SUBCELLULAR COMPARTMENTALIZATION OF PLANT ANTIOXIDANTS AND ROS GENERATING SYSTEMS

EDITED BY: Francisco J. Corpas and José Manuel Palma

PUBLISHED IN: Frontiers in Plant Science

frontiers Research Topics

frontiers

ISSN 1664-8714
ISBN 978-2-88966-632-4
DOI 10.3389/978-2-88966-632-4

About Frontiers

Frontiers is more than just an open-access publisher of scholarly articles: it is a pioneering approach to the world of academia, radically improving the way scholarly research is managed. The grand vision of Frontiers is a world where all people have an equal opportunity to seek, share and generate knowledge. Frontiers provides immediate and permanent online open access to all its publications, but this alone is not enough to realize our grand goals.

Frontiers Journal Series

The Frontiers Journal Series is a multi-tier and interdisciplinary set of open-access, online journals, promising a paradigm shift from the current review, selection and dissemination processes in academic publishing. All Frontiers journals are driven by researchers for researchers; therefore, they constitute a service to the scholarly community. At the same time, the Frontiers Journal Series operates on a revolutionary invention, the tiered publishing system, initially addressing specific communities of scholars, and gradually climbing up to broader public understanding, thus serving the interests of the lay society, too.

Dedication to Quality

Each Frontiers article is a landmark of the highest quality, thanks to genuinely collaborative interactions between authors and review editors, who include some of the world's best academicians. Research must be certified by peers before entering a stream of knowledge that may eventually reach the public - and shape society; therefore, Frontiers only applies the most rigorous and unbiased reviews.
Frontiers revolutionizes research publishing by freely delivering the most outstanding research, evaluated with no bias from both the academic and social point of view. By applying the most advanced information technologies, Frontiers is catapulting scholarly publishing into a new generation.

What are Frontiers Research Topics?

Frontiers Research Topics are very popular trademarks of the Frontiers Journals Series: they are collections of at least ten articles, all centered on a particular subject. With their unique mix of varied contributions from Original Research to Review Articles, Frontiers Research Topics unify the most influential researchers, the latest key findings and historical advances in a hot research area! Find out more on how to host your own Frontiers Research Topic or contribute to one as an author by contacting the Frontiers Editorial Office: frontiersin.org/about/contact

SUBCELLULAR COMPARTMENTALIZATION OF PLANT ANTIOXIDANTS AND ROS GENERATING SYSTEMS

Topic Editors:
Francisco J. Corpas, Biología Celular y Molecular de Plantas, Estación Experimental del Zaidín (EEZ), Spain
José Manuel Palma, Consejo Superior de Investigaciones Científicas (CSIC), Spain

Citation: Corpas, F. J., Palma, J. M., eds. (2021). Subcellular Compartmentalization of Plant Antioxidants and ROS Generating Systems. Lausanne: Frontiers Media SA. doi: 10.3389/978-2-88966-632-4

Table of Contents

frontiers in Plant Science

EDITORIAL
published: 18 February 2021
doi: 10.3389/fpls.2021.643239

Editorial: Subcellular Compartmentalization of Plant Antioxidants and ROS Generating Systems

José M. Palma and Francisco J. Corpas**

Group of Antioxidants, Free Radicals and Nitric Oxide in Biotechnology, Food and Agriculture, Department of Biochemistry, Cell and Molecular Biology of Plants, Estación Experimental del Zaidín, Consejo Superior de Investigaciones Científcas, Granada, Spain

Keywords: chloroplasts, mitochondria, peroxisomes, reactive oxygen species, antioxidants, reactive nitrogen species

OPEN ACCESS

Edited by:
Deyu Xie,
North Carolina State University, United States

Reviewed by:
Christine Helen Foyer,
University of Birmingham, United Kingdom
Sixue Chen,
University of Florida, United States

****Correspondence:***
José M. Palma
josemanuel.palma@eez.csic.es
Francisco J. Corpas
javier.corpas@eez.csic.es

Specialty section:
This article was submitted to Plant Metabolism and Chemodiversity, a section of the journal Frontiers in Plant Science

Received: *17 December 2020*
Accepted: *01 February 2021*
Published: *18 February 2021*

Citation:
Palma JM and Corpas FJ (2021) Editorial: Subcellular Compartmentalization of Plant Antioxidants and ROS Generating Systems. Front. Plant Sci. 12:643239. doi: 10.3389/fpls.2021.643239

Editorial on the Research Topic

Subcellular Compartmentalization of Plant Antioxidants and ROS Generating Systems

The oxygen paradox is a very well-known issue which encounters the necessity of oxygen for life with its toxic potentiality. This simplistic but real fact is molded by the prevailing oxygen concentrations that must be controlled for the optimal functioning of aerobic living beings. In plants, oxygen gains special relevance because, besides being fundamental for respiration, it is also product of the water photolysis occurring at the photosystem II (PSII). This converts chloroplasts into oxygen-enriched organelles and, in fact, this gas is target of the reducing events which take place in this compartment as a consequence of two light reactions at both PSII and PSI. As long as plant colorful organs (mainly green, including leaves, shoots, and fruits) are illuminated, photosynthesis is always operating if $NADP^+$ is conveniently available. But, subsidiarily, bypass processes always occur with the concomitant production of reactive oxygen species (ROS), either singlet oxygen ($^1O_2$) at the PSII, and superoxide radicals ($O_2^{\cdot-}$) at the PSI with subsequent dismutation to hydrogen peroxide (H_2O_2) (Foyer and Noctor, 2003; Asada, 2006; Gill and Tuteja, 2010; Corpas et al., 2015).

Under unfavorable stressful conditions, with enhanced ROS production and with chloroplast electron transport overcoming the ferredoxin-NADP reductase (FNR) capacity to reduce $NADP^+$ to NADPH for further use in the CO_2-fixing Calvin-Benson cycle, the oxygenase side of the RuBisCO is stimulated, thus promoting the photorespiratory pathway. This last route involves chloroplasts, peroxisomes and mitochondria. The first peroxisomal enzyme of this route is glycolate oxidase (GOX) which converts glycolate into glyoxylate with the concomitant production of H_2O_2. What it started as a stress condition imposed to chloroplast is then translocated to other cell organelles, i.e., peroxisomes, which increase their H_2O_2 production by the GOX activity. Additional systems located in other cell compartments like the mitochondrial electron transport chain and the respiratory burst oxidase homolog (Rboh) from plasma membrane are also ROS sources which may contribute to exacerbated ROS levels under stressful conditions. Thus, through the interconnection of organelles in the cell homeostasis, any sudden disturbing situation can be expanded as a snowball to the whole-cell where a set of mechanisms is prone to be activated to control the ROS excess (Asada, 2006; Gill and Tuteja, 2010; Corpas et al., 2015; Czarnocka and Karpinski, 2018; Janku et al., 2019; Kohli et al., 2019).

This ROS-modulating set includes enzymatic and non-enzymatic antioxidants. As plant antioxidative enzymes, superoxide dismutase (SOD), catalase, and the ascorbate-glutathione cycle are the most prominent members, while ascorbate (ASC), glutathione (GSH), carotenoids, α-tocopherol, and polyphenols are the main low-molecular-weight antioxidants. Within these latter ones, ASC is perhaps the most paradigmatic, powerful and versatile antioxidant since it can directly scavenge ROS, either $O_2^{\cdot-}$, H_2O_2, or hydroxyl radicals ($^{\cdot}OH$), but its effectiveness in controlling H_2O_2 levels may increase with the aid of ascorbate peroxidase (APX). ASC also contributes to quench $^1O_2$ by regenerating α-tocopherol, and in the dynamics of carotenoids (also $^1O_2$ scavengers), through the xanthophylls' cycle (Gupta et al., 2018). Each organelle contains its own antioxidative equipment, but the participation of ASC and GSH cell-wide grants to these molecules a relevant role in the oxidative homeostasis. ASC is synthesized in the mitochondrial membrane whereas the synthesis of GSH takes place in the cytosol and chloroplasts (Arisi et al., 1997; Zechmann, 2014, 2018; Rodríguez-Ruiz et al., 2017; Jez, 2019; Martí et al.). However, in still little known processes, these compounds migrate to all organelles to exert their antioxidant role, either directly or through the participation of enzymatic partners (**Figure 1**).

Accordingly, this Research Topic includes articles focused on the main plant cell organelles which harbor the most active ROS and antioxidant metabolism in the cell: chloroplasts, mitochondria and peroxisomes. Thus, it has been reported that in mulberry (*Morus* ssp.), a chloroplast drought-induced stress protein (MaCDSP32), with thioredoxin nature, is upregulated under drought conditions and appears to confer drought tolerance and ROS homeostasis, what triggers the stress response during seed germination and growth of this plant species (Sun et al.). Salt and osmotic stresses have been also addressed in this volume, and it was found that the exogenous application of the flavonoid naringenine protected bean (*Phaseolus vulgaris*) chloroplast against those stress conditions by regulating the PSII efficiency and the organelle antioxidant machinery (Yildiztugay et al.). The involvement of chloroplasts in plant immunity and disease with the assistance of other organelles such as apoplast, mitochondria, and peroxisomes and their respective ROS-redox systems was reviewed, and the integration between photosynthesis and plant immunity for future food demand was proposed (Kuzniak and Kopczewski). The role of ROS and antioxidant agents from mitochondria and plastids, and the profile of DNA damage in those organelles were also analyzed in different organs during maize development and under dark and light conditions (Tripathi et al.).

The involvement of signaling processes mediated by ROS, reactive nitrogen species (RNS) and H_2S in the response to biotic and abiotic was also investigated at mitochondrial level in this Research Topic. It was discussed how these chemical species operate in these organelles through diverse post-translational modifications (PTMs) including *S*-oxidation, *S*-glutathionylation and *S*-nitrosation, paying special attention to the thioredoxin/peroxiredoxin system as target and following its response to environmental stress (Martí et al.). *S*-nitrosation and nitration promoted by RNS, and persulfidation mediated by H_2S are PTMs which take part as strategic tools for the autoregulation of the peroxisomal metabolism to adapt these

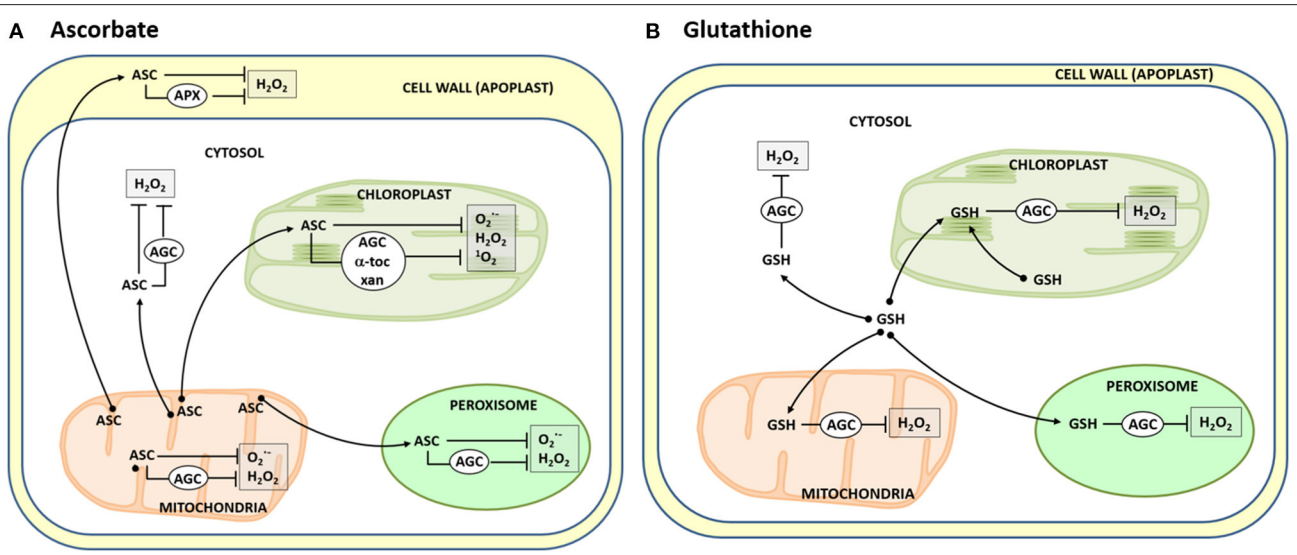

FIGURE 1 | Dynamics of ascorbate **(A)** and glutathione **(B)** in plant cells. Ascorbate (ASC) generated in the mitochondrial membranes [see Rodríguez-Ruiz et al. (2017) and Martí et al.] is driven to the different cell loci where it is used to neutralize diverse ROS [superoxide radicals ($O_2^{\cdot-}$), hydrogen peroxide (H_2O_2), and singlet oxygen ($^1O_2$)] generated in the organelles. This occurs directly or indirectly through either the participation of the ascorbate peroxidase (APX) and the enzymes of the ascorbate-glutathione cycle (AGC), regenerating α-tocopherol (α-toc), or the xanthophylls' cycle (xan). Likewise, glutathione (GSH), synthesized in the cytosol and chloroplasts, is basically used as well in different cell compartments to indirectly scavenge H_2O_2 through the AGC.

organelles to their target organ, the developmental stage, and to face external stimuli including pathogens and abiotic agents. These signaling processes, together with the crosstalk among ROS, RNS, reactive sulfur species (RSS), and peroxisomes under the prevailing conditions have been also reviewed here (Corpas et al.).

Additionally, this Research Topic covers glycosylation of antioxidant molecules and phytohormones achieved by UDP-glycosyltransferases with consequences in their cell and histological repartition. By this modification, plants upgrade their adaptation and fitness capacities in a scenario of climate change which can influence the productivity of many crops (Behr et al.). In this context, a synergistic regulation of nitrogen (N) and sulfur (S) on the redox and amino acid balances has been proposed to be a key point to improve the maize sustainable yield and its nutritional quality. Consequently, a balanced N-S stoichiometry promoted enhanced GSH content and photosynthetic rate (Liu et al.).

Overall, this Research Topic provides an updated overview on how the synergy among diverse strategies at subcellular and molecular levels can bring light to many aspects of the ROS and antioxidant cell homeostasis, what conveys the potential repercussion of these promising investigations for the upcoming modern agriculture.

AUTHOR CONTRIBUTIONS

All authors listed have made a substantial, direct and intellectual contribution to the work, and approved it for publication.

REFERENCES

Arisi, A. C. M., Noctor, G., and Foyer, C. H. (1997). Modification of thiol contents in poplars (*Populus tremula* x *P. alba*) overexpressing enzymes involved in glutathione synthesis. *Planta* 203, 362–372. doi: 10.1007/s004250050202

Asada, K. (2006). Production and scavenging of reactive oxygen species in chloroplasts and their functions. *Plant Physiol.* 141, 391–396. doi: 10.1104/pp.106.082040

Corpas, F. J., Gupta, D. K., and Palma, J. M. (2015). "Production sites of reactive oxygen species (ROS) in organelles from plant cells," in *Reactive Oxygen Species and Oxidative Damage in Plants Under Stress*, eds Gupta, D. K., Palma, J. M., and Corpas, F. J. (Heidelberg: Springer Internation Publushing), 1–22. doi: 10.1007/978-3-319-20421-5_1

Czarnocka, W., and Karpinski, S. (2018). Friend or foe? Reactive oxygen species production, scavenging and signaling in plant response to environmental stresses. *Free Rad. Biol. Med.* 122, 4–20. doi: 10.1016/j.freeradbiomed.2018.01.011

Foyer, C. H., and Noctor, G. (2003). Redox sensing and signaling associated with reactive oxygen in chloroplasts, peroxisomes and mitochondria. *Physiol. Plant* 119, 355–364. doi: 10.1034/j.1399-3054.2003.00223.x

Gill, S. S., and Tuteja, N. (2010). Reactive oxygen species and antioxidant machinery in abiotic stress tolerance in crop plants. *Plant Physiol. Biochem.* 48, 909–930. doi: 10.1016/j.plaphy.2010.08.016

Gupta, D. K., Palma, J. M., and Corpas, F. J. (eds.). (2018). "Preface: Generation and scavenging of reactive oxygen species (ROS) in plant cells: an overview" in *Antioxidants and Antioxidant Enzymes in Higher Plants* (Cham: Springer International Publishing), 5–9. doi: 10.1007/978-3-319-75088-0

Janku, M., Luhova, L., and Petrivalsky, M. (2019). On the origin and fate of reactive oxygen species in plant cell compartments. *Antioxidants* 8:105. doi: 10.3390/antiox8040105

Jez, J. M. (2019). Structural biology of plant sulfur metabolism: from sulfate to glutathione. *J. Exp. Bot.* 70, 4089–4103. doi: 10.1093/jxb/erz094

Kohli, S. K., Khanna, K., Bhardwaj, R., Abd Allah, E. F., Ahmad, P., and Corpas, F. J. (2019). Assessment of subcellular ROS and NO metabolism in higher plants: multifunctional signaling molecules. *Antioxidants* 8:641. doi: 10.3390/antiox8120641

Rodríguez-Ruiz, M., Mateos, R. M., Codesido, V., Corpas, F. J., and Palma, J. M. (2017). Characterization of the galactono-1,4-lactone dehydrogenase from pepper fruits and its modulation in the ascorbate biosynthesis. Role of nitric oxide. *Redox Biol.* 12, 171–181. doi: 10.1016/j.redox.2017.02.009

Zechmann, B. (2014). Compartment-specific importance of glutathione during abiotic and biotic stress. *Front. Plant Sci.* 5:566. doi: 10.3389/fpls.2014.00566

Zechmann, B. (2018). Compartment-specific importance of ascorbate during environmental stress in plants. *Antiox. Redox Signal.* 29, 1488–1501. doi: 10.1089/ars.2017.7232

Conflict of Interest: The authors declare that the research was conducted in the absence of any commercial or financial relationships that could be construed as a potential conflict of interest.

frontiers in Plant Science

ORIGINAL RESEARCH
published: 16 April 2020
doi: 10.3389/fpls.2020.00419

MaCDSP32 From Mulberry Enhances Resilience Post-drought by Regulating Antioxidant Activity and the Osmotic Content in Transgenic Tobacco

*Hongmei Sun, Wenrui Zhao, Hui Liu, Chao Su, Yonghua Qian and Feng Jiao**

Institute of Sericulture and Silk, College of Animal Science and Technology, Northwest A&F University, Yangling, China

Desiccation tolerance is a complex phenomenon that depends on the regulated expression of numerous genes during dehydration and subsequent rehydration. Our previous study identified a chloroplast drought-induced stress protein (MaCDSP32) in mulberry, a thioredoxin (Trx) that is upregulated under drought conditions and is likely to confer drought tolerance to transgenic plants. Mulberry (*Morus* spp.) is an ecologically and economically important perennial woody plant that is widely used in forest management to combat desertification. However, its stress tolerance physiology is not well understood. In this study, the functions of *MaCDSP32* gene were investigated. The expression of *MaCDSP32* exhibited a circadian rhythm and was induced by mild and severe water deficits. Under abiotic stress, *MaCDSP32*-overexpressing plants exhibited increased stress sensitivity with lower water retention capacity and more severe lipid peroxidation than the wild-type (WT) plants. Furthermore, the activity of superoxide dismutase (SOD), the contents of proline and soluble sugars and the expression of stress-related transcription factors were lower in the *MaCDSP32*-overexpressing plants than in the WT plants. However, the *MaCDSP32*-overexpressing lines exhibited stronger recovery capability after rewatering post-drought. Moreover, the SOD enzyme activity, proline content, and soluble sugar content were higher in the transgenic plants after rewatering than in the WT plants. The production of the reactive oxygen species (ROS) H_2O_2 and O_2^- was significantly lower in the transgenic plants than in the WT plants. In addition, under abiotic stress, the *MaCDSP32*-overexpressing lines exhibited improved seed germination and seedling growth, these effects were regulated by a positive redox reaction involving *MaCDSP32* and one of its targets. In summary, this study indicated that *MaCDSP32* from mulberry regulates plant drought tolerance and ROS homeostasis mainly by controlling SOD enzyme activity and proline and soluble sugar concentrations and that this control might trigger the stress response during seed germination and plant growth. Overall, *MaCDSP32* exerts pleiotropic effects on the stress response and stress recovery in plants.

Keywords: mulberry *MaCDSP32*, transgenic tobacco, abiotic stress, resilience, antioxidant activity, osmotic accumulation

OPEN ACCESS

Edited by:
José Manuel Palma, Spanish National Research Council, Spain

Reviewed by:
Rosa Porcel, Universitat Politècnica de València, Spain
Renu Deswal, University of Delhi, India

****Correspondence:***
Feng Jiao
fjiao@nwsuaf.edu.cn

Specialty section:
This article was submitted to Plant Abiotic Stress, a section of the journal Frontiers in Plant Science

Received: *23 November 2019*
Accepted: *23 March 2020*
Published: *16 April 2020*

Citation:
Sun H, Zhao W, Liu H, Su C, Qian Y and Jiao F (2020) MaCDSP32 From Mulberry Enhances Resilience Post-drought by Regulating Antioxidant Activity and the Osmotic Content in Transgenic Tobacco. Front. Plant Sci. 11:419. doi: 10.3389/fpls.2020.00419

INTRODUCTION

Plants, as sessile organisms, are constantly facing challenges from their surroundings and have thus evolved a set of precise defense mechanisms and self-repair systems during the long process of survival of the fittest (Zhu, 2016). Reactive oxygen species (ROS), as an inevitable metabolite produced during plant growth or due to environmental hazards, play integral roles as signaling molecules in numerous biological processes but can also cause oxidative damage to cells (Baxter et al., 2014). Excess ROS cause biochemical changes, such as protein unfolding, denaturation or aggregation, which results in the inactivation of various enzymes, and these effects are mostly ascribed to changes in intermolecular disulfide bonds (Rey et al., 1998). However, it is important to maintain the normal physiological functions of some response proteins in plants under stress (Vieira Dos Santos and Rey, 2006). ROS accumulation within chloroplasts is controlled by a complex antioxidant-scavenging system that includes thioredoxins (Trxs) and 2-Cys peroxiredoxins (Prxs), as well as antioxidant enzymes, such as superoxide dismutase (SOD) and ascorbate peroxidase (APX) (Foyer and Shigeoka, 2011). Trxs contain active cysteine residues (Cys-Gly-Pro-Cys), and this disulfide center appears to be highly involved in their function (Vieira Dos Santos et al., 2007; Laugier et al., 2010) by supplying reducing power to the oxidized disulfide of Prxs (Buchanan et al., 2000). Chloroplasts house a large number of different Trx forms. Trx-*x*, Trx-*y* and CDSP32 are Trxs that play important roles in the responses of chloroplast to oxidative stress (Foyer, 2018). Moreover, Trxs reduce the disulfide bridges of target proteins during the Calvin cycle. These Trxs can be reduced by two pathways, which show some overlap with regard to their target proteins: the ferredoxin-dependent Trx system and the NADPH-dependent Trx reductase (NTRC) pathway. These two systems function together with 2-Cys Prxs. The Prx/Trx system is a ubiquitous antioxidant system that removes harmful ROS and is specifically involved in the detoxification of hydrogen peroxide (H_2O_2). Trxs modulate the activities of various antioxidant enzymes and the redox status to directly scavenge ROS, and these effects contribute to oxidative stress-linked signaling pathways and ROS homeostasis. Although it is clear that Trxs play a fundamental role in regulating diverse processes in living cells (Montrichard et al., 2009), further studies are needed to determine the specific enzymes targeted by certain Trxs and their interaction regulatory processes in chloroplasts under different abiotic stresses.

Mulberry (*Morus* spp.) is a widely planted economically and ecologically important woody plant species that is used in modern farming, environmental management, and the clothing industry. Its economic value in sericulture, nutritional benefits and medicinal value have received increasing attention (Zeng et al., 2015). In addition, mulberry has worldwide ecological value due to its environmental adaptability, which is reflected in its tolerance to adverse conditions, such as drought, cold, saline-alkali conditions, waterlogging and barren soil (Li et al., 2018). However, the molecular mechanisms involved in tolerance to drought stress are not well understood. Notably, certain species known as resurrection plants have evolved unique mechanisms of desiccation tolerance and can thus tolerate relatively severe water loss. Drought tolerance is a complex phenomenon that depends on the regulated expression of numerous genes during dehydration and subsequent rehydration (Dinakar and Bartels, 2013), but the underlying regulatory mechanisms remain unclear. Thus, an understanding of the mulberry genes involved in responses to adverse conditions should provide useful genetic resources for future molecular plant breeding. In particular, since the announcement of the mulberry genome in 2013, studies of genes related to tolerance in mulberry have been gradually conducted (He et al., 2013). Our preliminary work identified a wide range of differentially expressed proteins in drought-treated mulberry *ShinIchinose* (*Morus alba* L.), and among these proteins, we identified an upregulated protein, denoted mulberry chloroplast drought-induced stress protein (MaCDSP32), which is a plastidial Trx-like protein with two Trx domains (Rey et al., 1998). CDSP32 is involved in both the regeneration of plant Prxs (Dietz, 2007) and catalysis of the thiol-disulfide interchange (Sugiura et al., 2019). A previous study revealed that plants overexpressing *CDSP32* display increased sensitivity to oxidative stress (Broin et al., 2002). However, transgenic potato plants deficient in the CDSP32 protein present higher levels of overoxidized forms of Prx monomers and increased lipid peroxidation (Broin et al., 2003). These results are contradictory, and the reasons remain unclear. The last review of *CDSP32* provided little detailed functional knowledge (Dietz, 2007), but recent studies have shown that *CDSP32* is involved in a variety of physiological and biochemical processes, including the anthocyanin biosynthetic pathway in arctic mustard (Butler et al., 2014) and the cadmium tolerance process in oilseed rape (Zhang et al., 2018). In addition, B-type methionine sulphoxide reductase (MSRB) is a target of CDSP32 (Rey et al., 2005, 2013). Methionine sulphoxide reductase (MSR) regulates the life of seeds, and the metabolites of methionine specifically facilitate seed germination (Catusse et al., 2011; Chatelain et al., 2013). Whether *MaCDSP32* participates in the regulation of seed germination through a mechanism related to MSRB has not been previously reported. Thus, the function of MaCDSP32 in mulberry piqued our interest. In this study, its coding gene, *MaCDSP32*, was transformed into tobacco (*N, benthamiana*) to assess the changes in the various abiotic stress tolerances of the transgenic plants. We found that the ectopic expression of *MaCDSP32* altered the stress signal transduction pathway and the production of ROS under abiotic stress and stress relief conditions. Furthermore, the potential action of *MaCDSP32* in seed germination was evaluated. The aim of this work was to characterize the functions of *MaCDSP32* during exposure to abiotic stress. Overall, our results suggest a novel functional model for Trx MaCDSP32 in plant stress tolerance and post-stress recovery and provide a reference for the exploitation of mulberry germplasm resources.

MATERIALS AND METHODS

Plant Materials and Growth Conditions

Laboratory mulberry plants of the *ShinIchinose* cultivar were produced by tissue culture from winter buds. Laboratory

mulberry *Luza* seedlings were grown from seeds. Five-month-old laboratory *ShinIchinose* plants and laboratory *Luza* plants were prepared for use in this study. The plants were grown in a mixed nursery substrate composed of turfy soil and vermiculite. In addition, the mature leaves from the annual shoots of *ShinIchinose* trees grown in the field were used for the expression assay of circadian rhythm gene. The growth of these trees was completely dependent on the natural conditions, without artificial watering. Tobacco (*N. benthamiana*) was used for the generation of overexpression transgenic plants. The laboratory mulberry and tobacco plants were grown in a greenhouse under the controlled conditions (23°C, 16-h light/8-h dark, 50% humidity) and supplied 1/4-strength Hoagland nutrition solution once per week.

Gene Cloning, Sequencing and Bioinformatics Analysis

Total RNA from the leaves of *ShinIchinose* was extracted using an Ultrapure RNA kit (CWBIO, China) according to the manufacturer's recommended protocol. First-strand cDNA was synthesized from 1 μg of total RNA using the PrimeScript RT reagent kit with gDNA Eraser (Takara, Japan). The primers used for amplification of the full-length sequence of *MaCDSP32* (the coding gene of mulberry chloroplast drought-induced stress protein, MaCDSP32) (**Supplementary Table S1**) were designed according to the sequence of *Morus notabilis CDSP32* (XM_010101817.1). PCR was performed using 2 × Taq MasterMix (CWBIO) according to the manufacturer's recommended protocol. After detection by agarose gel electrophoresis, the PCR product bands were recovered using a gel recovery kit (Omega, United States) and sequenced. Bioinformatics analysis was conducted as described by Wang et al. (2018). The phylogenetic tree was constructed through neighbor-joining analysis using MEGA 6.0.

Expression Pattern of *MaCDSP32*

To detect the circadian expression patterns of *MaCDSP32*, mature leaf samples from the annual shoots of *ShinIchinose* plants in the field were collected over 3 days (during sunny weather). Leaf samples were collected every 3 h from 06:00 to 21:00 in each day, with three biological replicates per day. To detect the tissue-specific expression patterns of *MaCDSP32*, the leaves (1st, 2nd, 3rd, 4th, 6th, and 9th from the top), petioles and stems from five-month-old laboratory *ShinIchinose* plants were collected at 10:00 under normal water conditions. Three biological replicates were included. Samples were frozen in liquid nitrogen and stored at −80°C.

Plasmid Construction and Plant Transformation

Full-length *MaCDSP32* was ligated into the pCAM35S-GFP botany vector using a homologous recombination system. The recombinant pCAM35S-*MaCDSP32*-GFP plasmids were transformed into *A. tumefaciens* (GV3101) for plant transformation. Transient transformation was performed in the leaves of *ShinIchinose* according to a vacuum immersion protocol (Matsuo et al., 2016). Three days after transformation, the *MaCDSP32* gene expression in the leaves was confirmed by RT-PCR. The leaves with successful expression were designated *Inst* (*Inst*-1 and *Inst*-2 were selected for subsequent study due to their higher *MaCDSP32* expression), and the wild type was designated WT_{Ma}. Stable transformation was performed in tobacco using a leaf disk co-cultivation protocol (Horsch et al., 1985; Bao et al., 2017). The positive transgenic tobacco lines were selected by 35 mg/ml kanamycin and confirmed by genomic DNA PCR (Rahim et al., 2019). The presence of *MaCDSP32* in each selected transgene was verified by qRT-PCR (La Mantia et al., 2018). The identified positive lines were subcultured until roots formed and then transferred to soil. The tobacco lines with successful overexpression of *MaCDSP32* were named OE lines. The OE-2 and OE-7 lines had higher *MaCDSP32* expression than the other lines and were therefore selected for subsequent experiments. The wild-type tobacco lines were named WT. Seeds from the homozygous transgenic lines were harvested and dried for subsequent use.

Subcellular Localization

The constructed pCAM35S-*MaCDSP32*-GFP plasmids and the control pCAM35S-GFP vector plasmids were transformed into tobacco (*N. benthamiana*) leaves mediated by *A. tumefaciens* (GV3101) to express fusion proteins with green fluorescence protein (GFP). After 3 d of incubation, the GFP fluorescence in tobacco leaves was imaged using a laser-scanning confocal microscope (TCS SP8 CARS; Leica, Germany). This experiment was performed three times with identical results, and at least six leaves were included in each experimental repeat.

Abiotic Stress Treatment, Water Loss Rate and Gene Expression

For the drought treatment, 5-month-old *Luza* and *ShinIchinose* plants were subjected to a watering halt for 6 d. Leaves from *Luza* were collected after 0, 1, 2, 3, 4, 5 and 6 d of drought, and leaves from *ShinIchinose* were collected after 0, 3 and 6 d of drought. Three-month-old plants of the OE-2, OE-7 and WT tobacco lines were subjected to drought for 10 d and then rewatered for 4 d. The percentage of wilted leaves in each whole plant at different times points during treatment was recorded. For the NaCl and oxidative stress treatments, three-month-old plants of the OE-2, OE-7 and WT tobacco lines were watered with 200 mM NaCl for 13 d or sprayed with 10 μM methyl viologen (MV) for 25 h according to Li et al. (2009). At least three replicates per treatment were established. All samples were collected at 10:00, frozen in liquid nitrogen and stored at −80°C.

The water loss rate was measured according to Rao et al. (2015). Mulberry leaves (*Inst*-1, *Inst*-2 and WT_{Ma}, at least five leaves per set) were placed on dry filter paper to measure their natural rate dehydration. The water loss rate of tobacco leaves (OE-2, OE-7 and WT, at least five leaves per set) was also measured. All the leaves were weighed every 10 min, for a total of 120 min. The stomatal apertures was measured at 0, 30, and 60 min of dehydration. The expression levels of *MaCDSP32*, the dehydration responsive element binding protein

gene (*MaDREB1*) and the mitogen-activated protein kinase gene (*MaMAPK*) in the treated *Inst*-1, *Inst*-2 and WT_{Ma} leaves were examined. Measurements were conducted with at least three replicates.

Seed Germination and Seedling Growth Under Abiotic Stress

Seeds of the transgenic (OE-2 and OE-7) and WT tobacco lines were germinated on 1/2 MS medium containing mannitol or NaCl at one of two concentrations (100 mM and 200 mM). Medium without additives was used as control medium. The seed germination rate at 5, 6, 7 and 8 d after sowing was scored, and the production of H_2O_2 and O_2^- and the gene expression of *MaCDSP32* and *NtMSRB* after 6 d of treatment with 100 mM NaCl or 100 mM mannitol were measured. Nine days after germination under normal conditions, the germinated seedlings of the transgenic (OE-2 and OE-7) and WT tobacco lines were transplanted to 1/2 MS medium containing 200 mM NaCl for an additional 16 d of growth or to medium without additives (control). Seedlings length at initial transplantation and after 16 d of treatment was measured as described by Cui et al. (2019). The gene expression of *MaCDSP32* and *NtMSRB* in treated seedlings was detected after 16 d of growth under stress treatment. At least three replicates were established for each treatment.

Quantitative Real-Time PCR (qRT-PCR)

qRT-PCR was performed using a TB Green Premix Ex Taq II kit (Tli RNaseH Plus) (Takara) according to the manufacturer's instructions for gene expression analysis. The template cDNA fragment was synthesized from the extracted total RNA and was diluted to 1/10 for use in the qRT-PCR system. All the primers are detailed in **Supplementary Table S1**. The procedure was performed with a LightCycler 480II machine (Roche, Switzerland) using a 45-cycle program (95°C for 5 s and 60°C for 30 s). The relative expression of genes was calculated based on the threshold cycle according to the $_{\Delta}$ $_{\Delta}$ Ct method (Schmittgen and Livak, 2008). The result was normalized to the expression of the reference gene *actin* in mulberry (Chen et al., 2018) or *L25* in tobacco (Liu et al., 2018). Expression was determined for at least three replicates per treatment.

Quantification of Relative Water Content (RWC)

The RWC of the leaf samples was determined by measuring the fresh leaf weight (FW) and the dry weight (DW) after drying at 65°C for 24 h, as well as the saturated weight (SW) after soaking in water for 1 h, as described by Wang et al. (2015). The following formula was used: RWC (%) = (FW – DW)/(SW – DW) × 100%.

Measurement of Malondialdehyde (MDA), Proline and Soluble Sugars Contents

The MDA content was detected through the thiobarbituric acid (TBA) reaction as described by Duan et al. (2012). The leaf samples (0.3 g) were homogenized in 5 ml of 50 mM phosphate buffer (pH 7.8) and centrifuged at 10000 × *g* for 10 min. Two milliliters of supernatant was added to 5 ml of 0.5% (w/v) TBA in 10% (w/v) trichloroacetic acid (TCA). The mixture was incubated in boiling water for 10 min, cooled at room temperature and then centrifuged at 3000 × *g* for 10 min. The absorbance of the supernatant was determined at 450 nm, 532 nm, and 600 nm and the following formula was used: MDA ($\mu M \cdot g^{-1}$) = 6.45 (A_{532}-A_{600}) – 0.56A_{450}.

The proline content was determined using acid ninhydrin. The leaf samples (0.2 g) were homogenized in 3 ml of 3% aqueous sulfosalicylic acid and centrifuged at 12000 × *g* for 10 min. Subsequently, 500 μl of the supernatant was added to 1 ml of distilled water and 2 ml of 2% ninhydrin in acetone. The mixture was boiled for 15–30 min until it turned pink, cooled, added to 3 ml of toluene, mixed and allowed to stand for 5 min. The absorbance of the upper phase was determined at 520 nm. The proline content in the samples was calculated according to the standard curve and the formula described by Chen et al. (2019).

The soluble sugar content was determined using anthrone. A portion of each sample (0.2 g) was added to 3 ml of 80% ethanol and extracted in a water bath at 80°C for 30 min. Subsequently, 0.1 ml of the extract was added to 3 ml of anthrone reagent (0.2 g of anthrone and 1.0 g of thiourea in 100 ml of concentrated sulfuric acid). The mixture was placed in a boiling water bath for 10 min. The absorbance of the mixture was determined at 620 nm. The soluble sugar content was calculated according to the standard curve and the formula described by Chen et al. (2019). Measurements were obtained for at least three replicates per treatment.

In vivo Localization and Quantification of H_2O_2 and O_2^-

The *in vivo* detection of H_2O_2 and O_2^- was accomplished by histochemical staining with 3,3'-diaminobenzidine (DAB) and nitro blue tetrazolium (NBT) as described by Yadav et al. (2012). The presence of H_2O_2 and O_2^- in transgenic and WT leaves exposed to drought and salt stress was detected by immersing the leaf samples in solutions of DAB (1 mg/ml, pH 3.8) and NBT (1 mg/ml) in 10 mM phosphate buffer (pH 7.8). For the detection of O_2^-, the leaves were illuminated for 12 h until blue spots, which are indicative of formazan precipitates, appeared. To determine the localization of H_2O_2, the immersed leaves were incubated in the presence of light at room temperature for 24 h until brown spots became visible; these spots occurred due to the reaction of DAB with H_2O_2. After incubation, the leaf chlorophyll was bleached in absolute ethanol to enable visualization of the blue and brown spots.

The O_2^- content was determined according to the methods described by Yadav et al. (2012). The leaf tissue was extracted in 10 ml of 65 mM potassium phosphate buffer (pH 7.8) and centrifuged at 5000 × *g* for 10 min. A reaction mixture containing 0.9 ml of 65 mM phosphate buffer (pH 7.8), 0.1 ml of 10 mM hydroxylamine hydrochloride, and 1 ml of the extract was incubated at 25°C for 20 min. Subsequently, 17 mM sulphanilamide and 7 mM α-naphthylamine were added, and the mixture was further incubated at 25°C for 20 min. The absorbance was read at 530 nm. A standard curve

(10–200 nM) was prepared with $NaNO_2$ to calculate the production rate of O_2^-.

The H_2O_2 content in the leaf samples was measured as described by Yadav et al. (2012). The leaf tissue was extracted with cold acetone. Two milliliters of extract was mixed with 0.5 ml of 0.1% titanium dioxide in 20% (v/v) H_2SO_4, and the mixture was centrifuged at 6000 × *g* for 15 min. The absorbance of the supernatant was measured at 415 nm, and the concentration of H_2O_2 was calculated based on the established standard curve. Measurements were obtained for at least three replicates.

Quantification of Antioxidant Activity

The activity of antioxidant enzymes was detected as described by Wang et al. (2008). The leaf samples (0.3 g) were ground in liquid nitrogen and then homogenized in 5 ml of 50 mM phosphate buffer (pH 7.0). The homogenate was centrifuged at 10000 × *g* for 20 min at 4°C, and the supernatant was assayed for the activities of antioxidant enzymes. Protein quantification was determined using a BCA protein assay kit (Jiancheng, China) according to the manufacturer's recommended protocol, with bovine serum albumin used as the standard. SOD activity was measured with 0.1 ml of supernatant by monitoring the superoxide radical-induced reduction of NBT at 560 nm. One unit of SOD was defined as the amount of enzyme causing 50% inhibition of the reaction compared with the reaction in a blank sample. Catalase (CAT) and APX activities were determined with 0.2 ml of supernatant by following the breakdown of H_2O_2 and the ascorbate oxidation at 240 nm and 290 nm over 3 min, respectively. The reaction was initiated by the addition of H_2O_2. Peroxidase (POD) activity was measured with 0.2 ml of supernatant at 470 nm, following the oxidation of guaiacol. One unit of enzyme activity was defined as the amount of enzyme causing 50% inhibition per mg of protein and was expressed as $U{\cdot}mg^{-1}$ protein. Measurements were obtained for at least three replicates.

Gas Exchange Parameters and Photosynthetic Pigments Related to Photosynthesis

To evaluate the changes in the photosynthetic system, the gas exchange parameters of the WT and transgenic tobacco lines after 10 d of drought, 13 d of treatment with 200 mM NaCl and 25 h of treatment with 10 μM MV were determined. The gas exchange parameters, including the net photosynthetic rate (*Pn*), stomatal conductance, intercellular CO_2 concentration, transpiration rate and leaf temperature, were assessed using a portable photosynthetic transpiration system (Yaxin-1102, Yaxin, China) according to the operating instructions. An open-circuit automatic measurement mode was selected. Each measurement was repeated three times, and at least three plants were included in each treatment group.

The chlorophyll and carotenoid contents were measured according to Grzeszczuk et al. (2018) and Rey et al. (2013). The leaf samples were homogenized in 80% acetone and centrifuged at 3000 × *g* for 3 min. The absorbance of the supernatant was recorded at 663 nm, 645 nm and 470 nm. The contents of chlorophyll *a* (C_a) and chlorophyll *b* (C_b) were determined as follows: $C_a = 12.21 \times A_{663} - 2.81 \times A_{645}$, $C_b = 20.13 \times A_{645} - 5.03 \times A_{663}$. The carotenoid content was determined as follows: carotenoid contents = $(1000 \times A_{470} - 3.27 \times C_a - 104 \times C_b)/229$. Measurements were obtained for at least three replicates.

Statistical Analysis

Statistical analyses were performed using SAS 9.1 and Excel software, and figures were prepared using GraphPad Prism 6.0 software. At least three biological replicates were included in each experiment. The data are presented as the means ± SDs of the biological replicates. The significance of differences was analyzed using Student's *t*-test. $^*P < 0.05$, $^{**}P < 0.01$ and $^{***}P < 0.001$.

RESULTS

MaCDSP32 Cloning, Bioinformatics Analysis and Expression Pattern

A full-length gene fragment of *MaCDSP32* was amplified from mulberry *ShinIchinose* by RT-PCR (**Figure 1A**). The coding region (909 bp) was cloned, sequenced, and submitted to GenBank (accession number: KY799583). The deduced amino acid sequence was 302 amino acids. A phylogenetic tree was constructed using MEGA 6.0 (**Figure 1B**). The amino acid sequence of MaCDSP32 showed the highest similarity with the protein sequences from *Morus notabilis* (XM 010101817.1),

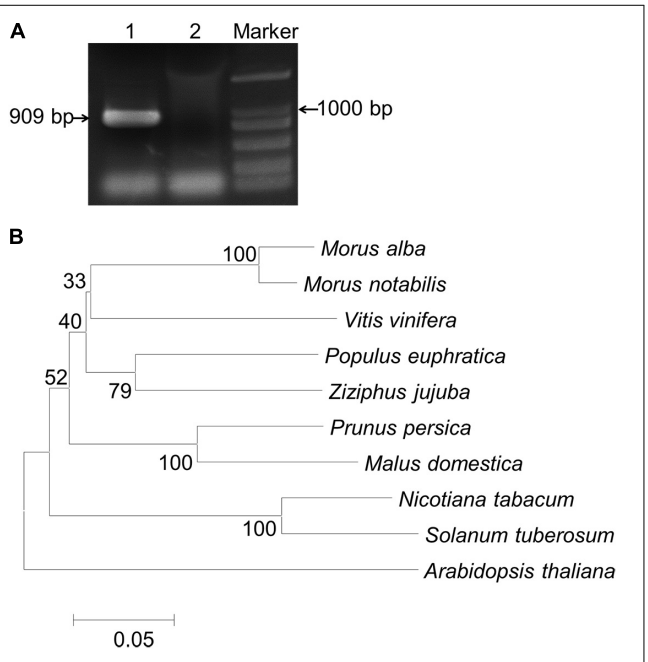

FIGURE 1 | PCR products of *MaCDSP32* and neighbor-joining phylogenetic analysis. **(A)** PCR amplification products of *MaCDSP32*. Lane 1: products of MaCDSP32; Lane 2: negative control (distilled water) used as a template for PCR. **(B)** A phylogenetic tree of the amino acid sequences of CDSP32 proteins from *Rosales* and several typical plant species was constructed using the MEGA 6.0 program.

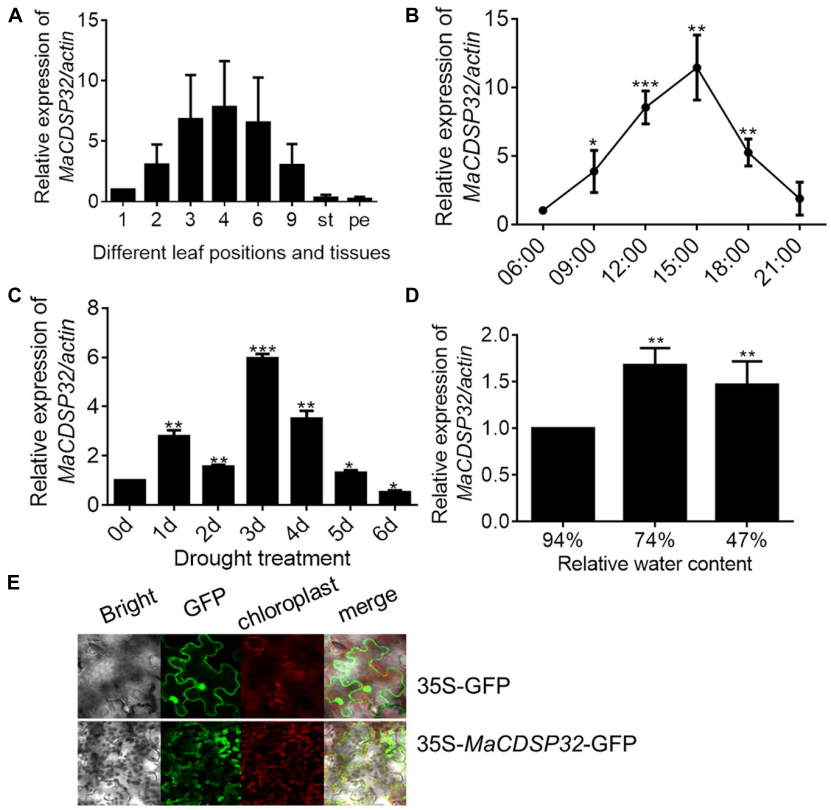

FIGURE 2 | Expression pattern of *MaCDSP32* in mulberry. **(A)** Measurements were obtained from the aboveground parts of the *ShinIchinose* mulberry cultivar; 1, 2, 3, 4, 6, and 9 represent the different leaf positions from top to bottom; st, stem; pe, petiole. **(B)** Measurements obtained within a day. Samples were collected on 3 consecutive days (during sunny weather), with three replicate samples collected per time point. **(C)** Measurements obtained during 6 days of drought in *Luza* cultivar. **(D)** Measurements obtained under different relative water contents (RWCs) of leaves of the *ShinIchinose* cultivar. **(E)** Subcellular localization of MaCDSP32. The control (plasmid with 35S-*GFP* alone) and fusion plasmid (35S-*MaCDSP32-GFP*) are shown. At least three biological replicates were included. Asterisks indicate significant differences between the transgenic and wild-type leaves (*t*-test, $^{*}P < 0.05$, $^{**}P < 0.01$, $^{***}P < 0.001$).

followed by that from *Vitis vinifera*, and the least similarity with the proteins from *Arabidopsis* and *Solanum tuberosum*. Therefore, it is likely that the physiological function of *MaCDSP32* is very different from that known in potato.

The gene expression analyses showed that *MaCDSP32* was mainly expressed in mature leaves (of the 3rd, 4th, and 6th leaf positions) rather than in young (1st leaf position) or senescent (9th leaf position) leaves or other tissues, such as stems and petioles in *ShinIchinose* mulberry plants (**Figure 2A**). Analysis of the expression changes with the circadian rhythm showed that compared to that at 06:00, *MaCDSP32* gene expression was markedly increased at 09:00 and 12:00, peaked at 15:00, and was substantially decreased at 18:00 and 21:00. Moreover, the level at 21:00 was similar to that at 06:00 (**Figure 2B**). *MaCDSP32* is involved in photosynthesis; accordingly, circadian transcriptional activity was detected. Additionally, the expression products of *MaCDSP32* were localized in chloroplasts (**Figure 2E**). The results suggest that *MaCDSP32* might function as a clock gene expressed during the day in association with sun exposure to affect chloroplast function. Regarding abiotic stress treatments, *MaCDSP32* expression under drought conditions was detected in the two mulberry cultivars. In the *Luza* cultivar, *MaCDSP32* gene expression was upregulated after 5 d of drought and peaked at 3 d (**Figure 2C**). In the *ShinIchinose* cultivar, leaf RWC decreased with increasing soil desiccation during the drought treatment (hydrated leaf, 94% RWC); mildly wilted leaf, 74% RWC), severely wilted leaf, 47% RWC). The gene expression of *MaCDSP32* was increased at RWC 74% than that at RWC94%, while was slightly downregulated at RWC 47% than that at 74% (**Figure 2D**). These results suggest that *MaCDSP32* expression is induced by water deficit but that expression does not increase linearly with drought intensity, declining only slightly under severe water deficit.

MaCDSP32 Overexpression Increases Leaf Water Loss Under Dehydration

Three days after transient transformation in mulberry leaves, the expression level of *MaCDSP32* in *Inst* (*Inst*-1 and *Inst*-2) and WT_{Ma} leaves was detected. *MaCDSP32* expression was higher in *Inst*-1 and *Inst*-2 than in WT_{Ma} (at 0 min, baseline condition), and upregulated after 60 min under dehydration (**Figure 3C**). These findings confirmed the effectiveness of the transient transformation, ensuring the reliability of the experiment results.

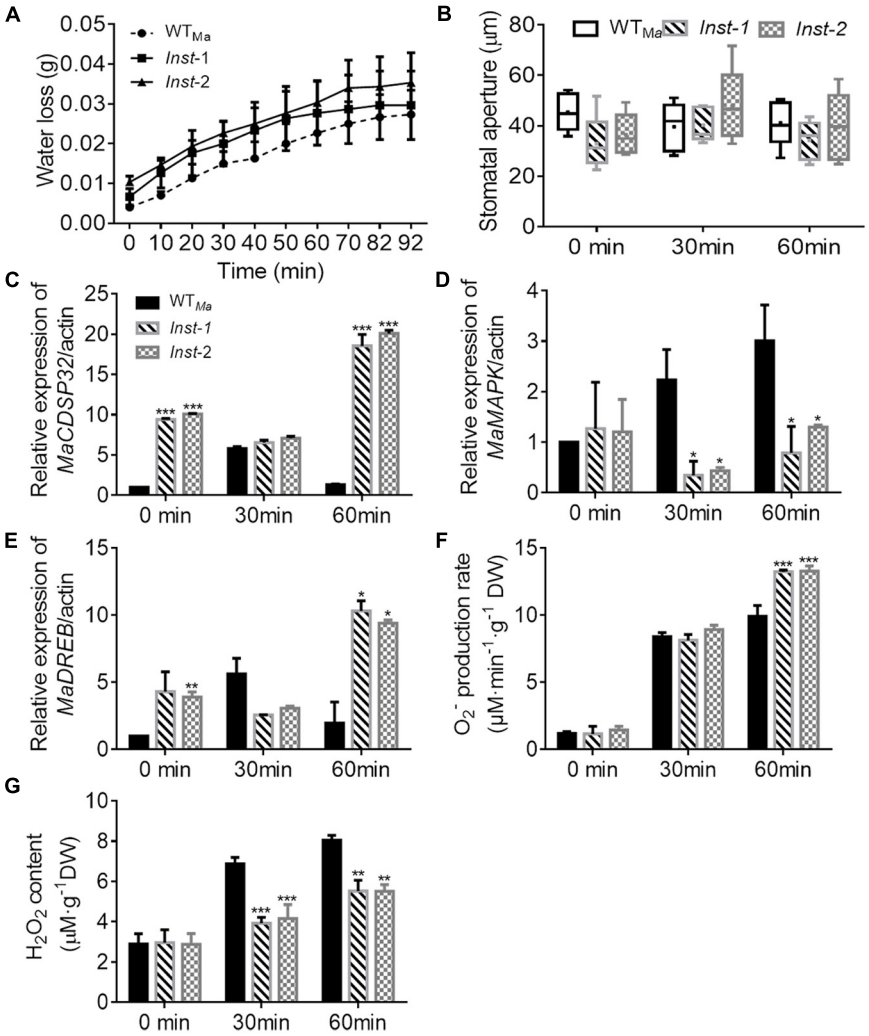

FIGURE 3 | The transient overexpression of *MaCDSP32* increases leaf water loss under desiccation conditions in mulberry. **(A)** Water loss, **(B)** Stomatal aperture after 0, 30, and 60 min of desiccation. **(C–E)** Relative expression of *MaCDSP32* **(C)**, *MaMAPK* **(D)**, and *MaDREB1* **(E)** genes. **(F–G)** Quantification of H_2O_2 **(F)** and O_2^- **(G)** contents. WT$_{Ma}$, leaves of wild-type *Shinlchinose*; *Inst*-1 and *Inst*-2, leaves of *Shinlchinose* transiently overexpressing *MaCDSP32*. At least three biological replicates were included. Asterisks indicate significant differences between the transgenic and wild-type leaves (*t*-test, $^*P < 0.05$, $^{**}P < 0.01$, $^{***}P < 0.001$).

During desiccation treatment, the water loss in *Inst*-1 and *Inst*-2 leaves was higher than that in WT$_{Ma}$ leaves over the 92 min of observation (**Figure 3A**). Because water evaporation is often related to the stomatal aperture, the changes in the stomatal aperture were measured. The stomatal aperture in *Inst*-1 and *Inst*-2 was not significantly different from that in WT$_{Ma}$ at both baseline (0 min) and during the desiccation treatment (30 and 60 min) (**Figure 3B**). At 30 min of rehydration, *MaCDSP32* expression was increased in WT$_{Ma}$ but significantly decreased in *Inst*-1 and *Inst*-2; however, after 60 min of rehydration, *MaCDSP32* expression was decreased in WT$_{Ma}$ and markedly increased in *Inst*-1 and *Inst*-2 (**Figure 3C**). *MaMAPK* expression did not significantly differ between WT$_{Ma}$ and *Inst*-1 or *Inst*-2 at baseline (at 0 min) but was upregulated in WT$_{Ma}$ and downregulated in *Inst*-1 and *Inst*-2 under stress conditions (at 30 and 60 min of dehydration) (**Figure 3D**). Under stress conditions, *MaDREB1* expression in *Inst*-1 and *Inst*-2 showed the same trends as *MaCDSP32* expression (**Figure 3E**). Additionally, the production of O_2^- was increased in WT$_{Ma}$, *Inst*-1 and *Inst*-2 at 30 min of dehydration, with no significant difference among the three leaf types. However, after 60 min of dehydration, O_2^- production was significantly higher in *Inst*-1and *Inst*-2 than in WT$_{Ma}$ (**Figure 3F**). H_2O_2 content did not significantly differ among *Inst*-1, *Inst*-2 and WT$_{Ma}$ under control conditions, but was significantly lower in *Inst*-1 and *Inst*-2 than in WT$_{Ma}$ during dehydration (30 and 60 min) (**Figure 3G**).

Two *MaCDSP32*-overexpression transgenic tobacco lines, OE-2 and OE-7, were selected for exploring the function of the *MaCDSP32* gene (**Figure 4C**). Detached leaves from the transgenic and WT plants were weighed at regular intervals to record the water loss over the natural drying process. The results showed that the cumulative water loss in the OE-2 and

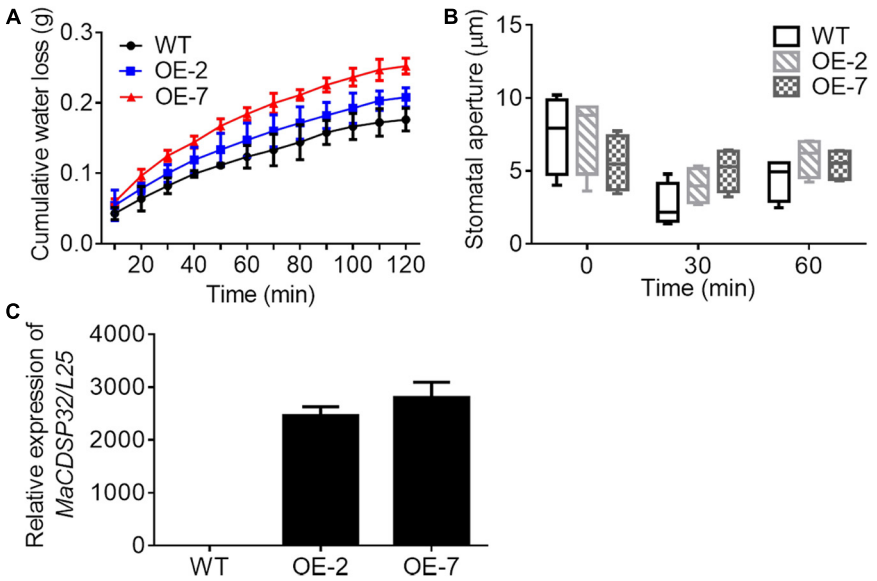

FIGURE 4 | Gene overexpression of *MaCDSP32* increases water loss under dehydration conditions in transgenic tobacco. **(A)** The accumulated water loss of detached leaves under natural desiccation. **(B)** Stomatal aperture of leaves after 0, 30, and 60 min under natural desiccation. **(C)** Detection of *MaCDSP32* gene expression in transgenic tobacco. WT, wild-type tobacco (*N. benthamiana*); OE-2 and OE-7, two transgenic tobacco lines with *MaCDSP32* overexpression. At least three biological replicates were included. No significant difference was observed between the transgenic and WT lines.

OE-7 lines was higher than that in the WT lines during the dehydration process (**Figure 4A**). In particular, the OE-7 line, which exhibited the highest *MaCDSP32* expression, showed the greatest water loss. Stomatal aperture in the OE-2 and OE-7 lines was slightly larger than that in the WT lines after 30 and 60 min of dehydration, although the difference was not significant (**Figure 4B**).

MaCDSP32 Attenuates Abiotic Stress Tolerance but Strengthens Resilience After Rewatering

The OE-2 and OE-7 lines exhibited a wilting phenotype earlier than the WT lines, with wilting appear at 10 d of drought (**Figure 5A**). At this time, a higher abundance of the blue precipitate derived from O_2^- was obtained from the OE-2 and OE-7 lines than from the WT lines (**Figure 5B**), whereas a lower abundance of the brown precipitate derived from H_2O_2 was obtained from the OE-2 and OE-7 lines than from the WT lines (**Figure 5C**). The quantitative ROS assay showed results consistent with the *in vivo* localization, with more O_2^- (**Figure 5F**) and less H_2O_2 (**Figure 5E**) produced in the OE-2 and OE-7 lines than in the WT plants. In addition, the OE-2, OE-7 and WT lines exhibited no significant phenotypic differences after 13 d of treatment with 200 mM NaCl, but more severe ROS production was found in the OE-2 and OE-7 lines than in the WT plants (**Supplementary Figures S1A–E**). Moreover, the MDA contents under both drought and NaCl stress conditions were significantly higher in the OE-2 and OE-7 lines than that in the WT plants (**Figure 5G** and **Supplementary Figure S1F**), which indicated a more severe oxidative damage in the transgenic lines.

The determination of antioxidant enzymes activities showed that the OE-2 and OE-7 lines exhibited higher CAT activity than the WT plants under both drought and NaCl stress conditions (**Figure 6A**). The POD activities in the OE-2 and OE-7 lines were significantly higher than that of WT plants under drought and NaCl treatments (**Figure 6B**). No difference in APX activity was found among the OE-2, OE-7 and WT lines under drought and NaCl conditions (**Figure 6C**). However, the OE-2 and OE-7 lines exhibited significantly lower SOD activity than the WT plants under drought and NaCl conditions (**Figure 6D**). The proline and soluble sugar contents were substantially increased under drought and NaCl conditions in both the WT and transgenic lines, and significantly lower contents were obtained in the OE-2 and OE-7 lines than in the WT plants (**Figures 6E,F**), which indicated that *MaCDSP32* obstructs the accumulation of proline and soluble sugars in response to abiotic stress. Overall, the overexpression of *MaCDSP32* appears to increase sensitivity to drought and NaCl stress in transgenic tobacco.

We found that the OE-2 and OE-7 lines completely recovered after 4 d of rewatering, whereas the WT lines became severely wilted, and their leaves severely yellowed (**Figure 5A**). During drought stress, the proportion of wilted leaves was higher in the OE-2 and OE-7 lines than in the WT lines; however, it decreased markedly in the transgenic lines after rewatering, becoming lower than that in the WT plants (**Figure 5D**). Furthermore, the production of H_2O_2 and O_2^- in the OE-2 and OE-7 lines was markedly decreased after rewatering compared with that under drought, whereas corresponding changes were not observed in the WT plants (**Figures 5E,F**). Decreases in MDA content were obtained with the production of ROS in the OE-2 and OE-7 lines, whereas MDA content increased continuously in WT

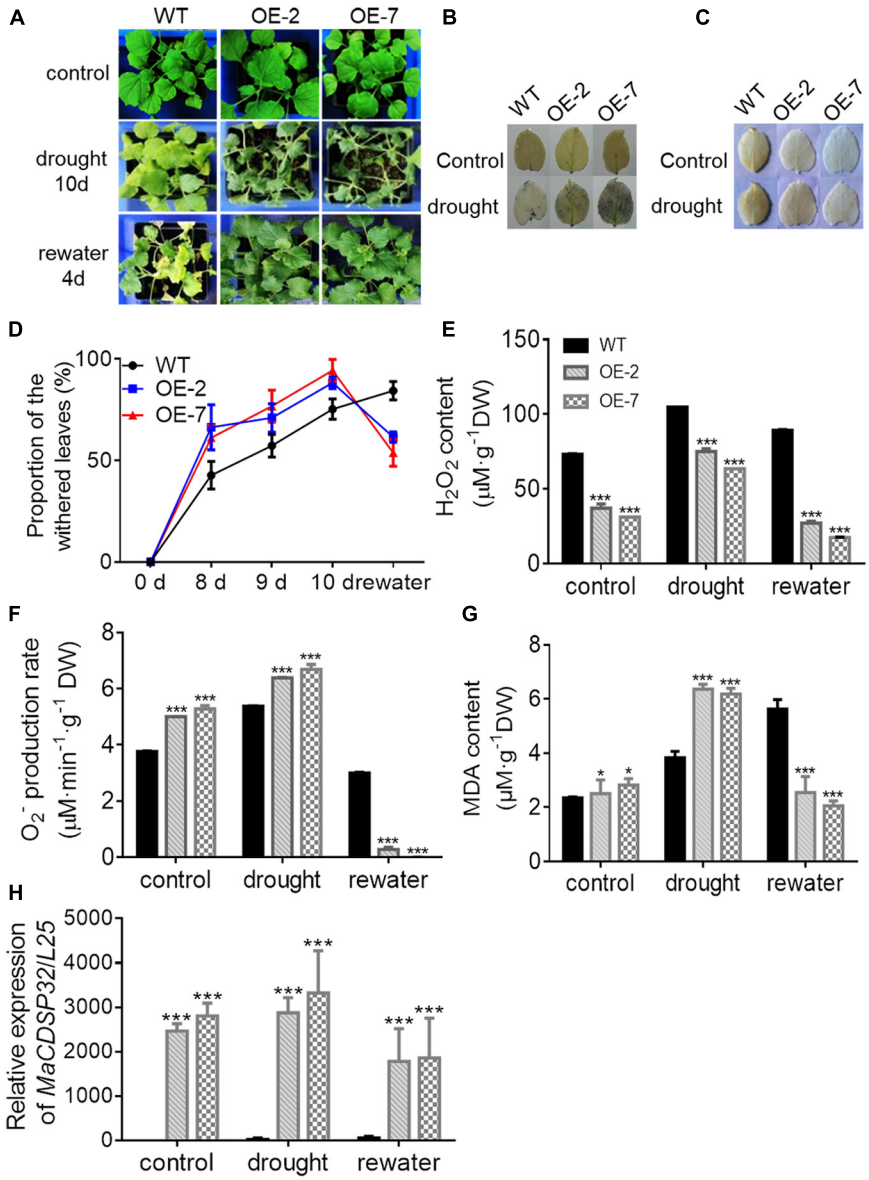

FIGURE 5 | Overexpression of the *MaCDSP32* gene increases drought sensitivity but strengthens recovery during post-drought rewatering in transgenic tobacco. **(A)** Phenotypes of 3-month-old WT plants and two transgenic (OE-2 and OE-7) tobacco lines after 10 days of drought and 4 days of rewatering treatment. **(B,C)** *In vivo* histochemical detection of O_2^- **(B)** and H_2O_2 **(C)** after 10 days of drought. **(D)** Proportions of wilted leaves per plant under the treatment. **(E,F)** Quantification of H_2O_2 **(E)** and O_2^- **(F)** contents in leaves under the treatment. **(G)** Malondialdehyde (MDA) content in leaves under the treatment. **(H)** Gene expression of *MaCDSP32* under treatment. At least three biological replicates were included. Asterisks indicate significant differences between the transgenic and WT lines (*t*-test, $^*P < 0.05$, $^{***}P < 0.001$).

plants (**Figure 5G**). In the WT plants, *MaCDSP32* expression was upregulated under drought and rewatering conditions compared with that under control conditions. In contrast, *MaCDSP32* expression in the OE-2 and OE-7 lines was strongly upregulated under drought conditions and slightly downregulated after rewatering (**Figure 5H**). The physiological parameters that significantly differed between the transgenic lines and WT plants in response to drought treatment were measured again after rewatering. Decreased CAT activity was obtained after 4 d of rewatering, but no significant difference was found among the OE-2, OE-7 and WT lines (**Figure 6A**). Decreased POD activity was also observed after rewatering, although significantly higher recovery of POD activity was observed in the OE-2 and OE-7 lines than in the WT plants (**Figure 6B**). After rewatering, significantly higher SOD activity was observed in the OE-2 and OE-7 lines than in the WT lines (**Figure 6D**). In addition, the proline and soluble sugar contents after rewatering were significantly higher in the transgenic lines than in the WT plants

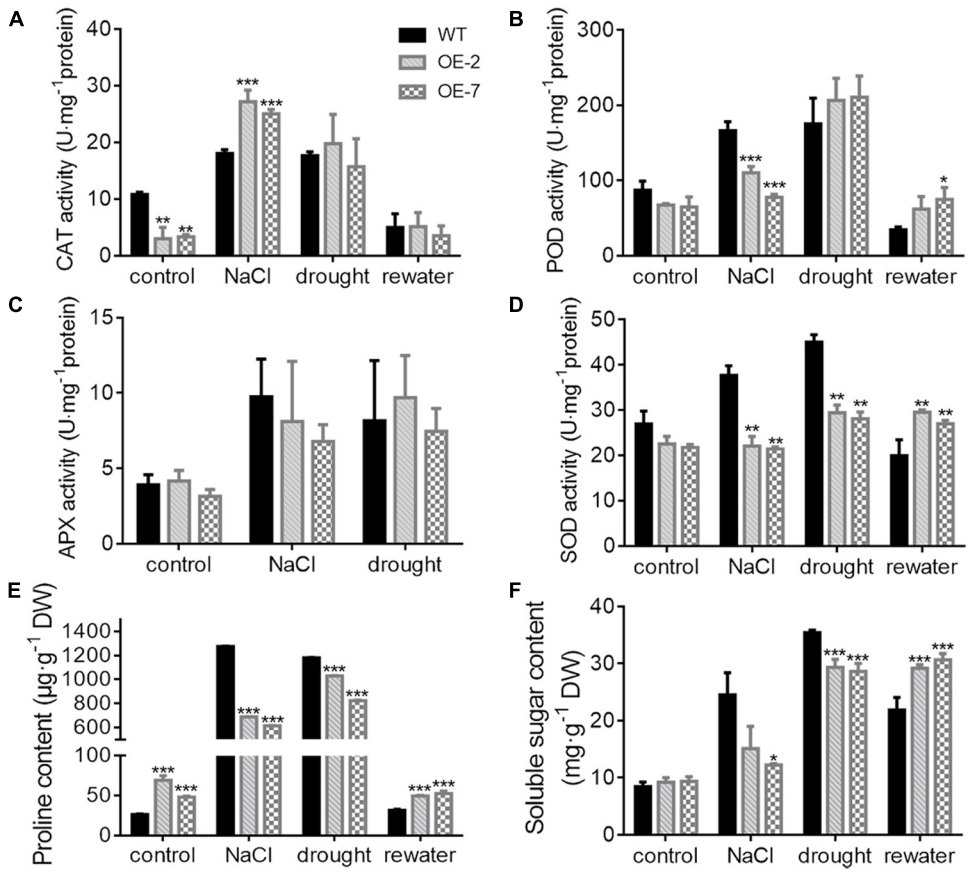

FIGURE 6 | Antioxidant activity and osmotic content in transgenic tobacco under abiotic stress. **(A–D)** Activities of catalase (CAT) **(A)**, peroxidase (POD) **(B)**, ascorbate peroxidase (APX) **(C)**, and superoxide dismutase (SOD) **(D)** enzymes after 13 days of treatment with 200 mM NaCl, 10 days of drought and 4 days of post-drought rewatering. The activity units are expressed as U·mg^{-1} protein. CAT activity was calculated by following the breakdown of H_2O_2. POD activity was calculated by following the guaiacol oxidation. APX activity was calculated by following the ascorbate oxidation. SOD activity was calculated by monitoring the superoxide radical-induced reduction of nitro blue tetrazolium (NBT). One unit of enzyme activity was defined as the amount of enzyme causing 50% inhibition per mg of protein. **(E)** Proline content, **(F)** Soluble sugar content. At least three biological replicates were included. Asterisks indicate significant differences between the transgenic and WT lines (*t*-test, $^*P < 0.05$, $^{**}P < 0.01$, $^{***}P < 0.001$).

(**Figures 6E,F**). These differences suggested that *MaCDSP32* is involved in the bidirectional regulation of the associated physiological pathways in response to both drought stress and drought release in plants.

MaCDSP32 Affects Photosynthetic System Parameters Under Abiotic Stress

Because the expression of the *MaCDSP32* gene had a circadian rhythm and because the gene product was located in chloroplasts, parameters related to the photosynthetic system were detected under various abiotic stress treatments (10 d of drought, 13 d of NaCl and 25 h of MV) to assess the effects on photosynthetic efficiency. Both the two OE and WT lines exhibited severe wilting after 25 h of MV treatment, and no significant difference in phenotype was observed among the lines (**Supplementary Figure S2F**). In general, no significant difference in *Pn* values was found among the OE-2, OE-7 and WT lines under the drought, NaCl or oxidation conditions (**Supplementary Figure S2A**). Under the drought and oxidation conditions, stomatal conductance was lower in the OE-2 and OE-7 lines than in the WT plants (**Supplementary Figure S2B**). The intercellular CO_2 concentration was significantly lower in the OE-2 and OE-7 lines than in WT under NaCl stress (**Supplementary Figure S2C**). Leaf temperature was significantly higher in the OE-2 and OE-7 lines than in the WT plants under the control and drought conditions (**Supplementary Figure S2D**). Interestingly, the results obtained for the transpiration rate were highly consistent with those obtained for the stomatal conductance under the stress treatments, and the OE-2 and OE-7 lines exhibited a significantly lower transpiration rates than the WT plants (**Supplementary Figure S2E**). These results indicated that *MaCDSP32* might affect the regulation of gas parameters under abiotic stress in plants. Additionally, after 13 d of NaCl treatment, the concentrations of C_a, C_b, total chlorophyll and carotenoids were significantly higher in the OE-2 and OE-7 lines than in the WT lines (**Supplementary Figure S3**). These results indicate that *MaCDSP32* might protect photosynthetic pigments under NaCl stress.

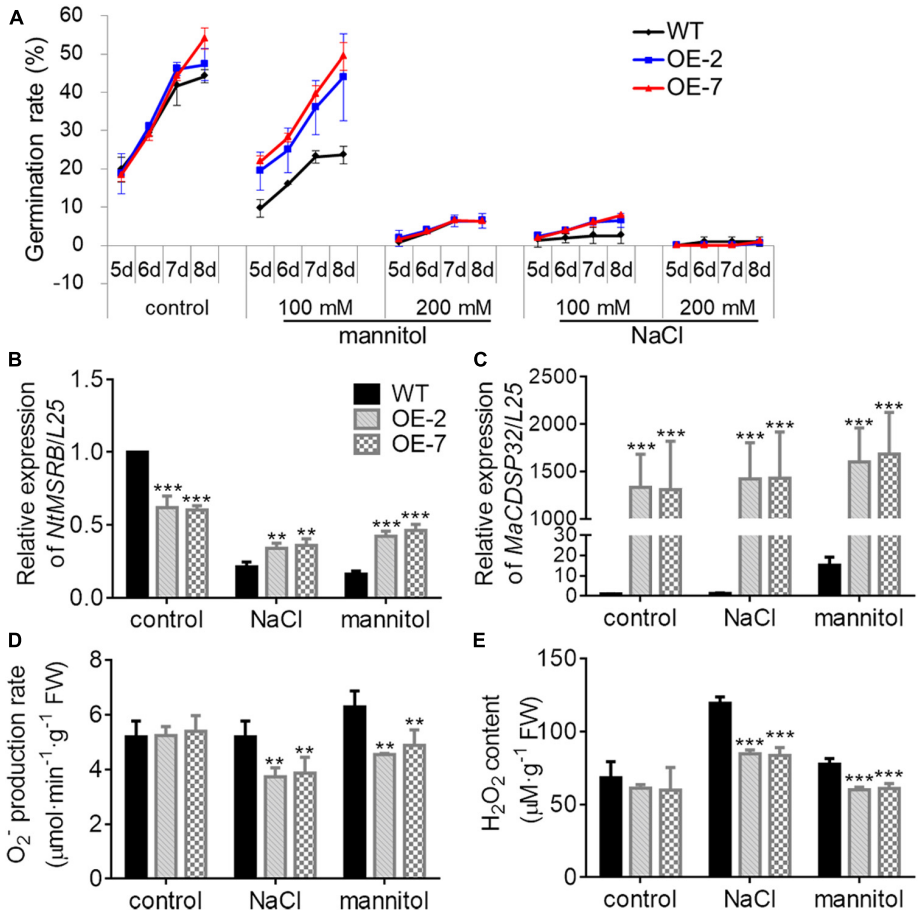

FIGURE 7 | Overexpression of *MaCDSP32* enhances seed germination in transgenic tobacco under osmotic stress. **(A)** Seed germination rates after sowing at 5, 6, 7, and 8 days of treatment with mannitol or NaCl at various concentrations (100 mM and 200 mM). **(B,C)** Relative gene expression of *NtMSRB* **(B)** and *MaCDSP32* **(C)** in germinating seeds after 6 days of treatment with 100 mM NaCl or mannitol. **(D,E)** Production of O_2^- **(D)** and H_2O_2 **(E)** after 6 days of treatment with 100 mM NaCl or mannitol. At least three biological replicates were included. Asterisks indicate significant differences between the transgenic and WT lines (*t*-test, $^{**}P < 0.01$, $^{***}P < 0.001$).

MaCDSP32 Enhances Seed Germination and Seedling Growth Under Osmotic Stress

MSRB protein is considered a well-known target of CDSP32, and is involved in the regulation of seed viability, and the metabolites of methionine can facilitate seed germination (Catusse et al., 2011; Chatelain et al., 2013). Therefore, the seed germination of two transgenic tobacco OE lines were estimated in this study (**Figure 7A**). Under normal conditions, the germination rates of WT, OE-2 and OE-7 seeds at the early stage were not significantly different. However, by day 8, the germination rates of the OE-2 (47.29%) and OE-7 seeds (54.03%) were markedly higher than that of the WT seeds (44.15%). Under exposure to 100 mM mannitol or 100 mM NaCl, the higher germination capacity of OE-2 and OE-7 seeds than of WT seeds was more pronounced. Germination was suppressed in the OE-2, OE-7, and WT seeds during exposure to a high NaCl or mannitol concentration (200 mM). The expression of *NtMSRB* in germinating seeds was downregulated under 100 mM NaCl or mannitol treatment compared with the control expression, but was higher in the OE-2 and OE-7 seeds than in the WT seeds (**Figure 7B**). The expression of *MaCDSP32* in germinating seeds was upregulated under 100 mM NaCl or mannitol treatment compared with the control expression level, and was significantly higher in the seeds of the OE-2 and OE-7 lines those that of the WT lines (**Figure 7C**). H_2O_2 and O_2^- levels were significantly lower in the germinating seeds of the OE-2 and OE-7 lines than in those of the WT lines under 100 mM mannitol or NaCl treatment (**Figures 7D,E**). These results revealed that *MaCDSP32* enhanced the seed germination rate under osmotic stress. Regarding seedling growth no significant difference was found between the two OE and WT seedlings at the initial time point or after 16 d of growth under control condition; however, after 16 days of growth under 200 mM NaCl treatment, the lengths of OE-2 and OE-7 seedlings were significantly greater than the length of WT seedlings (**Figures 8A,B**). Furthermore, after 16 d of NaCl treatment, the expression of *NtMSRB* was upregulated

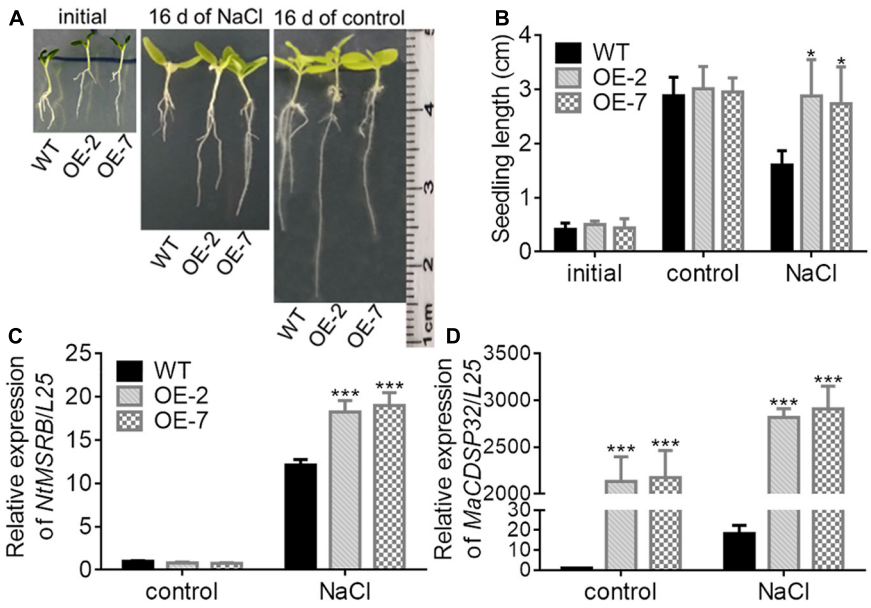

FIGURE 8 | Overexpression of *MaCDSP32* enhances the growth of transgenic tobacco seedlings under NaCl stress. **(A)** Phenotypes of two transgenic lines of tobacco seedlings (OE-2 and OE-7) and of WT tobacco seedlings at transplant (initial), after 16 days of 200 mM NaCl stress and after 16 days under normal conditions. **(B)** Seedlings lengths of treated tobacco. **(C,D)** Relative expression of *NtMSRB* **(C)** and *MaCDSP32* **(D)** in tobacco seedlings after 16 days of 200 mM NaCl stress. Initial: newly transplanted seedlings, which germinated 9 days after sowing under normal conditions. At least three biological replicates were included. Asterisks indicate significant differences between the transgenic and WT lines (*t*-test, $^{*}P < 0.05$, $^{***}P < 0.001$).

relative to control levels in the seedlings of both the OE and WT genotypes and was significantly higher in the OE-2 and OE-7 seedlings than in the WT seedlings (**Figure 8C**). In addition, *MaCDSP32* expression was upregulated under NaCl treatment and was significantly higher in the OE-2 and OE-7 seedlings than in the WT seedlings (**Figure 8D**). These results revealed that *MaCDSP32* potentially strengthens seedling growth under NaCl stress and might participate in regulating the expression of *NtMSRB*.

DISCUSSION

A previous study revealed that CDSP32 protein was synthesized extensively under water deficit conditions (Rey et al., 1998), particularly under severe conditions (Broin et al., 2000). Here, we demonstrate that *MaCDSP32* is a drought-induced gene in mulberry that is mainly expressed in mature leaves rather than young leaves, old leaves, stems or petioles. Furthermore, MaCDSP32 is localized to the chloroplasts, and we deduced that *MaCDSP32* was involved in photosynthesis. In addition, the expression of *MaCDSP32* within a photoperiod was regular, and higher expression was detected during the middle of the day; these findings indicated that *MaCDSP32* is a circadian-regulated gene and closely related to photosynthetic light reactions.

Under dehydration, *MaMAPK* and *MaDREB1* were more strongly downregulated in *Inst* than in WT_{Ma}, which indicated a negative correlation between *MaMAPK*/*MaDREB1* and *MaCDSP32* under water deficit conditions. The MAPK cascade and DREB1 pathway are involved in the transmission of stress signals and can activate the expression of stress tolerance genes (Sakuma et al., 2002; Choudhury et al., 2017). In general, plants respond to a variety of environmental constraints via orchestrated signaling events that coordinate modifications to transcriptional profiles, physiological processes and redox homeostasis. *MaCDSP32* might reduce drought tolerance through stress signal transduction by inhibiting the expression of *MaMAPK* and *MaDREB1*. Additionally, the transgenic *Inst* (*Inst*-1 and *Inst*-2) leaves and OE (OE-2 and OE-7) lines showed higher water loss rate or an earlier wilting phenotype than did the WT plants under drought and NaCl stress. Lower H_2O_2 production and higher O_2^- production were found in transgenic tobacco lines than in the WT plants under both stress conditions, which indicated that *MaCDSP32* is involved in ROS metabolism in response to abiotic stress. *MaCDSP32* is likely to promote the removal of H_2O_2 but not O_2^- under stress for the following reasons: Trxs participate in the sulfide oxidation by reducing H_2O_2 in cells (Broin et al., 2002), and MaCDSP32 is a Trx-like protein that has an active center similar to the functional domain of other Trxs. Moreover, larger amounts of MDA were detected in the transgenic tobacco lines than in the WT lines under stress conditions, which indicated more severe membrane lipid peroxidation damage in the former due to *MaCDSP32* overexpression. Significantly lower SOD activity was found in the transgenic lines than in the WT lines under the stress conditions, suggesting inefficient O_2^- metabolism in the transgenic lines and consistent with the higher O_2^- production observed in these lines. In addition, the concentrations of proline

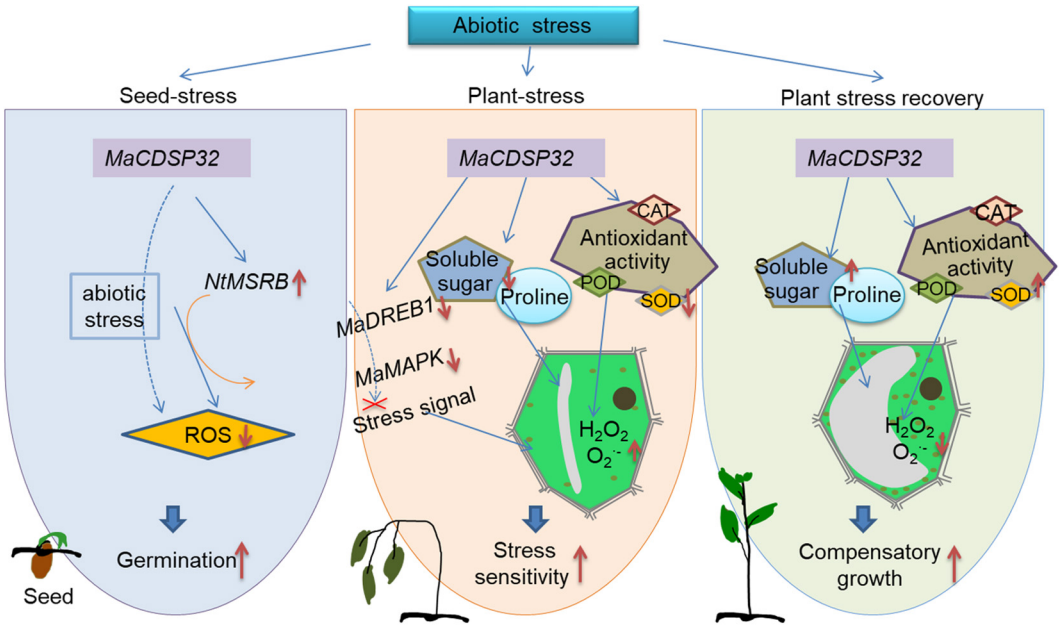

FIGURE 9 | Schematic of the contribution of *MaCDSP32* to plant drought tolerance through the regulation of redox metabolism, signal transduction and osmotic pressure. The solid orange arrows represent findings from the literature; the solid blue arrows represent finding of the present study; the dashed blue arrows represent our speculations based on the findings of the present study; the red bold solid down arrows indicates downregulation; the red bold solid up arrows indicates upregulation; and the red cross mark indicates inhibition.

and soluble sugars were significantly lower in the transgenic lines than in the WT plants under stress conditions. We propose that *MaCDSP32* is likely a negative regulatory factor for the accumulation of these two osmotic substances under abiotic stress. The overexpression of *MaCDSP32* disrupts the redox equilibrium and the regulation of cellular turgor in response to abiotic stress. Notably, the opposite results were obtained after rewatering. Transgenic tobacco lines showed complete post-drought recovery, whereas the WT plants did not. The OE-2 and OE-7 lines exhibited higher SOD activity, increased proline and soluble sugar contents, and substantially lower detectable H_2O_2 and O_2^- contents after rewatering compared with the WT plants. Downregulated *MaCDSP32* expression was obtained after rewatering compared with during drought in both OE lines, but the expression of *MaCDSP32* remained upregulated in the WT plants. This result suggests that the drought response mechanism involves *MaCDSP32*, which might antagonize the mechanism of osmotic pressure regulation in the cell, and that in the ROS scavenging pathway, *MaCDSP32* may be functionally redundant with the enzyme system and antioxidant enzyme system.

We deduced that *MaCDSP32* participates in multiple regulatory mechanisms by inhibiting or promoting antioxidant activity and the accumulation of osmotic-adjustment substances under abiotic stress so that plants can endure changes in the environment. We conjecture that the intricate regulatory network enmeshing *MaCDSP32* is responsible for the rapid wilting of the transgenic lines during severe water deficit and their maintenance of the minimum water consumption, which allows their survival under drought conditions. The SOD enzyme is the main site of the conversion of superfluous O_2^- via its disproportionation in the chloroplast (Chen et al., 2018). Based on the results obtained for SOD activity and O_2^- production demonstrate that *MaCDSP32* plays a key role in the regulation of ROS homeostasis by particularly targeting the SOD enzyme. Under drought conditions, *MaCDSP32* causes a decrease in SOD activity. A previous study showed that most Trxs are involved in the regulation of antioxidant enzyme activity (Arnér and Holmgren, 2000), and each member interacts with a specific antioxidant (Mata-Perez and Spoel, 2018). For instance, Trx-*y* specifically affects the activity of glutathione peroxidase (Navrot et al., 2006). These findings provide strong evidence supporting our conjecture that SOD is a target of *MaCDSP32*. Additionally, previous studies have revealed that CDSP32 is involved in osmoregulation (Pruvot et al., 1996) and that the accumulation of osmotic substances can enhance tolerance to stress by increasing cell turgor in plants (Ashraf and Foolad, 2007; Boriboonkaset et al., 2013). However, the compound that serves as the substrate is unclear. Our results suggest that proline and soluble sugars are two types of potential substrates of *MaCDSP32*.

ROS act as signaling molecules involved in the biological processes of plants under favorable conditions, whereas excess ROS can cause oxidative damage under adverse conditions (Mittler, 2017; Schneider et al., 2018). With a similar bimodality to that of ROS, *MaCDSP32* overexpression attenuates the tolerance of plants during drought stress and promotes post-drought recovery. Other events also arise from the same cause but have completely opposite results. A previous study revealed that P53 protein plays completely different roles in animal cells

at 40°C and 43°C by promoting cell survival and apoptosis, respectively, because these different temperatures lead to different P53 protein stabilization mechanisms and activate different signaling pathways (Gong et al., 2016). Similarly, transgenic lines overexpressing *MaCDSP32* might have altered tolerance thresholds to mild and severe drought stress and show differences post-drought rewatering. Plants exhibit two types of drought tolerance: tolerance during drought and resilience after drought (Tyree et al., 2002). We hypothesize that the drought tolerance of transgenic tobacco involving *MaCDSP32* mainly belongs to the latter type, which is similar to the drought tolerance pattern of resurrection plants.

The expression of CDSP32 is regulated by posttranscriptional events, which are closely related to the plant developmental stage and environmental conditions (Broin et al., 2003). In addition, CDSP32 expression is mainly induced under severe stress conditions; a high abundance of CDSP32 in transgenic overexpression plants under mild stress conditions could disturb the plastidic redox state and might divert the reducing power (or electron transport direction) necessary for other protection systems (Broin et al., 2002). Therefore, we hypothesize that although the activities of antioxidative enzymes in *MaCDSP32*-overexpressing transgenic tobacco plants were quite similar under the control and rewatering conditions, the feedback responses in the plants differed among the different physiological and environmental conditions. The reducing power provided by the products of *MaCDSP32* expression was diverted and reallocated, which led to a different distribution of the *MaCDSP32*-related upstream and downstream processes involved in ROS homeostasis regulation and thereby resulted in differences in superoxide production. Furthermore, the specific regulatory mechanism induced by severe drought stress in transgenic tobacco plants is one of the possible reasons for the reduced production of O_2^-. This process might involve a complex mechanism, and further exploration and verification are needed.

Under NaCl stress, transgenic tobacco lines maintain higher chlorophyll and carotenoid contents than the WT, which suggested that *MaCDSP32* plays a positive role in protecting chloroplast photosynthetic pigments against NaCl stress. This result indicated that *MaCDSP32* might affect the activity of chlorophyll-related enzymes under NaCl stress. Although NaCl treatment can increase the activity of chlorophyllase, the synthesis and degradation of chlorophyll are mainly affected by the activity of chlorophyll enzymes (Chen et al., 2018). This increased chlorophyllase activity might induce CDSP32 activity, which functions to protect photosynthetic system elements (Broin et al., 2002). Moreover, *MaCDSP32* enhanced seed germination and seedling growth in transgenic tobacco under NaCl and mannitol stress. Because MSRB participates involved in the regulation of seed vitality by reducing oxidized methionine (Laugier et al., 2010; Chatelain et al., 2013), we suggest that *MaCDSP32* and its target *NtMSRB* work together to reduce the production of H_2O_2 and O_2^- and facilitate seed germination. We propose that the *MaCDSP32*/*NtMSRB* reduction system plays an important role in the effective scavenging of ROS produced under osmotic stress.

CONCLUSION

The present study provides novel insights into the functions of *MaCDSP32* in plants. A schematic that incorporates the abiotic stress response mechanism mediated by *MaCDSP32* is shown in **Figure 9**. *MaCDSP32* overexpression promotes the gene expression of *NtMSRB*, which enhances seed germination under stress conditions. *MaCDSP32* influences ROS production by regulating the expression of *MaDREB1* and *MaMAPK*, the accumulation of soluble sugars and proline and the activities of antioxidant enzymes (especially POD and SOD) to affect the resistance of transgenic plants.

Due to the rapid development of human civilization, plants inevitably face increasingly serious environmental constraints. Plants with stronger vitality and adaptability are urgently needed for future plant and crop breeding. The abundant resources available in nature, such as the resurrection plant *Selaginella tamariscina*, might lead to enlightenment. Under water deficit conditions, these desiccation-tolerant species maintain significantly higher levels of soluble sugars, amino acids and other metabolites, which help the detoxification of excess ROS and contribute to desiccation tolerance (Xu et al., 2018). Our study suggests that *MaCDSP32* positively contributes to the post-drought recovery strategy and repair mechanisms of plants, and these effects give plants the ability to survive water stress and enhance the plant survival rate after stress relief.

DATA AVAILABILITY STATEMENT

The raw data supporting the conclusions of this article will be made available by the authors, without undue reservation, to any qualified researcher.

AUTHOR CONTRIBUTIONS

HS and FJ conceived the original research plans, performed most of the experiments, analyzed the data, and wrote the manuscript. WZ, HL, CS, and YQ provided much assistance in the sampling and data analysis stage. All the authors reviewed and interpreted the data, edited the manuscript, reviewed the results, and approved the final version of the manuscript.

FUNDING

This project was supported by the Fundamental Research Funds for the Central Universities of Northwest A&F University (2452019041), the National Special Research Fund for Non-Profit Sector (Agriculture) (Grant No. 201303057), the National Key Research and Development Project of China (No. 2019YFD1000600), and the China Agriculture Research System (No. CARS-18).

ACKNOWLEDGMENTS

We thank the Grassland Science Lab for sharing the laboratory equipment needed for these experiments.

SUPPLEMENTARY MATERIAL

The Supplementary Material for this article can be found online at: https://www.frontiersin.org/articles/10.3389/fpls.2020.00419/full#supplementary-material

FIGURE S1 | Production of reactive oxygen species (ROS) in tobacco under NaCl stress. **(A)** Phenotypes of 3-month-old WT and transgenic (OE-2 and OE-7) tobacco lines under 13 days of treatment with 200 mM NaCl. **(B,C)** *In vivo* histochemical detection of O_2^- **(B)** and H_2O_2 **(C)** in plants under treatment. **(D,E)** Quantification of H_2O_2 **(D)**, O_2^- **(E)**, and **(F)** MDA contents. At least three biological replicates were included. Asterisks indicate significant differences between the transgenic and WT lines (*t*-test, $*P < 0.05$, $***P < 0.001$).

FIGURE S2 | Gas exchange parameters in transgenic tobacco under abiotic stress. **(A)** Net photosynthetic rate (*Pn*). **(B)** Stomatal conductance. **(C)** Intercellular CO_2 concentration. **(D)** Leaf temperature. **(E)** Transpiration rate. **(F)** Phenotypes of 3-month-old WT and transgenic (OE-2 and OE-7) tobacco lines treated with 10 μM methyl viologen (MV) for 25 h. The following treatments were used: 10 days of soil drought, 13 days of treatment with 200 mM NaCl and 25 h of treatment with 10 μM MV. At least three biological replicates were included. Asterisks indicate significant differences between the transgenic and WT lines (*t*-test, $*P < 0.05$, $**P < 0.01$ and $***P < 0.001$).

FIGURE S3 | Overexpression of *MaCDSP32* helps maintain chloroplast pigment levels in transgenic tobacco under NaCl stress. **(A)** Total chlorophyll content. **(B)** Chlorophyll *a* content. **(C)** Chlorophyll *b* content. **(D)** Carotenoids content. Three-month-old WT and transgenic (OE-2 and OE-7) tobacco lines were treated with 200 mM NaCl for 13 days. At least three biological replicates were included. Asterisks indicate significant differences between the transgenic and WT lines (*t*-test, $**P < 0.01$).

REFERENCES

Arnér, E., and Holmgren, A. (2000). Physiological functions of thioredoxin and thioredoxin reductase. *FEBS J.* 267, 6102–6109. doi: 10.1046/j.1432-1327.2000.01701.x

Ashraf, M., and Foolad, M. R. (2007). Roles of glycine betaine and proline in improving plant abiotic stress resistance. *Environ. Exp. Bot.* 59, 206–216. doi: 10.1016/j.envexpbot.2005.12.006

Bao, F., Du, D., An, Y., Yang, W., Wang, J., Cheng, T., et al. (2017). Overexpression of *Prunus mume* dehydrin genes in tobacco enhances tolerance to cold and drought. *Front. Plant Sci.* 8:151. doi: 10.3389/fpls.2017.00151

Baxter, A., Mittler, R., and Suzuki, N. (2014). ROS as key players in plant stress signalling. *J. Exp. Bot.* 65, 1229–1240. doi: 10.1093/jxb/ert375

Boriboonkaset, T., Theerawitaya, C., Yamada, N., Pichakum, A., Supaibulwatana, K., Suriyan , M., et al. (2013). Regulation of some carbohydrate metabolism-related genes, starch and soluble sugar contents, photosynthetic activities and yield attributes of two contrasting rice genotypes subjected to salt stress. *Protoplasma* 250, 1157–1167. doi: 10.1007/s00709-013-0496-9

Broin, M., Besse, I., and Rey, P. (2003). Evidence for post-translational control in the expression of a gene encoding a plastidic thioredoxin during leaf development in *Solanum tuberosum* plants. *Plant Physiol. Biochem.* 41, 303–308. doi: 10.1016/s0981-9428(03)00023-8

Broin, M., Cuine, S., Eymery, F., and Rey, P. (2002). The plastidic 2-cysteine peroxiredoxin is a target for a thioredoxin involved in the protection of the photosynthetic apparatus against oxidative damage. *Plant Cell* 14, 1417–1432. doi: 10.1105/tpc.001644

Broin, M., Cuine, S., Peltier, G., and Rey, P. (2000). Involvement of CDSP 32, a drought-induced thioredoxin, in the response to oxidative stress in potato plants. *FEBS Lett.* 467, 245–248. doi: 10.1016/s0014-5793(00)01165-0

Buchanan, B. B., Gruissem, W., and Jones, R. L. (eds) (2000). Biochemistry & molecular biology of plants. *J. Plant Growth Regul.* 35, 105–106.

Butler, T., Dick, C., Carlson, M. L., and Whittall, J. B. (2014). Transcriptome analysis of a petal anthocyanin polymorphism in the arctic mustard, *Parrya nudicaulis*. *PLoS One* 9:e101338. doi: 10.1371/journal.pone.0101338

Catusse, J., Meinhard, J., Job, C., Strub, J. M., Fischer, U., Pestsova, E., et al. (2011). Proteomics reveals potential biomarkers of seed vigor in sugarbeet. *Proteomics* 11, 1569–1580. doi: 10.1002/pmic.201000586

Chatelain, E., Satour, P., Laugier, E., Ly Vu, B., Payet, N., Rey, P., et al. (2013). Evidence for participation of the methionine sulfoxide reductase repair system in plant seed longevity. *Proc. Natl. Acad. Sci. U.S.A.* 110, 3633–3638. doi: 10.1073/pnas.1220589110

Chen, H., Feng, H., Zhang, X., Zhang, C., Wang, T., and Dong, J. (2019). An *Arabidopsis* E3 ligase *HUB2* increases histone H2B monoubiquitination and enhances drought tolerance in transgenic cotton. *Plant Biotechnol. J.* 17, 556–568. doi: 10.1111/pbi.12998

Chen, L., Hou, Y., Hu, W., Qiu, X., Lu, H., Wei, J., et al. (2018). The molecular chaperon AKR2A increases the mulberry chilling-tolerant capacity by maintaining SOD activity and unsaturated fatty acids composition. *Sci. Rep.* 8:12120.

Choudhury, F. K., Rivero, R. M., Blumwald, E., and Mittler, R. (2017). Reactive oxygen species, abiotic stress and stress combination. *Plant J.* 90, 856–867. doi: 10.1111/tpj.13299

Cui, D., Yin, Y., Wang, J., Wang, Z., Ding, H., Ma, R., et al. (2019). Research on the physio-biochemical mechanism of non-thermal plasma-regulated seed germination and early seedling development in *Arabidopsis*. *Front. Plant Sci.* 10:1322. doi: 10.3389/fpls.2019.01322

Dietz, K.-J. (2007). The dual function of plant peroxiredoxins in antioxidant defence and redox signaling. *Subcell. Biochem.* 44, 267–294. doi: 10.1007/978-1-4020-6051-9_13

Dinakar, C., and Bartels, D. (2013). Desiccation tolerance in resurrection plants: new insights from transcriptome, proteome and metabolome analysis. *Front. Plant Sci.* 4:482. doi: 10.3389/fpls.2013.00482

Duan, M., Feng, H. L., Wang, L. Y., Li, D., and Meng, Q. W. (2012). Overexpression of thylakoidal ascorbate peroxidase shows enhanced resistance to chilling stress in tomato. *J. Plant Physiol.* 169, 867–877. doi: 10.1016/j.jplph.2012.02.012

Foyer, C. H. (2018). Reactive oxygen species, oxidative signaling and the regulation of photosynthesis. *Environ. Exp. Bot.* 154, 134–142. doi: 10.1016/j.envexpbot.2018.05.003

Foyer, C. H., and Shigeoka, S. (2011). Understanding oxidative stress and antioxidant functions to enhance photosynthesis. *Plant Physiol.* 155, 93–100. doi: 10.1104/pp.110.166181

Gong, L., Pan, X., Chen, H., Rao, L., Zeng, Y., Hang, H., et al. (2016). p53 isoform Δ133p53 promotes efficiency of induced pluripotent stem cells and ensures genomic integrity during reprogramming. *Sci. Rep.* 6:37281.

Grzeszczuk, M., Salachna, P., and Meller, E. (2018). Changes in photosynthetic pigments, total phenolic content, and antioxidant activity of *Salvia coccinea* Buc'hoz Ex Etl. induced by exogenous salicylic acid and soil salinity. *Molecules* 23:1296. doi: 10.3390/molecules23061296

He, N., Zhang, C., Qi, X., Zhao, S., Tao, Y., Yang, G., et al. (2013). Draft genome sequence of the mulberry tree *Morus notabilis*. *Nat. Commun.* 4:2445.

Horsch, R., Fry, J., Hoffmann, N., Eichholtz, D., Rogers, S., and Fraley, R. (1985). A simple and general method for transferring genes into plants. *Science* 4691, 1229–1231. doi: 10.1126/science.227.4691.1229

La Mantia, J., Unda, F., Douglas, C. J., Mansfield, S. D., and Hamelin, R. (2018). Overexpression of At*GolS3* and Cs*RFS* in poplar enhances ROS tolerance and represses defense response to leaf rust disease. *Tree Physiol.* 38, 457–470. doi: 10.1093/treephys/tpx100

Laugier, E., Tarrago, L., Vieira Dos Santos, C., Eymery, F., Havaux, M., and Rey, P. (2010). *Arabidopsis thaliana* plastidial methionine sulfoxide reductases B, MSRBs, account for most leaf peptide MSR activity and are essential for growth under environmental constraints through a role in the preservation of

photosystem antennae. *Plant J.* 61, 271–282. doi: 10.1111/j.1365-313x.2009.04053.x

Li, R., Liu, L., Dominic, K., Wang, T., Fan, T., Hu, F., et al. (2018). Mulberry (*Morus alba*) *MmSK* gene enhances tolerance to drought stress in transgenic mulberry. *Plant Physiol. Biochem.* 132, 603–611. doi: 10.1016/j.plaphy.2018.10.007

Li, Y. J., Hai, R. L., Du, X. H., Jiang, X. N., and Lu, H. (2009). Over-expression of a Populus peroxisomal ascorbate peroxidase (*PpAPX*) gene in tobacco plants enhances stress tolerance. *Plant Breeding* 128, 404–410. doi: 10.1111/j.1439-0523.2008.01593.x

Liu, L. H., Fan, T. F., Shi, D. X., Li, C. J., He, M. J., Chen, Y. Y., et al. (2018). Coding-sequence identification and transcriptional profiling of nine *AMT*s and four *NRT*s from tobacco revealed their differential regulation by developmental stages, nitrogen nutrition, and photoperiod. *Front. Plant Sci.* 9:210. doi: 10.3389/fpls.2018.00210

Mata-Perez, C., and Spoel, S. H. (2018). Thioredoxin-mediated redox signalling in plant immunity. *Plant Sci.* 279, 27–33. doi: 10.1016/j.plantsci.2018.05.001

Matsuo, K., Fukuzawa, N., and Matsumura, T. (2016). A simple agroinfiltration method for transient gene expression in plant leaf discs. *J. Biosci. Bioeng.* 122, 351–356. doi: 10.1016/j.jbiosc.2016.02.001

Mittler, R. (2017). ROS are good. *Trends Plant Sci.* 22, 11–19. doi: 10.1016/j.tplants.2016.08.002

Montrichard, F., Alkhalfioui, F., Yano, H., Vensel, W., Hurkman, W., and Buchanan, B. (2009). Thioredoxin targets in plants: The first 30 years. *J. Proteom.* 72, 452–474. doi: 10.1016/j.jprot.2008.12.002

Navrot, N., Collin, V. R., Gualberto, J., Gelhaye, E., Hirasawa, M., Rey, P., et al. (2006). Plant glutathion: still mysterious reducing systems. *Plant Physiol.* 142, 1364–1379.

Pruvot, G., Massimino, J., Peitier, G., and Rey, P. (1996). Effects of low temperature, high salinity and exogenous ABA on the synthesis of two chloroplastic drought-induced proteins in *Solanum tuberosum*. *Physiol. Plant.* 97, 123–131. doi: 10.1034/j.1399-3054.1996.970119.x

Rahim, M. A., Resentini, F., Dalla Vecchia, F., and Trainotti, L. (2019). Effects on plant growth and reproduction of a peach R2R3-MYB transcription factor overexpressed in tobacco. *Front. Plant Sci.* 10:1143. doi: 10.3389/fpls.2019.01143

Rao, Y., Yang, Y., Xu, J., Li, X., Leng, Y., Dai, L., et al. (2015). Early senescence1 encodes a SCAR-LIKE PROTEIN2 that affects water loss in rice. *Plant Physiol.* 169, 1225–1239. doi: 10.1104/pp.15.00991

Rey, P., Cuine, S., Eymery, F., Garin, J., Court, M., Jacquot, J. P., et al. (2005). Analysis of the proteins targeted by CDSP32, a plastidic thioredoxin participating in oxidative stress responses. *Plant J.* 41, 31–42. doi: 10.1111/j.1365-313x.2004.02271.x

Rey, P., Pruvot, G., Becuwe, N., Eymery, F., Rumeau, D., and Peltier, G. (1998). A novel thioredoxin-like protein located in the chloroplast is induced by water deficit in *Solanum tuberosum* L. plants. *Plant J.* 13, 97–107. doi: 10.1046/j.1365-313x.1998.00015.x

Rey, P., Sanz-Barrio, R., Innocenti, G., Ksas, B., Courteille, A., Rumeau, D., et al. (2013). Overexpression of plastidial thioredoxins f and m differentially alters photosynthetic activity and response to oxidative stress in tobacco plants. *Front. Plant Sci.* 4:390. doi: 10.3389/fpls.2013.00390

Sakuma, Y., Liu, Q., Dubouzet, J. G., Abe, H., Shinozaki, K., and Yamaguchi-Shinozaki, K. (2002). DNA-binding specificity of the ERF/AP2 domain of *Arabidopsis* DREBs, transcription factors involved in dehydration- and cold-inducible gene expression. *Biochem. Biophys. Res. Commun.* 290, 998–1009. doi: 10.1006/bbrc.2001.6299

Schmittgen, T. D., and Livak, K. J. (2008). Analyzing real-time PCR data by the comparative CT method. *Nat. Protoc.* 3, 1101–1108. doi: 10.1038/nprot.2008.73

Schneider, J. R., Caverzan, A., and Chavarria, G. (2018). Water deficit stress, ROS involvement, and plant performance. *Arch. Agron. Soil Sci.* 65, 1160–1181. doi: 10.1080/03650340.2018.1556789

Sugiura, K., Yokochi, Y., Fu, N., Fukaya, Y., Yoshida, K., Mihara, S., et al. (2019). The thioredoxin (Trx) redox state sensor protein can visualize Trx activities in the light/dark response in chloroplasts. *J. Biol. Chem.* 294, 12091–12098. doi: 10.1074/jbc.ra119.007616

Tyree, M. T., Vargas, G., Engelbrecht, B. M., and Kursar, T. A. (2002). Drought until death do us part: a case study of the desiccation-tolerance of a tropical moist forest seedling-tree, *Licania platypus* (Hemsl.) Fritsch. *J. Exp. Bot.* 53, 2239–2247. doi: 10.1093/jxb/erf078

Vieira Dos Santos, C., and Rey, P. (2006). Plant thioredoxins are key actors in the oxidative stress response. *Trends Plant Sci.* 11, 329–334. doi: 10.1016/j.tplants.2006.05.005

Vieira Dos Santos, C., Laugier, E., Tarrago, L., Massot, V., Issakidis-Bourguet, E., Rouhier, N., et al. (2007). Specificity of thioredoxins and glutaredoxins as electron donors to two distinct classes of Arabidopsis plastidial methionine sulfoxide reductases B. *FEBS Lett.* 581, 4371–4376. doi: 10.1016/j.febslet.2007.07.081

Wang, D., Zhao, L., Jiang, J., Liu, J., Wang, D., Yu, X., et al. (2018). Cloning, expression, and functional analysis of lysine decarboxylase in mulberry (*Morus alba* L.). *Protein Expr. Purif.* 151, 30–37. doi: 10.1016/j.pep.2018.06.004

Wang, R., Chen, S., Zhou, X., Shen, X., Deng, L., Zhu, H., et al. (2008). Ionic homeostasis and reactive oxygen species control in leaves and xylem sap of two poplars subjected to NaCl stress. *Tree Physiol.* 28, 947–957. doi: 10.1093/treephys/28.6.947

Wang, X., Zeng, J., Li, Y., Rong, X., Sun, J., Sun, T., et al. (2015). Expression of *TaWRKY44*, a wheat *WRKY* gene, in transgenic tobacco confers multiple abiotic stress tolerances. *Front. Plant Sci.* 6:615. doi: 10.3389/fpls.2015.00615

Xu, Z., Xin, T., Bartels, D., Li, Y., Gu, W., Yao, H., et al. (2018). Genome analysis of the ancient tracheophyte *selaginella tamariscina* reveals evolutionary features relevant to the acquisition of desiccation tolerance. *Mol. Plant* 11, 983–994. doi: 10.1016/j.molp.2018.05.003

Yadav, N., Shukla, P., Jha, A., Agarwal, P., and Jha, B. (2012). The *SbSOS1* gene from the extreme halophyte *Salicornia brachiata* enhances Na+ loading in xylem and confers salt tolerance in transgenic tobacco. *BMC Plant Biol.* 12:188. doi: 10.1186/1471-2229-12-188

Zeng, Q., Chen, H., Zhang, C., Han, M., Li, T., Qi, X., et al. (2015). Definition of eight mulberry species in the genus morus by internal transcribed spacer-based phylogeny. *PLoS One* 10:e0135411. doi: 10.1371/journal.pone.0135411

Zhang, F., Xiao, X., Yan, G., Hu, J., Cheng, X., Li, L., et al. (2018). Association mapping of cadmium-tolerant QTLs in *Brassica napus* L. and insight into their contributions to phytoremediation. *Environ. Exp. Bot.* 155, 420–428. doi: 10.1016/j.envexpbot.2018.07.014

Zhu, J. K. (2016). Abiotic stress signaling and responses in plants. *Cell* 167, 313–324. doi: 10.1016/j.cell.2016.08.029

Conflict of Interest: The authors declare that the research was conducted in the absence of any commercial or financial relationships that could be construed as a potential conflict of interest.

frontiers in Plant Science

ORIGINAL RESEARCH
published: 19 May 2020
doi: 10.3389/fpls.2020.00596

Reactive Oxygen Species, Antioxidant Agents, and DNA Damage in Developing Maize Mitochondria and Plastids

*Diwaker Tripathi, Andy Nam, Delene J. Oldenburg and Arnold J. Bendich**

Department of Biology, University of Washington, Seattle, WA, United States

Maize shoot development progresses from non-pigmented meristematic cells at the base of the leaf to expanded and non-dividing green cells of the leaf blade. This transition is accompanied by the conversion of promitochondria and proplastids to their mature forms and massive fragmentation of both mitochondrial DNA (mtDNA) and plastid DNA (ptDNA), collectively termed organellar DNA (orgDNA). We measured developmental changes in reactive oxygen species (ROS), which at high concentrations can lead to oxidative stress and DNA damage, as well as antioxidant agents and oxidative damage in orgDNA. Our plants were grown under normal, non-stressful conditions. Nonetheless, we found more oxidative damage in orgDNA from leaf than stalk tissues and higher levels of hydrogen peroxide, superoxide, and superoxide dismutase in leaf than stalk tissues and in light-grown compared to dark-grown leaves. In both mitochondria and plastids, activities of the antioxidant enzyme peroxidase were higher in stalk than in leaves and in dark-grown than light-grown leaves. In protoplasts, the amount of the small-molecule antioxidants, glutathione and ascorbic acid, and catalase activity were also higher in the stalk than in leaf tissue. The data suggest that the degree of oxidative stress in the organelles is lower in stalk than leaf and lower in dark than light growth conditions. We speculate that the damaged/fragmented orgDNA in leaves (but not the basal meristem) results from ROS signaling to the nucleus to stop delivering DNA repair proteins to mature organelles producing large amounts of ROS.

Keywords: maize, ROS, plastids, mitochondria, protoplasts, DNA damage

OPEN ACCESS

Edited by:
Francisco J. Corpas, Consejo Superior de Investigaciones Científicas (CSIC), Spain

Reviewed by:
Carlos Guillermo Bartoli, Instituto de Fisiología Vegetal (INFIVE), Argentina
Daniel Gallie, University of California, Riverside, United States

****Correspondence:***
Arnold J. Bendich
bendich@uw.edu

Specialty section:
This article was submitted to Plant Abiotic Stress, a section of the journal Frontiers in Plant Science

Received: *28 November 2019*
Accepted: *20 April 2020*
Published: *19 May 2020*

Citation:
Tripathi D, Nam A, Oldenburg DJ and Bendich AJ (2020) Reactive Oxygen Species, Antioxidant Agents, and DNA Damage in Developing Maize Mitochondria and Plastids. Front. Plant Sci. 11:596. doi: 10.3389/fpls.2020.00596

INTRODUCTION

Reactive oxygen species (ROS) can have both detrimental and beneficial effects on plants. At high concentrations, ROS can lead to oxidative stress by causing damage to various biomolecules. ROS are produced as unavoidable byproducts of electron transport reactions in both respiration and photosynthesis, and damage-defense measures are employed to ameliorate oxidative stress. But ROS also function in modifying the cell wall during development, as signaling molecules to maintain cellular and organismal homeostasis, and to regulate plant development (Mittler, 2017; Smirnoff and Arnaud, 2019). For example, ROS can affect the distribution of chloroplasts within a cell and the ability to resist pathogen attack (Park et al., 2018; Ding et al., 2019), as well as the fate of stem cells (Zeng et al., 2017; Yang et al., 2018).

Reactive oxygen species can be produced in chloroplasts, mitochondria, and several other plant cell compartments (Janku et al., 2019). Since ROS are produced during the partial reduction of molecular oxygen, one way to avoid the potential damaging effects of ROS is to maintain certain cells under hypoxic conditions. In mammals, a hypoxic niche is maintained during early development in cells that will develop into gametes (embryonic stem cells) and later in the stem cells that provide the differentiated cells of adult tissues (Mohyeldin et al., 2010). Similarly, the non-green cells of the shoot apical meristem in Arabidopsis are also maintained in a hypoxic niche for 5 weeks during the development of the inflorescence meristem of the adult plant (Weits et al., 2019). Thus, in both animals and plants, the DNA that will be transmitted to the next generation is protected from potential oxidative stress associated with respiration and photosynthesis (Mohyeldin et al., 2010; Considine et al., 2017).

Although the nucleus is not a major site of ROS production, ROS signaling molecules generated elsewhere in the cell can be moved to the nucleus to modulate expression of nuclear genes (Noctor and Foyer, 2016). The highest concentration of ROS should be found in the parts of the cell that produce most of the ROS, such as chloroplasts and mitochondria, but most research on DNA damage has focused on nuclear DNA. The most severe type of DNA damage is a double-strand break, and both homologous recombination (HR) and non-homologous end-joining (NHEJ) are used to repair this break in the nuclear DNA of yeasts and mammals (Runge and Li, 2018; Scully et al., 2019). Both HR and NHEJ are also found in the plant nucleus (Spampinato, 2017), but thus far only HR has been identified in either mitochondria or plastids of plants (Boesch et al., 2011; Christensen, 2018). Other DNA damage repair systems found in the nucleus may also be found in mitochondria and plastids. For example, Arabidopsis organellar DNA (orgDNA) polymerases can perform microhomology-mediated end-joining (MMEJ) *in vitro* (Garcia-Medel et al., 2019), proteins associated with base excision repair (BER) have been found in Arabidopsis plastids and mitochondria (Gutman and Niyogi, 2009; Boesch et al., 2011), and the BER system is the major pathway for repair of oxidatively damaged DNA (Markkanen, 2017).

As maize plants develop from the meristem at the base of the shoot (the basal meristem) to the leaves, the size of orgDNA [referring to both plastid DNA (ptDNA) and mitochondrial DNA (mtDNA)] decreases from molecules equal to or greater than the size of the genome (570 kb for mtDNA and 140 kb for ptDNA) in the meristem to much smaller fragments in the leaf (Oldenburg and Bendich, 2004, 2015; Kumar et al., 2014). In dark-grown plants, high-integrity ptDNA (large complex-branched molecules) is retained in the leaves, and a rapid decline in ptDNA copy number is observed after transfer from dark to light growth conditions (Zheng et al., 2011). We interpreted this decline in molecular integrity to ROS-induced DNA damage that was not repaired, followed by degradation of the unrepaired orgDNA molecules (Oldenburg and Bendich, 2015).

Through the decades, research has focused on the damage caused by ROS. More recently, however, the positive aspects of ROS signaling have been appreciated when oxidative stress is increased by environmental change (extreme temperature, intense light, high salinity, water or nutrient deprivation) or deleterious mutations (Halliwell, 2006; Noctor and Foyer, 2016; Brunkard and Burch-Smith, 2018; Foyer, 2018; Bokhari and Sharma, 2019; Zandalinas et al., 2019). Our approach has been to monitor changes in orgDNA during the normal development of the wild-type plant, without the imposition of genotoxic agents or extreme environments. In particular, we wish to investigate potential ROS signaling that leads to the demise of orgDNA in differentiated somatic cells but not in germline cells.

Here, we report on the types and levels of ROS in mitochondria, plastids, and whole cells during maize seedling development in light and dark growth conditions so as to assess the correlation between ROS and orgDNA degradation. We also report on antioxidant agents and oxidative damage to orgDNA as assessed by levels of 8-hydroxydeoxyguanasine (8-OHdG) and 8-oxoguanine (8-oxoG).

MATERIALS AND METHODS

Plant Tissue

Zea mays (inbred line B73) seeds were imbibed overnight and sown in Sunshine soil Mix #4 and vermiculite (1:1 ratio). The seedlings were grown for 12 days with a 16 h light/8 h dark photoperiod (light-grown) or in continuous dark for 12 days (dark-grown). The light intensity was ∼500 μmol s^{-1} m^{-2}. Seedlings were washed with 0.5% sarkosyl for ∼3 min and then rinsed with distilled water. For each assay, tissue was harvested from 20 to 25 plants as follows: Stalk lower (base of stalk 5 mm above the node); Stalk upper (top of stalk 5 mm below the ligule of the first leaf), leaf blades (L1 or L1 + L2 + L3). Stalk tissue was composed of several concentric rings of leaves, the outermost being the first leaf sheath. L1 was the fully expanded blade, whereas L2 and L3 were still developing. The coleoptile was removed before the extraction of plastids, mitochondria, and protoplasts.

Isolation of Plastids and Mitochondria

Plastids and mitochondria were isolated using high-salt buffer (HSB; 1.25 M NaCl, 40 mM HEPES pH 7.6, 2 mM EDTA pH 8, 0.1% BSA) (Oldenburg et al., 2006, 2013). 0.1% β-mercaptoethanol (Sigma-Aldrich) was added to the buffer before grinding the tissue samples. Briefly, leaf and stalk tissues were homogenized in HSB using a blender, and the homogenate was filtered through 1–3 layers of Miracloth (EMD Millipore). The homogenate was differentially centrifuged first at low speed (500 × *g* for 5 min) to remove nuclei. Then the supernatant was centrifuged (3,000 × *g* for 10 min) to pellet plastids. The resulting supernatant was centrifuged at 20,000 × *g* for 15 min) to pellet mitochondria. The plastid and mitochondria pellets were washed three times with chloroplast dilution buffer (CDB; 0.33 M D-sorbitol, 20 mM HEPES pH 7.6, 2 mM EDTA, 1 mM $MgCl_2$, 0.1% BSA) and mitochondria dilution buffer (MDB; 0.4 M D-sorbitol, 0.1 M HEPES pH 7.6, 2 mM EDTA, 1 mM $MgCl_2$, 0.1% BSA), respectively. The plastids and mitochondria were further purified using discontinuous (step) Percoll gradients as

follows. For plastids, 30% and 70% Percoll solutions adjusted to the equivalent osmolarity of 1x CDB were prepared (for example: for 30%, 12 mL Percoll + 8 mL 5x Chlp Gradient Buffer + 20 mL dH_2O and for 70%, 28 mL Percoll + 8 mL 5x Chlp Gradient Buffer + 4 mL dH_2O; 5x Chlp Gradient Buffer is 1.65 M D-sorbitol, 40 mM Hepes pH 7.6, 4 mM EDTA, 2 mM $MgCl_2$, 0.2% BSA). For two-step gradients, 15 mL 30% Percoll was layered onto 15 mL of 70% Percoll in a 40-mL centrifuge tube. Then 2–4 mL of plastid solution was gently layered on top, followed by centrifuged for 30 min at 1,500 × *g* using a JA-20 fixed-angle rotor. Plastids were removed from the 30/70 Percoll interface, transferred to a centrifuge tube and washed 2–3 times with CDB (using 10x the volume of recovered plastid solution), followed by centrifugation of 3,000 × *g* for 8 min to pellet plastids. The purified plastids were then resuspended in a small volume of CDB. A similar process was used for purification of mitochondria, except for the following minor changes. A two-step 28% and 45% Percoll gradient, with solutions adjusted to the equivalent osmolarity of 1x MDB, was used (for example: for 28%, 11.2 mL Percoll + 20 mL 2x Mito Gradient Buffer + 8.8 mL dH_2O and for 45%, 18 mL Percoll + 20 mL 2x Mito Gradient Buffer + 2 mL dH_2O; 2x Mito Gradient Buffer is 0.8 M D-sorbitol, 40 mM Hepes pH 7.6, 4 mM EDTA, 2 mM $MgCl_2$, 0.2% BSA). Centrifugation was done for 20 min at 20,000 × *g* using a JA-20 fixed-angle rotor, mitochondria were recovered from the 28/45 Percoll interface, washed 2–3 times with MDB, pelleted by centrifugation for 15 min at 20,000 × *g*, and resuspended in small volume of MDB. Finally, plastids and mitochondria were stored in CDB or MDB. Freshly isolated plastids and mitochondria were used in the ROS assays.

Isolation of DNA From Organelles

Plastid and mtDNA were extracted using cetyltrimethylammonium bromide (CTAB) as described by Rogers and Bendich (1985) with minor modifications. An equal volume of 2x CTAB buffer [2% CTAB (w/v), 100 mM Tris/HCl (pH 8.0), 20 mM EDTA, 1.4 M NaCl, 1% polyvinylpyrrolidone (M 40000; w/v); preheated to 65°C] and Proteinase K (20 μg/ml) were added to the resuspended plastids or mitochondria and incubated at 65°C for 1 h. Then 0.1 M phenylmethylsulfonyl fluoride was added, followed by incubation at room temperature for 1 h. Then RNase A was added to 100 μg/mL, and the samples were kept at 60°C for 15 min. Next, potassium acetate was added to 400 mM, and the mixtures were kept on ice for 15 min before centrifugation at 12,000 × *g* for 10 min at 4°C. Equal volumes of chloroform:isoamyl alcohol (24:1) were added, the tubes were shaken, and then centrifuged at 12,000 × *g* for 1 min. After isopropanol precipitation, the DNA pellet was suspended in 10 mM Tris (pH 8), 1 mM EDTA (TE), and precipitated with two volumes of 100% ethanol overnight at −20°C before pelleting. DNA pellets were washed three times with 70% ethanol, dried, and then resuspended in TE. Quantitation was performed using the Quant-IT DNA quantitation kit (Thermo Fisher Scientific).

Protoplast Isolation

Maize protoplasts were isolated from the leaf and stalk tissues, as described by Sheen (1995). Briefly, seedlings were washed with 0.5% Sarkosyl (5 min), 0.6% sodium hypochlorite (10 min), and 70% ethanol (10 s) and rinsed with sterile water. 0.5 mm strips were cut from the middle part of four or five leaves and stalks. Tissues were digested in the enzyme solution (1.5% cellulase R10 and 0.3% macerozyme (Yakult Honsha) in 0.6 M mannitol, 10 mM MES pH 5.7, 1 mM $CaCl_2$, 5mM β-mercaptoethanol, 0.1% BSA for 30 min in a vacuum and 2 h at room temperature with agitation at 80 rpm. Protoplasts were stored overnight at 4°C. The suspension containing protoplasts was filtered through a 35 μm nylon mesh. Protoplasts were pelleted by centrifuging at 150 × *g*, and the pellet was washed twice and then stored in W1 buffer (154 mM NaCl, 125 mM $CaCl_2$, 5 mM KCl, 2 mM MES pH 5.7). Protoplasts were counted using a counting chamber slide. Freshly isolated protoplasts were used for the assays.

Assays of ROS and Antioxidant Agents

ROS Marker Dyes

Fluorescein and rhodamine dyes are chemically reduced to colorless, non-fluorescent dyes. These "dihydro" derivatives are readily oxidized back to the parent dye by ROS and thus can serve as fluorogenic probes for detecting oxidative activity in cells and tissues. The fluorogenic probes and CellROX Green reagent (Thermo Fisher Scientific) were used to measure ROS in plastids, and the rhodamine dye DHR123 (Thermo Fisher Scientific) was used to measure ROS in mitochondria and protoplasts. Equal volumes of centrifuged pellets of isolated plastids, mitochondria, and protoplasts from leaf/stalk were used for each comparative measurement. Resuspended plastids/mitochondria/protoplasts were incubated with 5 μM CellROX or DHR123 for 30 min at 37°C before the fluorescence units were measured using a Victor plate reader (Perkin Elmer) at 485/520 nm (for CellROX) and 507/529 nm (for DHR123).

For superoxide detection, MitoSOX Red (Thermo Fisher Scientific) was used as a mitochondrial superoxide indicator. Oxidation of MitoSOX Red indicator (or dihydroethidium) by superoxide results in the formation of 2-hydroxyethidium that exhibits fluorescence at 510/580 nm.

Amplex Red Assays for H_2O_2 and Peroxidase Activity

For measuring H_2O_2 and peroxidase levels, we used the Amplex red dye. Amplex red reagent (10-acetyl-3,7-dihydroxyphenoxazine from Thermo Fisher Scientific) reacts with H_2O_2 in a 1:1 stoichiometry to produce highly fluorescent resorufin that can be measured by absorbance at 560 nm. The manufacturer's protocol was followed to measure H_2O_2 and peroxidase. Briefly, H_2O_2 and peroxidase standards were prepared by serial dilution. Equal volumes (as above) of plastids/mitochondria/protoplasts and H_2O_2/peroxidase standard solutions were added to the Amplex red reagent and incubated at room temperature for 30 min. The absorbance was measured, and H_2O_2 and peroxidase levels were calculated using standard curves.

SOD Activity Assay

Superoxide dismutase (SOD) activity was measured using a SOD colorimetric activity kit and the manufacturer's protocol (Thermo Fisher Scientific). This assay measures all types of

SOD activity, including Cu/Zn, Mn, and FeSOD types. Samples (plastids/mitochondria/protoplasts) were diluted in colored sample diluent and added to the wells of a 96-well plate. The substrate was added followed by Xanthine Oxidase Reagent and incubation at room temperature for 20 min. Superoxide is generated by the xanthine oxidase that converts a colorless substrate to a yellow-colored product, which was quantified at 450 nm by an absorbance assay. A SOD standard curve was used for all samples.

Catalase Assay

Catalase activity in protoplasts was quantified using the OxiSelect^{TM} catalase activity assay according to the manufacturer's protocol (Cell Biolabs) that involves decomposition of H_2O_2 into water and oxygen, which is proportional to the concentration of catalase. After the reaction, the catalase is quenched with sodium azide, and the remaining H_2O_2 facilitates the coupling reaction of 4-aminophenazone (4-aminoantipyrene, AAP) and 3,5-dichloro-2-hydroxy-benzenesulfonic acid (DHBS) in the presence of horseradish peroxidase (HRP) catalyst. The product, quinoneimine dye, was measured at 520 nm using a 96-well microtiter plate. Hydrogen peroxide 'working solution' was added to each well. Incubation was at room temperature for 40–60 min with vigorous mixing. The absorbance was read at 520 nm. The activity in the samples was determined by interpolation of the catalase standard curve.

Ascorbic Acid Assays

The levels of ascorbic acid (AsA) in protoplasts were quantified using the Cell Biolabs' OxiSelect^{TM} Ascorbic Acid Assay kit according to the manufacturer's protocol (Cell Biolabs). The assay was based on the Ferric Reducing/Antioxidant Ascorbic Acid (FRASC) chemistry driven by the electron-donating reducing power of antioxidants. The assay employs ascorbate oxidase, which allows the user to differentiate the AsA content from other antioxidants present within the samples. AsA levels in a sample are determined by measuring the difference in optical density between two sample wells, one with and one without the enzyme. In samples, the ferrous iron was chelated to a colorimetric probe to form a product that was measured at 540. AsA levels (nM) were determined using the standard curve.

Glutathione Assays

Total glutathione (GSH) levels in protoplasts were determined by the OxiSelect^{TM} Total Glutathione Assay Kit as per the manufacturer's protocol (Cell Biolabs). In this assay, GSH reductase reduces oxidized glutathione (GSSG) to reduced glutathione (GSH) in the presence of NADPH. Subsequently, the chromogen reacts with the thiol group of GSH to produce a colored compound that absorbs at 405 nm. The total glutathione content (μM) was determined by comparison with the predetermined GSH standard curve.

DNA Damage Assays

ELISA 8-OHdG assay

The quantitative measurement of 8-OHdG was determined by the OxiSelect^{TM} Oxidative DNA Damage ELISA kit (Cell Biolabs) following the manufacturer's protocol, which includes digestion of DNA to nucleosides. Equal amounts of the digested ptDNA and mtDNA and 8-OHdG standards were added to wells of 8-OHdG/BSA-conjugate preabsorbed microwell strips and incubated at room temperature for 10 min on an orbital shaker. Then anti-8-OHdG antibody was added to each well, and the plate was incubated at room temperature for 1 h. The strips were washed with Wash Buffer three times, and the diluted secondary antibody-enzyme conjugate was added for incubation at room temperature for 1 h. After washing, a substrate solution was added, and incubation was at room temperature for 2 min. The absorbance of each microwell was measured using 450 nm, and the 8-OHdG level was measured using a standard curve.

8-OxoG immunofluorescence assay

Plastids and mitochondria from light-grown stalk lower, stalk upper and L1 tissues were fixed in 4% formaldehyde/Dulbecco's phosphate buffered saline (PBS; Gibco) in 1 mM EDTA for 10 min, pelleted, and washed twice in PBS/EDTA. Then organelles were permeabilized in 0.1% Triton X-100/PBS/EDTA for 5 min, followed by washing twice. Fixed and permeabilized plastids were incubated in blocking solution (2% BSA/PBS/EDTA) for 30 min. Organelles were incubated with primary antibody anti-8-oxoguanine mouse monoclonal (1:1000 dilution; 1 μL of 0.5 mg/mL anti-8-oxoG in 1 mL 1% BSA/PBS/EDTA blocking solution) (Millipore-Sigma MAB3560-C) for 1 h at room temperature, then washed three times. Next, organelles were incubated with secondary antibody goat anti-mouse IgM conjugated with Alexa Fluor 488 (1:1000 dilution; 1 μL of 2 mg/mL Alexa in 1 mL 1% BSA/PBS/EDTA blocking solution) (Invitrogen A21042) for 1 h at room temperature, then washed three times.

For plastids, immunofluorescence imaging was done using a Nikon Microphot Epifluorescence microscope and images acquired with a QImaging Retiga 1300 10-bit digital camera using OpenLab image capture and analysis software. Imaging of 8-oxoG/Alexa 488 plastids was done using a 470/40ex and 525/50em filter set and autofluorescence imaging of plastids with a 470/20ex and 514em filter set. For individual plastids, the 8-oxoG/Alexa 488 mean fluorescence intensity (FI) was measured as pixel values (0 to 1023) (background mean FI was also measured and subtracted from plastid mean FI). As a control, plastids incubated with the Alexa secondary Ab and without the 8-oxoG primary antibody were also imaged. Immunofluorescence analysis of 8-oxoG/Alexa was also performed with plastids from light- and dark-grown entire seedling shoots (stalk and leaves), and the fluorescence intensity was evaluated visually ("by eye") using a scale of undetectable, weak, or high fluorescence.

The mitochondria were stained with MitoTracker Red CMXRos (Invitrogen/Molecular Probes) (incubation in 1x PBS/EDTA/200 nM CMXRos for 1 h) prior to fixation. Imaging of mitochondria with the MitoTracker dye and 8-oxoG/Alexa 488 was done using an Olympus IX81 microscope and images were acquired with a Hamamatsu Orca Flash 2.8 CMOS 12-bit digital camera. A TRITC filter set (556/20 ex and 614/30

em) was used for the MitoTracker dye and a FITC filter set (485/20 ex and 516/11 em) for 8-oxoG/Alexa 488. For individual mitochondria, the 8-oxoG/Alexa 488 mean fluorescence intensity (FI) was measured as pixel values (0 to 4096) (background mean FI was also measured and subtracted from mitochondria mean FI). As a control, mitochondria incubated with the Alexa secondary Ab and without the 8-oxoG primary antibody were also imaged. Differences in fluorescence intensity, higher for mitochondria (**Figure 6B**) than plastids (**Figure 6A**), can be attributed to the use of two different systems for image acquisition, the Hamamatsu 12-bit and the QImaging 10-bit, respectively.

Statistical Analysis

All assays were performed at least three times with similar results. For **Figures 1–5**, the values in each bar graph are shown as mean relative values ± SE from three independent assays (biological replicates). Statistically significant differences between tissues were assessed by the Student's *t*-test and/or by the ANOVA, and Tukey honest significant difference test and are shown as asterisks, where $^{*}P$-value ≤ 0.05, $^{**}P$-value ≤ 0.01, $^{***}P$-value ≤ 0.001, and P-values > 0.05 are indicated on respective graphs (see **Supplementary Material**).

RESULTS

We previously reported changes in the structure of orgDNA molecules during maize development and proposed that light triggers orgDNA degradation probably due to ROS-induced damage without subsequent repair (Oldenburg and Bendich, 2004; Oldenburg et al., 2006, 2013; Zheng et al., 2011; Kumar et al., 2014). There is a gradient in cell and organellar development from the base of the stalk to the tip of the maize leaf (Sylvester et al., 1990; Stern et al., 2004). Here, we measured the levels of ROS, antioxidant agents, and orgDNA damage at three stages of maize development: stalk lower (the base of the stalk), stalk upper (top of the stalk), and the blades from the first three leaves (**Table 1** and see "Materials and Methods" section). L1 refers to the first and oldest leaf. L2 and L3 refers to the second and third leaves, respectively. The tissue with the lowest value in each set of assays was used as the baseline for comparison with other tissues and is set at 1 (see "Materials and Methods" section and see **Supplementary Material** for statistical analyses).

In order to compare properties of orgDNA molecules during maize development, we previously used equal volumes of isolated packed organelles, and here we use the same standard to assess changes in ROS and orgDNA damage. Organelle number per cell, organelle size, and protein amount and composition per organelle all change greatly during the transition from promitochondria and proplastids to mature organelles. Therefore, neither an equal number of organelles nor an equal amount of protein is a good standard for comparison. How changes in ROS assessed using isolated organelles might reflect changes in the organelles within the plant will be considered later (see "Discussion" section).

ROS Levels Increase During Development

To measure the ROS level, we used ROS-indicator dyes that quantify general ROS components or that are specific for either superoxide anion ($O_2^{\bullet -}$) or hydrogen peroxide (H_2O_2). We used these dyes (see "Materials and Methods" section) with isolated plastids and mitochondria and with whole-cell protoplasts. The ROS-indicator dyes are oxidized to fluorescent products that were quantified using a microplate reader.

Figure 1 shows relative ROS levels using the dyes DHR123 for mitochondria and protoplasts and CellROX for plastids (**Supplementary Table S1**). **Figure 1A** shows that the ROS level is lowest in the plastids isolated from the stalk lower tissue. As the developmental gradient proceeds from stalk lower to stalk upper to the blade of L1, the ROS level increases to 2.6 in L1 compared to stalk lower. Unless accompanied by a corresponding increase in antioxidant defense, we would expect greater ROS damage to molecules of ptDNA in the green leaf blade than in the stalk (see "Discussion" section). A similar developmental increase of 2.7-fold was found for ROS in mitochondria isolated from the same tissues (**Figure 1B**), as well as 2.6-fold for protoplasts obtained from the total leaf (L1 + L2 + L3) blades and total stalk (stalk lower + stalk upper) tissues (**Figure 1C**). These data indicate that the increase in ROS during the development from stalk lower to leaf blade can be attributed to the maturation of plastids and mitochondria (and probably to the ROS byproducts of electron transport chains used in both photosynthesis and respiration), rather than other parts of the cell where ROS can be produced.

Since DHR123 and CellROX report ROS in a general sense, we used other dyes to focus on specific types of ROS molecules. Hydrogen peroxide is a major non-radical oxygen species that is generated during photosynthetic and respiratory electron transport chain reactions, as well as in peroxisomes (Mhamdi et al., 2010). We used the Amplex red assay for H_2O_2 in organelles isolated from leaf and stalk tissues. The lowest H_2O_2 level was detected in stalk lower (plastids and mitochondria) and stalk (for protoplasts) tissues, with the highest level in L1 and leaf (**Figures 1D–F** and **Supplementary Table S3**).

Superoxide, a free-radical oxygen species, is also present in plant organelles. Using the mitochondrial-specific superoxide dye, MitoSOX red, we measured the superoxide level in mitochondria and protoplasts of leaf and stalk tissues (**Figures 1G,H** and **Supplementary Table S5**). We found that MitoSOX red, which was developed for mitochondria, did not work with isolated chloroplasts. The level of superoxide in mitochondria was higher by 2.3-fold for L1 than in stalk lower and 3-fold for leaf tissue than in stalk, respectively (**Figures 1G,H**). To summarize, both H_2O_2 and $O_2^{\bullet -}$ were lower in stalk than leaves, so that the level of ROS clearly increases as the seedlings develop from stalk to leaf blade tissue.

ROS Levels Are Higher in Light-Grown Than Dark-Grown Plants

We previously reported that orgDNA maintenance is influenced by responses to light signals: light that led to the greening of seedling leaves also triggered the demise of both ptDNA

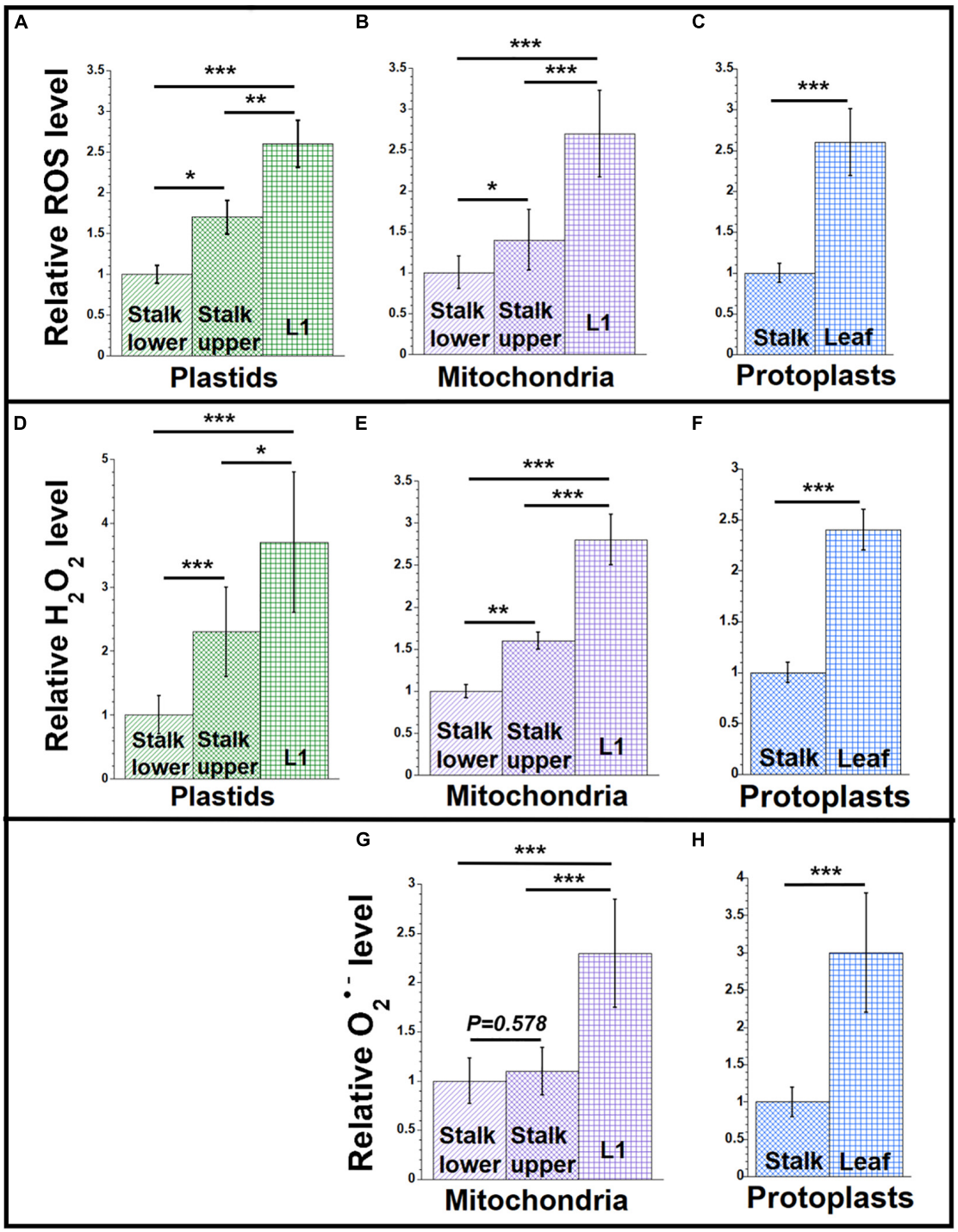

FIGURE 1 | ROS levels during maize development. Plastids and mitochondria were isolated from light-grown maize seedling tissues (Stalk lower, basal 1/3 of stalk; Stalk upper, upper 2/3 of stalk; L1, leaf 1). Protoplasts were isolated from Leaf (combined leaves L1, L2, and L3) and the entire Stalk (stalk lower and upper). For each set of assays, equal volumes of plastids, mitochondria, or protoplasts were used. Measurements are given relative to the tissue with the lowest value (stalk lower or stalk), which is set at one (see the section "Materials and Methods"). **(A–C)** The level of reactive oxygen species (ROS; superoxide anion ($O_2^{\bullet -}$), hydroxyl radical ($HO^{\bullet}$), and H_2O_2) was measured using the oxidative stress marker fluorescence dyes DHR123 for mitochondria and protoplasts and CellROX green for plastids. **(D–F)** H_2O_2 in was measured using the Amplex red assay. The hydrogen peroxide concentrations in μM were measured. **(G,H)** Superoxide anion was measured using the mitochondrial-specific superoxide fluorescence dye, MitoSOX. All assays were performed at least three times. Statistically significant differences were measured using ANOVA statistic test with *post hoc* analysis using Tukey's HSD and are shown as asterisks, where *P-value ≤ 0.05, **P-value ≤ 0.01, ***P-value ≤ 0.001. P-values > 0.05 are indicated on respective graphs.

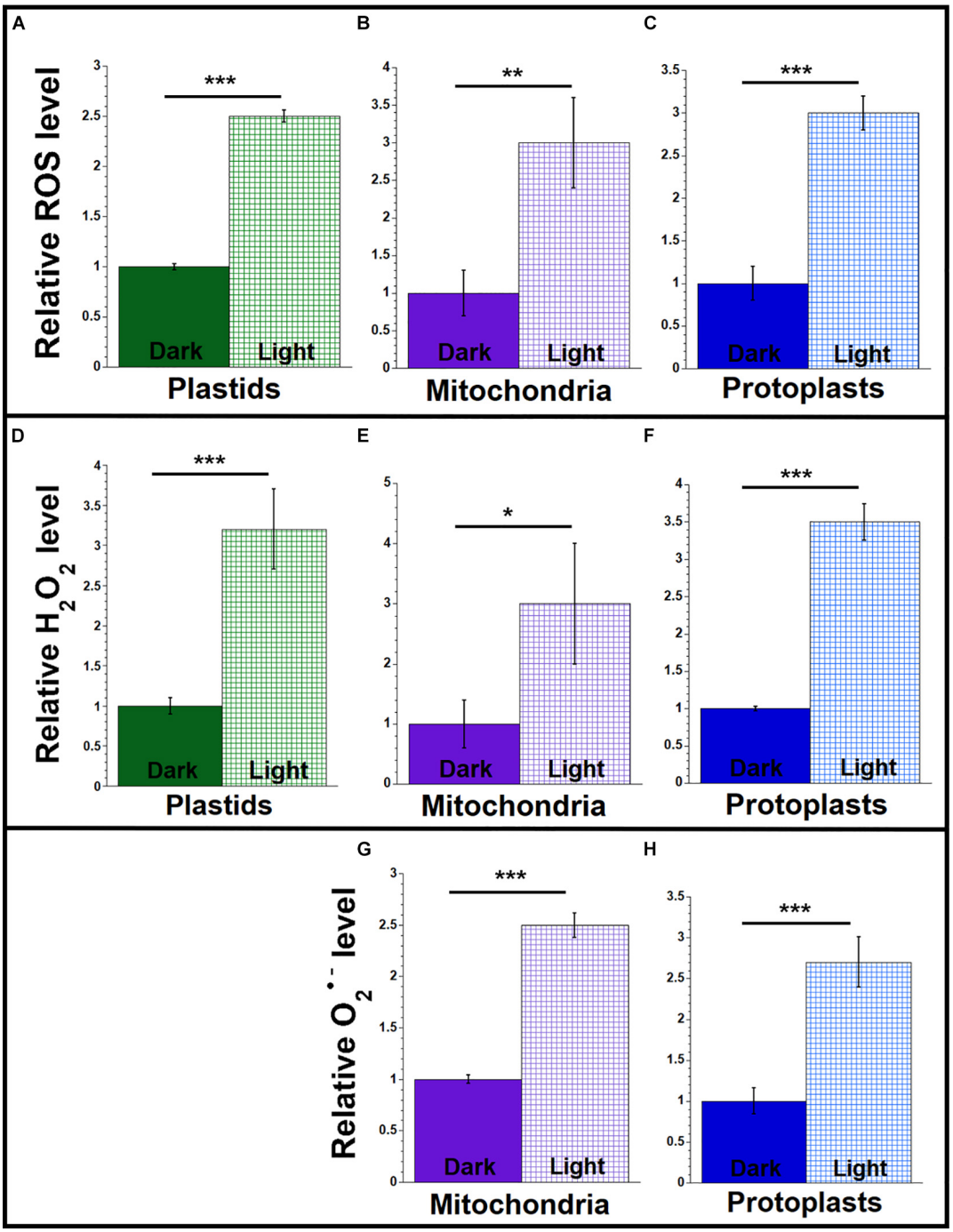

FIGURE 2 | ROS levels in light and dark conditions. Plastids, mitochondria, and protoplasts were isolated from light-grown (light) and dark-grown (dark) maize seedling leaves (L1 + L2 + L3). Equal volumes of plastids, mitochondria or protoplasts were used for each set of assays. The assay measurements are given relative to the tissue with the lowest value (dark-grown samples) which is set at one. **(A–C)** The levels of ROS (DHR123 for plastids and mitochondria and CellROX for protoplasts) were assayed as in **Figure 1**. **(D–F)** The level of H_2O_2 was measured using the Amplex red as in **Figure 1**. **(G,H)** The levels of superoxide anion ($O_2^{\bullet-}$) were measured using MitoSOX as in **Figure 1**. All assays were performed at least three times. Statistically significant differences were measured using ANOVA statistic test with *post hoc* analysis using Tukey's HSD and are shown as asterisks, where *P-value ≤ 0.05, **P-value ≤ 0.01, ***P-value ≤ 0.001.

and mtDNA in maize (Oldenburg et al., 2006; Zheng et al., 2011; Kumar et al., 2014). Here, we test the hypothesis that the increased level of ROS in light-grown maize correlates with increased damage to orgDNA. We quantified ROS in plastids, mitochondria, and protoplasts from light- and dark-grown total leaf blade (L1 + L2 + L3) tissues, using the tissue with the

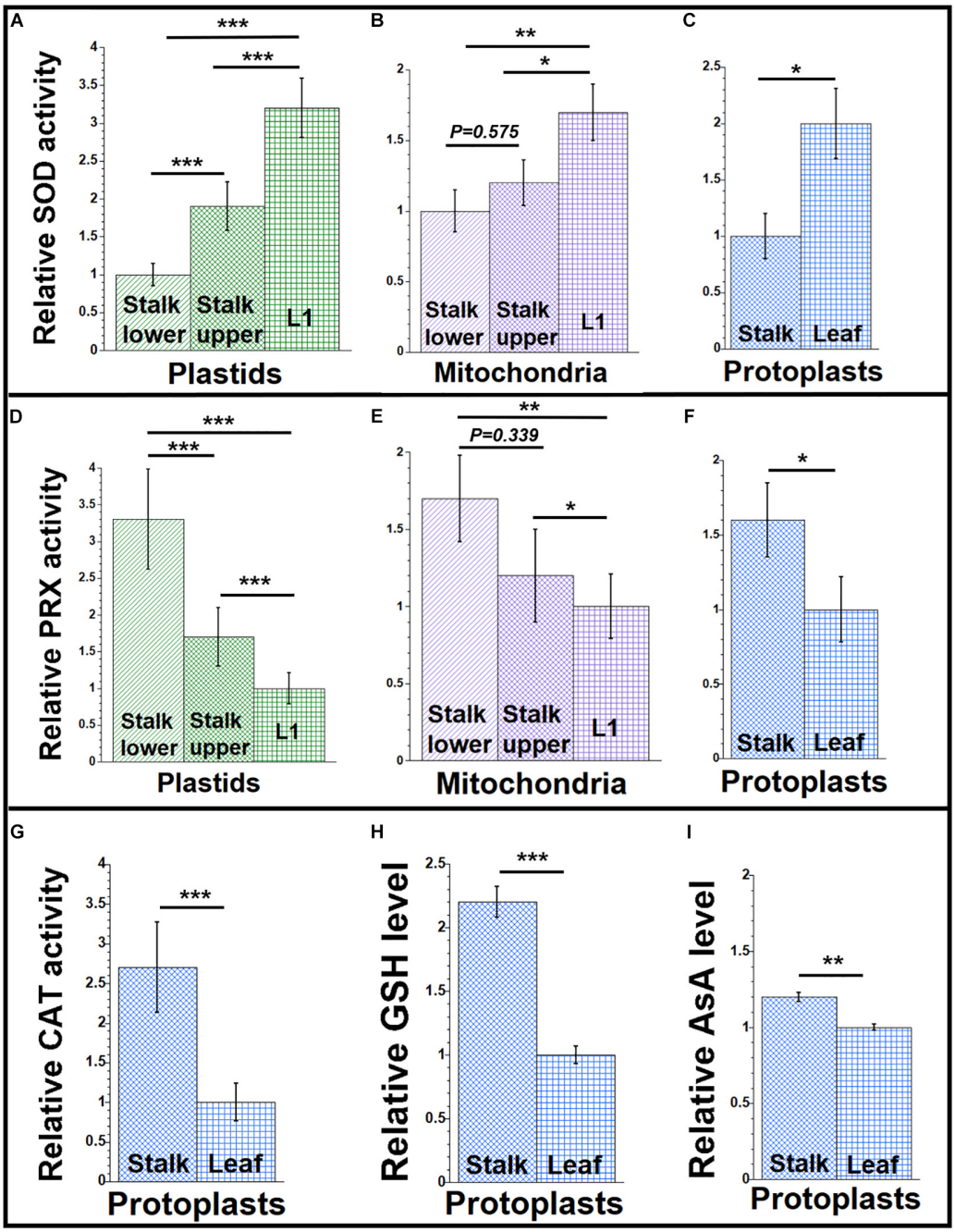

FIGURE 3 | Antioxidant agents during maize development. Organelles and protoplasts were isolated, as in **Figure 1**. The assay measurements are given relative to the tissue with the lowest value which is set at one. **(A–C)** The level of superoxide dismutase (SOD) enzyme activity was measured as U/mL using an immunoassay. **(D–F)** The Amplex red assay was used for the peroxidase (PRX) enzyme activity and measured as mU/mL. **(G)** A colorimetric assay was used for determining catalase (CAT) enzyme activity and measured as U/mL. **(H)** Total glutathione (GSH) and **(I)** ascorbic acid (AsA) levels (μM and nM, respectively) in protoplasts were determined by colorimetric assays. All assays were performed at least three times. Statistically significant differences were measured using ANOVA statistic test with *post hoc* analysis using Tukey's HSD and are shown as asterisks, where *P-value ≤ 0.05, **P-value ≤ 0.01, ***P-value ≤ 0.001. P-values > 0.05 are indicated in the respective graphs.

lower amount of ROS as the baseline for comparison. The light/dark ratios were similar, ranging from 2.5 to 3.5, for general ROS (**Figures 2A–C** and **Supplementary Table S2**), H_2O_2 (**Figures 2D–F** and **Supplementary Table S4**), and $O_2^{\bullet-}$ (**Figures 2G,H** and **Supplementary Table S6**). Although it might be expected that these light/dark ratios would be similar for plastids and protoplasts, it is notable that the light/dark ratios are also in the range of 2.5 to 3 for isolated, non-green

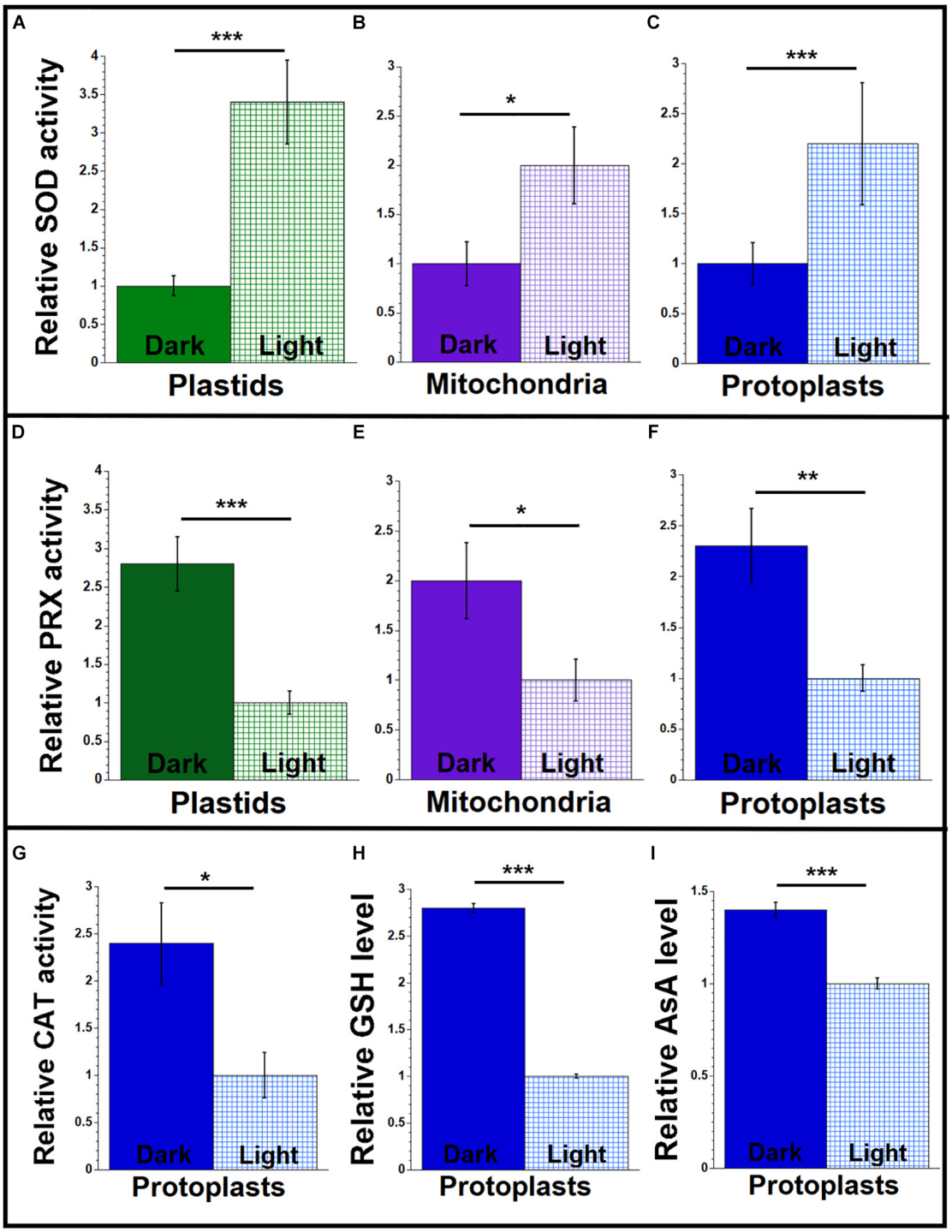

FIGURE 4 | Antioxidant agents from maize seedlings grown under light or dark conditions. Organelles and protoplasts were isolated, as in **Figure 2**. The assay measurements are given relative to the tissue with the lowest value, which is set at one. **(A–C)** The level of superoxide dismutase (SOD) enzyme activity was measured as U/mL using an immunoassay. **(D–F)** The level of peroxidase (PRX) enzyme activity was measured as mU/mL using the Amplex red assay. **(G)** A colorimetric assay was used for determining catalase (CAT) enzyme activity and measured as U/mL. **(H)** Total glutathione (GSH) and **(I)** ascorbic acid (AsA) levels (μM and nM, respectively) in protoplasts were determined by colorimetric assays. All assays were performed at least three times. Statistically significant differences were measured using ANOVA statistic test with *post hoc* analysis using Tukey's HSD and are shown as asterisks, where *P-value ≤ 0.05, **P-value ≤ 0.01, ***P-value ≤ 0.001.

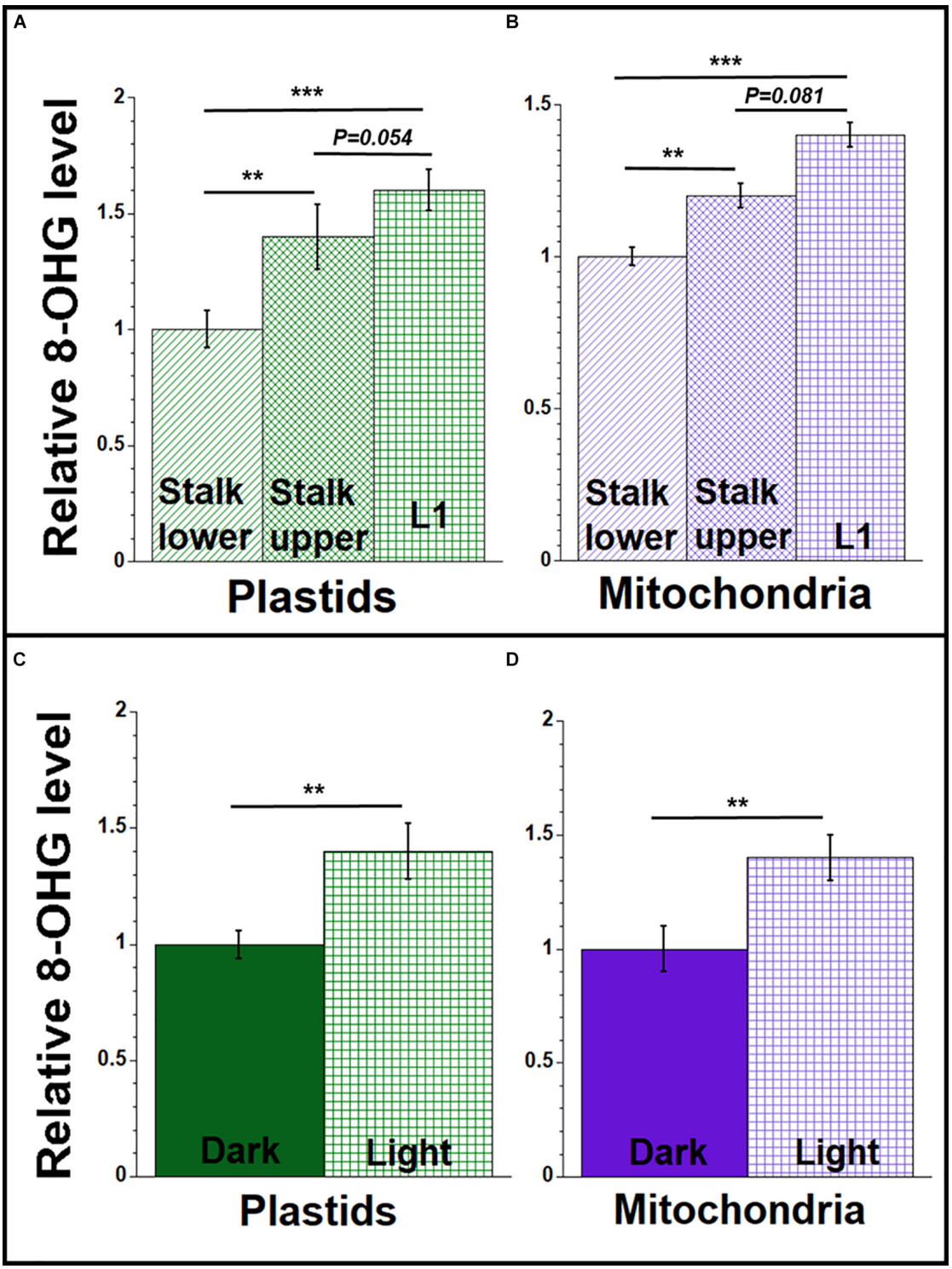

FIGURE 5 | 8-hydroxydeoxyguanosine (8-OHdG) representing orgDNA damage during maize development. Equal amounts of DNA extracted from isolated plastids and mitochondria were used to measure the 8-OHdG levels using a competitive ELISA assay. The levels of 8-OHdG in ptDNA and mtDNA were determined (ng/mL) and shown relative to stalk lower for **(A,B)** and relative to dark-grown leaves for **(C,D)**. All assays were performed at least three times. Statistically significant differences were measured using ANOVA statistic test with *post hoc* analysis using Tukey's HSD and are shown as asterisks, where **P*-value $\leq$ 0.05, ***P*-value $\leq$ 0.01, ****P*-value $\leq$ 0.001. *P*-values $>$ 0.05 are indicated on respective graphs.

TABLE 1 | Assays for ROS and antioxidant agents.

Assay	Method	Mechanism	Detection
General ROS	Dihydrorhodamine 123 and CellROX dyes	Dyes fluoresce green upon oxidation	Fluorescence
Hydrogen peroxide	Amplex red assay (Amplex red reagent + horseradish peroxidase)	Generation of fluorescent resorufin	Absorbance/ fluorescence
Superoxide	MitoSOX dye	Dye oxidized by superoxide in mitochondria	Fluorescence
Superoxide dismutase	Colorimetric immunoassay	Generation of a yellow product	Absorbance
Peroxidase	Amplex red assay (Amplex red reagent + hydrogen peroxide)	Generation of fluorescent resorufin	Absorbance/ fluorescence
Catalase	Colorimetric assay	Coupling of quinoneimine dye with H_2O_2	Absorbance
Glutathione	Colorimetric assay	Generation of a colored compound by a reaction of chromogen with glutathione	Absorbance
Ascorbic acid	Colorimetric assay	Ferric reducing/antioxidant ascorbic acid (FRASC) chemistry	Absorbance

mitochondria because there are no known photoreceptors in mitochondria.

Change in Antioxidant Enzyme Activity During Development

Antioxidant enzymes can modulate the levels of ROS and reduce oxidative stress (Asada, 2006; Soares et al., 2019). The SOD enzymes remove superoxide by catalyzing its dismutation and reducing it to H_2O_2. Plants have MnSODs in the mitochondria and peroxisomes, Cu/ZnSODs in the chloroplast, peroxisomes, and cytosol, and FeSODs in the chloroplast (Alscher et al., 2002; Pilon et al., 2011). Our SOD assay measured all types of SOD activities. We measured SOD activity in organelles and protoplasts isolated from leaf and stalk tissues. As shown in **Figures 3A–C** and **Supplementary Table S7**, SOD activity was highest in organelles isolated from L1 and higher in protoplasts from leaf than from stalk.

The stability and accumulation of H_2O_2 are mainly influenced by the activity of the antioxidative system. In plants, several antioxidant enzymes metabolize H_2O_2. Ascorbate peroxidases (APX), peroxiredoxins, glutathione/thioredoxin peroxidases, glutathione *S*-transferases, and catalases are such enzymes (Cerny et al., 2018; Foyer, 2018). APXs have high specificity for H_2O_2, are present in chloroplast and mitochondria, and perform the final step of conversion of free radicals to water and oxygen (Maruta et al., 2016). Other peroxidases, such as peroxiredoxins, are localized to the cytosol, plastids, mitochondria, and peroxisomes in plants (Liebthal et al., 2018). Our peroxidase assay measured all types of peroxidase activities. We found more peroxidase activity in organelles isolated from stalk lower compared to organelles from L1 and more in protoplasts from stalk than from leaf (**Figures 3D–F** and **Supplementary Table S9**).

Catalase has high specificity for H_2O_2 and acts by the dismutation of two molecules of H_2O_2 to water and O_2 (Mhamdi et al., 2010). Although the CAT-3 isoform of catalase was reported in maize mitochondria (Scandalios et al., 1980), and some catalase was reported in other cellular compartments including chloroplasts (Mhamdi et al., 2010), the peroxisome has been considered as the main location of catalase within plant cells, with mitochondrial/chloroplast catalase as possible contamination from broken peroxisomes (Corpas et al., 2017). Here, we report total cellular catalase activity in maize protoplasts prepared from stalk and leaf tissue. In our assays, catalase activity was higher in protoplasts from stalk than from leaf (**Figure 3G** and **Supplementary Table S11**).

In all antioxidant enzyme assays, the tissue with the lowest enzyme activity was used as the baseline for comparison with other tissues. Our assays suggest that high peroxidase and catalase activities result in the relatively low H_2O_2 level in the stalk, whereas low peroxidase and catalase activities result in high H_2O_2 levels in the leaf.

Antioxidant Enzyme Activity in Light and Dark Conditions

The ROS level in the organelles isolated from leaf tissue of maize was higher for light-grown than dark-grown plants (**Figure 2**), and this difference may be attributed to lower antioxidant enzyme activity in the light. To test this idea, we measured the antioxidant activities of SOD, peroxidase, and catalase in leaves (L1 + L2 + L3) grown in light and dark conditions, as described above. We found 2–3.4 times higher SOD activity in the organelles and protoplasts of light-grown than dark-grown plants (**Figures 4A–C** and **Supplementary Table S8**). In contrast, the activity of peroxidase was 2–2.7 times lower for light-grown than dark-grown plants (**Figures 4D–F** and **Supplementary Table S10**). The catalase activity was 2.4 times lower in protoplasts from light compared to dark (**Figure 4G** and **Supplementary Table S12**).

Levels of Small-Molecule Antioxidants

The non-enzymatic antioxidant system in plants includes low-mass metabolites like GSH, AsA, phenolic compounds, and proline. These antioxidants manage the ROS homeostasis by removing, transforming, or neutralizing the oxidant pool (Diaz-Vivancos et al., 2015; Smirnoff, 2018; Soares et al., 2019). To determine if small antioxidants are involved in maintaining low levels of ROS in maize, we quantified the levels of GSH and AsA in protoplasts isolated from leaf and stalk tissues. We found that the level of GSH was 2.2 times higher in stalk compared to leaf (**Figure 3H** and **Supplementary Table S11**). And we found that the level of AsA was 1.2 times higher in stalk than in leaf (**Figure 3I** and **Supplementary Table S11**).

We also performed the GSH and AsA assays in protoplasts isolated from the light-and dark-grown leaves. As shown in **Figures 4H,I** and **Supplementary Table S12**, both GSH and AsA levels were higher in the protoplasts isolated from the dark-grown plants. In protoplasts from the dark-grown leaves, the GSH level was 2.8 times higher, and the AsA level was 1.4 times higher than protoplasts from light-grown plants.

In summary (**Table 2**), we found higher levels of ROS (H_2O_2 and superoxide) and higher SOD activity in leaf than stalk tissues, but lower activities for peroxidase and catalase in leaf than stalk tissues. Light-grown leaves had higher levels of H_2O_2, superoxide, and SOD but lower activities of peroxidase and catalase than dark-grown leaves. Levels of GSH and AsA also changed, lower in light-grown leaf than in stalk tissue.

Levels of orgDNA Oxidative Damage Change During Development and in Light/Dark Conditions

Reactive oxygen species generate various modified DNA bases, and 7,8-dihydro-8-oxoguanine (8-oxoguanine, 8-oxoG) is the most common modified base found in DNA from bacteria, the eukaryotic nucleus, and mitochondria of animals, plants, and yeast (Imlay, 2013; Wallace, 2013; Bokhari and Sharma, 2019). During repair via the BER pathway, the damaged nucleoside, 8-hydroxydeoxyguanasine (8-OHdG), is released and has been used as a biomarker for oxidative stress (Shen et al., 2007). 8-oxoG lesions in DNA have also been assessed in rat liver cells by immunofluorescence (Kemeleva et al., 2006).

We used antibodies to 8-OHdG and a competitive ELISA method to measure the relative amounts of oxidative damage in orgDNA from maize tissues. In our ELISA assay, we found a higher level of 8-OHdG in ptDNA and mtDNA isolated from the blade of L1 compared to stalk lower tissue (**Figures 5A,B** and **Supplementary Table S13**). The level was 1.4–1.6 times higher in orgDNAs isolated from L1 compared to orgDNAs isolated from stalk lower. We also found 1.4 times higher 8-OHdG in the orgDNA of leaves from seedlings grown in the light than in the dark (**Figures 5C,D** and **Supplementary Table S14**). The higher 8-OHdG levels strongly suggest greater oxidative damage in the organelles from leaf than stalk.

Immunofluorescence microscopy was performed using isolated plastids and mitochondria from light-grown maize tissues (stalk lower, stalk upper, and L1) with a primary antibody to 8-oxoG and a secondary antibody containing the fluorescent dye Alexa 488. For both plastids and mitochondria, the fluorescence intensity per organelle was higher for the leaf than the stalk tissues (**Figures 6A,B**). 8-OxoG immunofluorescence was also evaluated for plastids from light- and dark-grown entire seedling shoots (stalk and leaves). In this assay, the fluorescence intensity was assessed visually and scored as undetectable, weak, or high. For light, 75 out of 107 plastids were scored as "high"; for dark, 0 of 48 plastids were scored as "high." Each of these results indicate that there are more 8-oxoG lesions in ptDNA from photosynthetically active leaf chloroplasts than non-photosynthetic stalk plastids.

TABLE 2 | Results summary for plastids, mitochondria, and protoplasts.

Assay	Results
General ROS	Leaf > stalk
	Light > dark
Hydrogen peroxide	Leaf > stalk
	Light > dark
Superoxide*	Leaf > stalk
	Light > dark
Superoxide dismutase	Leaf > stalk
	Light > dark
Peroxidase	Leaf < stalk
	Light < dark
Catalase**	Leaf < stalk
	Light < dark
Glutathione**	Leaf < stalk
	Light < dark
Ascorbic acid**	Leaf < stalk
	Light < dark

**Superoxide assay was not performed for plastids. **Assays were performed only for protoplasts.*

DISCUSSION

Most of the changes we report for ROS and antioxidant agents during maize development might have been anticipated as a mitigating response to damage resulting from oxidative stress. In some cases, however, the anticipated damage-defense relationship was not observed suggesting a beneficial role for ROS unrelated to damage. We now consider how ROS and antioxidant agents may influence the maintenance or degradation of orgDNA during the transition from stem cell to leaf.

ROS and Antioxidant Agents in Plant Cells and Organelles: An Overview

Although chloroplasts and mitochondria are the main sites of ROS production, ROS profoundly influence the chemistry in peroxisomes, cytosol, and vacuoles (Asada, 2006; Noctor and Foyer, 2016; Kohli et al., 2019). Cells also contain many protein and small-molecule antioxidant agents that both counteract oxidative stress and facilitate signaling the redox status of the cell to the nucleus, probably in the form of H_2O_2 (Cerny et al., 2018; Locato et al., 2018; Smirnoff and Arnaud, 2019; Soares et al., 2019). These include various SOD enzymes that convert the highly reactive $O_2^{\bullet-}$ to the mobile but less reactive H_2O_2 (Alscher et al., 2002; Pilon et al., 2011), catalases that remove H_2O_2 (Zamocky et al., 2008; Corpas et al., 2017), and APXs and glutathione peroxidases (GTXs) (Maruta et al., 2016; Liebthal et al., 2018) that also remove H_2O_2, as well as GSH, AsA, and other small-molecule antioxidants (Noctor et al., 2012; Diaz-Vivancos et al., 2015; Smirnoff, 2018). The redox "objective" indicated by levels of these antioxidant agents, as well as oxygen content, seems to be directed at suppressing oxidative damage in the meristem while tolerating some oxidative damage in the green leaf. One consequence is seen as pristine orgDNA in the

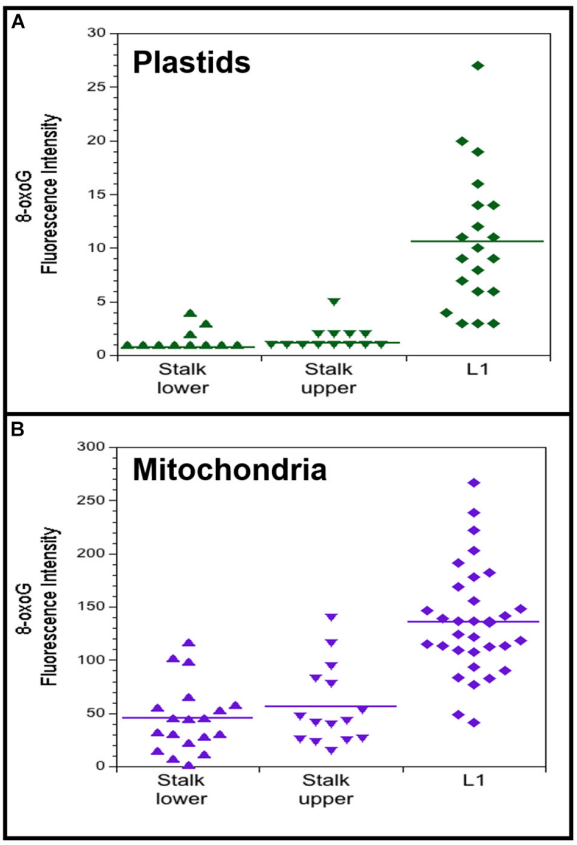

FIGURE 6 | 8-oxoguanine (8-oxoG) in maize plastids and mitochondria. Plastids **(A)** and mitochondria **(B)** were isolated from light-grown maize seedling tissues (Stalk lower, basal 1/3 of stalk; Stalk upper, upper 2/3 of stalk; L1, leaf 1). Fluorescence intensity was measured for individual plastids and mitochondria that were imaged by immunofluorescence microscopy using a primary antibody to 8-oxoG coupled with a secondary fluorescence antibody. All assays were performed at least three times. **(A)** The number of plastids measured and the average mean fluorescence intensity ± standard error was 22 and 0.8 ± 0.2 for Stalk lower, 18 and 1.2 ± 0.3 for Stalk upper, and 20 and 10.6 ± 1.4 for L1. **(B)** The number of mitochondria measured and the average mean fluorescence intensity ± standard error was 19 and 45 ± 7 for Stalk lower, 15 and 56 ± 10 for Stalk upper, and 33 and 136 ± 9 for L1. For both plastids and mitochondria, Stalk lower and Stalk upper are significantly different compared to L1 with P-value < 0.0001 using ANOVA with *post hoc* Tukey HSD, and there is no significant difference between Stalk lower and Stalk upper. Differences in the Fluorescence intensity may be attributed to different systems used to acquire images for plastids and mitochondria (see "Materials and Methods" section).

germline meristem and highly fragmented/damaged orgDNA in developing somatic cells.

Relative and Absolute Levels of ROS and Antioxidant Agents

Our data are shown as the relative levels of several types of ROS and antioxidant agents, using the tissue with the lowest level as the reference point. Most assays report fluorescence units from reactive dyes or enzyme activity, neither of which provide concentration level. For example, we find that superoxide increases from stalk to green leaf (**Figure 1G**), but we do not know the molar concentration in either tissue. And superoxide levels were determined only for mitochondria, not for plastids, even in the protoplast assays. The assay for H_2O_2 does report concentration, although this is for a given volume of pooled organelles or protoplasts. For plastids from the stalk lower, the concentration ranged from 2.5–5.3 μM H_2O_2 and increased to 8.5–19.6 in the green leaf. Similar values were found for mitochondria, 3.3–4.3 in stalk lower and 8.2–11.7 in leaf. Not surprisingly, the cellular H_2O_2 concentration was higher, 18.7–24.5 μM for protoplasts from light-grown leaves. The molarity of H_2O_2 extracted from various plants has been reported, but these values enormously exceed the values for animal cells, probably do the extremely high levels in the apoplastic parts of plant tissues (cell walls and intercellular spaces) (Foyer and Noctor, 2016; Noctor et al., 2018). Previous estimates of the absolute concentrations of ROS molecules within plant cells are problematic, in part due to technical difficulties, and even newer methods employing genetically engineered ROS-sensor proteins (HyPer) only report relative differences in ROS levels between samples (such as control and high light exposure) or along a cellular gradient (Exposito-Rodriguez et al., 2017; Smirnoff and Arnaud, 2019). Our data were obtained with isolated organelles and protoplasts, including many wash steps, so that apoplastic sources do not affect our ROS and antioxidant data. Maize is a C4 plant containing both mesophyll and bundle sheath cells. The isolated organelles and protoplasts prepared using our methods are mostly derived from mesophyll cells (Kumar et al., 2015), so that our ROS and antioxidant data represent a specific subset of differentiated maize cells. Whereas accurate measurements of the concentrations of ROS molecules and antioxidants in plant cell compartments are needed to better understand the influence of ROS in oxidative stress and signaling, comparisons of the relative levels in isolated organelles can provide insights, as described below.

Isolated Organelles and Organelles in the Plant

Any biochemical property may be altered by removing molecules or organelles from intact tissue before analysis, and the nature of ROS can make measurements especially challenging (Noctor et al., 2016). In order to mitigate effects of inadvertent oxidation on subsequent assays of ROS, antioxidant enzymes, and orgDNA damage, we employed low temperature and reducing conditions during the isolation of organelles. Furthermore, our data are reported as relative values among tissues handled and analyzed in parallel, so that potential isolation artifacts were controlled. The overall conclusions, summarized in **Figure 7**, present a relationship between redox status and DNA damage that would not be anticipated from artifactual data.

The Transition From Stem Cells to Leaf Cells

During maize leaf development, new cells arise from the basal meristem, begin expansion/elongation in the stalk region, and become fully differentiated in the leaf blade. The developing

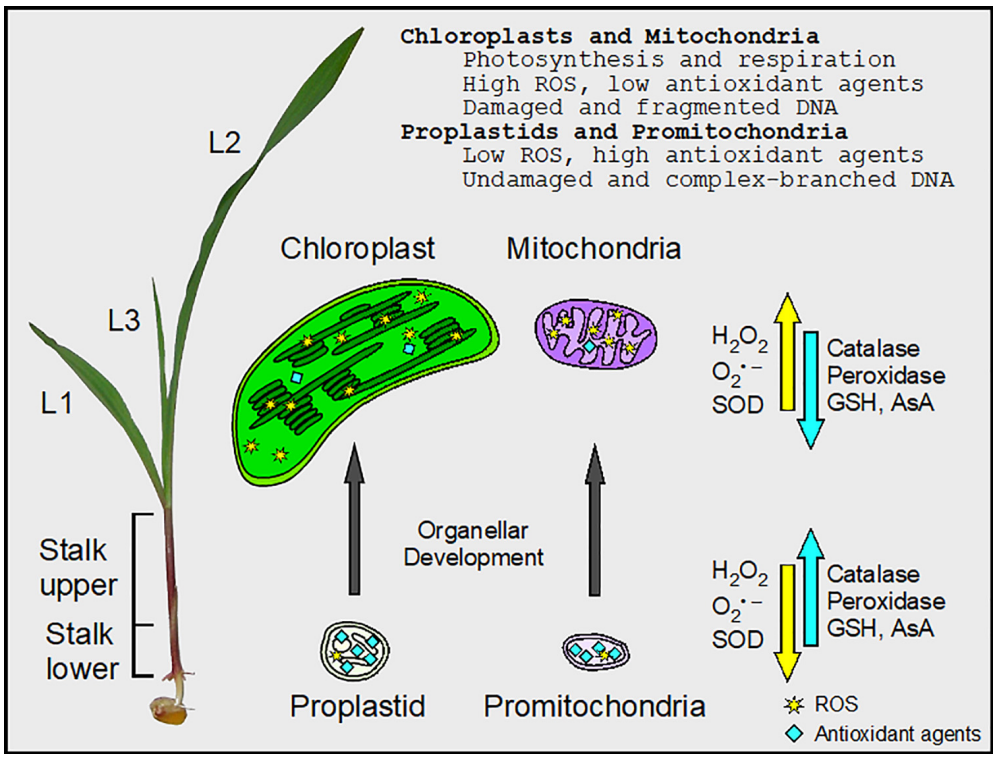

FIGURE 7 | Changes in ROS and antioxidant agents during maize chloroplast and mitochondrial development. There is a gradient in cellular and organellar development from the basal meristem (Stalk lower) to the fully expanded leaf blade in maize. In the undeveloped proplastids and promitochondria, the activity of peroxidase was high, facilitating the maintenance of minimal ROS levels and protecting orgDNA from oxidative damage. In chloroplasts and mitochondria, there were high levels of ROS, the byproducts of photosynthesis and respiration. Superoxide dismutase (SOD) converted some superoxide ($O_2^{\bullet-}$) to H_2O_2, but the activity of peroxidase was low. Thus, the orgDNA was subjected to extensive oxidative damage and became fragmented. Levels of glutathione (GSH), ascorbic acid (AsA), and catalase activity were obtained from protoplasts from the entire stalk and leaf blades (L1–L3), whereas both protoplasts and isolated organelles were used to assay ROS and enzyme activities for SOD and peroxidase.

cells in the stalk are in an etiolated state, shielded from light first by the coleoptile and later by the outer leaf sheath. Only after the leaf blade tip emerges are the cells exposed to light and begin the final differentiation process to photosynthetic capability. It is this final step where a sudden increase in ROS due to photosynthesis may result in oxidative stress or may merely be part of the normal cellular signaling process.

Antioxidant agents are usually considered as defensive agents that relieve oxidative stress and damage caused by high levels of ROS. We find that superoxide, SOD, and 8-oxoG all increase during leaf development (**Table 2** and **Figure 7**), a result consistent with a damage-response function for the antioxidant enzyme SOD. But perhaps SOD does not act only to reduce oxidative stress when it converts superoxide to H_2O_2 for two reasons. Since H_2O_2 is more stable than superoxide, a consequence of SOD activity is the replacement of one type of ROS with a more persistent type. The neutralization of superoxide as a damaging agent involves a second step in which H_2O_2 is removed by catalase and peroxidases. But as the leaf develops from the lower stalk, the increase in cellular H_2O_2 is accompanied by a *decrease* in cellular catalase and peroxidase activities and GSH and AsA levels. The second reason is that mutations that either over-express or reduce levels of some SODs reveal that these proteins have only minor roles in photoprotection or protection from oxidative damage (Alscher et al., 2002; Pilon et al., 2011). However, severe developmental defects were observed in mutants deficient for two plastid FeSODs, and H_2O_2 was proposed to coordinate chloroplast-nuclear gene expression (Myouga et al., 2008). Therefore, a major function of SOD may be to convert an immobile ROS species (superoxide) to a mobile species (H_2O_2), which is the likely signaling molecule that communicates the redox status of the cell to the nucleus (Brunkard and Burch-Smith, 2018; Mullineaux et al., 2018; Janku et al., 2019). In the lower stalk, however, the low level of SOD combined with the high activities of catalase and peroxidase and higher levels of GSH and AsA (**Figure 3**) serves to maintain a relatively high ratio of superoxide to H_2O_2 that is thought to be required for "stemness" in the stem cells of the shoot apical meristem of Arabidopsis (Zeng et al., 2017; Yang et al., 2018).

To summarize, our data support a signaling role for ROS in the lower stalk to maintain the stem cells (that later lead to the gametes) and in leaf cells developing photosynthetic capacity. Furthermore, mitochondria and plastids may comprise the major

source of the H_2O_2 signaling molecules produced during leaf development (**Figures 1**, **7**).

Damage and Repair of Organellar DNA

In maize, the DNA molecules in mitochondria and plastids isolated from the stalk lower tissue are pristine, as expected for stem cells, but these orgDNAs are highly degraded in green leaves (Oldenburg and Bendich, 2004, 2015; Oldenburg et al., 2013). Our present data show that during leaf development there is an increase in ROS and 8-oxoG (representing orgDNA damage). We infer that the demise of orgDNA begins with increased ROS production and that damaged-but-not-repaired orgDNA is degraded by default as occurs in *Escherichia coli* (Skarstad and Boye, 1993). Our data show that ROS, H_2O_2, superoxide, and SOD levels are lower in dark-grown leaves than in those grown in the light. Previously, we reported that the amount and molecular integrity of ptDNA rapidly decline upon transfer of maize seedlings from dark to light growth conditions (Zheng et al., 2011). We speculate that in the dark, the ROS byproducts of respiration lead to mtDNA damage and that a small amount of H_2O_2 signals the nucleus to express and deliver DNA repair proteins to the mitochondria and plastids. In the light, the green cells of the maize leaf blade produce sufficient ATP by photophosphorylation and no longer require transcription from either mtDNA to support respiration or ptDNA to support photosynthesis. A larger amount of H_2O_2 from the chloroplasts now signals the nucleus to cut off the supply of DNA repair proteins (such as RecA) and the damaged DNA in both organelles disintegrates. [The theoretical problem of continued photosynthesis in single-season grasses, such as maize, using long-lived mRNAs without the support of functional ptDNA has been considered elsewhere (Oldenburg and Bendich, 2015)].

The changes in ROS and antioxidant enzyme levels (SOD and peroxidase) during maize seedling development and under light and dark growth conditions show the same trends in both plastids and mitochondria. However, since mitochondria have no known light receptors, it is unclear why the mtDNA suffers the same light-induced demise as does ptDNA. One possible explanation comes from cultured human retinal pigment epithelial cells: the electron transport chain generates ROS when cells are exposed to blue light (King et al., 2004). In maize, we reported lower amounts of DNA per plastid in blue light than in white light and concluded that blue light suppresses ptDNA replication/repair and induces degradation (Oldenburg et al., 2006). One way for the nucleus to coordinate organellar activities is expression of dual-targeted proteins (those delivered to both plastids and mitochondria), including the replication/repair protein RecA (Oldenburg and Bendich, 2015). Thus, regardless of the organellar source of H_2O_2, considered the main signaling molecule, the nucleus perceives the redox status of the cell and dictates the fate of the orgDNA.

Although mechanisms for orgDNA repair in plants have been addressed recently (Baruch-Torres and Brieba, 2017; Garcia-Medel et al., 2019), additional insight may be found elsewhere. The "SOS response" in *E. coli* is initiated by accumulation of single-stranded DNA (ssDNA) during replication of DNA containing lesions (Maslowska et al., 2019). For both bacteria and eukaryotes, Bantele and Pfander (2019) propose a mechanism for responding to DNA damage that is based on the persistence of ssDNA: (1) repair locally if the damage level is low and ssDNA is short-lived; and (2) halt cell division until global repair of high-level damage is accomplished. The overall amount of ssDNA in a given cell must exceed a threshold to activate a DNA damage "checkpoint" for cell division. How might these precedents influence the integrity of orgDNA in plants?

Pristine DNA in the gametes is required for maintaining the lineage of a sexually reproducing organism. High-quality DNA is maintained by damage repair in a eukaryote with a single cell type, such as yeast or *Chlamydomonas*, regardless of the metabolic cost of DNA repair. But for a species with embryonic development (like maize), the high cost of DNA repair can be reduced by powering germline cells with "quiet" metabolism (neither respiration nor photosynthesis) and the somatic cells with "active" metabolism (both respiration and photosynthesis) (Bendich, 2010). Of course, full repair of DNA damage is required in the meristem. But low oxygen, low H_2O_2, and high peroxidase and catalase reduce the potential for oxidative DNA damage, lowering the cost to repair both orgDNA and nuclear DNA. Thus, the local repair of a low level of damage to orgDNA would suffice, and repair pathways including BER, HR, and perhaps MMEJ operate in both plastids and mitochondria in some plants (Boesch et al., 2011; Garcia-Medel et al., 2019). Maize was not among those investigated, although its plastid proteome does contain DNA repair proteins, and most of these (including RecA) were found in greater abundance in the proplastids at the leaf base than in chloroplasts at the leaf tip (Majeran et al., 2012). Although wild type Arabidopsis ptDNA contains some ssDNA, a large increase in ssDNA regions was found in a *cprecA* mutant (Rowan et al., 2010). In maize leaf, if RecA expression is turned off following ROS signaling, ssDNA should accumulate in orgDNA leading to its demise. For somatic cells in the leaf, the plant can "afford" to not repair all of the high oxidatively damaged copies of their organellar genomes, thereby reducing the high cost of orgDNA repair, although repair of nuclear DNA is required for cellular homeostasis and checkpoint control of cell division.

CONCLUSION

Studies on ROS in plants typically consider the effects following biotic and abiotic stress. Here, we focus on changes in ROS and antioxidant agents under normal, non-stressful growth conditions and show that the ROS levels increase in whole cells and in plastids and mitochondria during maize leaf development. Although we report changes in the relative levels of ROS and antioxidant agents, a deeper understanding of ROS in oxidative stress and signaling may be gained when new methods are developed to measure absolute concentrations. Previously, we showed differences in the maintenance and degradation of ptDNA between maize and other plants, including tobacco and Arabidopsis (Shaver et al., 2006; Rowan and Bendich, 2009). These differences could be due to variations in response to ROS signaling. We propose that orgDNA degradation in maize leaf is a result of an increase in oxidative damage to orgDNA and ROS-signaling that leads to a decrease in orgDNA repair systems.

DATA AVAILABILITY STATEMENT

All datasets generated for this study are included in the article/**Supplementary Material**.

AUTHOR CONTRIBUTIONS

DT and AN performed the experiments. DT, AN, and DO analyzed the data. DT, DO, and AB wrote the manuscript. All authors have read and approved the final version of the manuscript.

FUNDING

This research was funded by the Junat Fund (a private charitable fund). Mitochondrial immunofluorescence data were acquired using an Olympus IX81 microscope located in the Biology Imaging Facility at the University of Washington.

SUPPLEMENTARY MATERIAL

The Supplementary Material for this article can be found online at: https://www.frontiersin.org/articles/10.3389/fpls.2020.00596/full#supplementary-material

REFERENCES

Alscher, R. G., Erturk, N., and Heath, L. S. (2002). Role of superoxide dismutases (SODs) in controlling oxidative stress in plants. *J. Exp. Bot.* 53, 1331–1341.

Asada, K. (2006). Production and scavenging of reactive oxygen species in chloroplasts and their functions. *Plant Physiol.* 141, 391–396. doi: 10.1104/pp.106.082040

Bantele, S. C. S., and Pfander, B. (2019). Quantitative mechanisms of DNA damage sensing and signaling. *Curr. Genet.* 66, 59–62. doi: 10.1007/s00294-019-01007-4

Baruch-Torres, N., and Brieba, L. G. (2017). Plant organellar DNA polymerases are replicative and translesion DNA synthesis polymerases. *Nucleic Acids Res.* 45, 10751–10763. doi: 10.1093/nar/gkx744

Bendich, A. J. (2010). Mitochondrial DNA, chloroplast DNA and the origins of development in eukaryotic organisms. *Biol. Direct.* 5:42. doi: 10.1186/1745-6150-5-42

Boesch, P., Weber-Lotfi, F., Ibrahim, N., Tarasenko, V., Cosset, A., Paulus, F., et al. (2011). DNA repair in organelles: pathways, organization, regulation, relevance in disease and aging. *Biochim. Biophys. Acta* 1813, 186–200. doi: 10.1016/j.bbamcr.2010.10.002

Bokhari, B., and Sharma, S. (2019). Stress marks on the genome: use or lose? *Int. J. Mol. Sci.* 20:364. doi: 10.3390/ijms20020364

Brunkard, J. O., and Burch-Smith, T. M. (2018). Ties that bind: the integration of plastid signalling pathways in plant cell metabolism. *Essays Biochem.* 62, 95–107. doi: 10.1042/EBC20170011

Cerny, M., Habanova, H., Berka, M., Luklova, M., and Brzobohaty, B. (2018). Hydrogen peroxide: its role in plant biology and crosstalk with signalling networks. *Int. J. Mol. Sci.* 19:2812. doi: 10.3390/ijms19092812

Christensen, A. C. (2018). "Mitochondrial DNA Repair and Genome Evolution," In *Annual Plant Reviews*, 2nd Edn, ed J. A. Roberts (New York, NY: Wiley-Blackwell), 11–31. doi: 10.1093/gbe/evt069

Considine, M. J., Diaz-Vivancos, P., Kerchev, P., Signorelli, S., Agudelo-Romero, P., Gibbs, D. J., et al. (2017). Learning to breathe: developmental phase transitions in oxygen status. *Trends Plant Sci.* 22, 140–153. doi: 10.1016/j.tplants.2016.11.013

Corpas, F. J., Barroso, J. B., Palma, J. M., and Rodriguez-Ruiz, M. (2017). Plant peroxisomes: a nitro-oxidative cocktail. *Redox Biol.* 11, 535–542. doi: 10.1016/j.redox.2016.12.033

Diaz-Vivancos, P., de Simone, A., Kiddle, G., and Foyer, C. H. (2015). Glutathione–linking cell proliferation to oxidative stress. *Free Radic. Biol. Med.* 89, 1154–1164. doi: 10.1016/j.freeradbiomed.2015.09.023

Ding, X., Jimenez-Gongora, T., Krenz, B., and Lozano-Duran, R. (2019). Chloroplast clustering around the nucleus is a general response to pathogen perception in *Nicotiana benthamiana*. *Mol. Plant Pathol.* 20, 1298–1306. doi: 10.1111/mpp.12840

Exposito-Rodriguez, M., Laissue, P. P., Yvon-Durocher, G., Smirnoff, N., and Mullineaux, P. M. (2017). Photosynthesis-dependent H2O2 transfer from chloroplasts to nuclei provides a high-light signalling mechanism. *Nat. Commun.* 8:49. doi: 10.1038/s41467-017-00074-w

Foyer, C. H. (2018). Reactive oxygen species, oxidative signaling and the regulation of photosynthesis. *Environ. Exp. Bot.* 154, 134–142. doi: 10.1016/j.envexpbot.2018.05.003

Foyer, C. H., and Noctor, G. (2016). Stress-triggered redox signalling: what's in pROSpect? *Plant Cell Environ.* 39, 951–964. doi: 10.1111/pce.12621

Garcia-Medel, P. L., Baruch-Torres, N., Peralta-Castro, A., Trasvina-Arenas, C. H., Torres-Larios, A., and Brieba, L. G. (2019). Plant organellar DNA polymerases repair double-stranded breaks by microhomology-mediated end-joining. *Nucleic Acids Res.* 47, 3028–3044. doi: 10.1093/nar/gkz039

Gutman, B. L., and Niyogi, K. K. (2009). Evidence for base excision repair of oxidative DNA damage in chloroplasts of *Arabidopsis thaliana*. *J. Biol. Chem.* 284, 17006–17012. doi: 10.1074/jbc.M109.008342

Halliwell, B. (2006). Reactive species and antioxidants. Redox biology is a fundamental theme of aerobic life. *Plant Physiol.* 141, 312–322. doi: 10.1104/pp.106.077073

Imlay, J. A. (2013). The molecular mechanisms and physiological consequences of oxidative stress: lessons from a model bacterium. *Nat. Rev. Microbiol.* 11, 443–454. doi: 10.1038/nrmicro3032

Janku, M., Luhova, L., and Petrivalsky, M. (2019). On the origin and fate of reactive oxygen species in plant cell compartments. *Antioxidants* 8, 105. doi: 10.3390/antiox8040105

Kemeleva, E. A., Sinitsyna, O. I., Conlon, K. A., Berrios, M., Kolosova, N. G., Zharkov, D. O., et al. (2006). Oxidation of guanine in liver and lung DNA of prematurely aging OXYS rats. *Biochemistry* 71, 612–618. doi: 10.1134/s0006297906060046

King, A., Gottlieb, E., Brooks, D. G., Murphy, M. P., and Dunaief, J. L. (2004). Mitochondria-derived reactive oxygen species mediate blue light-induced death of retinal pigment epithelial cells. *Photochem. Photobiol.* 79, 470–475. doi: 10.1562/le-03-17.1

Kohli, S. K., Khanna, K., Bhardwaj, R., Abd Allah, E. F., Ahmad, P., and Corpas, F. J. (2019). Assessment of subcellular ROS and NO metabolism in higher plants: multifunctional signaling molecules. *Antioxidants* 8:641. doi: 10.3390/antiox8120641

Kumar, R. A., Oldenburg, D. J., and Bendich, A. J. (2014). Changes in DNA damage, molecular integrity, and copy number for plastid DNA and mitochondrial DNA during maize development. *J. Exp. Bot.* 65, 6425–6439. doi: 10.1093/jxb/eru359

Kumar, R. A., Oldenburg, D. J., and Bendich, A. J. (2015). Molecular integrity of chloroplast DNA and mitochondrial DNA in mesophyll and bundle sheath cells of maize. *Planta* 241, 1221–1230. doi: 10.1007/s00425-015-2253-0

Liebthal, M., Maynard, D., and Dietz, K. J. (2018). Peroxiredoxins and redox signaling in plants. *Antioxid. Redox. Signal.* 28, 609–624. doi: 10.1089/ars.2017.7164

Locato, V., Cimini, S., and De Gara, L. (2018). ROS and redox balance as multifaceted players of cross-tolerance: epigenetic and retrograde control of gene expression. *J. Exp. Bot.* 69, 3373–3391. doi: 10.1093/jxb/ery168

Majeran, W., Friso, G., Asakura, Y., Qu, X., Huang, M., Ponnala, L., et al. (2012). Nucleoid-enriched proteomes in developing plastids and chloroplasts from maize leaves: a new conceptual framework for nucleoid functions. *Plant Physiol.* 158, 156–189. doi: 10.1104/pp.111.188474

Markkanen, E. (2017). Not breathing is not an option: how to deal with oxidative DNA damage. *DNA Repair* 59, 82–105. doi: 10.1016/j.dnarep.2017.09.007

Maruta, T., Sawa, Y., Shigeoka, S., and Ishikawa, T. (2016). Diversity and evolution of ascorbate peroxidase functions in chloroplasts: more than just a classical antioxidant enzyme? *Plant Cell Physiol.* 57, 1377–1386. doi: 10.1093/pcp/pcv203

Maslowska, K. H., Makiela-Dzbenska, K., and Fijalkowska, I. J. (2019). The SOS system: a complex and tightly regulated response to DNA damage. *Environ. Mol. Mutagen.* 60, 368–384. doi: 10.1002/em.22267

Mhamdi, A., Queval, G., Chaouch, S., Vanderauwera, S., Van Breusegem, F., and Noctor, G. (2010). Catalase function in plants: a focus on *Arabidopsis* mutants as stress-mimic models. *J. Exp. Bot.* 61, 4197–4220. doi: 10.1093/jxb/erq282

Mittler, R. (2017). ROS are good. *Trends Plant Sci.* 22, 11–19. doi: 10.1016/j.tplants.2016.08.002

Mohyeldin, A., Garzon-Muvdi, T., and Quinones-Hinojosa, A. (2010). Oxygen in stem cell biology: a critical component of the stem cell niche. *Cell Stem Cell.* 7, 150–161. doi: 10.1016/j.stem.2010.07.007

Mullineaux, P. M., Exposito-Rodriguez, M., Laissue, P. P., and Smirnoff, N. (2018). ROS-dependent signalling pathways in plants and algae exposed to high light: comparisons with other eukaryotes. *Free Radic. Biol. Med.* 122, 52–64. doi: 10.1016/j.freeradbiomed.2018.01.033

Myouga, F., Hosoda, C., Umezawa, T., Iizumi, H., Kuromori, T., Motohashi, R., et al. (2008). A heterocomplex of iron superoxide dismutases defends chloroplast nucleoids against oxidative stress and is essential for chloroplast development in *Arabidopsis*. *Plant Cell* 20, 3148–3162. doi: 10.1105/tpc.108.061341

Noctor, G., and Foyer, C. H. (2016). Intracellular redox compartmentation and ROS-related communication in regulation and signaling. *Plant Physiol.* 171, 1581–1592. doi: 10.1104/pp.16.00346

Noctor, G., Mhamdi, A., Chaouch, S., Han, Y., Neukermans, J., Marquez-Garcia, B., et al. (2012). Glutathione in plants: an integrated overview. *Plant Cell Environ.* 35, 454–484. doi: 10.1111/j.1365-3040.2011.02400.x

Noctor, G., Mhamdi, A., and Foyer, C. H. (2016). Oxidative stress and antioxidative systems: recipes for successful data collection and interpretation. *Plant Cell Environ.* 39, 1140–1160. doi: 10.1111/pce.12726

Noctor, G., Reichheld, J. P., and Foyer, C. H. (2018). ROS-related redox regulation and signaling in plants. *Semin. Cell Dev. Biol.* 80, 3–12. doi: 10.1016/j.semcdb.2017.07.013

Oldenburg, D. J., and Bendich, A. J. (2004). Changes in the structure of DNA molecules and the amount of DNA per plastid during chloroplast development in maize. *J. Mol. Biol.* 344, 1311–1330. doi: 10.1016/j.jmb.2004.10.001

Oldenburg, D. J., and Bendich, A. J. (2015). DNA maintenance in plastids and mitochondria of plants. *Front. Plant Sci.* 6:883. doi: 10.3389/fpls.2015.00883

Oldenburg, D. J., Kumar, R. A., and Bendich, A. J. (2013). The amount and integrity of mtDNA in maize decline with development. *Planta* 237, 603–617. doi: 10.1007/s00425-012-1802-z

Oldenburg, D. J., Rowan, B. A., Zhao, L., Walcher, C. L., Schleh, M., and Bendich, A. J. (2006). Loss or retention of chloroplast DNA in maize seedlings is affected by both light and genotype. *Planta* 225, 41–55. doi: 10.1007/s00425-006-0329-6

Park, E., Caplan, J. L., and Dinesh-Kumar, S. P. (2018). Dynamic coordination of plastid morphological change by cytoskeleton for chloroplast-nucleus communication during plant immune responses. *Plant Signal. Behav.* 13:e1500064. doi: 10.1080/15592324.2018.1500064

Pilon, M., Ravet, K., and Tapken, W. (2011). The biogenesis and physiological function of chloroplast superoxide dismutases. *Biochim. Biophys. Acta* 1807, 989–998. doi: 10.1016/j.bbabio.2010.11.002

Rogers, S. O., and Bendich, A. J. (1985). Extraction of DNA from milligram amounts of fresh, herbarium and mummified plant tissues. *Plant Mol. Biol.* 5, 69–76. doi: 10.1007/BF00020088

Rowan, B. A., and Bendich, A. J. (2009). The loss of DNA from chloroplasts as leaves mature: fact or artefact? *J. Exp. Bot.* 60, 3005–3010. doi: 10.1093/jxb/erp158

Rowan, B. A., Oldenburg, D. J., and Bendich, A. J. (2010). RecA maintains the integrity of chloroplast DNA molecules in *Arabidopsis*. *J. Exp. Bot.* 61, 2575–2588. doi: 10.1093/jxb/erq088

Runge, K. W., and Li, Y. (2018). A curious new role for MRN in *Schizosaccharomyces pombe* non-homologous end-joining. *Curr. Genet.* 64, 359–364. doi: 10.1007/s00294-017-0760-1

Scandalios, J. G., Tong, W.-F., and Roupakias, D. G. (1980). *Cat3*, a third gene locus coding for a tissue-specific catalase in maize: Genetics, intracellular location, and some biochemical properties. *Mol. Gen. Genet.* 179, 33–41. doi: 10.1007/BF00268443

Scully, R., Panday, A., Elango, R., and Willis, N. A. (2019). DNA double-strand break repair-pathway choice in somatic mammalian cells. *Nat. Rev. Mol. Cell Biol.* 20, 698–714. doi: 10.1038/s41580-019-0152-0

Shaver, J. M., Oldenburg, D. J., and Bendich, A. J. (2006). Changes in chloroplast DNA during development in tobacco, *Medicago truncatula*, pea, and maize. *Planta* 224, 72–82. doi: 10.1007/s00425-005-0195-7

Sheen, J. (1995). Methods for mesophyll and bundle sheath cell separation. *Methods Cell Biol.* 49, 305–314. doi: 10.1016/s0091-679x(08)61462-4

Shen, J., Deininger, P., Hunt, J. D., and Zhao, H. (2007). 8-Hydroxy-2'-deoxyguanosine (8-OH-dG) as a potential survival biomarker in patients with nonsmall-cell lung cancer. *Cancer*109, 574–580. doi: 10.1002/cncr.22417

Skarstad, K., and Boye, E. (1993). Degradation of individual chromosomes in *recA* mutants of *Escherichia coli*. *J. Bacteriol.* 175, 5505–5509.

Smirnoff, N. (2018). Ascorbic acid metabolism and functions: a comparison of plants and mammals. *Free Radic. Biol. Med.* 122, 116–129. doi: 10.1016/j.freeradbiomed.2018.03.033

Smirnoff, N., and Arnaud, D. (2019). Hydrogen peroxide metabolism and functions in plants. *New Phytol.* 221, 1197–1214. doi: 10.1111/nph.15488

Soares, C., Carvalho, M. E. A., Azevedo, R. A., and Fidalgo, F. (2019). Plants facing oxidative challenges—A little help from the antioxidant networks. *Environ. Exp. Bot.* 161, 4–25. doi: 10.1016/j.envexpbot.2018.12.009

Spampinato, C. P. (2017). Protecting DNA from errors and damage: an overview of DNA repair mechanisms in plants compared to mammals. *Cell Mol. Life. Sci.* 74, 1693–1709. doi: 10.1007/s00018-016-2436-2

Stern, D. B., Hanson, M. R., and Barkan, A. (2004). Genetics and genomics of chloroplast biogenesis: maize as a model system. *Trends Plant Sci.* 9, 293–301. doi: 10.1016/j.tplants.2004.04.001

Sylvester, A. W., Cande, W. Z., and Freeling, M. (1990). Division and differentiation during normal and *liguleless-1* maize leaf development. *Development* 110, 985–1000.

Wallace, S. S. (2013). DNA glycosylases search for and remove oxidized DNA bases. *Environ. Mol. Mutagen.* 54, 691–704. doi: 10.1002/em.21820

Weits, D. A., Kunkowska, A. B., Kamps, N. C. W., Portz, K. M. S., Packbier, N. K., Nemec Venza, Z., et al. (2019). An apical hypoxic niche sets the pace of shoot meristem activity. *Nature* 569, 714–717. doi: 10.1038/s41586-019-1203-6

Yang, S., Yu, Q., Zhang, Y., Jia, Y., Wan, S., Kong, X., et al. (2018). ROS: the fine-tuner of plant stem cell fate. *Trends Plant Sci.* 23, 850–853. doi: 10.1016/j.tplants.2018.07.010

Zamocky, M., Furtmuller, P. G., and Obinger, C. (2008). Evolution of catalases from bacteria to humans. *Antioxid. Redox. Signal.* 10, 1527–1548. doi: 10.1089/ars.2008.2046

Zandalinas, S. I., Sengupta, S., Burks, D., Azad, R. K., and Mittler, R. (2019). Identification and characterization of a core set of ROS wave-associated transcripts involved in the systemic acquired acclimation response of *Arabidopsis* to excess light. *Plant J.* 98, 126–141. doi: 10.1111/tpj.14205

Zeng, J., Dong, Z., Wu, H., Tian, Z., and Zhao, Z. (2017). Redox regulation of plant stem cell fate. *EMBO J.* 36, 2844–2855. doi: 10.15252/embj.201695955

Zheng, Q., Oldenburg, D. J., and Bendich, A. J. (2011). Independent effects of leaf growth and light on the development of the plastid and its DNA content in *Zea* species. *J. Exp. Bot.* 62, 2715–2730. doi: 10.1093/jxb/erq441

Conflict of Interest: The authors declare that the research was conducted in the absence of any commercial or financial relationships that could be construed as a potential conflict of interest.

frontiers in Plant Science

ORIGINAL RESEARCH
published: 03 June 2020
doi: 10.3389/fpls.2020.00682

Flavonoid Naringenin Alleviates Short-Term Osmotic and Salinity Stresses Through Regulating Photosynthetic Machinery and Chloroplastic Antioxidant Metabolism in *Phaseolus vulgaris*

*Evren Yildiztugay[1], Ceyda Ozfidan-Konakci[2], Mustafa Kucukoduk[3] and Ismail Turkan[4]**

[1] Department of Biotechnology, Faculty of Science, Selcuk University, Konya, Turkey, [2] Department of Molecular Biology and Genetics, Faculty of Science, Necmettin Erbakan University, Konya, Turkey, [3] Department of Biology, Faculty of Science, Selcuk University, Konya, Turkey, [4] Department of Biology, Faculty of Science, Ege University, Bornova, Turkey

OPEN ACCESS

Edited by:
Francisco J. Corpas, Estación Experimental del Zaidín (EEZ), Spain

Reviewed by:
José A. Hernández, Consejo Superior de Investigaciones Científicas (CSIC), Spain
Mirza Hasanuzzaman, Sher-e-Bangla Agricultural University, Bangladesh

***Correspondence:**
Ismail Turkan
ismail.turkan@ege.edu.tr

Specialty section:
This article was submitted to Plant Metabolism and Chemodiversity, a section of the journal Frontiers in Plant Science

Received: *19 February 2020*
Accepted: *30 April 2020*
Published: *03 June 2020*

Citation:
Yildiztugay E, Ozfidan-Konakci C, Kucukoduk M and Turkan I (2020) Flavonoid Naringenin Alleviates Short-Term Osmotic and Salinity Stresses Through Regulating Photosynthetic Machinery and Chloroplastic Antioxidant Metabolism in Phaseolus vulgaris. Front. Plant Sci. 11:682. doi: 10.3389/fpls.2020.00682

The current study was conducted to demonstrate the possible roles of exogenously applied flavonoid naringenin (Nar) on the efficiency of PSII photochemistry and the responses of chloroplastic antioxidant of salt and osmotic-stressed *Phaseolus vulgaris* (*cv. Yunus90*). For this aim, plants were grown in a hydroponic culture and were treated with Nar (0.1 mM and 0.4 mM) alone or in a combination with salt (100 mM NaCl) and/or osmotic (10% Polyethylene glycol, −0.54 MPa). Both caused a reduction in water content (RWC), osmotic potential (Ψ_Π), chlorophyll fluorescence (F_v/F_m), and potential photochemical efficiency (F_v/F_o). Nar reversed the changes on these parameters. The phenomenological fluxes (TR_o/CS and ET_o/CS) altered by stress were induced by Nar and Nar led to a notable increase in the performance index (PI_{ABS}) and the capacity of light reaction [$\Phi P_o/(1-\Phi P_o)$]. Besides, Nar-applied plants exhibited higher specific fluxes values [ABS/RC, ET_o/RC, and $\Psi E_o/(1-\Psi E_o)$] and decreasing controlled dissipation of energy (DI_o/CS_o and DI_o/RC). The transcripts levels of psbA and psbD were lowered in stress-treated bean but upregulated in Nar-treated plants after stress exposure. Nar also alleviated the changes on gas exchange parameters [carbon assimilation rate (A), stomatal conductance (g_s), intercellular CO_2 concentrations (C_i), transpiration rate (E), and stomatal limitation (L_s)]. By regulating the antioxidant metabolism of the isolated chloroplasts, Nar was able to control the toxic levels of hydrogen peroxide (H_2O_2) and TBARS (lipid peroxidation) produced by stresses. Chloroplastic superoxide dismutase (SOD) activity reduced by stresses was increased by Nar. In response to NaCl, Nar increased the activities of ascorbate peroxidase (APX), glutathione reductase (GR), monodehydroascorbate reductase (MDHAR), and dehydroascorbate reductase (DHAR), as well as peroxidase (POX). Nar protected the bean chloroplasts by minimizing disturbances caused by NaCl exposure via the ascorbate (AsA) and glutathione (GSH) redox-based systems. Under Nar plus PEG, Nar maintained the AsA regeneration by

the induction of MDHAR and DHAR, but not GSH recycling by virtue of no induction in GR activity and the reduction in GSH/GSSG and GSH redox state. Based on these advances, Nar protected in bean chloroplasts by minimizing disturbances caused by NaCl or PEG exposure via the AsA or GSH redox-based systems and POX activity.

Keywords: antioxidant enzymes, chloroplast isolation, naringenin, photosynthetic efficiency, stress

INTRODUCTION

Plants are simultaneously subjected to the combination of salinity and osmotic stresses rather than the effects of an individual stress. Plants have common defense responses against these stresses. Photosynthesis is inhibited by decreasing intercellular CO_2 concentrations depending on stomatal closure under both salt and osmotic stresses (Cheeseman, 2013). Chloroplasts, one of the cell compartments, have a central role in cell pathways such as biosynthesis of aromatic amino acids, fatty acids and carotenoids, and sulfate and nitrogen assimilation, as well as photosynthesis and are sensitive to stress conditions. Some of symptoms triggered by stress in plants is associated with the process occurred in chloroplasts. Due to the highly energetic reactions of photosynthesis, the reduction of molecular oxygen generates toxic reactive oxygen species (ROS), which interacts with essential and important molecules such as DNA, photosynthetic pigments, and proteins (Miller et al., 2010; Flowers et al., 2015). The accumulation of ROS causes the photoinhibition of photosystem I (PSI), the disruption in the structure of photosynthetic pigments, the inactivation of the elongation factor of D1 protein, the inhibition in the repair of photosystem II (PSII) and the decline of rubisco activity (Acosta-Motos et al., 2017; Bose et al., 2017). Stress treatments easily occur the damage in the reaction centers (RCs) of PSII (Strauss et al., 2006). The data on the photosynthetic performance is provided with the phenomenological and biophysical parameters in plants (Gururani et al., 2015). The responses of photosynthetic apparatus with these parameters are evaluated through OJIP fluorescence transients (called a JIP test). The OJIP test was developed by Strasser et al. (1995), and the parameters are calculated using the generated chlorophyll fluorescence induction curve according to the JIP-test method (Zeliou et al., 2009). The JIP test shows the measurement of several phenological and biophysical expressions of PSII including the fluxes of absorption, trapping, and electron transport (Strasser et al., 2000).

Cell detoxification mechanisms against ROS accumulation include the induced gene expression of enzymatic antioxidants including superoxide dismutase (SOD), peroxidase (POX), and ascorbate peroxidase (APX), glutathione reductase (GR), monodehydroascorbate reductase (MDHAR), dehydroascorbate reductase (DHAR) that are related to AsA-GSH cycle (Asada-Halliwell pathway) (Dai et al., 2012; Uzilday et al., 2012; Carvalho et al., 2015). APX, along with the oxidation of AsA, generates monodehydroascorbate (MDHA). MDHA is spontaneously turned into the oxidized state (dehydroascorbate, DHA). MDHA and DHA are reduced to AsA by the activities of NADPH-dependent MDHAR and GSH-dependent DHAR, respectively. As well as AsA, GSH has important roles to cope with the damage caused by ROS (Batth et al., 2017). To maintain of GSH pool, oxidized glutathione (GSSG) is reduced by GR via the consumption of NADPH (de Sousa et al., 2016).

Flavonoids are small molecular secondary metabolites synthesized by plants. The phenylpropanoid pathway is responsible for the synthesis of flavonoids (D'Amelia et al., 2018). After stress exposure to plants, the biosynthesis of flavonoids is induced. The flavonoids diminished the negative effects of stressful conditions by inhibition of ROS-generating enzymes such as lipoxygenase and xanthine oxidase, the chelation of transition metal ions, and the scavenging activity as an antioxidant agent (Baskar et al., 2018). Their eliminating feature against ROS comes from their catechol group in the B-ring of the flavonoid skeleton. They accumulate in mesophyll cells, vacuole and chloroplasts and stabilize the chloroplast membrane against stress (Martinez et al., 2016). Depending on the location of the flavonoids, some reports suggested them as an important component in photoprotection under stress (Agati and Tattini, 2010). For example, chloroplast-localized flavonoids reduced the ROS generation in excess light irradiance-treated *Phyllirea latifolia* (Agati et al., 2002). Also, flavonoids within chloroplasts protect the function of the membrane during cellular dehydration (Inoue, 2011). Many data revealed that there is an interaction between the levels of induced flavonoids and antioxidant action under different stress treatments such as ozone, heat and salinity (Gondor et al., 2016; Martinez et al., 2016; Pheomphun et al., 2019). Mahajan and Yadav (2013) found that exogenous flavonoid quercetin and epicatechin regulates the antioxidant enzymes at transcriptional levels in tobacco seedlings. As well as abiotic factors, upon exposure to biotic stress conditions, bacterial or fungal-mediated infection is inhibited by flavanols (such as myricetin) and anthocyanins (such as delphinidin) (Karageorgou and Manetas, 2006).

Naringenin (Nar) is a flavonoid belonging to flavanones subclass. It is widely distributed in several citrus fruits, bergamot, tomatoes, and other fruits, being found in its glycosides form (mainly naringin) as well. The chemical name of Nar is 2,3-dihydro-5,7-dihydroxy-2-(4-hydroxyphenyl)-4H-1-benzopyran-4-one (Salehi et al., 2019). Nar is derived from the hydrolysis of glycone forms of this flavanone, such as naringin or narirutin. The effects of Nar have been one of the immense study topics in animal systems (Salehi et al., 2019). However, the number of researches on its possible roles on plant growth, metabolism, and stress responses in plants is rather scanty. In several of those, Nar has been reported to suppress the growth of annual plant species, acting as an

allelochemical. Similarly, Nar has been reported to cause a decrease in the growth of *Arabidopsis thaliana* (Hernandez and Munne-Bosch, 2012). This inhibitory effect of Nar was attributed at least to some extent, through impaired auxin transport. Deng et al. (2004) suggested that it exert its inhibitory effect by inhibiting the activity of the key enzyme of the phenylpropanoid pathway, 4-coumarate: CoA ligase, whereas Bido et al. (2010) assumed that the action site of naringenin may be related to other enzymes working at later steps of the phenylpropanoid pathway, such as cell wall–bound POX or, perhaps, cinnamyl alcohol dehydrogenase. Hence, the mode of action of naringenin still remains an open question in plant systems. However, the information about the interaction flavonoids including Nar with the activity of antioxidants localized in chloroplasts under individual or combined-treated stress treatments is unclear. Besides, hardly any data is available about the influence of exogenous applied flavonoid on quantum efficiencies and phenomenological energy fluxes indicating the vitality of PSII in photosynthetic machinery after stress exposure. In this regard, after chloroplast isolation of sampling groups in bean (*Phaseolus vulgaris* L.) leaves, we have focused on explanation the effects of exogenously applied Nar in five steps: (i) the effects of Nar on water content and osmotic potential under salt and/or osmotic stresses; (ii) the effects of Nar on gas exchange parameters such as carbon assimilation rate, transpiration rate, stomatal conductance and stomatal limitation; (iii) the determination the effects of Nar on the photochemical reactions and fluorescence transients and, on the expression levels of genes encoding the major extrinsic proteins of PSII such as psbA and psbD; (iv) the effects of Nar on the responses of antioxidant in chloroplasts of stress-treated plants; and (v) the effects of Nar on ROS content and lipid peroxidation in chloroplasts.

MATERIALS AND METHODS

Plant Material

Common bean seeds (*P. vulgaris cv. Yunus90*) were obtained from the Bahri Dagdas International Agricultural Research Institute, Turkey. The procedures of germination and growth were cited from Yildiztugay et al. (2014).

The Applications of Stress and Naringenin and the Sampling

For naringenin (Nar; 0.1 mM and 0.4 mM) and salt (NaCl, 100 mM)/osmotic Polyethylene glycol, 10% PEG6000, −0.54 MPa (Hellal et al., 2018) stress treatments, it was prepared by being dissolved in Hoagland solution and was added to the growth medium at the stage of 21 days old. An experiment was designed as twelve groups and was listed in **Supplementary Table S1**. The toxic levels of NaCl and PEG were chosen base on the study of Kurniasih et al. (2016) and Shatpathy et al. (2018), respectively. For determination of Nar application, the doses of Nar were selected as 0.1 mM and 0.4 mM according to Liu et al. (2012). Plants were harvested after 72 hours (h) of treatment.

Determination of Water Content and Osmotic Potential

After harvest, six leaves were obtained and their fresh weight (FW) was determined. The leaves were floated on de-ionized water for 6 h and the turgid tissue was blotted dry prior to determining turgid weight (TW). Dry weight (DW) was determined after oven drying at 70°C. The leaf relative water content (RWC) was calculated by the following formula (Smart and Bingham, 1974):

$$RWC(\%) = [(FW - DW)/(TW - DW)] \times 100$$

Leaves were extracted by crushing the material with a glass rod. Leaf osmotic potential (Ψ_{Pi}) was measured by Vapro Vapor pressure Osmometer 5600. Ψ_{Pi} was converted to MPa according to Santa-Cruz et al. (2002) by multiplying by a coefficient of 2.408×10^{-3}.

Determination of Photosynthetic Efficiency and OJIP Analysis

A portable fluorometer (Handy PEA, Hansatech Instruments Ltd., Norfolk, United Kingdom) was used to determine the maximal quantum yield of PSII photochemistry (F_v/F_m), physiological state of the photosynthetic apparatus (F_o/F_m) and potential photochemical efficiency (F_v/F_o). Many parameters showing the structure and function of photosynthetic apparatus were detected by Handy PEA (Plant Efficiency Analyzer, Hansatech Instruments Ltd). The measurement was defined in **Table 1** and the radar plot included the average values of the photosynthetic parameters of treatments groups in bean plants.

Gene Expression Analysis

RNA isolation was completed given by Ozgur et al. (2015). The nucleic acid concentrations of total RNA and cDNA were measured by a Multiskan Go (Thermo Fisher Scientific, Waltham, MA, United States). To detect relative gene expression for each group, the threshold cycle value was normalized the actin and each sample was evaluated with three replications. The primer sequences and qRT-PCR conditions are given in **Supplementary Table S2**.

Determination of Gas Exchange Parameters

Carbon assimilation rate (A), stomatal conductance (g_s), intercellular CO_2 concentration (C_i) and transpiration rate (E) were detected with a portable gas exchange system (LCpro$^+$; ADC, Hoddesdon, United Kingdom). The stomatal limitation value (L_s) was calculated as $1 - C_i/C_a$ (Ma et al., 2011).

The Isolation Procedure for Chloroplasts of *Phaseolus vulgaris*

The leaves were homogenized using a blender in isolation buffer containing 0.1 M Tris–HCl (pH 7·8), 0.3 M sorbitol, 5 mM $MgCl_2$, 10 mM NaCl, 0.1% bovine serum albumin (BSA). The homogenate was filtered through four layers of cheesecloth, and

TABLE 1 | The abbreviations and definitions of terms used by the JIP-test.

Abbreviations	Definitions
Area	Total complementary area between the fluorescence induction curve and F_m
RC	Reaction center
CS	Cross section or measured area of sample
F_o	Minimal fluorescence of dark-adapted leaves
F_m	Maximal fluorescence of dark-adapted leaves
F_v	Variable chlorophyll fluorescence (F_m-F_o)
ET	Electron transfer
F_v/F_m	Maximum quantum yield of primary photochemistry of PSII
F_o/F_m or φDo	Quantum yield of absorbed photons for electron transport
F_v/F_o	Efficiency of the water-splitting complex on the donor side of PSII
ET_o/CS_o	Electron transport flux per cross section (CS) at $t = 0$
TR_o/CS_o	Trapping per excited cross section
DI_o/CS_o	Dissipated energy flux per cross section (CS) at $t = 0$
ABS/RC	Absorption flux (of antenna chlorophylls) per RC
ET_o/RC	Electron transport flux (further than Q_A^-) per RC
TR_o/RC	Trapped energy flux (leading to Q_A reduction) per RC
$\Phi P_o/(1-\Phi P_o)$	Q_A-reducing RCs per PSII antenna chlorophyll
$\Psi E_o/(1-\Psi E_o)$	the efficiency with which a trapped exciton transfers an electron to the photosynthetic ET chain
γRC/(1-γRC)	The fraction of PSII chlorophyll a molecule that function as reaction centers
DI_o/RC	Dissipated energy flux per reaction center
PI_{ABS}	Performance index (potential) for energy conservation from exciton to the reduction of intersystem electron acceptors
PI_{total}	Performance index (potential) for energy conservation from exciton to the reduction of PSI and acceptors

the filtrate was centrifuged at 1000 × *g* for 6 min at 4°C. The supernatant was discarded, and the pellet was resuspended in the isolation buffer. Resuspended chloroplasts were overlaid on a 40% Percoll solution and centrifuged at 1700 × *g* for 7 min at 4°C. Intact chloroplasts were obtained after this centrifugation as a pellet which was resuspended again in the isolation buffer without BSA. Intactness of the chloroplasts was determined by using a ferricyanide reduction test (Lilley et al., 1975). For analysis of enzyme activity and for the native activity gels, chloroplasts were lysed with a lysis solution (10 mM HEPES-KOH (pH 7.2), 0.1 mM EDTA, 1 mM $MgCl_2$, 0.1% Triton-X100) for 1 h at 4°C. Where APX was estimated, 5 mM ascorbate was added into the isolation buffer.

Determination of Isozyme and/or Enzyme Compositions

The total soluble protein content was analyzed (Bradford, 1976). The electrophoretic separation was detected on non-denaturing polyacrylamide miniature slab gels (8 cm × 10 cm) using the Mini PROTEAN Tetra Cell electrophoresis (Bio-Rad). Due to the high number of treatment groups and the low number of wells in the electrophoresis apparatus, the groups were divided into two as (i) C, Nar1, Nar2, S, S + Nar1, S + Nar2; and (ii) D, S, D + Nar1, D + Nar2, SD, SD + Nar1, SD + Nar2 and the gels were loaded to two different running modules at the same time. Samples were exposed to non-denaturing polyacrylamide gel electrophoresis (PAGE) as shown by Laemmli (1970). Chloroplastic SOD (EC 1.15.1.1) activity assay was based on the method of Beauchamp and Fridovich (1971). SOD isozyme activity was detected by staining with riboflavin and nitroblue tetrazolium. SOD isozyme patterns were determined by incubating the gels with 5 mM H_2O_2 to inhibit both Cu/Zn-SOD and Fe-SOD, or with 5 mM KCN to inhibit only Cu/Zn-SOD. Before staining of SOD activity, the control group was preincubated with 50 mM potassium phosphate buffer (pH 7.8) alone, buffer plus H_2O_2, or buffer plus KCN. POX isozymes were detected according to Seevers et al. (1971). The POX (EC 1.11.1.7) activity was done according to the procedure given by Herzog and Fahimi (1973). Electrophoretic APX separation was performed according to Mittler and Zilinskas (1993). Glutathione S-transferase (GST, EC: 2.5.1.18) activity was calculated following the method of Hossain et al. (2006). For GST isozyme activity, the method of Ricci et al. (1984) was used. NADPH oxidase (NOX) isozymes were identified by NBT reduction method as described by Sagi and Fluhr (2001). The samples containing 40 mg protein was loaded per lane. Total NOX (EC 1.6.3.1) activity was measured according to Jiang and Zhang (2002). The assay medium contained 50 mM Tris–HCl buffer, 0.5 mM XTT, 100 mM NADPH.Na_4 and 20 mg of protein sample. After addition of NADPH, XTT reduction was followed at 470 nm. Activity was calculated using the extinction coefficient, 2.16×10^4 M^{-1} cm^{-1}. One unit of NOX was defined as 1 nmol ml^{-1} XTT oxidized min^{-1}.

Determination of Enzyme Activity Related to AsA-GSH Cycle

Chloroplastic activities of APX (EC 1.11.1.11), GR (EC 1.6.4.2), monodehydroascorbate reductase (MDHAR; EC 1.6.5.4), dehydroascorbate reductase (DHAR; EC 1.8.5.1) were detected according to Foyer and Halliwell (1976); Nakano and Asada (1981), Dalton et al. (1986), and Miyake and Asada (1992), respectively. Total and reduced contents of ascorbate (AsA) were determined according to the method of Dutilleul et al. (2003). The oxidized form of ascorbate (DHA, dehydroascorbate) was calculated using the formula DHA = Total AsA - Reduced AsA. Glutathione (GSH) was assayed according to Paradiso et al. (2008). Oxidized glutathione (GSSG) was determined after removal of GSH by 2-vinylpyridine derivatization.

Gels stained with chloroplastic SOD, POX, APX, NOX, and GST activities were photographed with the Gel Doc XR^+ System and then analyzed with Image Lab software v4.0.1 (Bio-Rad, Hercules, CA, United States). Activities of isoenzymes (0.5 units of SOD and 0.2 units of POX) were measured according to the known standard amounts.

Determination of H_2O_2 Content and Lipid Peroxidation Levels

H_2O_2 was determined according to Cheeseman (2006) using eFOX reagent. This modified ferrous ammonium sulphate/xylenol orange (FOX) assay was used due to its sensitivity, stability, and adaptability to a large number of

samples. In this assay, 1% ethanol is added to the reagent, which increases its sensitivity to H_2O_2 by 50% (i.e., eFOX). Extraction was carried out using ice-cold acetone containing 25 mM H_2SO_4 for intact chloroplasts. Samples were then centrifuged for 5 min at 3000 × *g* at 4°C. eFOX reagent [950 μL of 250 μM ferrous ammonium sulfate, 100 μM xylenol orange, 100 μM sorbitol, 1% ethanol (v/v)] was used for 50 μL of supernatant. Reaction mixtures were incubated at room temperature for 30 min and then absorbance at 550 and 800 nm was measured. H_2O_2 concentrations were calculated using a standard curve prepared with known concentrations of H_2O_2.

Lipid peroxidation (thiobarbituric acid reactive substances (TBARS) content) was determined according to Rao and Sresty (2000). TBARS concentration was calculated from the absorbance at 532 nm, and measurements were corrected for non-specific turbidity by subtracting the absorbance at 600 nm. The concentration of TBARS was calculated using an extinction coefficient of 155 mM^{-1} cm^{-1}.

Statistical Analysis

The experiments were repeated thrice independently, and each data point was the mean of six replicates. All data obtained were subjected to a one-way analysis of variance (ANOVA). Statistical analysis of the values was performed by using SPSS 20.0. Tukey's post-test was used to compare the treatment groups. Comparisons with $p < 0.05$ were considered significantly different. In all figures, the error bars represent standard errors of the means.

RESULTS

The Effects of Nar on Physiological Parameters in Response to Stress

Figure 1A shows that there was a significant decrement in RWC under the alone or the combined treatments of stresses. There was a maximum reduction in the combination form of stresses (NaCl plus PEG) by 1.4-fold. The presence of Nar provided the high levels of RWC under stress-treated plants. On the other hand, Nar alone did not affect RWC compared to the control group.

Salinity and osmotic stresses led to a considerable decrease in Ψ_Π of bean (**Figure 1B**). The decreased values of Ψ_Π were reversed by exogenously applied Nar in response to stress. Similar to the results of RWC, no effect was created on Ψ_Π through Nar alone under control conditions.

The Effects of Nar on Photosynthetic Efficiency in Response to Stress

Figures 2A–C revealed that both stress treatments significantly inhibited F_v/F_m and F_v/F_o of bean leaves. The lowest levels of F_v/F_m and F_v/F_o were at the combination form of stresses (by 18.5 and 54.6% declines, respectively). However, stress caused an induction in F_o/F_m and this effect induced by stress was more noticeable at NaCl + PEG group by 88.2% increase (**Figure 2B**). When bean plants were treated with Nar applications under stress, remarkable responses were created on F_v/F_m, F_o/F_m, and F_v/F_o levels. The results for these parameters were close to control group or higher than that of one. However, no effect on F_v/F_m, F_o/F_m, and F_v/F_o was detected after the solo applications of Nar (except for Nar2 on F_v/F_o).

The phenomenological energy fluxes are presented in **Figures 2D–F**. Stress treatments resulted in a decline in ET_o/CS_o (**Figure 2D**), and TR_o/CS_o (**Figure 2E**), but the increment in DI_o/CS_o was observed at NaCl and/or PEG stress (**Figure 2F**). On the other hand, there was the opposite changes in all these parameters of Nar-treated bean plants, as compared to the stress alone. Similar to stress + Nar groups, Nar applications under control conditions promoted the levels of ET_o/CS_o and TR_o/CS_o.

The Effects of Nar on Photosynthetic Machinery in Response to Stress

Figure 3 showed the values of photosynthetic parameters in all the treatment groups as a radar plot. NaCl or PEG and their combined form caused the similar responses in photosynthetic machinery. While, the specific energy fluxes in thylakoid membranes per reaction centers of sample (ABS/RC, ET_o/RC, and TR_o/RC) decreased in chloroplasts of bean with stress, this effect was reversed by Nar applications. These parameters were similar to the control group or increased in Nar-treated plants.

NaCl and/or PEG caused a decrease in the efficiency of light reaction [$\Phi P_o/(1-\Phi P_o)$] and the rate of biochemical reaction [$\Psi E_o/(1-\Psi E_o)$] and γRC/(1-γRC), but Nar applications resulted in an increase in these parameters. Interestingly, stress resulted in an increment in energy dissipation (DI_o/RC) of bean chloroplasts. However, these values were reversed by the Nar applications. Depending on the changes of these parameters [ΦPo/(1-ΦPo), ΨEo/(1-ΨEo) and γRC/(1-γRC)], stress lowered the performance index detected on energy absorption of chloroplasts (PI_{ABS} and PI_{total}) and the reduction rate was lower in PEG-treated plants than that of the NaCl ones. Also, the lowest reduction was under the combined stress treatments. Both Nar applications alone were provided the high index levels.

The Effects of Nar on the Transcription Levels of psbA and psbD in Response to Stress

Stress had considerable effect on the relative transcription of the psbA gene in bean leaves, which was a maximum reduction in NaCl-treated plants (**Figure 4A**). Both Nar alone and Nar together with stress assuaged the stress-triggered reduction in psbA transcription compared to that of the control and stress alone group, respectively. The transcription levels of this gene were noticeably increased by a 0.4 mM Nar application under stress or non-stress.

While NaCl-induced salinity suppressed the gene expression of psbD to its lowest levels (by 37.5% decrease), there was no significant difference among the control plants, PEG- and NaCl + PEG-treated plants (**Figure 4B**). Exogenously applied Nar to stressed plants upregulated the psbD gene to a level above that observed in the stress-treated alone. The psbD gene detected the highest upregulation after S + D + Nar1

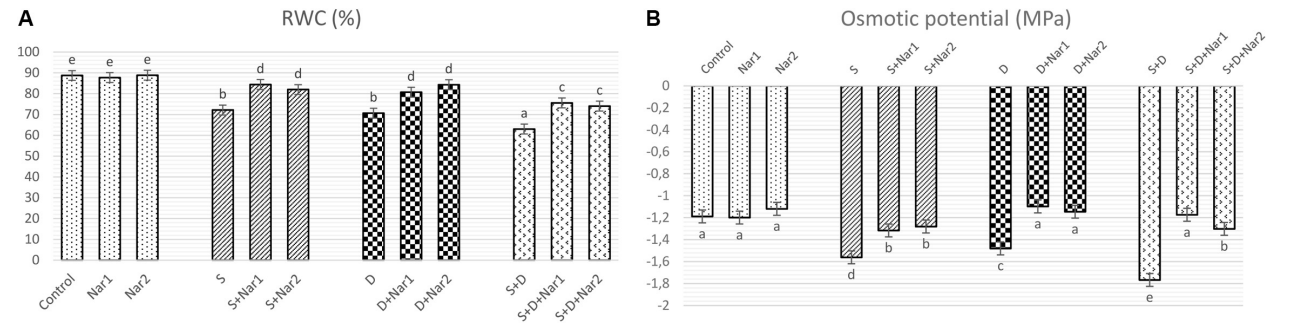

FIGURE 1 | The effects of exogenously applied Nar (Nar1, 0.1 mM and Nar2, 0.4 mM) on water status in bean leaves under alone or combination of salt (S, 100 mM NaCl) and PEG-induced osmotic (D, 10% PEG6000) stress. **(A)** the relative water content (RWC), **(B)** the osmotic potential (Ψ_{II}). For each group, vertical bars indicate ± SE and the different lowercase letters are significantly different ($p < 0.05$) values according to the Tukey test.

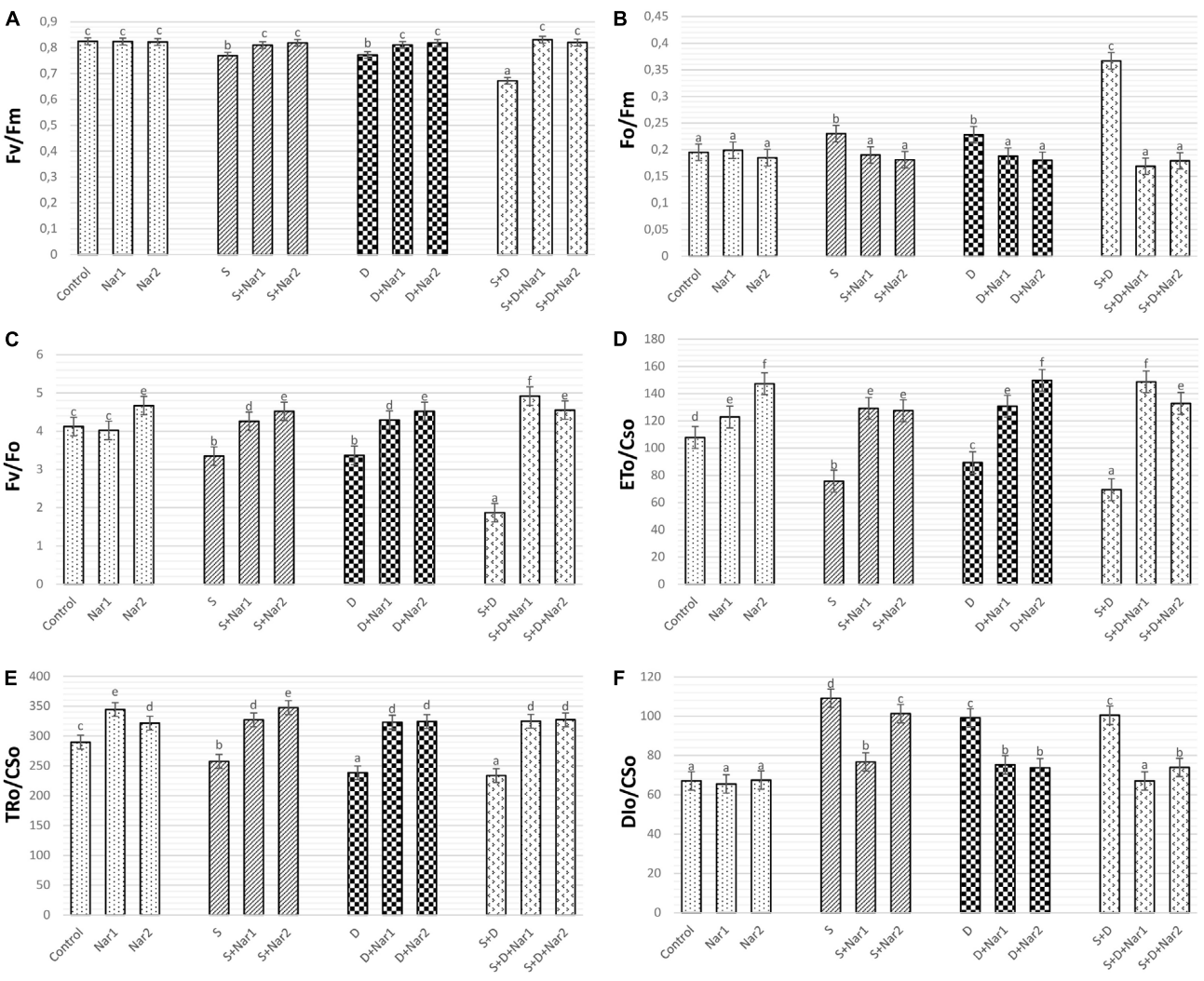

FIGURE 2 | The effects of exogenously applied Nar (Nar1, 0.1 mM and Nar2, 0.4 mM) on the photosynthetic machinery and the phenomenological energy fluxes in bean leaves under alone or combination of salt (S, 100 mM NaCl) and PEG-induced osmotic (D, 10% PEG6000) stress. **(A)** the maximal quantum yield of PSII photochemistry (F_v/F_m), **(B)** the physiological state of the photosynthetic apparatus (F_o/F_m), **(C)** the potential photochemical efficiency (F_v/F_o), **(D)** the electron transport flux per cross section (ET_o/CS_o), **(E)** the energy flux trapped per cross section (CS) (TR_o/CS_o), **(F)** The dissipated energy flux per cross section (DI_o/CS_o). For each group, vertical bars indicate ± SE and the different lowercase letters are significantly different ($p < 0.05$) values according to the Tukey test.

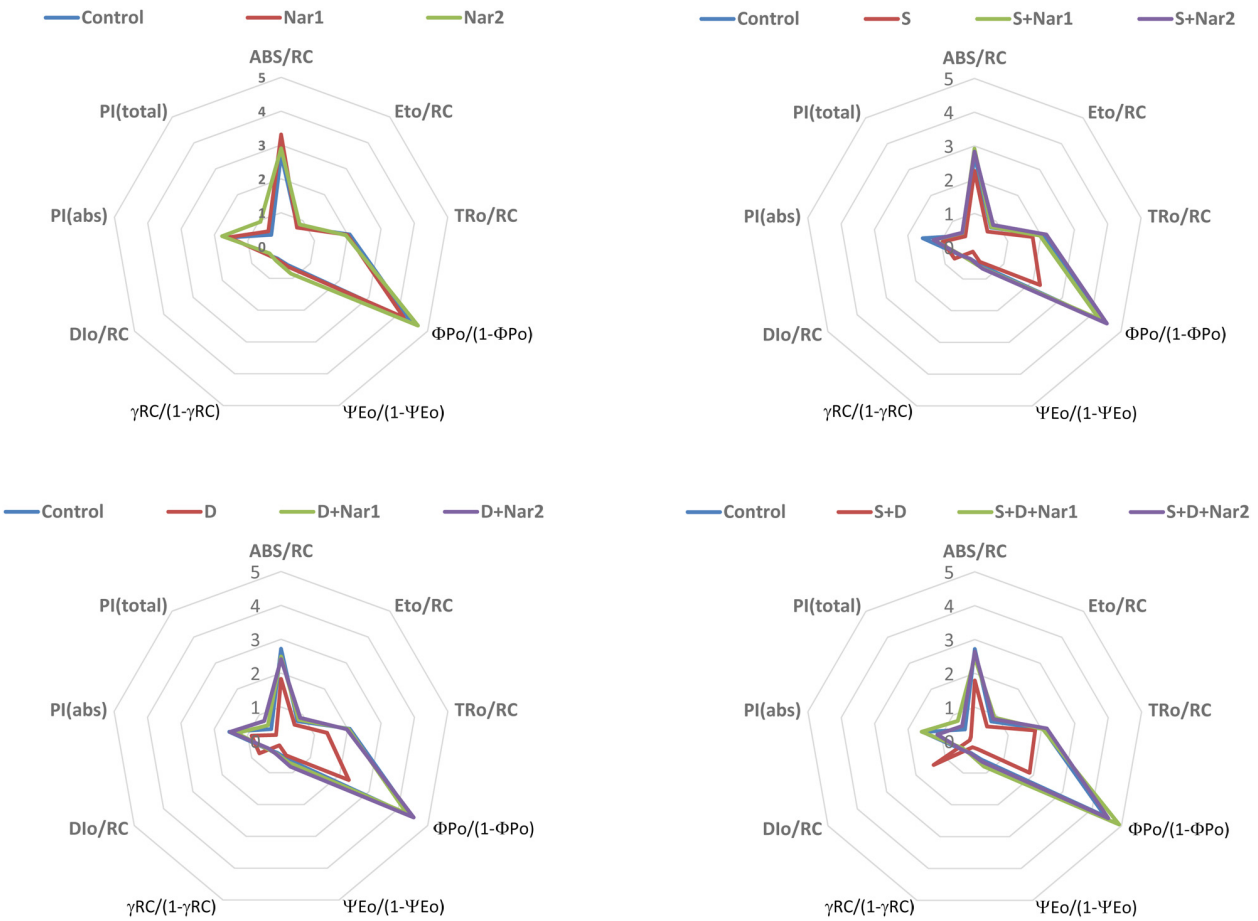

FIGURE 3 | The effects of exogenously applied Nar (Nar1, 0.1 mM and Nar2, 0.4 mM) on the radar plot with a series parameter derived from JIP-test analyses of the experimental fluorescence OJIP transients in bean leaves under alone or combination of salt (S, 100 mM NaCl) and PEG-induced osmotic (D, 10% PEG6000) stress. ABS/RC, average absorption per active reaction center; ET_o/RC, electron transport flux per active reaction centers; TR_o/RC, flux or exciton trapped per active reaction center; $\Phi P_o/(1-\Phi P_o)$, Q_A-reducing RCs per PSII antenna chlorophyll; $\Psi E_o/(1-\Psi E_o)$, the efficiency with which a trapped exciton transfers an electron to the photosynthetic electron transfer chain; γRC/(1-γRC), Q_A- reducing reaction centers per PSII antenna chlorophyll; DI_o/RC, ratio of total dissipation to the amount of active reaction center; PI_{ABS}, performance index based on the absorption of light energy; PI_{total}, performance index (potential) for energy conservation from exciton to the reduction of PSI and acceptors.

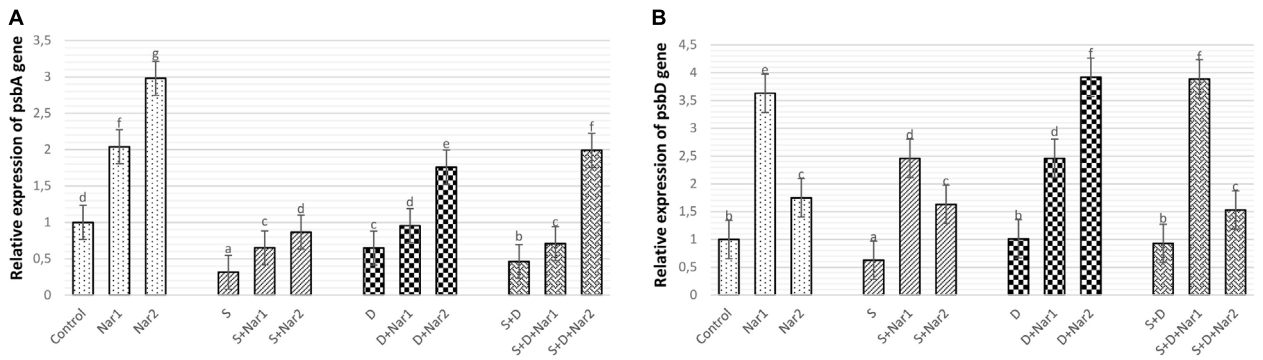

FIGURE 4 | The effects of exogenously applied Nar (Nar1, 0.1 mM and Nar2, 0.4 mM) on the relative expression of genes encoding reaction center core proteins in photosystem of bean chloroplasts under alone or combination of salt (S, 100 mM NaCl) and PEG-induced osmotic (D, 10% PEG6000) stress. **(A)** the relative expression of psbA, **(B)** the relative expression of psbD. For each group, vertical bars indicate ± SE and the different lowercase letters are significantly different ($p < 0.05$) values according to the Tukey test.

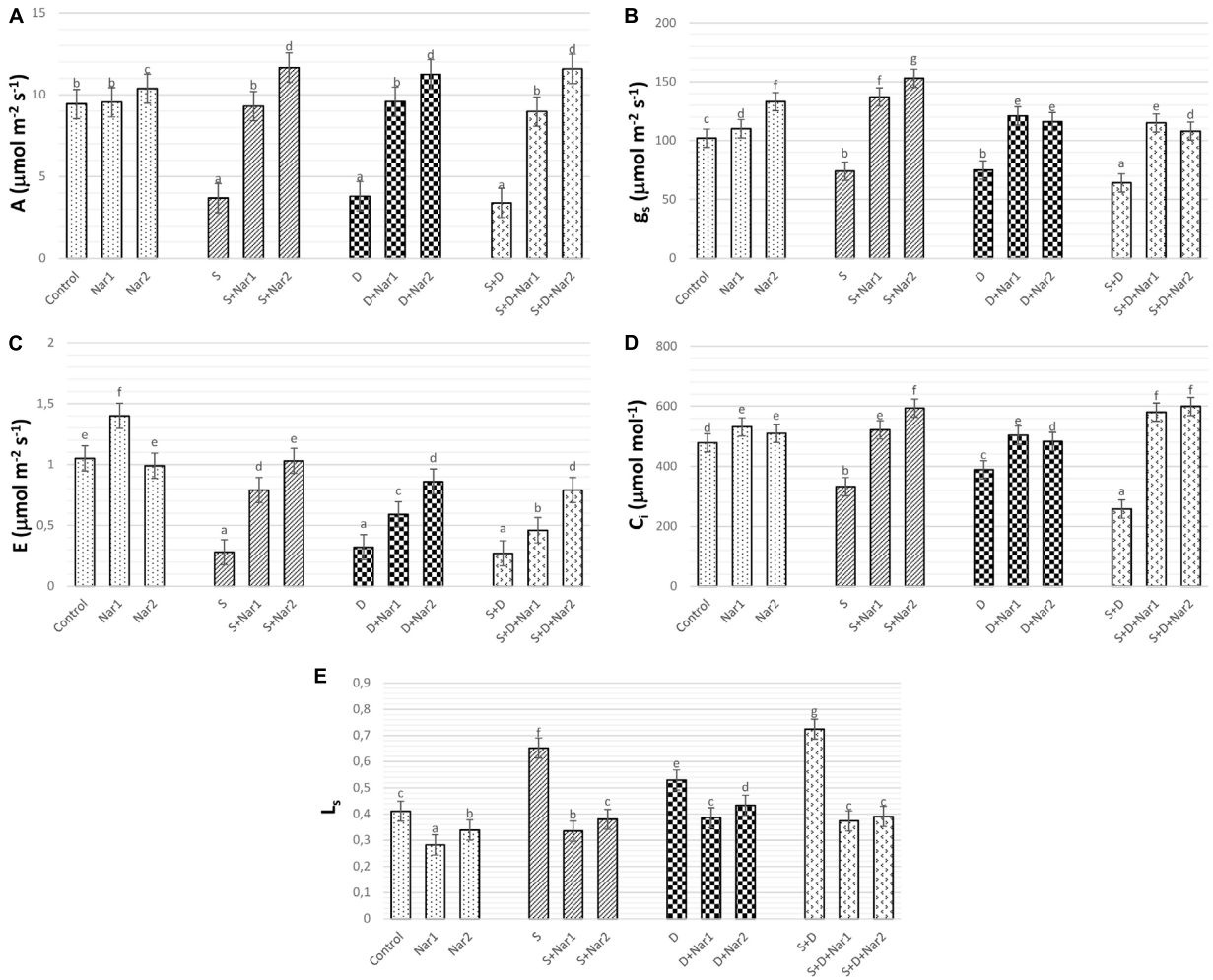

FIGURE 5 | The effects of exogenously applied Nar (Nar1, 0.1 mM and Nar2, 0.4 mM) on the gas exchange parameters in bean leaves under alone or combination of salt (S, 100 mM NaCl) and PEG-induced osmotic (D, 10% PEG6000) stress. **(A)** Carbon assimilation rate (A), **(B)** stomatal conductance (g_s), **(C)** transpiration rate (E), **(D)** intercellular CO_2 concentration (C_i), **(E)** stomatal limitation value (L_s). For each group, vertical bars indicate ± SE and the different lowercase letters are significantly different ($p < 0.05$) values according to the Tukey test.

by 4.1-fold. In terms of the transcript levels of psbD gene, similar response was observed at Nar alone as compared to the control group.

The Effects of Nar on Gas Exchange in Response to Stress

As well as the combined treatment, salt and osmotic stresses reduced A values, which reached the minimum levels at NaCl + PEG by 64.05% (**Figure 5A**). Similar trend was observed in g_s (**Figure 5B**), E (**Figure 5C**), and C_i (**Figure 5D**) values of stress-treated bean plants. The reduction rate of A, g_s, E, and C_i was higher in the combination form of stresses. Also, these reductions in A, g_s, E, and C_i were prevented by Nar treatments under stress conditions. On the other hand, after exposure to NaCl or PEG, the stomatal limitations resulted in 58.6 or 28.9% increase, respectively (**Figure 5E**). Both Nar applications caused a decline in L_s in response to stress or control conditions.

The Effects of Nar on the Isozyme and/or Enzyme Compositions in Response to Stress

As illustrated by **Figure 6A**, three SOD isozymes (Fe-SODs, Fe-SOD1-3) were detected by native page analysis in bean chloroplasts. However, Cu/Zn-SOD could not be identified. As compared to the control group, the chloroplastic SOD activity was reduced by PEG and NaCl + PEG (**Figure 6B**), depending on especially the intensities of Fe-SOD2 (**Figure 6A**). However, the plants treated with NaCl exhibited any effect in SOD activity. There was an increment in SOD activity of Nar-treated plants under stress. The induction in SOD (24.8%) was only observed the high Nar application under non-stress conditions.

Gel analysis revealed that four chloroplastic POX isozymes (POX1-4) were viewed in the evaluation of POX isozyme profiles (**Figure 6C**). The isozyme activity of POX of bean was higher by NaCl or PEG, providing the intensities of POX1-2. Interestingly,

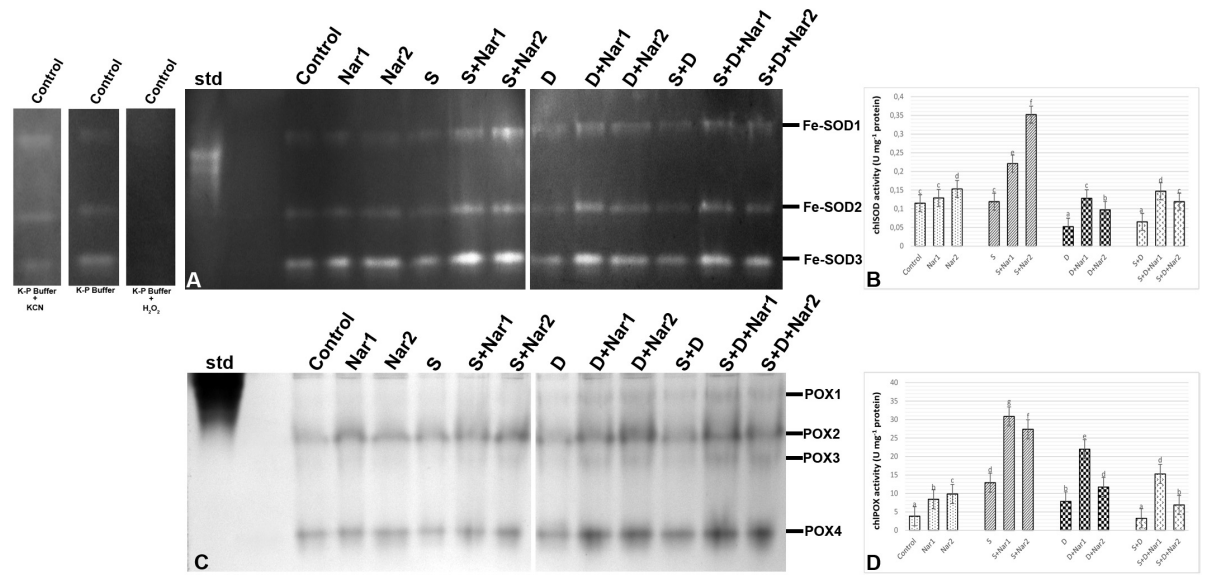

FIGURE 6 | The effects of exogenously applied Nar (Nar1, 0.1 mM and Nar2, 0.4 mM) on some antioxidant enzyme activities in bean leaves under alone or combination of salt (S, 100 mM NaCl) and PEG-induced osmotic (D, 10% PEG6000) stress. **(A)** The relative band intensity of chloroplastic superoxide dismutase isoenzymes (SOD), **(B)** chloroplastic SOD activity, **(C)** the relative band intensity of different types of chloroplastic peroxidase isoenzymes (POX), **(D)** chloroplastic POX activity. Due to the high number of treatment groups and the low number of wells in the electrophoresis apparatus, the groups were divided into two as (i) C, Nar1, Nar2, S, S + Nar1, S + Nar2) and (ii) D, S, D + Nar1, D + Nar2, SD, SD + Nar1, SD + Nar2) and the gels were loaded to two different running modules at the same time. For the determination of SOD isozymes, before staining of SOD activity, the control group was preincubated with 50 mM potassium phosphate buffer (pH 7.8) alone, buffer plus 5 mM H_2O_2, or buffer plus 4 mM KCN. For each group, vertical bars indicate ± SE and the different lowercase letters are significantly different ($p < 0.05$) values according to the Tukey test.

when applied a combination of both, no response was observed in POX activity (**Figure 6D**). In Nar plus stress-treated plants, the intensities of POX isoforms were stronger than stress treatments alone. This effect was related to the induced intensities of POX2-4 and the new defined isozyme, POX3. Exogenously applied Nar could maintain this induction produced by stress in POX under non-stress conditions as well.

Quantification of the GST band intensities detected that three GST isozymes (GST1-3) revealed during experimental period (**Figure 7A**). The chloroplastic enzyme activity increased under all the stress treatments, as compared to the control group (**Figure 7B**). This induction of GST activity was related to the intensities of GST1-2 and GST1-2-3 in NaCl or PEG and NaCl + PEG-treated bean plants, respectively (**Figure 7A**). After NaCl treatment, Nar-treated plants had in induction in GST activity and it reached to the maximum level at S + Nar1, which was observed an enhancement by 2.03-fold. Similar trend was detected in the bean exposed to Nar together with PEG. On the other hand, chloroplastic GST activity of bean was lowered by Nar plus NaCl + PEG. Also, there was an enhancement in GST activity of Nar-treated plants under non-stress, as demonstrated by the stronger intensities of all GST isoforms.

As shown in **Figure 7C**, a total of four NOX isoenzymes was detected as NOX1-4 by native PAGE analysis. Chloroplastic NOX activity in bean was either unaffected or lower by the alone and the combined form of stress treatments (**Figure 7D**). However, bean leaves exposed to Nar and stress treatments exhibited the high NOX activity. This induction in chloroplastic NOX activity reached the maximum levels in Nar1 + NaCl-treated plants (6.2-fold). Although NOX3 isoform decreased in this treatment group (Nar1 + NaCl), the induction of the intensities of NOX1-2 was responsible for the response in activity. While 0.1 mM Nar alone created no remarkable effect on NOX activity, 0.4 mM Nar caused an increase in this enzyme compared to the control group (1.22-fold enhancement).

The Effects of Nar on the Enzyme Activity Related to AsA-GSH Cycle in Response to Stress

Examination of chloroplastic APX isoenzymes in bean identified five isoforms (APX1-5) (**Figure 8A**). The bean leaves treated with NaCl or PEG had no change in the activity of APX enzyme. However, at both NaCl and PEG, a remarkable increase in APX was measured (66.2%) and especially APX1 and APX4 isozymes were responsible for this change. After Nar applications to the stress-applied bean, the activity levels of APX isozymes were induced throughout the experimental period. Also, this induction in APX activity was observed in only the 0.1 mM Nar-treated bean leaves under the combination form of stresses (**Figure 8B**), as provided the isozyme-staining pattern (**Figure 8A**). On the other hand, 0.1 and 0.4 mM Nar alone enhanced chloroplastic APX activity by 52.3% and 60.1% increment.

Except for PEG-treated plants, NaCl alone or together with PEG caused a reduction in chloroplastic GR activity (**Figure 8C**). Nar prevented this reduction in GR only in plants with NaCl.

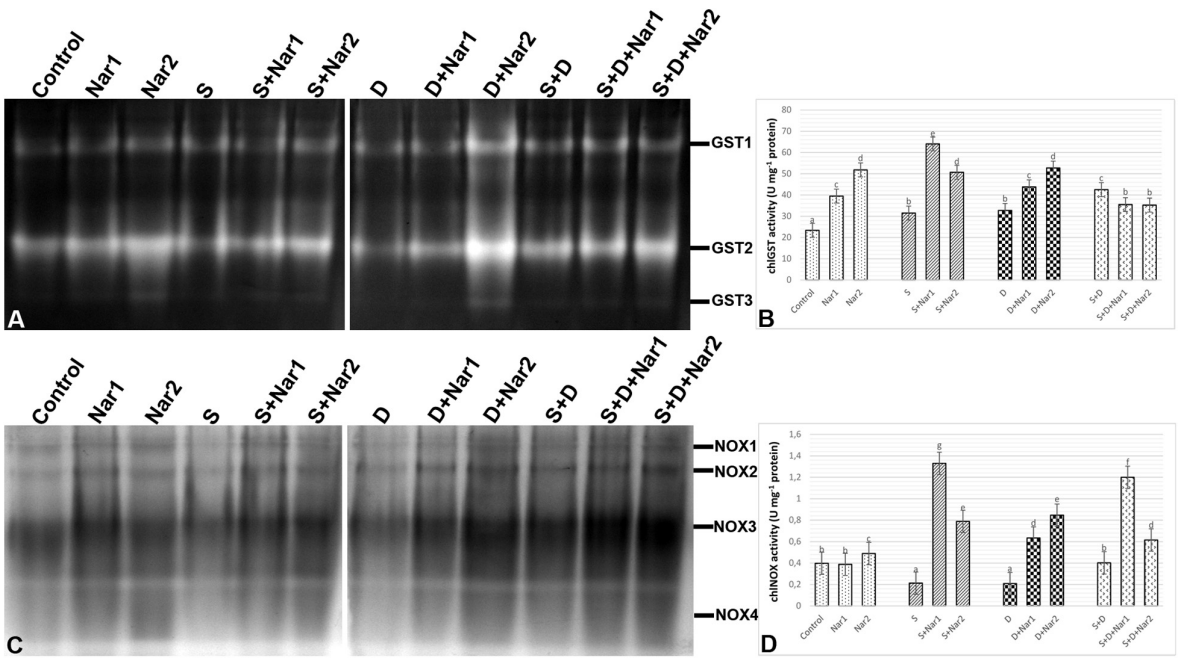

FIGURE 7 | The effects of exogenously applied Nar (Nar1, 0.1 mM and Nar2, 0.4 mM) on some antioxidant enzyme activities in bean leaves under alone or combination of salt (S, 100 mM NaCl) and PEG-induced osmotic (D, 10% PEG6000) stress. **(A)** The relative band intensity of different types of chloroplastic glutathione S-transferase (GST), **(B)** chloroplastic GST activity, **(C)** the relative band intensity of different types of chloroplastic NADPH oxidase isoenzymes (NOX), **(D)** chloroplastic NOX activity. Due to the high number of treatment groups and the low number of wells in the electrophoresis apparatus, the groups were divided into two as (i) C, Nar1, Nar2, S, S + Nar1, S + Nar2) and (ii) D, S, D + Nar1, D + Nar2, SD, SD + Nar1, SD + Nar2) and the gels were loaded to two different running modules at the same time. For each group, vertical bars indicate ± SE and the different lowercase letters are significantly different ($p < 0.05$) values according to the Tukey test.

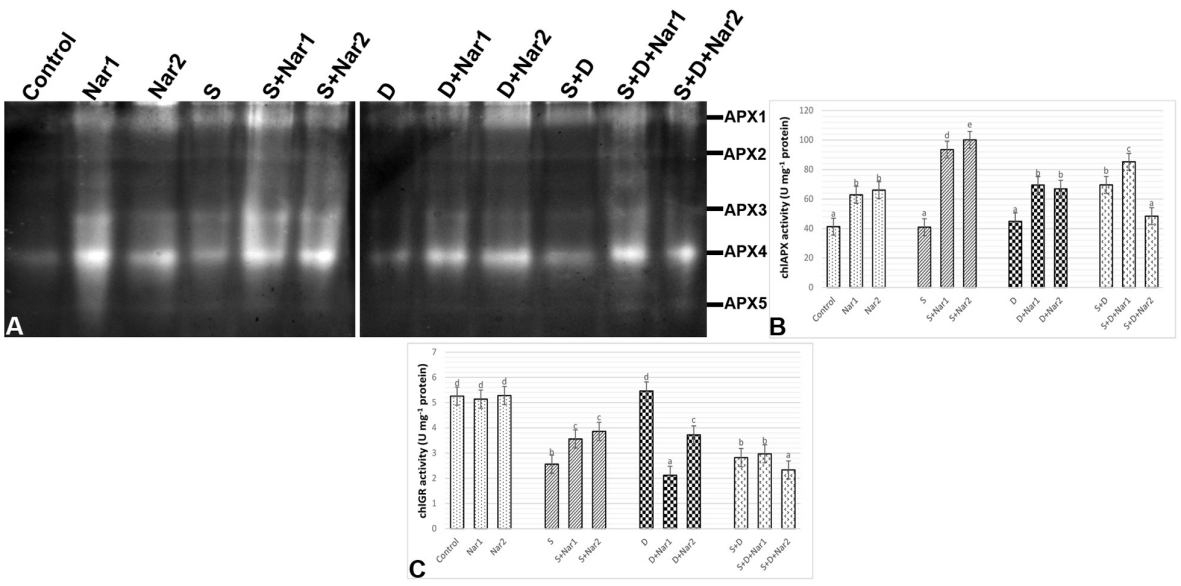

FIGURE 8 | The effects of exogenously applied Nar (Nar1, 0.1 mM and Nar2, 0.4 mM) on some antioxidant enzyme activities in bean leaves under alone or combination of salt (S, 100 mM NaCl) and PEG-induced osmotic (D, 10% PEG6000) stress. **(A)** The relative band intensity of different types of chloroplastic ascorbate peroxidase isoenzymes (APX), **(B)** chloroplastic APX activity, **(C)** chloroplastic glutathione reductase (GR). Due to the high number of treatment groups and the low number of wells in the electrophoresis apparatus, the groups were divided into two as (i) C, Nar1, Nar2, S, S + Nar1, S + Nar2) and (ii) D, S, D + Nar1, D + Nar2, SD, SD + Nar1, SD + Nar2) and the gels were loaded to two different running modules at the same time. For each group, vertical bars indicate ± SE and the different lowercase letters are significantly different ($p < 0.05$) values according to the Tukey test.

GR activity of the bean was either lower or unaffected by Nar + PEG and Nar+ the combined stress treatments. When compared to the control group, exogenously applied Nar created no remarkable effect on chloroplastic GR activity.

There was a similar response between chloroplastic MDHAR (**Figure 9A**) and DHAR (**Figure 9B**) in stress-treated bean plants. Single stress treatments (NaCl or PEG) were reduced or did not change the activities of MDHAR and DHAR. However, in response to the combined stress treatment, chloroplastic MDHAR activity was induced by 82.1% (**Figure 9A**). After Nar application was added to NaCl or PEG stress-treated plants, the activities of MDHAR and DHAR were elevated in comparison with those of the stress-treated plants alone. On the other hand, the increased activity of these enzymes was not maintained with the applications of Nar under the combined stress treatments. While, there was no effect on MDHAR activity in chloroplasts of bean exposed to 0.1 mM Nar, the elevated activity of MDHAR was detected by 0.4 mM Nar (1.2-fold), as compared to the control group. When Nar was applied alone, a reduction in DHAR of bean chloroplasts was observed (**Figure 9B**).

Compared with control group, when the bean plants were exposed to stress, chloroplastic AsA content decreased or was similar to levels of control (**Figure 9C**). The combined stress-treated plants had an increase in AsA content. A remarkable increase in AsA was detected only in bean plants with Nar plus stress (NaCl or PEG). However, the induction in AsA was not maintained by Nar applications along with NaCl + PEG. In contrast to the results of AsA, single stress treatments caused an increment in DHA content which not observe in the combination form of stresses (**Figure 9D**). NaCl or PEG-induced increment in DHA content was not maintained by exogenously applied Nar. Besides, the chloroplasts of bean with S + D + Nar2 exhibited the increment in DHA content. Under non-stress conditions, Nar alone decreased DHA content as compared to the control group.

The contents of GSH (**Figure 9E**) or GSSG (**Figure 9F**) in chloroplasts of the bean decreased or increased for the experimental period when under stress, compared to the content level of the control group, respectively. While, only the bean leaves with Nar plus NaCl had high GSH content (**Figure 9E**), there was a reduction in NaCl or PEG (exception for PEG + NaCl) in GSSG content of Nar-treated bean chloroplasts (**Figure 9F**). Besides, when comparison to the control group, the maximum induction in GSH and GSSG was at Nar2 and Nar1 by 1.6-fold and 1.2-fold, respectively. Additionally, Nar applications minimized the risk of reducing GSH redox state [the ratio of GSH content to total glutathione (GSH + GSSG)] in response to NaCl stress.

The Effects of Nar on H_2O_2 Content and Lipid Peroxidation Levels in Response to Stress

As detected in **Figure 10A**, H_2O_2 content gradually increased under stress treatments and reached the maximum levels (by 2.3-fold) in plants with NaCl plus PEG stress. While, Nar alone did not affect H_2O_2 content, after Nar treatments to the stress-treated bean plants, a decline in H_2O_2 content was detected.

Figure 10B reveals that stress treatments resulted in an induction in the levels of lipid peroxidation. The maximum rate of this increment in TBARS content was at NaCl + PEG by 74.1%. However, Nar alleviated the increased in TBARS content of both stress-treated plants. In contrast to H_2O_2 content, as compared to the control group, Nar applications had no increase in TBARS content.

DISCUSSION

Physiological Parameters

Many reports revealed that stress reduces the osmotic potential (Ψ_{Pi}) in plants (Sheldon et al., 2017). In the current study, when Ψ_{Pi} reached to more negative levels in bean under stress, the uptake of water or the efficiency of water use were reduced and then the water content (RWC) decreased. There was previous data where flavonoid levels can promote water content of rice seedlings under stress, as detected also in our study (Chutipaijit et al., 2009). In bean treated with Nar plus stress, Ψ_{Pi} reduced by NaCl and PEG was alleviated. This indicated that the induced levels of Ψ_{Pi} might help to conserve of RWC and to improve in hydration status, which was related to the higher levels of water content.

The Photochemical Performance of PSII and the Transcript Levels of psbA and psbD Genes

To investigate for determination of the tolerance range of plants against to stress, the photochemical performance of PSII plays essential roles as an informative tool. As mentioned earlier, the responses of PSII are important in determining the differences on the photosynthetic machinery between salinity and osmotic stresses (Kalaji et al., 2018). The induction kinetics in fluorescence show the reduction of electron acceptors in electron transport system (ETS) (Gururani et al., 2015). A decline in F_v/F_m and F_v/F_o levels is reported in stress-treated plants (Kalaji et al., 2011). This reduction is evidence of the damage of reaction centers in PSII, the decrease in electron transfer rates at oxidizing site of PSII and the declined number of quanta absorbed per unit time (Mehta et al., 2010). In our study, NaCl and PEG stresses caused a decrease in electron flow to reaction center of PSII, by providing a decline in F_m (acceptor side of PSII) and the area (reduced plastoquinone pool size, data not shown). However, Nar had positive effects on F_v/F_m and F_v/F_o by promotion of this value reduced by stress. By increased levels in F_v/F_m, Nar was able to induce the capacity of the energy absorbed to the reaction center by PSII under dark-adapted conditions, as suggested by Shu et al. (2016). The possible reason behind Nar-triggered increase of F_v/F_m and F_v/F_o in bean might be repairment of the degraded photosynthetic pigments in the thylakoid membrane of chloroplasts or regulation of the reduction/re-oxidation levels of quinones. Phenomenological fluxes include energy flux in the excited cross section (CS) of the sample (ET_o/CS and TR_o/CS). After NaCl treatments, a decrease in ET_o/CS_o caused the inactivation of reaction center.

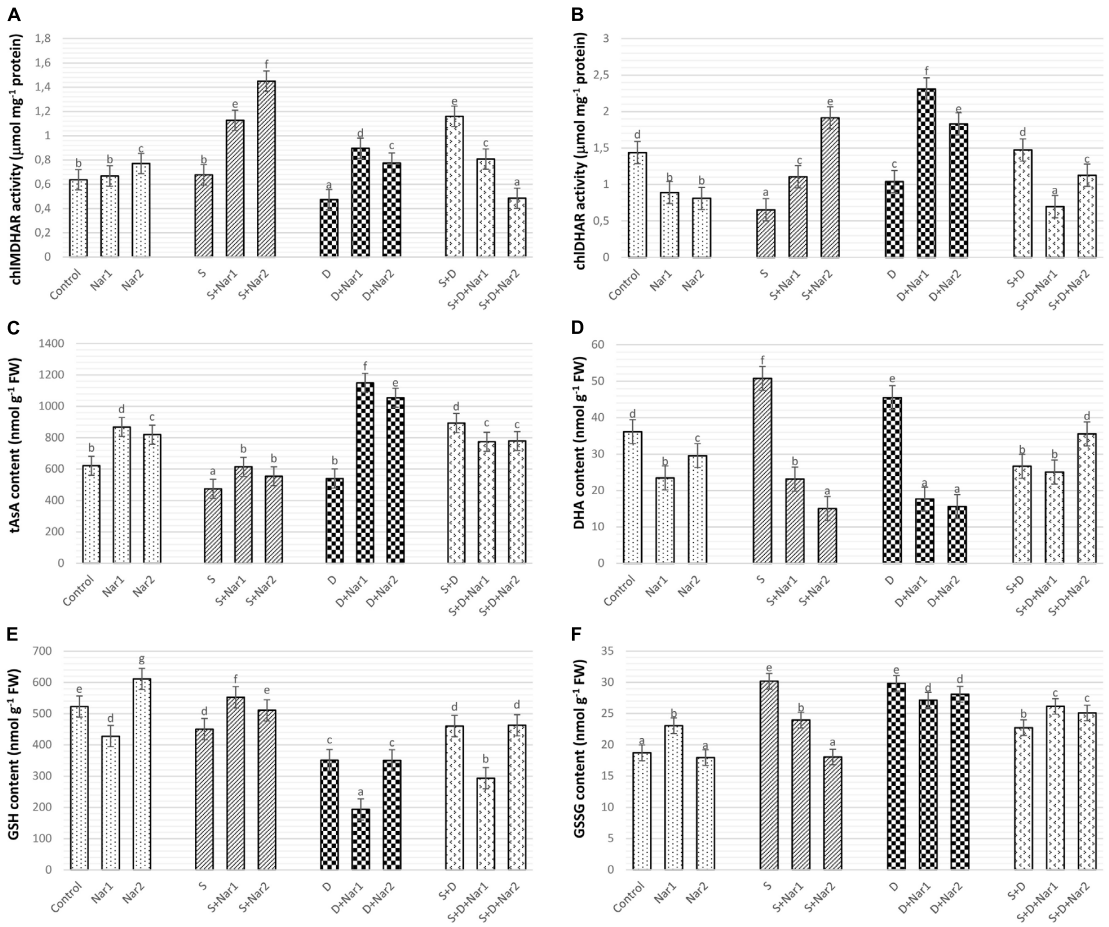

FIGURE 9 | The effects of exogenously applied Nar (Nar1, 0.1 mM and Nar2, 0.4 mM) on some antioxidant enzyme activities related to AsA-GSH cycle in bean leaves under alone or combination of salt (S, 100 mM NaCl) and PEG-induced osmotic (D, 10% PEG6000) stress. **(A)** Chloroplastic monodehydroascorbate reductase activity (MDHAR), **(B)** chloroplastic dehydroascorbate reductase activity (DHAR), **(C)** chloroplastic ascorbate content (tAsA), **(D)** chloroplastic dehydroascorbate content (DHA), **(E)** chloroplastic glutathione content (GSH), **(F)** chloroplastic oxidized glutathione (GSSG). For each group, vertical bars indicate ± SE and the different lowercase letters are significantly different ($p < 0.05$) values according to the Tukey test.

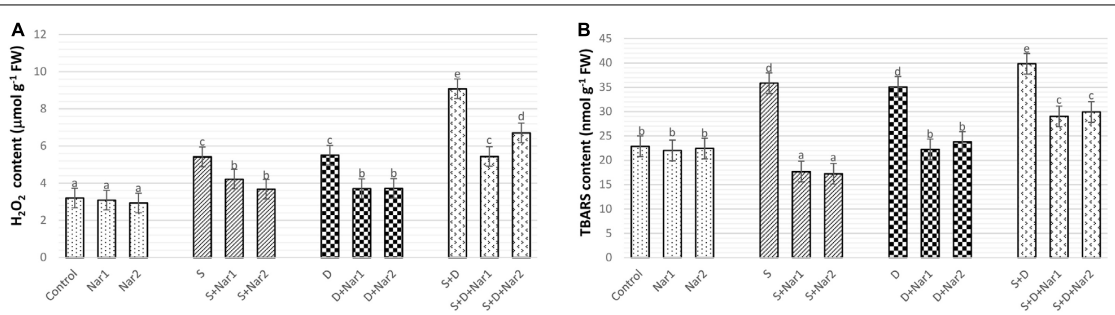

FIGURE 10 | The effects of exogenously applied Nar (Nar1, 0.1 mM and Nar2, 0.4 mM) on the ROS content and lipid peroxidation in bean leaves under alone or combination of salt (S, 100 mM NaCl) and PEG-induced osmotic (D, 10% PEG6000) stress. **(A)** hydrogen peroxide (H_2O_2), **(B)** lipid peroxidation (TBARS content). For each group, vertical bars indicate ± SE and the different lowercase letters are significantly different ($p < 0.05$) values according to the Tukey test.

However, in stress-treated bean, Nar might regulate re-oxidation of reduced quinone through electron transfer (ET) over a CS of active and inactive reaction center (RC). In the current study, the lowered the electron transport per CS (TR_o/CS) in stress-treated plants was alleviated by Nar application. NaCl and PEG-treated bean plants had a lower energy absorption by antenna pigments and energy trapping by RC. This is why there is a decrease in ET_o/CS and TR_o/CS under stress. However, the Nar-applied

bean had the ability to protection of photosynthetic pigments such as chlorophyll-a. Similar phenomenon had been observed by Dolatabadian et al. (2012) that flavonoid genistein promoted photosynthesis rate by enhancing chlorophyll content in soybean exposed to salt stress.

NaCl and/or PEG caused an induction in DI_o/CS, which was related to the levels of dissipated energy per leaf cross section. When DI_o/CS was reduced by Nar application, the energy trapping efficiency in RC of PSII was higher than that of the stressed plants, which was also connected with the higher values of F_v/F_m. ABS/RC, ET_o/RC and TR_o/RC are the specific energy flux in membranes measured per the RC of sample. ABS/RC is the ratio of a number of absorbed energies by chlorophylls to the number of active RCs (Gururani et al., 2015). In the present study, this ratio was reduced under stress conditions (NaCl and/or PEG). This reduction was related to the decline in the amount of energy flow reaching to the RC of PSII and the antenna size of RCs. The stress-induced damage in PSII in this study was reversible after Nar application and the values reached to the higher levels than that of stress alone. ET_o/RC and TR_o/RC denote electron transfer and trap per active RC of PSII, respectively (Varghese et al., 2019). Trapping of an excitation by the RC results in the reduction of Q_A to Q_A^- (Gururani et al., 2015). Under stress conditions, the overproduction of reduced Q_A^- causes a damage in reaction center (Zhao et al., 2017). In the present study, stress decreased these parameters indicating a disruption in the transport and capture of electrons by photosynthetic systems, but this situation was successfully reversed by both of two different Nar application levels. Nar also protected bean leaves from photoinhibition by maintaining the reduced quinone pool. Exogenously applied Nar resulted in the positive effects on the forward electron transport rates by increasing $\Psi E_o/(1\text{-}\Psi E_o)$ values. This recovery on $\Psi E_o/(1\text{-}\Psi E_o)$ was related to the increased fluxes of absorption, trapping and electron transport in photosynthetic machinery (Rapacz et al., 2019). As well as the rate of biochemical reaction, both Nar treatments promoted the capacity of light reaction by the alleviated levels of $\Phi P_o/(1\text{-}\Phi P_o)$. Besides, Nar promoted the reduction by stress on $\gamma RC/(1\text{-}\gamma RC)$, which shows contribution of ET beyond reduced form of quinone. As contradistinction to the other parameters, DI_o/RC was induced under stress treatments, as also suggested by Varghese et al. (2019). This situation has been regarded as an adaptive response for the dissipation of excess energy in a heat form based on the inactivation of PSII in photooxidative damage (Kalaji et al., 2014), in which electrons cannot be captured by RC of PSII. However, when Nar applied to the bean plants, this value did not need to increase, even it decreased in Nar alone and Nar + stress groups. The reason for this is that the excess energy caused stress-related damage did not occur in chloroplasts due to the exogenous application of Nar.

The other parameter of the OJIP test, the performance index (PI), indicates the vitality of sample under stress conditions and three critic steps in photosynthesis: absorption, trapping and electron transfer (Mehta et al., 2010; Varghese et al., 2019). In the present study, the reduced PI triggered by stress showed the decrement in density of the RC of PSII and this influence was greater under the combined stress treatments. Depending on efficiency of $\Psi E_o/(1\text{-}\Psi E_o)$ and $\Phi P_o/(1\text{-}\Phi P_o)$, Nar, in response to stress, encouraged the photosynthetic performance (PI_{ABS} and PI_{total}) in bean chloroplasts. Our data are in contention with previous reports where measurement of diminished fluorescence in different stressed plants (Mehta et al., 2010; Lazar et al., 2013; Varghese et al., 2019). When all the structural and functional parameters mentioned above were evaluated, stress conditions (NaCl and/or PEG) reversibly resulted an inactivation in photosynthetic machinery in bean chloroplasts. However, Nar applications recovered the damage at the acceptor/donor side of PSII, the decrease in the pool size of reduced quinones or maintained the stability of PSII by enhancing the turnover of D1 protein (as detected in the increased transcription levels of psbA gene).

Because of containing several components which are necessary for the photochemical reactions, the D1 protein is a functional protein in PSII complex (Mukherjee, 2020). The regulation of gene expression related to the photosynthesis shows the tolerance against the stress conditions (Wang et al., 2017). One of them is psbA gene, which encodes the D1 protein and is responsible for the reproduction of impaired D1 protein by stress. The other gene is psbD which protects the stability of PSII complex and regulates D2 protein expression (Chen et al., 2016). In the present study, our data showed that NaCl and PEG disrupted the relative expression of psbA and psbD by triggering damage in PSII system, as shown by the results of F_v/F_m and F_v/F_o. Similar conclusions were observed by Wang et al. (2018). However, both Nar applications protected transcription levels of psbA and psbD from the negative effects produced by NaCl or PEG, accelerating in the functional repair of PSII and assisting the synthesis of D2. This alleviation induced by Nar might be connected with newly synthesizing or repairing the impaired D1 protein.

Gas Exchange

One of the factors associated with reduction of the photosynthetic rate in stress-treated plants is disruption on gas exchange parameters and water management. The water status in the plants is directly correlated with the changes in stomatal conductance (Wada et al., 2019). In the present study, the decline in g_s observed in salt and/or PEG-treated bean, signed to stomatal closure, which was accordance with significant declines in A, C_i, and E. This data is consistent with report of Engineer et al. (2016). In the present study, the decline of A/C_i under NaCl and/or PEG showed that depending on decrease in A and C_i, the assimilation values of CO_2 in chloroplasts of NaCl or the PEG-treated bean might be influenced with the stomatal limitation, as evident by the increase in L_s ($1\text{-}\ C_i/C_a$). A similar observation was noted by Wang et al. (2018) in rice with stress. Nar applications could repair the restriction on photosynthetic regulation, as provided by a promotion of g_s, A, C_i, E, and a reduction in L_s. Exogenously applied Nar in response to stress triggered stomatal opening by increasing g_s levels. This situation promoted transport of internal CO_2 to chloroplasts (as proved increased C_i) and carboxylation efficiency was alleviated. Under stress conditions, Nar applications could provide an increase

in CO_2 from the mesophyll (non-stomatal), as well as the increased entrance of CO_2 through the stoma opening. C_i/g_s is an important tool for identification of mesophyll efficiency and there is an opposite relationship between C_i/g_s and mesophyll efficiency (Ramanjulu et al., 1998). In the current study, after individual treatments of NaCl or PEG to bean plants, both Nar applications caused a decline in C_i/g_s, which verified by the increased mesophyll efficiency, but that was not the case under the combined form of these stresses. Also, Nar applications in bean chloroplasts subjected to NaCl and/or PEG provided the recovery on the restriction in mesophyll and stomata, as evident from the results of A, E, g_s, E, L_s, and F_v/F_m.

ROS Production and Chloroplastic Antioxidant Enzyme Activity

Because of the disruption in redox regulation in photosynthesis, the electrons with a high energy state of chlorophyll reduce molecular oxygen by forming singlet oxygen ($^1O_2$). Also, the thylakoidal electron transport components on the PSI side such as the Fe-S centers result in the reduction of oxygen by a reaction called the Mehler reaction (Cruz de Carvalho, 2008) thus forming superoxide and H_2O_2. SOD, converting superoxide anion radical to oxygen and H_2O_2, is the front-line enzyme against toxic accumulation of ROS (Zou et al., 2018). In the present study, despite no observation in response of chloroplastic SOD activity under NaCl and/or PEG, H_2O_2 content was induced. This result contradict data presented by Guan et al. (2017) who reported an increase in chloroplastic Cu/Zn-SOD of rice under salinity. Other than photosynthesis, photorespiration also produces ROS. During carbon assimilation, ribulose-1,5-bisphosphate is also oxidized with oxygen by the activity of enzyme Rubisco. The yielding glycolate is transported from chloroplasts to peroxisomes and H_2O_2 is generated (Hodges et al., 2016). Hence, a possible source of H_2O_2 is also the activation of some enzymes such as glycolate oxidases, glucose oxidases, amino-acid oxidases, sulfite oxidases and NOX (Wu et al., 2018). In the chloroplasts of bean, there was no contribution of NOX activity in H_2O_2 accumulation under stress. The produced H_2O_2 is eliminated by POX or APX in the so-called water-water cycle (Asada, 1999). In present study, POX activity increased only after individual application of NaCl or PEG, but, not under combined application of NaCl and PEG. Whereas, APX activity was induced only under NaCl plus PEG stress. Our observations are in line with that of Zhang et al. (2017) who reported increased activity of APX under NaCl + PEG in *Glycyrrhiza uralensis*, but not in NaCl alone-treated plants. The bean leaves showed more sensitivity to NaCl or PEG due to the reduction in AsA/DHA and GSH/GSSG ratio. In response to stress, the inadequate enzyme activity might also be related to the increased accumulation of H_2O_2. This was accordance with the higher TBARS content in bean chloroplasts under NaCl and/or PEG, as also reported by Wang et al. (2019).

Naringenin applications to NaCl and/or PEG-applied bean resulted in an increase of SOD activity, resulting in an increase in H_2O_2 content. Also, the induction of NOX activity also contributed to this increase. After Nar applications to bean with NaCl or PEG treatments, the differences were observed in the responses for scavenging of H_2O_2. When Nar was applied under NaCl, H_2O_2 produced by SOD or NOX was eliminated by the activities of POX and, APX, GR, MDHAR and DHAR which activated the AsA-GSH cycle. In response to NaCl stress, Nar increased chloroplastic DHA levels, which are converted from MDHA, depending on APX activity. Nar might trigger the transformation to AsA from MDHA via the activation of MDHAR. The induced DHA was regenerated to AsA by the catalysis of DHAR. The GSH regeneration required for the activity of DHAR was provided by GR which regenerates GSH and so, maintains the GSH pool (Shan et al., 2020). Under salt stress, the applications of Nar had direct capability to protect a high level of AsA/DHA. Therefore, Nar could maintain the pool of AsA and GSH under salt stress in bean chloroplasts by the regulation the AsA-GSH cycle. Also, the overexpressed enzymes presented in regeneration and biosynthesis of AsA and GSH display the enhanced the tolerance to stress (Li et al., 2012). The high ratio in GSH/GSSG and the elevated GSH content/redox state, which was detected in Nar-treated bean chloroplasts in response to salinity, showed that it could have a role in recycling of AsA and GSH by providing a redox state and reducing oxidative stress, as mentioned by Wang et al. (2013) and Garg and Singla (2015). Another enzyme, GST detoxifies toxic lipid peroxides and reduces dehydroascorbate with GSH-dependent reductase activity (DHAR) and so maintains the reductant pools such as AsA (Souri et al., 2020). In the current study, induced GST activity was continued by Nar applications with NaCl or PEG. However, under the combination of stresses, the increase in GST was not maintained via Nar applications. This result was inconsistent with the changes in AsA and GSH which interacts with ROS and abscisic acid in signaling pathway (Szalai et al., 2009). Hence, Nar might have promoted the signaling pathway via the increased GSH activity under salinity.

Exogenous addition of Nar together with PEG-induced osmotic stress to bean plants removed H_2O_2 accumulation through the activities of POX, APX, MDHAR, and DHAR. Like the responses to NaCl stress, Nar could be role in recycling of AsA through the induction of chloroplastic AsA content. Although DHAR converts to GSSG from GSH, it was not possible to regenerate GSH from GSSG due to the inactivity of GR. Therefore, Nar had no effect on GSH regeneration in bean chloroplasts treated with PEG. These results were consistent with the high ratio of AsA/DHA and the reduced GSH/GSSG and GSH redox state.

Interestingly, the same variation in this cycle was not observed in the combination with Nar and NaCl + PEG stress. No increases in the activities of GR, MDHAR, DHAR not only was observed in bean chloroplasts but also exhibited a reduction in the contents of AsA, DHA and GSH. So, the regeneration of both AsA and GSH contents was reduced by Nar applications under the combined form of these stresses. However, POX activity induced by Nar was successfully stimulated to remove of the toxic levels of H_2O_2 produced under NaCl + PEG. Our findings are in accordance with Agati et al. (2013) that the accumulation of H_2O_2 are eliminated by flavonoid-peroxidase reaction.

Lipid Peroxidation

As a biomarker to measure the degree of damage, TBARS is important tool in plants treated with stress (Parvin et al., 2020) and TBARS is induced with salinity or osmotic stress in bean chloroplasts. When all this data was interpreted, Nar applications to stress-treated bean chloroplasts showed lower oxidative damage as indicated by lower H_2O_2 and TBARS levels. Similar observation was noted by Garg and Singla (2015), where Nar applications decreased both H_2O_2 and TBARS contents in *Cicer arietinum* under salt stress. Because of the decreasing amount of H_2O_2, Nar might trigger a signal role of H_2O_2 rather than its toxic effects.

CONCLUSION

Our study confirms that Nar applications prevented inhibition on RWC, osmotic potential and photosynthetic efficiency (F_v/F_m, F_v/F_o, and F_o/F_m) effected by NaCl and/or PEG in bean chloroplasts. Nar could reverse the restriction on stomatal regulation, as evident by alleviation of g_s, A, E and L_s. Nar recovered the photosynthetic machinery by altering the stability of PSII [ABS/RC, ET_o/RC and $\Psi E_o/(1\text{-}\Psi E_o)$] and regulation of dissipated energy levels absorbed energy by chlorophyll of all reaction center in PSII (DI_o/CS_o and DI_o/RC) and protection the damage at the acceptor/donor side of PSII. These regulations triggered by Nar led to a notable increase in the performance index (PI_{ABS}) and the capacity of light reaction [$\Phi P_o/(1\text{-}\Phi P_o)$]. Both Nar applications (0.1 and 0.4 mM) protected from the negative effects produced by NaCl or PEG on transcription levels of psbA and psbD, accelerating in the functional repair of PSII and assisting the synthesis of D2. By regulating the antioxidant metabolism in chloroplasts of bean plants, Nar was able to control the toxic levels of ROS and TBARS produced by stress. Chloroplastic SOD activity reduced by stress in bean exposed to stress was increased by Nar. Since Nar exposure increased the activities of APX, GR, MDHAR, and DHAR as well as POX, Nar could maintain both AsA and GSH redox state in response to NaCl, as evident by enhancement in AsA/DHA and GSH/GSSG. Nar protected the bean chloroplasts by minimizing disturbances caused by salinity via the ascorbate and glutathione redox-based systems. Despite of the induction of MDHAR and DHAR under Nar plus PEG, Nar maintained the AsA regeneration, but not GSH recycling because of no induction in GR activity and the reduction in GSH/GSSG and GSH redox state. Consequently, Nar protected bean chloroplasts by minimizing disturbances caused by NaCl or PEG exposure via the AsA or GSH redox-based systems and POX activity.

DATA AVAILABILITY STATEMENT

All datasets generated for this study are included in the article/**Supplementary Material**.

AUTHOR CONTRIBUTIONS

EY, CO-K, MK, and IT conceived and designed the research. CO-K and EY conducted the experiments. CO-K, EY, and IT analyzed the data. CO-K, EY, and IT wrote the manuscript. All authors read and approved the manuscript.

FUNDING

Financial support for this work was provided by the Selcuk University Scientific Research Projects Coordinating Office (Project number: 20401044).

ACKNOWLEDGMENTS

We are thankful to Dr. Ramazan Keles from Bahri Dagdas International Agricultural Research Institute for providing the seeds of wheat.

SUPPLEMENTARY MATERIAL

The Supplementary Material for this article can be found online at: https://www.frontiersin.org/articles/10.3389/fpls.2020.00682/full#supplementary-material

REFERENCES

Acosta-Motos, J., Ortuno, M. F., Bernal-Vicente, A., Diaz-Vivancos, P., Sanchez-Blanco, M., and Hernandez, J. A. (2017). Plant responses to salt stress: adaptive mechanisms. *Agronomy* 7:18. doi: 10.3390/agronomy7010018

Agati, G., Brunetti, C., Di Ferdinando, M., Ferrini, F., Pollastri, S., and Tattini, M. (2013). Functional roles of flavonoids in photoprotection: new evidence, lessons from the past. *Plant Physiol. Biochem.* 72, 35–45. doi: 10.1016/j.plaphy.2013.03.014

Agati, G., Galardi, C., Gravano, E., Romani, A., and Tattini, M. (2002). Flavonoid distribution in tissues of *Phillyrea latifolia* L. leaves as estimated by microspectrofluorometry and multispectral fluorescence microimaging. *Photochem. Photobiol.* 76, 350–360. doi: 10.1562/0031-8655(2002)0760350fditop2.0.co2

Agati, G., and Tattini, M. (2010). Multiple functional roles of flavonoids in photoprotection. *New Phytol.* 186, 786–793. doi: 10.1111/j.1469-8137.2010.03269.x

Asada, K. (1999). The water–water cycle in chloroplasts: scavenging of active oxygen and dissipation of excess photons. *Annu. Rev. Plant Physiol. Plant Mol. Biol.* 50, 601–639. doi: 10.1146/annurev.arplant.50.1.601

Baskar, V., Venkatesh, R., and Ramalingam, S. (2018). *Flavonoids (Antioxidants Systems) in Higher Plants and their Response to Stresses, in Antioxidants and Antioxidant Enzymes in Higher Plants*. Cham: Springer, 253–268.

Batth, R., Singh, K., Kumari, S., and Mustafiz, A. (2017). Transcript profiling reveals the presence of abiotic stress and developmental stage specific ascorbate oxidase genes in plants. *Front. Plant Sci.* 8:2. doi: 10.3389/fpls.2017.00198

Beauchamp, C., and Fridovich, I. (1971). Superoxide dismutase: improved assays and an assay applicable to acrylamide gels. *Anal. Biochem.* 44, 276–287. doi: 10.1016/0003-2697(71)90370-8

Bido, G. S., Ferrarese, M. L. L., Marchiosi, R., and Ferrarese-Filho, O. (2010). Naringenin inhibits the growth and stimulates the lignification of soybean root. *Braz. Arch. Biol. Technol.* 53, 533–542. doi: 10.1590/s1516-89132010000300005

Bose, J., Munns, R., Shabala, S., Gilliham, M., Pogson, B., and Tyerman, S. D. (2017). Chloroplast function and ion regulation in plants growing on saline soils: lessons from halophytes. *J. Exp. Bot.* 68, 3129–3143. doi: 10.1093/jxb/erx142

Bradford, M. M. (1976). A rapid and sensitive method for the quantitation of microgram quantities of protein utilizing the principle of protein-dye binding. *Anal. Biochem.* 72, 248–254. doi: 10.1016/0003-2697(76)90527-3

Carvalho, L. C., Vidigal, P., and Amâncio, S. (2015). Oxidative stress homeostasis in grapevine (*Vitis vinifera* L.). *Front. Environ. Sci.* 3:20. doi: 10.3389/fenvs.2015.00020

Cheeseman, J. M. (2006). Hydrogen peroxide concentrations in leaves under natural conditions. *J. Exp. Bot.* 57, 2435–2444. doi: 10.1093/jxb/erl004

Cheeseman, J. M. (2013). The integration of activity in saline environments: problems and perspectives. *Funct. Plant Biol.* 40, 759–774.

Chen, Y. E., Yuan, S., and Schroder, W. P. (2016). Comparison of methods for extracting thylakoid membranes of *Arabidopsis* plants. *Physiol. Plant.* 156, 3–12. doi: 10.1111/ppl.12384

Chutipaijit, S., Cha-Um, S., and Sompornpailin, K. (2009). Differential accumulations of proline and flavonoids in indica rice varieties against salinity. *Pakistan J. Bot.* 41, 2497–2506.

Cruz de Carvalho, M. H. (2008). Drought stress and reactive oxygen species: production, scavenging and signaling. *Plant Signal. Behav.* 3, 156–165. doi: 10.4161/psb.3.3.5536

Dai, A. H., Nie, Y. X., Yu, B., Li, Q., Lu, L. Y., and Bai, J. G. (2012). Cinnamic acid pretreatment enhances heat tolerance of cucumber leaves through modulating antioxidant enzyme activity. *Environ. Exp. Bot.* 79, 1–10. doi: 10.1016/j.envexpbot.2012.01.003

Dalton, D. A., Russell, S. A., Hanus, F. J., Pascoe, G. A., and Evans, H. J. (1986). Enzymatic-reactions of ascorbate and glutathione that prevent peroxide damage in soybean root-nodules. *Proc. Natl. Acad. Sci. U.S.A.* 83, 3811–3815. doi: 10.1073/pnas.83.11.3811

D'Amelia, V., Aversano, R., Ruggiero, A., Batelli, G., Appelhagen, I., Dinacci, C., et al. (2018). Subfunctionalization of duplicate MYB genes in *Solanum commersonii* generated the cold-induced ScAN2 and the anthocyanin regulator ScAN1. *Plant Cell Environ.* 41, 1038–1051. doi: 10.1111/pce.12966

de Sousa, A., Abdelgawad, H., Han, A., Teixeira, J., Matos, M., and Fidalgo, F. (2016). Oxidative metabolism of rye (*Secale cereale* L.) after short term exposure to aluminum: uncovering the glutathione–ascorbate redox network. *Front. Plant Sci.* 7:685. doi: 10.3389/fpls.2016.00685

Deng, F., Aoki, M., and Yogo, Y. (2004). Effect of naringenin on the growth and lignin biosynthesis of gramineous plants. *Weed Biol. Manag.* 4, 49–55. doi: 10.1111/j.1445-6664.2003.00119.x

Dolatabadian, A., Sanavy, S. A. M. M., Ghanati, F., and Gresshoff, P. M. (2012). Morphological and physiological response of soybean treated with the microsymbiont *Bradyrhizobium japonicum* pre-incubated with genistein. *South Afr. J. Bot.* 79, 9–18. doi: 10.1016/j.sajb.2011.11.001

Dutilleul, C., Driscoll, S., Cornic, G., De Paepe, R., Foyer, C. H., and Noctor, G. (2003). Functional mitochondrial complex I is required by tobacco leaves for optimal photosynthetic performance in photorespiratory conditions and during transients. *Plant Physiol.* 131, 264–275. doi: 10.1104/pp.011155

Engineer, C. B., Hashimoto-Sugimoto, M., Negi, J., Israelsson-Nordström, M., Azoulay-Shemer, T., Rappel, W.-J., et al. (2016). CO2 sensing and CO2 regulation of stomatal conductance: advances and open questions. *Trends Plant Sci.* 21, 16–30. doi: 10.1016/j.tplants.2015.08.014

Flowers, T. J., Munns, R., and Colmer, T. D. (2015). Sodium chloride toxicity and the cellular basis of salt tolerance in halophytes. *Ann. Bot.* 115, 419–431. doi: 10.1093/aob/mcu217

Foyer, C. H., and Halliwell, B. (1976). The presence of glutathione and glutathione reductase in chloroplasts: a proposed role in ascorbic acid metabolism. *Planta* 133, 21–25. doi: 10.1007/bf00386001

Garg, N., and Singla, P. (2015). Naringenin- and Funneliformis mosseae-mediated alterations in redox state synchronize antioxidant network to alleviate oxidative stress in *Cicer arietinum* L. genotypes under salt stress. *J. Plant Growth Regul.* 34, 595–610. doi: 10.1007/s00344-015-9494-9

Gondor, O. K., Szalai, G., Kovacs, V., Janda, T., and Pal, M. (2016). Relationship between polyamines and other cold-induced response mechanisms in different cereal species. *J. Agron. Crop Sci.* 202, 217–230. doi: 10.1111/jac.12144

Guan, Q., Liao, X., He, M., Li, X., Wang, Z., Ma, H., et al. (2017). Tolerance analysis of chloroplast OsCu/Zn-SOD overexpressing rice under NaCl and NaHCO3 stress. *PLoS One* 12:e0186052. doi: 10.1371/journal.pone.0186052

Gururani, M. A., Venkatesh, J., Ganesan, M., Strasser, R. J., Han, Y., Kim, J. I., et al. (2015). *In vivo* assessment of cold tolerance through chlorophyll-a fluorescence in transgenic zoysiagrass expressing mutant phytochrome a. *PLoS One* 10:5. doi: 10.1371/journal.pone.0127200

Hellal, F., El-Shabrawi, H., El-Hady, M. A., Khatab, I., El-Sayed, S., and Abdelly, C. (2018). Influence of PEG induced drought stress on molecular and biochemical constituents and seedling growth of Egyptian barley cultivars. *J. Genet. Eng. Biotechnol.* 16, 203–212. doi: 10.1016/j.jgeb.2017.10.009

Hernandez, I., and Munne-Bosch, S. (2012). Naringenin inhibits seed germination and seedling root growth through a salicylic acid-independent mechanism in *Arabidopsis thaliana*. *Plant Physiol. Biochem.* 61, 24–28. doi: 10.1016/j.plaphy.2012.09.003

Herzog, V., and Fahimi, H. (1973). Determination of the activity of peroxidase. *Anal. Biochem.* 55:e62.

Hodges, M., Dellero, Y., Keech, O., Betti, M., Raghavendra, A. S., Sage, R., et al. (2016). Perspectives for a better understanding of the metabolic integration of photorespiration within a complex plant primary metabolism network. *J. Exp. Bot.* 67, 3015–3026. doi: 10.1093/jxb/erw145

Hossain, M. Z., Hossain, M. D., and Fujita, M. (2006). Induction of pumpkin glutathione S-transferases by different stresses and its possible mechanisms. *Biol. Plant.* 50, 210–218. doi: 10.1007/s10535-006-0009-1

Inoue, K. (2011). Emerging roles of the chloroplast outer envelope membrane. *Trends Plant Sci.* 16, 550–557. doi: 10.1016/j.tplants.2011.06.005

Jiang, M., and Zhang, J. (2002). Involvement of plasma-membrane NADPH oxidase in abscisic acid- and water stress-induced antioxidant defense in leaves of maize seedlings. *Planta* 215, 1022–1030. doi: 10.1007/s00425-002-0829-y

Kalaji, H. M., Govindjee, G., Bosa, K., Koscielniak, J., and Zuk-Golaszewska, K. (2011). Effects of salt stress on photosystem II efficiency and CO2 assimilation of two Syrian barley landraces. *Environ. Exp. Bot.* 73, 64–72. doi: 10.1016/j.envexpbot.2010.10.009

Kalaji, H. M., Rackova, L., Paganova, V., Swoczyna, T., Rusinowski, S., and Sitko, K. (2018). Can chlorophyll-a fluorescence parameters be used as bio-indicators to distinguish between drought and salinity stress in *Tilia cordata* Mill? *Environ. Exp. Bot.* 152, 149–157. doi: 10.1016/j.envexpbot.2017.11.001

Kalaji, H. M., Schansker, G., Ladle, R. J., Goltsev, V., Bosa, K., Allakhverdiev, S. I., et al. (2014). Frequently asked questions about in vivo chlorophyll fluorescence: practical issues. *Photosynth. Res.* 122, 121–158.

Karageorgou, P., and Manetas, Y. (2006). The importance of being redwhen young: anthocyanins and the protection of young leaves of Quercus coccifera from insect herbivory and excess light. *Tree Physiol.* 26, 613–621. doi: 10.1093/treephys/26.5.613

Kurniasih, B., Greenway, H., and Colmer, T. D. (2016). Energetics of acclimation to NaCl by submerged, anoxic rice seedlings. *Ann. Bot.* 119, 129–142. doi: 10.1093/aob/mcw189

Laemmli, U. K. (1970). Cleavage of structural proteins during the assembly of the head of bacteriophage T4. *Nature* 227, 680–685. doi: 10.1038/227680a0

Lazar, D., Murch, S. J., Beilby, M. J., and Al Khazaaly, S. (2013). Exogenous melatonin affects photosynthesis in characeae *Chara australis*. *Plant Signal. Behav.* 8:e23279. doi: 10.4161/psb.23279

Li, Y. H., Liu, Y. J., Xu, X. L., Jin, M., An, L. Z., and Zhang, H. (2012). Effect of 24-epibrassinolide on drought stress-induced changes in *Chorispora bungeana*. *Biol. Plant.* 56, 192–196. doi: 10.1007/s10535-012-0041-2

Lilley, R. M., Fitzgerald, M., Rienits, K., and Walker, D. (1975). Criteria of intactness and the photosynthetic activity of spinach chloroplast preparations. *New Phytol.* 75, 1–10. doi: 10.1111/j.1469-8137.1975.tb01365.x

Liu, M. H., Zou, W., Yang, C. P., Peng, W., and Su, W. W. (2012). Metabolism and excretion studies of oral administered naringin, a putative antitussive, in rats and dogs. *Biopharm. Drug Disposition* 33, 123–134. doi: 10.1002/bdd.1775

Ma, Y., An, Y., Shui, J., and Sun, Z. (2011). Adaptability evaluation of switchgrass (*Panicum virgatum* L.) cultivars on the Loess Plateau of China. *Plant Science* 181, 638–643. doi: 10.1016/j.plantsci.2011.03.003

Mahajan, M., and Yadav, S. K. (2013). Effect of quercetin and epicatechin on the transcript expression and activity of antioxidant enzymes in tobacco seedlings. *Am. J. Biochem. Mol. Biol. Fertil. Soils* 3, 81–90. doi: 10.3923/ajbmb.2013.81.90

Martinez, V., Mestre, T. C., Rubio, F., Girones-Vilaplana, A., Moreno, D. A., Mittler, R., et al. (2016). Accumulation of flavonols over hydroxycinnamic acids favors oxidative damage protection under abiotic stress. *Front. Plant Sci.* 7:3. doi: 10.3389/fpls.2016.00838

Mehta, P., Jajoo, A., Mathur, S., and Bharti, S. (2010). Chlorophyll a fluorescence study revealing effects of high salt stress on Photosystem II in wheat leaves. *Plant Physiol. Biochem.* 48, 16–20. doi: 10.1016/j.plaphy.2009.10.006

Miller, G., Suzuki, N., Ciftci-Yilmaz, S., and Mittler, R. (2010). Reactive oxygen species homeostasis and signaling during drought and salinity stresses. *Plant Cell Environ.* 33, 453–467. doi: 10.1111/j.1365-3040.2009.02041.x

Mittler, R., and Zilinskas, B. A. (1993). Detection of ascorbate peroxidase-activity in native gels by inhibition of the ascorbate-dependent reduction of nitroblue tetrazolium. *Anal. Biochem.* 212, 540–546. doi: 10.1006/abio.1993.1366

Miyake, C., and Asada, K. (1992). Thylakoid-bound ascorbate peroxidase in spinach-chloroplasts and photoreduction of its primary oxidation-product monodehydroascorbate radicals in thylakoids. *Plant Cell Physiol.* 33, 541–553.

Mukherjee, A. (2020). Role of DnaK-DnaJ proteins in PSII repair. *Plant Physiol.* 182, 1804–1805. doi: 10.1104/pp.20.00265

Nakano, Y., and Asada, K. (1981). Hydrogen peroxide is scavenged by ascorbate-specific peroxidase in spinach chloroplasts. *Plant Cell Physiol.* 22, 867–880.

Ozgur, R., Uzilday, B., Sekmen, A. H., and Turkan, I. (2015). The effects of induced production of reactive oxygen species in organelles on endoplasmic reticulum stress and on the unfolded protein response in *Arabidopsis*. *Ann. Bot.* 116, 541–553. doi: 10.1093/aob/mcv072

Paradiso, A., Berardino, R., De Pinto, M. C., Sanita Di Toppi, L., Storelli, M. M., Tommasi, F., et al. (2008). Increase in ascorbate-glutathione metabolism as local and precocious systemic responses induced by cadmium in durum wheat plants. *Plant Cell Physiol.* 49, 362–374. doi: 10.1093/pcp/pcn013

Parvin, K., Nahaar, K., Hasaanuzzaman, M., Bhuyan, B., Mohsin, S. M., and Fujita, M. (2020). Exogenous vanillic acid enhances salt tolerance of tomato: insight into plant antioxidant defense and glyoxalase systems. *Plant Physiol. Biochem.* 150, 109–120. doi: 10.1016/j.plaphy.2020.02.030

Pheomphun, P., Treesubsuntorn, C., Jitareerat, P., and Thiravetyan, P. (2019). Contribution of Bacillus cereus ERBP in ozone detoxification by *Zamioculcas zamiifolia* plants: effect of ascorbate peroxidase, catalase and total flavonoid contents for ozone detoxification. *Ecotoxicol. Environ. Saf.* 171, 805–812. doi: 10.1016/j.ecoenv.2019.01.028

Ramanjulu, S., Sreenivasulu, N., and Sudhakar, C. (1998). Effect of water stress on photosynthesis in two mulberry genotypes with different drought tolerance. *Photosynthetica* 35, 279–283.

Rao, K. M., and Sresty, T. (2000). Antioxidative parameters in the seedlings of pigeonpea (*Cajanus cajan* (L.) Millspaugh) in response to Zn and Ni stresses. *Plant Science* 157, 113–128. doi: 10.1016/s0168-9452(00)00273-9

Rapacz, M., Wójcik-Jagła, M., Fiust, A., Kalaji, H. M., and Koscielniak, J. (2019). Genome-wide associations of chlorophyll fluorescence OJIP transient parameters connected with soil drought response in barley. *Front. Plant Sci.* 10:78. doi: 10.3389/fpls.2019.00078

Ricci, G., Bello, M. L., Caccuri, A. M., Galiazzo, F., and Federici, G. (1984). Detection of glutathione S-transferase activity on polyacrylamide gels. *Anal. Biochem.* 143, 226–230. doi: 10.1016/0003-2697(84)90657-2

Sagi, M., and Fluhr, R. (2001). Superoxide production by plant homologues of the gp91phox NADPH oxidase. Modulation of activity by calcium and by tobacco mosaic virus infection. *Plant Physiol.* 126, 1281–1290. doi: 10.1104/pp.126.3.1281

Salehi, B., Fokou, P. V., Sharifi-Rad, M., Zucca, P., Pezzani, R., Martins, N., et al. (2019). The Therapeutic potential of naringenin: a review of clinical trials. *Pharmaceuticals* 12:11. doi: 10.3390/ph12010011

Santa-Cruz, A., Martinez-Rodriguez, M. M., Perez-Alfocea, F., Romero-Aranda, R., and Bolarin, M. C. (2002). The rootstock effect on the tomato salinity response depends on the shoot genotype. *Plant Sci.* 162, 825–831. doi: 10.1016/s0168-9452(02)00030-4

Seevers, P., Daly, J., and Catedral, F. (1971). The role of peroxidase isozymes in resistance to wheat stem rust disease. *Plant Physiol.* 48, 353–360. doi: 10.1104/pp.48.3.353

Shan, C. J., Jin, Y. Y., Zhou, Y., and Li, H. (2020). Nitric oxide participates in the regulation of ascorbate-glutathione cycle and water physiological characteristics of *Arabidopsis thaliana* by NaHS. *Photosynthetica* 58, 80–86. doi: 10.32615/ps.2019.158

Shatpathy, P., Kar, M., Dwibedi, S. K., and Dash, A. (2018). Seed priming with salicylic acid improves germination and seedling growth of rice (*Oryza sativa* L.) under PEG-6000 induced water stress. *Int. J. Curr. Microbiol. Appl. Sci.* 7, 907–924. doi: 10.20546/ijcmas.2018.710.101

Sheldon, A. R., Dalal, R. C., Kirchhof, G., Kopittke, P. M., and Menzies, N. W. (2017). The effect of salinity on plant-available water. *Plant Soil* 418, 477–491. doi: 10.1007/s11104-017-3309-7

Shu, S., Tang, Y. Y., Yuan, Y. H., Sun, J., Zhong, M., and Guo, S. R. (2016). The role of 24-epibrassinolide in the regulation of photosynthetic characteristics and nitrogen metabolism of tomato seedlings under a combined low temperature and weak light stress. *Plant Physiol. Biochem.* 107, 344–353. doi: 10.1016/j.plaphy.2016.06.021

Smart, R. E., and Bingham, G. E. (1974). Rapid estimates of relative water content. *Plant Physiol.* 53, 258–260. doi: 10.1104/pp.53.2.258

Souri, Z., Karimi, N., Farooq, M., and Sandalio, L. (2020). Nitric oxide improves tolerance to arsenic stress in Isatis cappadocica desv. shoots by enhancing antioxidant defenses. *Chemosphere* 239:124523. doi: 10.1016/j.chemosphere.2019.124523

Strasser, R. J., Srivastava, A., and Govindjee, G. (1995). Polyphasic chlorophyll a fluorescence transient in plants and cyanobacteria. *Photochem. Photobiol.* 61, 32–42. doi: 10.1111/j.1751-1097.1995.tb09240.x

Strasser, R. J., Tsimilli- Michael, M., and Srivastava, A. (2000). "The fluorescence transient as a tool to characterize and screen photosynthetic samples," in *Probing Photosynthesis: Mechanisms, Regulation and Adaptation*, eds M. Yunus, U. Pather, and P. Mohanly (Boca Raton, FL: CRC Press), 445–483.

Strauss, A. J., Kruger, G. H. J., Strasser, R. J., and Van Heerden, P. D. R. (2006). Ranking of dark chilling tolerance in soybean genotypes probed by the chlorophyll a fluorescence transient O-J-I-P. *Environ. Exp. Bot.* 56, 147–157. doi: 10.1016/j.envexpbot.2005.01.011

Szalai, G., Kellõs, T., Galiba, G., and Kocsy, G. (2009). Glutathione as an antioxidant and regulatory molecule in plants under abiotic stress conditions. *J. Plant Growth Regul.* 28, 66–80. doi: 10.1007/s00344-008-9075-2

Uzilday, B., Turkan, I., Sekmen, A. H., Ozgur, R., and Karakaya, H. (2012). Comparison of ROS formation and antioxidant enzymes in Cleome gynandra (C4) and Cleome spinosa (C3) under drought stress. *Plant Sci.* 182, 59–70. doi: 10.1016/j.plantsci.2011.03.015

Varghese, N., Alyammahi, O., Nasreddine, S., Alhassani, A., and Gururani, M. A. (2019). Melatonin positively influences the photosynthetic machinery and antioxidant system of *Avena sativa* during salinity stress. *Plants* 8:610. doi: 10.3390/plants8120610

Wada, S., Takagi, D., Miyake, C., Makino, A., and Suzuki, Y. (2019). Responses of the photosynthetic electron transport reactions stimulate the oxidation of the reaction center chlorophyll of Photosystem I, P700, under drought and high temperatures in rice. *Int. J. Mol. Sci.* 20:2068. doi: 10.3390/ijms20092068

Wang, C., Lu, G., Hao, Y., Guo, H., Guo, Y., Zhao, J., et al. (2017). ABP9, a maize bZIP transcription factor, enhances tolerance to salt and drought in transgenic cotton. *Planta* 246, 453–469. doi: 10.1007/s00425-017-2704-x

Wang, G. F., Li, W. Q., Li, W. Y., Wu, G. L., Zhou, C. Y., and Chen, K. M. (2013). Characterization of rice NADPH oxidase genes and their expression under various environmental conditions. *Int. J. Mol. Sci.* 14, 9440–9458. doi: 10.3390/ijms14059440

Wang, R., Zhao, J., Jia, M., Xu, N., Liang, S., Shao, J., et al. (2018). Balance between cytosolic and chloroplast translation affects leaf variegation. *Plant Physiol.* 176, 804–818. doi: 10.1104/pp.17.00673

Wang, Y., Zhang, X., Hu, Y., Teng, Z., Zhang, S., Chi, Q., et al. (2019). Phenotypic response of tobacco leaves to simulated acid rain and its impact on photosynthesis. *Int. J. Agric. Biol.* 21, 391–398.

Wu, D., Liang, M. L., Dang, H. X., Fang, F., Xu, F., and Liu, C. J. (2018). Hydrogen protects against hyperoxia-induced apoptosis in type II alveolar epithelial cells via activation of PI3K/Akt/Foxo3a signaling pathway. *Biochem. Biophys. Res. Commun.* 495, 1620–1627. doi: 10.1016/j.bbrc.2017.11.193

Yildiztugay, E., Ozfidan-Konakci, C., and Kucukoduk, M. (2014). Exogenous nitric oxide (as sodium nitroprusside) ameliorates polyethylene glycol-induced osmotic stress in hydroponically grown maize roots. *J. Plant Growth Regul.* 33, 683–696. doi: 10.1007/s00344-014-9417-1

Zeliou, K., Manetas, Y., and Petropoulou, Y. (2009). Transient winter leaf reddening in *Cistus creticus* characterizes weak (stress-sensitive) individuals, yet anthocyanins cannot alleviate the adverse effects on photosynthesis. *J. Exp. Bot.* 60, 3031–3042. doi: 10.1093/jxb/erp131

Zhang, W., Xie, Z., Wang, L., Li, M., Lang, D., and Zhang, X. (2017). Silicon alleviates salt and drought stress of *Glycyrrhiza uralensis* seedling by altering antioxidant metabolism and osmotic adjustment. *J. Plant Res.* 130, 611–624. doi: 10.1007/s10265-017-0927-3

Zhao, X., Chen, T. T., Feng, B. H., Zhang, C. X., Peng, S. B., Zhang, X. F., et al. (2017). Non-photochemical quenching plays a key role in light acclimation of rice plants differing in leaf color. *Front. Plant Sci.* 7:4. doi: 10.3389/fpls.2016.01968

Zou, P., Lu, X. L., Jing, C. L., Yuan, Y., Lu, Y., Zhang, C. S., et al. (2018). Low-molecular-weight polysaccharides from Pyropia yezoensis enhance tolerance of wheat seedlings (*Triticum aestivum* L.) to salt stress. *Front. Plant Sci.* 9:5. doi: 10.3389/fpls.2018.00427

Conflict of Interest: The authors declare that the research was conducted in the absence of any commercial or financial relationships that could be construed as a potential conflict of interest.

frontiers in Plant Science

REVIEW
published: 03 July 2020
doi: 10.3389/fpls.2020.00853

Plant Peroxisomes: A Factory of Reactive Species

Francisco J. Corpas, Salvador González-Gordo and José M. Palma*

Group of Antioxidants, Free Radicals and Nitric Oxide in Biotechnology, Food and Agriculture, Department of Biochemistry, Cell and Molecular Biology of Plants, Estación Experimental del Zaidín, Consejo Superior de Investigaciones Científicas (CSIC), Granada, Spain

Plant peroxisomes are organelles enclosed by a single membrane whose biochemical composition has the capacity to adapt depending on the plant tissue, developmental stage, as well as internal and external cellular stimuli. Apart from the peroxisomal metabolism of reactive oxygen species (ROS), discovered several decades ago, new molecules with signaling potential, including nitric oxide (NO) and hydrogen sulfide (H_2S), have been detected in these organelles in recent years. These molecules generate a family of derived molecules, called reactive nitrogen species (RNS) and reactive sulfur species (RSS), whose peroxisomal metabolism is autoregulated through posttranslational modifications (PTMs) such as *S*-nitrosation, nitration and persulfidation. The peroxisomal metabolism of these reactive species, which can be weaponized against pathogens, is susceptible to modification in response to external stimuli. This review aims to provide up-to-date information on crosstalk between these reactive species families and peroxisomes, as well as on their cellular environment in light of the well-recognized signaling properties of H_2O_2, NO and H_2S.

Keywords: catalase, reactive oxygen, nitrogen and sulfur species, superoxide dismutase, nitric oxide, *S*-nitrosation, persulfidation

OPEN ACCESS

Edited by:
Vasileios Fotopoulos, Cyprus University of Technology, Cyprus

Reviewed by:
Christine Helen Foyer, University of Birmingham, United Kingdom
Olga V. Voitsekhovskaja, Komarov Botanical Institute (RAS), Russia

****Correspondence:***
Francisco J. Corpas
javier.corpas@eez.csic.es

Specialty section:
This article was submitted to Plant Physiology, a section of the journal Frontiers in Plant Science

Received: *14 April 2020*
Accepted: *27 May 2020*
Published: *03 July 2020*

Citation:
Corpas FJ, González-Gordo S and Palma JM (2020) Plant Peroxisomes: A Factory of Reactive Species. Front. Plant Sci. 11:853. doi: 10.3389/fpls.2020.00853

INTRODUCTION

For many years, peroxisomes in higher plants have been given different names, such as glyoxysomes during seed germination and leaf senescence, as well as leaf, root and fruit peroxisomes according to their presence in different organs and at different physiological stages (Tolbert and Essner, 1981; Palma et al., 2018). This is explained by the presence of metabolic pathways which appear to be specific to each type of peroxisome. However, peroxisomes, which share a number of metabolites and enzymes common to all types of peroxisome, is now the preferred term regardless of their specific metabolic characteristics (Pracharoenwattana and Smith, 2008). The most noteworthy metabolites and enzymes include H_2O_2 and catalase, which are directly involved in the metabolism of reactive oxygen species (ROS) (Su et al., 2018; Sousa et al., 2019).

Peroxisomes have a simple morphological constitution composed of a single membrane surrounding an amorphous matrix. Over the last 30 years, an increasing number of new and often unexpected components and processes in these organelles have been identified (Bueno and del Río, 1992; del Río et al., 1992; Corpas et al., 1994, 2001, 2017a, 2019a, Barroso et al., 1999; Reumann et al., 2009; Clastre et al., 2011; Simkin et al., 2011; Chowdhary et al., 2012; Guirimand et al., 2012; Oikawa et al., 2015; Reumann and Bartel, 2016; Kao et al., 2018; Pan et al., 2018, 2020; Borek et al., 2019), indicating that the plant peroxisomal metabolism and

consequently peroxisomal enzymatic and non-enzymatic components are more diverse than previously predicted. The diverse complementary range of experimental approaches used to identify these new peroxisomal constituents includes: (i) the biochemical, proteomic and molecular analysis of purified peroxisomes combined with bioinformatics methodologies and (ii) cell biology studies of features such as immune localization with the aid of electron microscopy and specific fluorescent probes with appropriated controls. Although the model plant *Arabidopsis thaliana* has increased our knowledge of plant peroxisomes, it should be pointed out that studies of peroxisomes from other plant species have been essential, as the peroxisomal metabolism can be modulated depending on the plant organ, development time and plant species involved. Therefore, this review principally aims to provide an update of research on the metabolism of reactive species associated with oxygen, nitrogen and, more recently, sulfur, as well as to outline new challenges and possible future research perspectives regarding crosstalk between peroxisomes and other subcellular compartments such as oil bodies, mitochondria and plastids which are closely related both biochemically and structurally (Palma et al., 2006; Oikawa et al., 2019). Information on plant peroxisomes could also be useful in relation to peroxisome research into other organisms and vice versa.

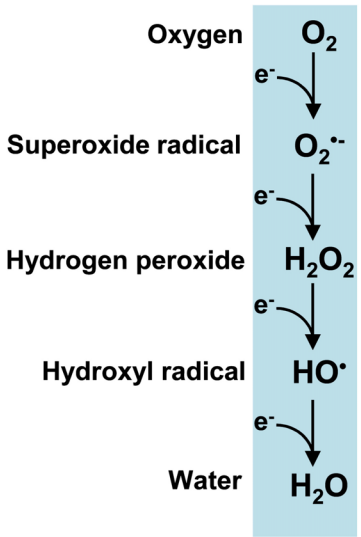

FIGURE 1 | Reactive oxygen species (ROS) produced from a sequential one-electron reduction from oxygen.

PEROXISOMAL ROS METABOLISM

Reactive oxygen species (ROS) are produced by a series of single-electron reductions in molecular oxygen which sequentially form superoxide ($O_2^{\bullet-}$), hydrogen peroxide (H_2O_2) and hydroxyl ($HO^\bullet$) radicals and ultimately ending in water (**Figure 1**). It is worth noting that the term peroxisomes, formerly known as microbodies, originates from their high H_2O_2 content (De Duve and Baudhuin, 1966; Corpas, 2015). Plant peroxisomes contain a significant number of enzymatic systems capable of generating H_2O_2 such as glycolate oxidase (GOX), acyl-CoA oxidase (AOX), urate oxidase (UO), polyamine oxidase, copper amine oxidase (CuAO), sulfite oxidase (SO), sarcosine oxidase (SOX), or superoxide dismutase (SOD) (Hauck et al., 2014; Corpas et al., 2017a and references therein). These H_2O_2-generating enzymes are involved in multiple biochemical pathways which are essential not only for the endogenous metabolism of plant peroxisomes but also for their interactions with other subcellular compartments such as plastids, mitochondria, cytosols, oil bodies and nuclei. In these subcellular interconnections, H_2O_2 itself plays a highly important role as a signal molecule in crosstalk between organelles in order to coordinate cell function.

Photorespiration has been estimated to be responsible for 70% of total H_2O_2 generated mainly from peroxisomal GOX in photosynthetic tissues (Noctor et al., 2002). Zhang et al. (2016) have described an elegant dynamic physical GOX-catalase association-dissociation mechanism that fine-tunes peroxisomal H_2O_2 in rice plants. Although peroxisomal H_2O_2 is kept under control when GOX and catalase are associated, under stress conditions and when mediated by salicylic acid (SA), this complex GOX-catalase dissociation mechanism inhibits catalase activity, leading to an increase in cellular H_2O_2 which acts as a signaling molecule (Zhang et al., 2016; Kohli et al., 2019). Another sophisticated mechanism, involving the interaction of the γb protein from the barley stripe mosaic virus with GOX, has been reported to inhibit GOX and to facilitate infection with the virus (Yang et al., 2018). More recently, Yamauchi et al. (2019) observed a connection between the H_2O_2-generating GOX and catalase, which is required in the stomatal movement. Thus, when there is an increase of oxidized peroxisomes they were removed by pexophagy allowing an increase in H_2O_2 in guard cells which mediated the stomatal closure. This mechanism of ROS homeostasis in guard cells seems to be relevant in response to environmental changes. On the other hand, the new peroxisomal small heat shock protein Hsp17.6CII, capable of increasing catalase activity especially under stress conditions, has been reported to be present in Arabidopsis plants (Li et al., 2017).

Acyl-CoA oxidase is another key peroxisomal H_2O_2-generating enzyme involved in fatty acid β-oxidation which, in collaboration with lipid bodies, enables triacylglyceride mobilization especially during seed germination and is also involved in the synthesis of signal molecules such as jasmonic acid (Baker et al., 2006; Chen et al., 2019b; Wang X. et al., 2019; Xin et al., 2019). However, under stress conditions such as salinity, ROS generated by peroxisomal fatty acid β-oxidation have a negative impact and contribute to oxidative damage (Yu et al., 2019).

Polyamines such as putrescine, spermidine and spermine are well known to be involved in multiple physiological processes, as well as mechanisms of response to various stress conditions (Wuddineh et al., 2018; Chen et al., 2019a; Wang W. et al., 2019). Several enzymes involved in the catabolism of polyamine, including H_2O_2-producing

polyamine oxidase (PAO) and copper amino oxidase (CuAO), have been reported to be present in plant peroxisomes (Moschou et al., 2008; Kusano et al., 2015). These enzymes are also involved in the γ-aminobutyric acid (GABA) biosynthesis signaling pathway (Zarei et al., 2015; Corpas et al., 2009b).

In addition, peroxisomal xanthine oxidoreductase (XOR) and superoxide dismutase (SOD), key enzymes in $O_2^{\bullet-}$ and H_2O_2 metabolism, can be regulated by stress conditions such as salinity, heavy metal and ozone stress (Corpas et al., 1993, 2008; Ueda et al., 2013).

Although catalase is the principal antioxidant enzyme in the matrix of all types of peroxisome (Mhamdi et al., 2010, 2012; Palma et al., 2020 and references therein), other enzymatic antioxidants are present in both the matrix and the membrane. It is also important to highlight the role of SOD isozymes, which differ according to peroxisomal origin (del Río et al., 2018). Thus, peroxisomes of watermelon cotyledons have two SOD isoenzymes, a CuZn-SOD located in the matrix and a Mn-SOD that is bound to the membrane (Bueno and del Río, 1992; Rodríguez-Serrano et al., 2007); pea leaf peroxisomes have a Mn-SOD present in the matrix; sunflower cotyledon peroxisomes have only a CuZn-SOD which is also located in the matrix (Corpas et al., 1998); carnation petal and pepper fruit peroxisomes have a Mn- and an Fe-SOD (Droillard and Paulin, 1990; Palma et al., 2018); and olive fruits peroxisomes contain four SOD isozymes, an Fe-SOD, two CuZn-SOD and a Mn-SOD (López-Huertas and del Río, 2014). Therefore, it could be hypothesized that the presence of two or more types of SOD in peroxisomes must have some physiological advantages. Thus, one of the SOD isozymes could be constitutive while the other one could be inducible under environmental or physiological stimuli such as seedling development, leaf senescence or fruit ripening.

In addition, it is worth noting the role of ascorbate-glutathione cycle components, including ascorbate peroxidase (APX), monodehydroascorbate reductase (MDAR), dehydroasrcorbate reductase (DAR) and glutathione reductase (GR) (Jiménez et al., 1998; Romero-Puertas et al., 2006; López-Huertas and del Río, 2014; Corpas et al., 2017a). While MDAR is present in both matrix and membrane (Leterrier et al., 2005; Lisenbee et al., 2005; Eastmond, 2007), APX is exclusively located in the membrane (Corpas et al., 1994; Yamaguchi et al., 1995; Bunkelmann and Trelease, 1996). With its high affinity for H_2O_2 (low *Km* value around 74 μM), membrane-bound APX appears to have fine-tuned control of H_2O_2 (Ishikawa et al., 1998) as compared to catalase, which, with a *Km* value in the mM range, is less efficient at low concentrations of H_2O_2 (Huang et al., 1983; Mhamdi et al., 2010). The *Km* values for plant catalase are reported to vary quite considerably, with, for example, a *Km* of 50 mM in *Beta vulgaris* (Dinçer and Aydemir, 2001), 100 mM in rice (Ray et al., 2012) and 190 mM in pea (del Río et al., 1977). Peroxisomal APX appears to be critical in a diverse range of processes such as seedling development (Corpas and Trelease, 1998) and leaf senescence (Ribeiro et al., 2017). To maintain the ascorbate-glutathione cycle at the GR level, NADPH needs to be supplied by NADP-dependent endogenous dehydrogenases including glucose-6-phosphate dehydrogenase (G6PDH), 6-phosphogluconate dehydrogenase (6PGDH) and isocitrate dehydrogenase (NADP-ICDH) (Leterrier et al., 2016; Corpas and Barroso, 2018b and references therein). In addition, Corpas et al. (2017b) have reported the presence of a protein immunologically related to plant peroxiredoxins, whose expression is differentially modulated under oxidative stresses such as those induced by $CdCl_2$ and the herbicide 2,4-dichlorophenoxyacetic acid (2,4-D); however, further research is necessary to clarify this phenomenon. **Figure 2** shows a working model of the ROS metabolism and its interaction with other reactive species, including NO and H_2S, which modulate the activity of peroxisomal enzymes through posttranslational modifications (PTMs), events which will be further discussed below.

Given the capacity of ROS to mediate several PTMs, particularly carbonylation and *S*-sulfenylation, certain amino acid residues, especially arginine, lysine, threonine and proline, are carbonylated, which affects target protein function in many cases (Debska et al., 2012; Lounifi et al., 2013). Several studies have identified peroxisomal proteins, such as catalase, malate synthase and the fatty acid β-oxidation multifunctional protein AIM1, which undergo carbonylation (Nguyen and Donaldson, 2005; Anand et al., 2009; Mano et al., 2014; Rodríguez-Ruiz et al., 2019). On the other hand, H_2O_2 can oxidize specific protein cysteine thiols to sulfenic acid (SOH), a process known as *S*-sulfenylation, which usually results in enzymatic inactivation. Using proteomic techniques, approximately 2% of peroxisomal proteins have been reported to be susceptible to *S*-sulfenylation (Akter et al., 2017; Huang et al., 2019). This PTM has been observed to occur with respect to fatty acid β-oxidation acyl-coenzyme A oxidase 1, the multifunctional proteins MFP2, and AIM1, as well as amine oxidase, phosphomevalonate kinase, MDAR and NADP-ICDH. **Table 1** shows a summary of peroxisomal enzymes targeted by carbonylation and *S*-sulfenylation, as well as other PTMs mediated by RNS and RSS, a subject which will be discussed below.

Given growing awareness of the important role of ROS peroxisomal metabolism in combating biotic stress, the expression of genes encoding for peroxisomal proteins involved in their biogenesis, fatty acid catabolism and the H_2O_2-generating glyoxylate cycle have been reported to increase during interactions between the pathogen *Sclerotinia sclerotiorum* and rapeseed (*Brassica napus*), thus facilitating pathogen cell wall degradation and metabolism detoxification (Chittem et al., 2020). On the other hand, using the Arabidopsis *nca1* mutant with no catalase activity 1, containing residual activity of the three catalase isozymes, Hackenberg et al. (2013) identified a link between catalase and ROS production as autophagy-dependent cell death progresses. **Table 2** shows some functional implications of peroxisomal H_2O_2 and other signal molecules generated in this organelle.

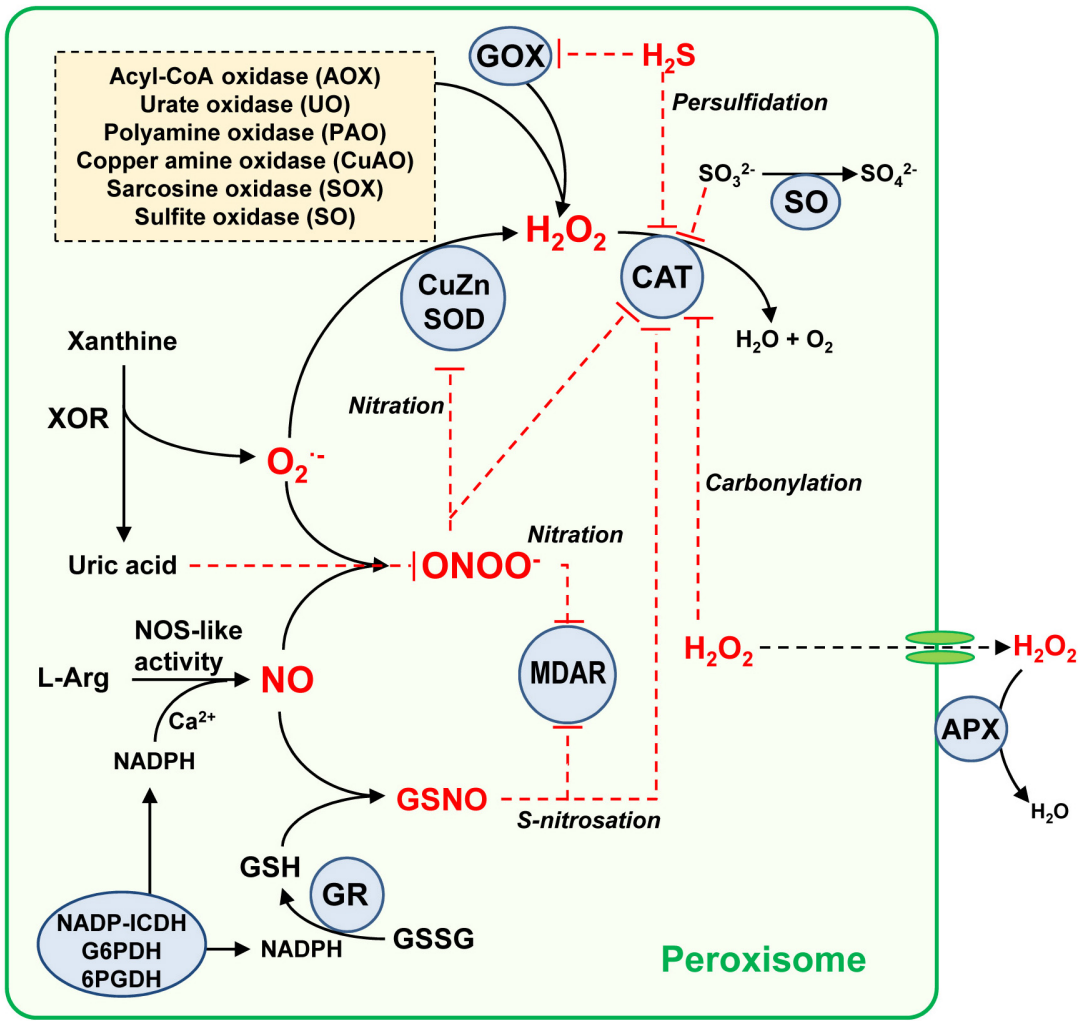

FIGURE 2 | Simple model of the global metabolism of reactive oxygen/nitrogen/sulfur species in plant peroxisomes. Peroxisomes have an important battery of H_2O_2-generating enzymes, being the photorespiratory glycolate oxidase (GOX) one of the most relevant. Peroxisomal xanthine oxidoreductase (XOR) activity generates uric acid which the concomitant generation of superoxide radical ($O_2^{\bullet -}$) which is dismutated to H_2O_2 by superoxide dismutase (SOD). All three SOD types have been described in plant peroxisomes from different origin, CuZ-SOD, Mn-SOD, and Fe-SOD. The H_2O_2 pool is mainly decomposed by catalase (CAT) but also by the membrane-bound ascorbate peroxidase (APX). An L-arginine (L-Arg) and Ca^{2+} dependent NOS-like activity generates NO which can react chemically with O_2^- to produce peroxynitrite ($ONOO^-$), a nitrating molecule that facilitates PTMs such as tyrosine nitration. NO can also interact with reduced glutathione (GSH) to form *S*-nitrosoglutathione (GSNO), a NO donor which mediates *S*-nitrosation. GSH is regenerated by glutathione reductase (GR) which requires NADPH supplied by several NADPH-generating enzymes (NADPH-ICDH, G6PDH, and 6PGDH). Uric acid is a $ONOO^-$ scavenger, this being a mechanism of peroxisomal auto-regulation. With all these components, and according to reported data, the peroxisomal targets of NO-derived PTMs identified so far are CAT, CuZn-SOD, and monodehydroascorbate reductase (MDAR) which can undergo an inhibitory effect either by nitration or *S*-nitrosation. Additionally, CAT and GOX can be inhibited by hydrogen sulfide (H_2S), and CAT is also inhibited by carbonylation. The H_2O_2-generating sulfite oxidase (SO) converts sulfite (SO_3^{2-}) to sulfate (SO_4^{2-}), which is a mechanism of protection because sulfite inhibits catalase activity. Red line denotes inhibition effect.

The generation of singlet oxygen ($^1O_2$) has always been associated with chloroplasts, particularly in photosystem II, responsible for various types of photo-damage which triggers distinct cellular responses (Wagner et al., 2004; Rosenwasser et al., 2011; Chen and Fluhr, 2018; Dogra et al., 2018). Using the green fluorescence probe to detect $^1O_2$, peroxisomes, mitochondria and nuclei have been shown to be either the origin or target of $^1O_2$, suggesting that this ROS is generated in a light-independent manner (Mor et al., 2014). These findings open up new questions about the importance of $^1O_2$ in the mechanism of response to plant stress in which several subcellular compartments including peroxisomes are involved.

PEROXISOMAL REACTIVE NITROGEN SPECIES (RNS)

Nitric oxide (NO) metabolism has a significant impact on cellular metabolisms due to its involvement in the important plant physiological processes of seed and pollen germination, root

TABLE 1 | Peroxisomal enzymes target of diverse posttranslational modifications (PTMs) whose activities are affected by either ROS, RNS, or RSS.

Peroxisomal enzyme	Pathway/Reaction	PTM	Effect on activity
Catalase (CAT)	H_2O_2 decomposition	Carbonylation	Inhibition
		Tyr-nitration	Inhibition
		S-nitrosation	Inhibition
		Persufidation	Inhibition
Monodehydroascorbate reductase (MDAR)	Ascorbate-glutathione cycle	Tyr-nitration	Inhibition
		S-nitrosation	Inhibition
		S-sulfenylation[a]	Not reported
Hydroxypyruvate reductase (HPR)	Photorespiration	Tyr-nitration	Inhibition
		S-nitrosation	Inhibition
Glycolate oxidase (GOX)	Photorespiration	*S*-nitrosation	Inhibition
		Persufidation	Inhibition
CuZn-superoxide dismutase (CSD3)	$O_2^{\bullet-}$ dismutation	Tyr-nitration	Inhibition
Malate dehydrogenase (MDH)	Fatty acid β-oxidation	Tyr-nitration	Inhibition
		S-nitrosation	Inhibition
Malate synthase (MS)	Glyoxylate cycle	Carbonylation	Inhibition
Isocitrate lyase (ICL)	Glyoxylate cycle	S-nitrosation[a]	Not reported
Acyl-coenzyme A oxidase 1	Fatty acid β-oxidation	Persulfidation[a]	Not reported
		S-sulfenylation[a]	Not reported
Multifunctional protein AIM1 isoform	Fatty acid β-oxidation	S-nitrosation[a]	Not reported
		S-sulfenylation[a]	Not reported
Lon protease homolog 2	Peroxisomal protein import	*S*-nitrosation[a]	Not reported
Phosphomevalonate kinase	Isoprenoid biosynthesis	*S*-sulfenylation[a]	Not reported
NADP-isocitrate dehydrogenase	NADPH supply	Tyr-nitration	Inhibition
		S-nitrosation	Inhibition
		Persufidation	Inhibition
		S-sulfenylation[a]	Not reported

[a]*Proteomic identification.*

development, stomatal closure, senescence and fruit ripening, as well as in the mechanism of response to many environmental stresses including salinity, drought, heavy metals and extreme temperature (Neill et al., 2008; León et al., 2014; Begara-Morales et al., 2018; Kolbert et al., 2019; Wei et al., 2020). NO belongs to a family of related molecules called reactive nitrogen species (RNS), with peroxynitrite ($ONOO^-$) and *S*-nitrosogluthione (GSNO) being the most studied. Using various experimental approaches including electron paramagnetic resonance (EPR) spectroscopy, as well as biochemical and cellular biology, some RNS including NO, $ONOO^-$ and GSNO have been detected in plant peroxisomes (Barroso et al., 2013; Corpas and Barroso, 2014b; Corpas et al., 2019). Identification of peroxisomal proteins undergoing PTMs mediated by these NO-derived species is strong evidence of an active RNS metabolism in peroxisomes. **Figures 3A–H** shows *in vivo* images of NO and $ONOO^-$ in Arabidopsis guard cell peroxisomes detected by confocal laser scanning microscopy (CLSM) and specific fluorescent probes.

$ONOO^-$ results from a reaction between NO with $O_2^{\bullet-}$, considered one of the fastest chemical reactions with a rate constant (k) of 1.9×10^{10} M^{-1} s^{-1} (Kissner et al., 1997). $ONOO^-$, a strong oxidant and nitrating molecule involved in protein tyrosine nitration (NO_2-Tyr), modifies protein function, mostly through inhibition (Corpas et al., 2009a; Mata-Pérez et al., 2016). This NO-derived PTM involves the covalent oxidative addition of a nitro group (-NO_2) to tyrosine residues, a highly selective process which depends on factors such as the protein environment of the Tyr and the nitration mechanism (Bartesaghi and Radi, 2018). **Table 1** shows some nitrated proteins identified in plant peroxisomes and how their function is affected. Interestingly, some of the proteins affected are directly involved in the ROS metabolism, indicating a close metabolic interconnection between both families of reactive species.

The antioxidant glutathione (GSH), a tripeptide (γ-Glu-Cys-Gly), undergoes *S*-nitrosation in order to generate GSNO, a low-molecular-weight NO reservoir, through a covalent addition of NO to the thiol group of Cys residues in order to form *S*-nitrosothiol (SNO) (Airaki et al., 2011). GSNO is a key molecule given its dynamic interaction with free cysteines, GSH and proteins through processes such as *S*-nitrosation, *S*-transnitrosation and *S*-glutathionylation (Broniowska et al., 2013; Corpas et al., 2013a,b). GSNO is enzymatically decomposed by GSNO reductase (GSNOR; Leterrier et al., 2011), an enzyme susceptible to *S*-nitrosation and consequently inhibition (Guerra et al., 2016). An increase in Tyr nitration, an irreversible process, is usually associated with nitro-oxidative stress; however, protein *S*-nitrosation, a reversible process, is a regulatory protein mechanism that occurs under physiological and stress conditions. **Table 1** shows some peroxisomal proteins targeted

TABLE 2 | Signal molecules generated in plant peroxisomes during different processes and their functional implications.

Peroxisomal signal	Functional implication	References
Hydrogen peroxide (H_2O_2)	Plant development and stress response	Zhang et al., 2016; Su et al., 2019
	Involved in peroxisome abundance under drought and heat stress	Hinojosa et al., 2019
	Pexophagy	Yamauchi et al., 2019
	Pathogen defense	Chittem et al., 2020
Nitric oxide (NO)	Pollen tube development	Prado et al., 2004
	Leaf senescence	Corpas et al., 2019
	Lateral root formation	Schlicht et al., 2013
	Heavy metal and root architecture	Piacentini et al., 2020
Hydrogen sulfide (H_2S)	Regulation of catalase	Corpas et al., 2019a
	Herbicide glyphosate response	
Jasmonic acid (JA)	Plant growth	Wang X. et al., 2019
	Environmental stimuli	Xin et al., 2019
	Insect defense	
γ-aminobutyric acid (GABA)	Fruit flavor and flower fragrance	Zarei et al., 2015
	Abiotic stress tolerance	Shelp and Zarei, 2017

by *S*-nitrosation, as well as proteins involved in ROS metabolism which are targeted by these NO-mediated PTMs.

The number of peroxisomal proteins targeted by NO-mediated PTMs is growing continuously. Using the biotin-switch technique and liquid chromatography/mass spectrometry/mass spectrometry (LC-MS/MS), several more *S*-nitrosated peroxisomal proteins have been identified during adventitious root growth induced by treatment with NO (Niu et al., 2019). These proteins include the peroxisomal LON2 protease, which is necessary for matrix protein import into peroxisomes (Lingard and Bartel, 2009); isocitrate lyase (ICL), involved in the glyoxylate cycle; and the multifunctional AIM1-like isoform, involved in fatty acid β-oxidation.

However, the source of enzymatic NO, as yet unelucidated, is currently the most controversial aspect of NO metabolism in higher plants (Kolbert et al., 2019). Two main candidates have been proposed: nitrate reductase (NR) (Mohn et al., 2019) and L-arginine-dependent NO synthase-like activity (Corpas et al., 2017a). Although no evidence of NR has been found in plant peroxisomes, NO synthase-like activity has been found and characterized in peroxisomes purified from pea leaves (Barroso et al., 1999). Though as yet unidentified, this protein is called NOS-like activity, as peroxisomal NO generation requires NOS proteins similar to those found in animals, including L-arginine, NADPH, FMN, FAD, tetrahydrobiopterin, calcium, and calmodulin (Corpas and Barroso, 2017b; Corpas et al., 2019). The protein responsible for NO generation is imported by a type 2 peroxisomal targeting signal involving a process dependent on calmodulin and calcium (Corpas and Barroso, 2014a, 2018a).

Peroxisomal NO metabolism is involved in processes such as pollen tube germination (Prado et al., 2004), lateral

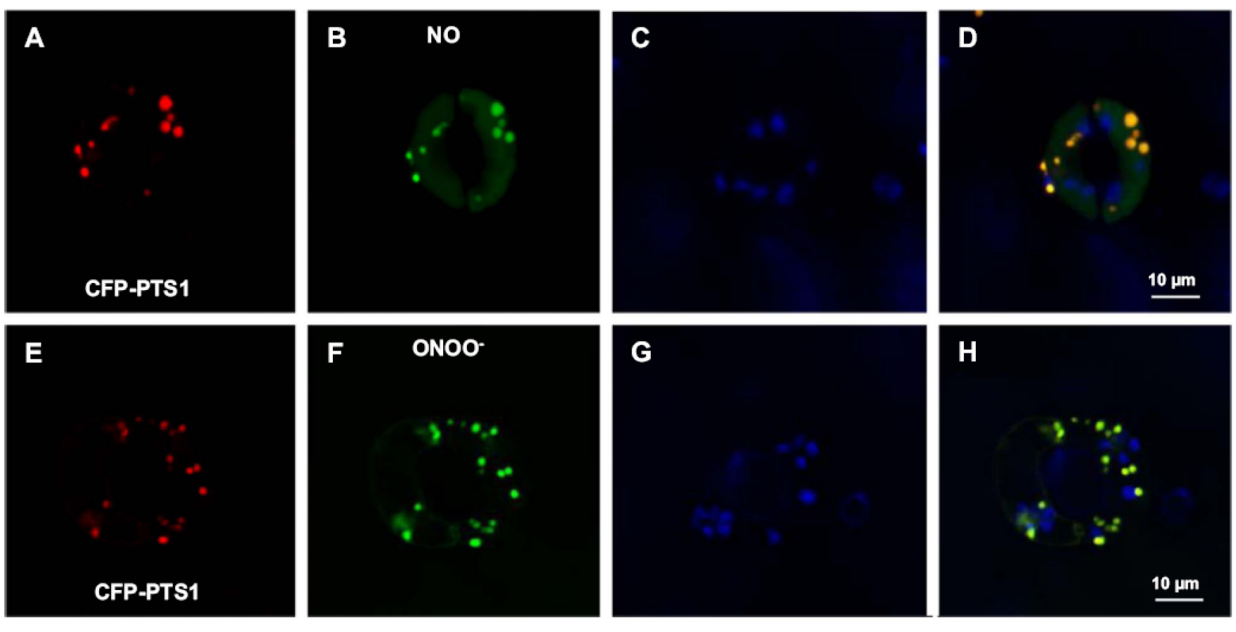

FIGURE 3 | Representative images illustrating the CLSM *in vivo* detection of nitric oxide (NO) and peroxynitrite ($ONOO^-$), peroxisomes (red) and chloroplasts (blue) in guard cells of transgenic Arabidopsis seedlings expressing CFP-PTS1. **(A,E)** Fluorescence punctate (red) attributable to CFP-PTS1, indicating the localization of peroxisomes in guard cells. **(B,F)** Fluorescence punctate (green) attributable to the detection in the same guard cells of NO and $ONOO^-$, respectively. **(C,G)** Chlorophyll autofluorescence (blue) attributable to the detection of chloroplasts. **(D,H)** Merged images for corresponding panels. Reproduced with permission from Corpas et al. (2017a) provided by Elsevier.

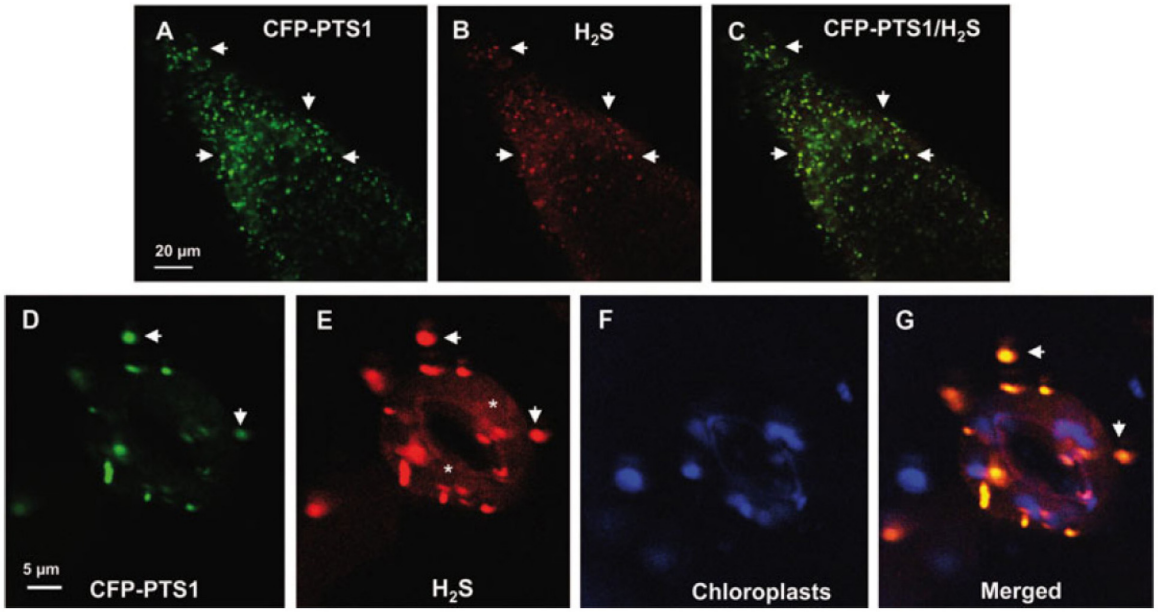

FIGURE 4 | Representative images illustrating the CLSM *in vivo* detection of H_2S (red color) and peroxisomes (green color) in root tips **(A–C)** and guard cells **(D–G)** of 10 days old Arabidopsis seedlings expressing CFP-PTS1. **(A,D)** Fluorescence puncta (green) attributable to CFP-PTS1, indicating the localization of peroxisomes. **(B,E)** Fluorescence punctate (red) attributable to H_2S detection in the same area. **(C)** Merged image of **(A,B)** showing colocalized fluorescence punctate (yellow). **(F)** Chlorophyll autofluorescence (blue) demonstrating location of chloroplasts. **(G)** Merged images of **(D–F)**. H_2S (red color) was detected by using 5 mM WSP-5, a fluorescence probe for H_2S. Arrows indicate representative punctate spots corresponding to the colocalization of H_2S with peroxisomes. Asterisks indicate localization of H_2S in the cytosol. Reproduced with permission from Corpas et al. (2019a) provided by John Wiley and Sons.

root formation (Schlicht et al., 2013), and leaf senescence (Corpas et al., 2019), as well as in responses to environmental and heavy metal stresses such as salinity (Corpas et al., 2009b), lead (Corpas and Barroso, 2017a), and cadmium (Corpas and Barroso, 2014b; Piacentini et al., 2020).

REACTIVE SULFUR SPECIES (RSS) IN PLANT PEROXISOMES

Reactive sulfur species (RSS) are chemically comparable to ROS (Olson, 2019) and can be generated from hydrogen sulfide (H_2S), some of these species are thiyl radical ($HS^{\bullet}$), hydrogen persulfide (H_2S_2), persulfide radical ($HS_2^{\bullet-}$), sulfite (SO_3^{2-}) or sulfate (SO_4^{2-}) among others (Gruhlke and Slusarenko, 2012; Ono et al., 2014; Mishanina et al., 2015; Park et al., 2015; Schöneich, 2016). However, the biochemistry of H_2S in cells, given its multiple interactions with other reactive species, is more complex than previously thought (see Filipovic et al., 2018 for a more in-depth review); for example, protein thiyl radicals are generated during the reaction of H_2O_2 with heme proteins, possibly inducing protein degradation (Schöneich, 2016).

Different molecules and enzymes, such as GSH (Müller et al., 2004), glutathione reductase (Romero-Puertas et al., 2006), and sulfite oxidase (Nowak et al., 2004; Hänsch and Mendel, 2005), involved in sulfur metabolism, are present in plant peroxisomes. Sulfite oxidase (SO) catalyzes the conversion of sulfite to sulfate by producing H_2O_2. The functional relevance of this enzyme is that it can protect catalase activity since sulfite, at low concentration, has the capacity to inhibit catalase activity (Veljovic-Jovanovic et al., 1998). Nevertheless, despite the greater importance attributed to peroxisomal SO in a recent study, mitochondrial SO in animal cells has the capacity to generate NO from nitrite (Bender et al., 2019), while NO enzymatic generation from SO in plant peroxisomes remains to be proven. An earlier study confirmed the important role played by the peroxisomal RSS metabolism (Corpas and Barroso, 2015).

H_2S has recently been proven to be present in plant peroxisomes (Corpas et al., 2019a). **Figures 4A–G** shows representative images of H_2S in peroxisomes from the root tips and guard cells of Arabidopsis seedlings detected by *in vivo* CLSM and a specific fluorescent probe. Using proteomic techniques, some peroxisomal enzymes have been identified as targets of persulfidation (Aroca et al., 2015, 2017). On the other hand, *in vitro* analysis shows that catalase activity from Arabidopsis and sweet pepper fruits is inhibited in the presence of H_2S (Corpas et al., 2019a). Although, to our knowledge, the enzymatic source of peroxisomal H_2S remains unknown, previous studies have proposed some potential candidates. For example, catalase, which functions as a sulfide oxidase or sulfur reductase, is capable of oxidizing or generating H_2S (Olson et al., 2017). SOD has also been reported to have the capacity to catalyze the reaction between O_2 and H_2S to generate persulfide (Olson et al., 2018). In a previous study by Corpas and Barroso (2015), the presence of these enzymatic and non-enzymatic components in plant

peroxisomes indicates that, in addition to ROS and RNS, these organelles also have an active RSS metabolism.

CROSSTALK BETWEEN PEROXISOMAL REACTIVE SPECIES

Functional interactions and inter-regulation through PTMs in these families of reactive species are shown in **Figure 2**. In this working model, under physiological conditions, catalase, the main antioxidant enzyme, regulates levels of H_2O_2 generated by different pathways, principally photorespiratory glycolate oxidase (GOX) (Noctor et al., 2002). On the other hand, peroxisomal xanthine oxidoreductase (XOR) activity involved in purine catabolism generates uric acid, with the concomitant formation of the $O_2^{\bullet-}$ (Corpas et al., 1997, 2008; Zarepour et al., 2010), which, in turn, is dismutated to H_2O_2 by SOD. The pool of H_2O_2 is mainly decomposed by catalase (CAT) and also by membrane-bound ascorbate peroxidase (APX). L-Arg-dependent NOS-like activity generates NO (Corpas et al., 2019) which chemically reacts with $O_2^{\bullet-}$ to produce peroxynitrite ($ONOO^-$), a nitrating molecule that facilitates PTMs such as tyrosine nitration. NO also interacts with reduced glutathione (GSH) to form *S*-nitrosoglutathione (GSNO), a NO donor that mediates *S*-nitrosation. Uric acid is a physiological $ONOO^-$ scavenger (Alamillo and García-Olmedo, 2001) involved in endogenous peroxisomal auto-regulation. Thus, the peroxisomal enzymes targeted by NO-derived PTMs, catalase (CAT), CuZn-SOD, and monodehydroascorbate reductase (MDAR), are inhibited by nitration and S-nitrosation. Both CAT, and GOX are inhibited by H_2S; the former is also inhibited by carbonylation when H_2O_2 is overproduced. In addition, H_2O_2-generating sulfite oxidase (SO) is involved in the conversion of sulfite to sulfate which, given sulfite's ability to inhibit SO, has been reported to be a catalase protection mechanism. These interconnections highlight the biochemical complexity of this self-regulated plant peroxisome network, in which the antioxidant catalase is one of the most regulated peroxisomal enzymes (Palma et al., 2020).

CONCLUSION

Much of our knowledge of reactive species metabolism in plant peroxisomes is now well established. The three molecular families ROS, RNS, and RSS are present in plant peroxisomes, which are considered to be potential producers of reactive species and to play an important role in the cell signaling network. However, our limited knowledge of reactive species families needs to be expanded by identifying new peroxisomal protein targets. We also need to determine the effect of the different PTMs, carbonylation, *S*-sulfenylation, *S*-nitrosation, tyrosine nitration, and persulfidation, on target protein function and peroxisomal metabolism. In addition, interactions with other subcellular compartments which share biochemical pathways such as photorespiration, fatty acid β-oxidation, isoprenoid biosynthesis and purine and polyamine metabolism (Clastre et al., 2011; Guirimand et al., 2012; Corpas et al., 2019b) should be investigated. Similarly, the relationship between reactive species and complex peroxisomal biogenesis, division and matrix/membrane protein import mechanisms (Reumann and Bartel, 2016; Kao et al., 2018) has been underexplored (López-Huertas et al., 2000). Further research should also be carried out to identify the proteins responsible for endogenous peroxisomal generation of NO and H_2S. This would increase our knowledge of how organelle biochemistry is modulated within the framework of the whole cell metabolism. This research could lead to biotechnological applications given the important role of peroxisomes in many physiological processes and in responses to biotic and abiotic stresses. Furthermore, in addition to harboring reactive species, with their known signaling properties, peroxisomes are a source of other signaling molecules such as jasmonic acid and γ-aminibutic acid (GABA), which extends the functional role of plant peroxisomes. **Table 2** shows signaling molecules generated in the plant peroxisomal metabolism and some examples of their role in various plant processes.

AUTHOR CONTRIBUTIONS

Authors have made a collaborative, direct and intellectual contribution to the work, and have approved it for publication.

FUNDING

This work was supported by the European Regional Development Fund co-financed grant from the Ministry of Economy and Competitiveness (AGL2015-65104-P and PID2019-103924GB-I00), the Plan Andaluz de Investigación, Desarrollo e Innovación (P18-FR-1359), and the Junta de Andalucía (group BIO192), Spain.

ACKNOWLEDGMENTS

SG-G acknowledges a "Formación de Personal Investigador" contract (BES-2016-078368) from the Ministry of Economy and Competitiveness, Spain.

REFERENCES

Airaki, M., Sánchez-Moreno, L., Leterrier, M., Barroso, J. B., Palma, J. M., and Corpas, F. J. (2011). Detection and quantification of S-nitrosoglutathione (GSNO) in pepper (*Capsicum annuum* L.) plant organs by LC-ES/MS. *Plant Cell Physiol.* 52, 2006–2015. doi: 10.1093/pcp/pcr133

Akter, S., Carpentier, S., Van Breusegem, F., and Messens, J. (2017). Identification of dimedone-trapped sulfenylated proteins in plants under stress. *Biochem. Biophys. Rep.* 9, 106–113. doi: 10.1016/j.bbrep.2016.11.014

Alamillo, J. M., and García-Olmedo, F. (2001). Effects of urate, a natural inhibitor of peroxynitrite-mediated toxicity, in the response of *Arabidopsis thaliana* to the

bacterial pathogen *Pseudomonas* syringae. *Plant J.* 25, 529–540. doi: 10.1046/j.1365-313x.2001.00984.x

Anand, P., Kwak, Y., Simha, R., and Donaldson, R. P. (2009). Hydrogen peroxide induced oxidation of peroxisomal malate synthase and catalase. *Arch. Biochem. Biophys.* 491, 25–31. doi: 10.1016/j.abb.2009.09.019

Aroca, A., Benito, J. M., Gotor, C., and Romero, L. C. (2017). Persulfidation proteome reveals the regulation of protein function by hydrogen sulfide in diverse biological processes in *Arabidopsis*. *J. Exp. Bot.* 68, 4915–4927. doi: 10.1093/jxb/erx294

Aroca, Á, Serna, A., Gotor, C., and Romero, L. C. (2015). S-sulfhydration: a cysteine posttranslational modification in plant systems. *Plant Physiol.* 168, 334–342. doi: 10.1104/pp.15.00009

Baker, A., Graham, I. A., Holdsworth, M., Smith, S. M., and Theodoulou, F. L. (2006). Chewing the fat: beta-oxidation in signalling and development. *Trends Plant Sci.* 11, 124–132. doi: 10.1016/j.tplants.2006.01.005

Barroso, J. B., Corpas, F. J., Carreras, A., Sandalio, L. M., Valderrama, R., Palma, J. M., et al. (1999). Localization of nitric-oxide synthase in plant peroxisomes. *J. Biol. Chem.* 274, 36729–36733.

Barroso, J. B., Valderrama, R., and Corpas, F. J. (2013). Immunolocalization of S-nitrosoglutathione, S-nitrosoglutathione reductase and tyrosine nitration in pea leaf organelles. *Acta Physiol. Plant* 35, 2635–2640. doi: 10.1007/s11738-013-1291-0

Bartesaghi, S., and Radi, R. (2018). Fundamentals on the biochemistry of peroxynitrite and protein tyrosine nitration. *Redox Biol.* 14, 618–625. doi: 10.1016/j.redox.2017.09.009

Begara-Morales, J. C., Chaki, M., Valderrama, R., Sánchez-Calvo, B., Mata-Pérez, C., Padilla, M. N., et al. (2018). Nitric oxide buffering and conditional nitric oxide release in stress response. *J. Exp. Bot.* 69, 3425–3438. doi: 10.1093/jxb/ery072

Bender, D., Tobias Kaczmarek, A., Niks, D., Hille, R., and Schwarz, G. (2019). Mechanism of nitrite-dependent NO synthesis by human sulfite oxidase. *Biochem. J.* 476, 1805–1815. doi: 10.1042/bcj20190143

Borek, S., Stefaniak, S., Śliwiński, J., Garnczarska, M., and Pietrowska-Borek, M. (2019). Autophagic machinery of plant peroxisomes. *Int. J. Mol. Sci.* 20:4754. doi: 10.3390/ijms20194754

Broniowska, K. A., Diers, A. R., and Hogg, N. (2013). S-nitrosoglutathione. *Biochim. Biophys. Acta* 1830, 3173–3181.

Bueno, P., and del Río, L. A. (1992). Purification and properties of glyoxysomal cuprozinc superoxide dismutase from watermelon cotyledons (*Citrullus vulgaris* Schrad). *Plant Physiol.* 98, 331–336. doi: 10.1104/pp.98.1.331

Bunkelmann, J. R., and Trelease, R. N. (1996). Ascorbate peroxidase. A prominent membrane protein in oilseed glyoxysomes. *Plant Physiol.* 110, 589–598. doi: 10.1104/pp.110.2.589

Chen, D., Shao, Q., Yin, L., Younis, A., and Zheng, B. (2019a). Polyamine function in plants: metabolism, regulation on development, and roles in abiotic stress responses. *Front. Plant Sci.* 9:1945.

Chen, S., Lu, X., Ge, L., Sun, X., and Xin, Z. (2019b). Wound- and pathogen-activated de novo JA synthesis using different ACX isozymes in tea plant (*Camellia sinensis*). *J. Plant Physiol.* 243:153047. doi: 10.1016/j.jplph.2019.153047

Chen, T., and Fluhr, R. (2018). Singlet oxygen plays an essential role in the root's response to osmotic stress. *Plant Physiol.* 177, 1717–1727. doi: 10.1104/pp.18.00634

Chittem, K., Yajima, W. R., Goswami, R. S., and Del Río Mendoza, L. E. (2020). Transcriptome analysis of the plant pathogen *Sclerotinia sclerotiorum* interaction with resistant and susceptible canola (*Brassica napus*) lines. *PLoS One* 15:e0229844. doi: 10.1371/journal.pone.0229844

Chowdhary, G., Kataya, A. R., Lingner, T., and Reumann, S. (2012). Non-canonical peroxisome targeting signals: identification of novel PTS1 tripeptides and characterization of enhancer elements by computational permutation analysis. *BMC Plant Biol.* 12:142. doi: 10.1186/1471-2229-12-142

Clastre, M., Papon, N., Courdavault, V., Giglioli-Guivarc'h, N., St-Pierre, B., and Simkin, A. J. (2011). Subcellular evidence for the involvement of peroxisomes in plant isoprenoid biosynthesis. *Plant Signal. Behav.* 6, 2044–2046. doi: 10.4161/psb.6.12.18173

Corpas, F. J. (2015). What is the role of hydrogen peroxide in plant peroxisomes? *Plant Biol.* 17, 1099–1103. doi: 10.1111/plb.12376

Corpas, F. J., Sandalio, L. M., del Río, L. A., Trelease, R. N. (1998). Copper–zinc superoxide dismutase is a constituent enzyme of the matrix of peroxisomes in the cotyledons of oilseed plants. *New Phytol.* 138, 307–314. doi: 10.1046/j.1469-8137.1998.00899.x

Corpas, F J., Barroso, J B., del Río, L A. (2001). Peroxisomes as a source of reactive oxygen species and nitric oxide signal molecules in plant cells. *Trends Plant. Sci.* 6, 145–50. doi: 10.1016/s1360-1385(01)01898-2

Corpas, F. J., Alché, J. D., and Barroso, J. B. (2013a). Current overview of S-nitrosoglutathione (GSNO) in higher plants. *Front. Plant Sci.* 4:126.

Corpas, F. J., Leterrier, M., Begara-Morales, J. C., Valderrama, R., Chaki, M., López-Jaramillo, J., et al. (2013b). Inhibition of peroxisomal hydroxypyruvate reductase (HPR1) by tyrosine nitration. *Biochim. Biophys. Acta* 1830, 4981–4989. doi: 10.1016/j.bbagen.2013.07.002

Corpas, F. J., and Barroso, J. B. (2014a). Peroxisomal plant nitric oxide synthase (NOS) protein is imported by peroxisomal targeting signal type 2 (PTS2) in a process that depends on the cytosolic receptor PEX7 and calmodulin. *FEBS Lett.* 588, 2049–2054. doi: 10.1016/j.febslet.2014.04.034

Corpas, F. J., and Barroso, J. B. (2014b). Peroxynitrite (ONOO-) is endogenously produced in *Arabidopsis* peroxisomes and is overproduced under cadmium stress. *Ann. Bot.* 113, 87–96. doi: 10.1093/aob/mct260

Corpas, F. J., and Barroso, J. B. (2015). Reactive sulfur species (RSS): possible new players in the oxidative metabolism of plant peroxisomes. *Front Plant Sci.* 6:116.

Corpas, F. J., and Barroso, J. B. (2017a). Lead-induced stress, which triggers the production of nitric oxide (NO) and superoxide anion (O2·-) in *Arabidopsis* peroxisomes, affects catalase activity. *Nitric Oxide* 68, 103–110. doi: 10.1016/j.niox.2016.12.010

Corpas, F. J., and Barroso, J. B. (2017b). Nitric oxide synthase-like activity in higher plants. *Nitric Oxide* 68, 5–6. doi: 10.1016/j.niox.2016.10.009

Corpas, F. J., and Barroso, J. B. (2018a). Calmodulin antagonist affects peroxisomal functionality by disrupting both peroxisomal Ca2+ and protein import. *J. Cell Sci.* 131:jcs201467. doi: 10.1242/jcs.201467

Corpas, F. J., and Barroso, J. B. (2018b). Peroxisomal plant metabolism - an update on nitric oxide, Ca2+ and the NADPH recycling network. *J. Cell Sci.* 131:jcs202978. doi: 10.1242/jcs.202978

Corpas, F. J., Barroso, J. B., González-Gordo, S., Muñoz-Vargas, M. A., and Palma, J. M. (2019a). Hydrogen sulfide: a novel component in *Arabidopsis* peroxisomes which triggers catalase inhibition. *J. Integr. Plant Biol.* 61, 871–883.

Corpas, F. J., del Río, L. A., and Palma, J. M. (2019b). Plant peroxisomes at the crossroad of NO and H2O2 metabolism. *J. Integr. Plant Biol.* 61, 803–816.

Corpas, F. J., Barroso, J. B., Palma, J. M., and Rodríguez-Ruiz, M. (2017a). Plant peroxisomes: a nitro-oxidative cocktail. *Redox Biol.* 11, 535–542. doi: 10.1016/j.redox.2016.12.033

Corpas, F. J., Pedrajas, J. R., Palma, J. M., Valderrama, R., Rodríguez-Ruiz, M., Chaki, M., et al. (2017b). Immunological evidence for the presence of peroxiredoxin in pea leaf peroxisomes and response to oxidative stress conditions. *Acta Physiol. Plant* 39:57.

Corpas, F. J., Bunkelmann, J., and Trelease, R. N. (1994). Identification and immunochemical characterization of a family of peroxisome membrane proteins (PMPs) in oilseed glyoxysomes. *Eur. J. Cell Biol.* 65, 280–290.

Corpas, F. J., Chaki, M., Leterrier, M., and Barroso, J. B. (2009a). Protein tyrosine nitration: a new challenge in plants. *Plant Signal. Behav.* 4, 920–923. doi: 10.4161/psb.4.10.9466

Corpas, F. J., Hayashi, M., Mano, S., Nishimura, M., and Barroso, J. B. (2009b). Peroxisomes are required for in vivo nitric oxide accumulation in the cytosol following salinity stress of *Arabidopsis* plants. *Plant Physiol.* 151, 2083–2094. doi: 10.1104/pp.109.146100

Corpas, F. J., de la Colina, C., Sánchez-Rasero, F., and del Río, L. A. (1997). A role for leaf peroxisomes in the catabolism of purines. *J. Plant Physiol.* 151, 246–250. doi: 10.1016/s0176-1617(97)80161-7

Corpas, F. J., del Río, L. A., and Palma, J. M. (2019). Impact of nitric oxide (NO) on the ROS metabolism of peroxisomes. *Plants* 8:E37.

Corpas, F. J., Gómez, M., Hernández, J. A., and del Rio, L. A. (1993). Metabolism of activated oxygen in peroxisomes from two *Pisum salivum* L. cultivars with different sensitivity to sodium chloride. *J. Plant Physiol.* 141, 160–165. doi: 10.1016/s0176-1617(11)80753-4

Corpas, F. J., Palma, J. M., Sandalio, L. M., Valderrama, R., Barroso, J. B., and del Río, L. A. (2008). Peroxisomal xanthine oxidoreductase: characterization of the enzyme from pea (*Pisum sativum* L.) leaves. *J. Plant Physiol.* 165, 1319–1330. doi: 10.1016/j.jplph.2008.04.004

Corpas, F. J., and Trelease, R. N. (1998). Differential expression of ascorbate peroxidase and a putative molecular chaperone in the boundary membrane of differentiating cucumber seedling peroxisomes. *J. Plant Physiol.* 153, 332–338. doi: 10.1016/s0176-1617(98)80159-4

De Duve, C., and Baudhuin, P. (1966). Peroxisomes (microbodies and related particles). *Physiol. Rev.* 46, 323–357. doi: 10.1152/physrev.1966.46.2.323

Debska, K., Bogatek, R., and Gniazdowska, A. (2012). Protein carbonylation and its role in physiological processes in plants. *Postepy Biochem.* 58, 34–43.

del Río, L. A., Ortega, M. G., López, A. L., and Gorgé, J. L. (1977). A more sensitive modification of the catalase assay with the Clark oxygen electrode. Application to the kinetic study of the pea leaf enzyme. *Anal Biochem.* 80, 409–415. doi: 10.1016/0003-2697(77)90662-5

del Río, L. A., Sandalio, L. M., Palma, J. M., Bueno, P., and Corpas, F. J. (1992). Metabolism of oxygen radicals in peroxisomes and cellular implications. *Free Radic. Biol. Med.* 13, 557–580. doi: 10.1016/0891-5849(92)90150-f

del Río, L. A., Corpas, F. J., López-Huertas, E., Palma, J. M. (2018). "Plant superoxide dismutases: function under abiotic stress conditions," in *Antioxidants and Antioxidant Enzymes in Higher Plants*, (Cham: Springer International Publishing), 1–26. doi: 10.1007/978?3?319?75088-0_1

Dinçer, A., and Aydemir, T. (2001). Purification and characterization of catalase from chard (*Beta vulgaris* var. cicla). *J. Enzyme Inhib.* 16, 165–175. doi: 10.1080/14756360109162366

Dogra, V., Rochaix, J. D., and Kim, C. (2018). Singlet oxygen-triggered chloroplast-to-nucleus retrograde signalling pathways: an emerging perspective. *Plant Cell Environ.* 41, 1727–1738. doi: 10.1111/pce.13332

Droillard, M. J., and Paulin, A. (1990). Isozymes of superoxide dismutase in mitochondria and peroxisomes isolated from petals of carnation (*Dianthus caryophyllus*) during senescence. *Plant Physiol.* 94, 1187–1192. doi: 10.1104/pp.94.3.1187

Eastmond, P. J. (2007). MONODEHYROASCORBATE REDUCTASE4 is required for seed storage oil hydrolysis and postgerminative growth in *Arabidopsis*. *Plant Cell* 19, 1376–1387. doi: 10.1105/tpc.106.043992

Filipovic, M. R., Zivanovic, J., Alvarez, B., and Banerjee, R. (2018). Chemical biology of H2S signaling through persulfidation. *Chem Rev.* 118, 1253–1337. doi: 10.1021/acs.chemrev.7b00205

Gruhlke, M. C., and Slusarenko, A. J. (2012). The biology of reactive sulfur species (RSS). *Plant Physiol. Biochem.* 59, 98–107. doi: 10.1016/j.plaphy.2012.03.016

Guerra, D., Ballard, K., Truebridge, I., and Vierling, E. (2016). S-Nitrosation of conserved cysteines modulates activity and stability of S-nitrosoglutathione reductase (GSNOR). *Biochemistry* 55, 2452–2464. doi: 10.1021/acs.biochem.5b01373

Guirimand, G., Simkin, A. J., Papon, N., Besseau, S., Burlat, V., St-Pierre, B., et al. (2012). Cycloheximide as a tool to investigate protein import in peroxisomes: a case study of the subcellular localization of isoprenoid biosynthetic enzymes. *J. Plant Physiol.* 169, 825–829. doi: 10.1016/j.jplph.2012.01.020

Hackenberg, T., Juul, T., Auzina, A., Gwizdz, S., Malolepszy, A., Van Der Kelen, K., et al. (2013). Catalase and NO CATALASE ACTIVITY1 promote autophagy-dependent cell death in *Arabidopsis*. *Plant Cell* 25, 4616–4626. doi: 10.1105/tpc.113.117192

Hänsch, R., and Mendel, R. R. (2005). Sulfite oxidation in plant peroxisomes. *Photosynth Res.* 86, 337–343. doi: 10.1007/s11120-005-5221-x

Hauck, O. K., Scharnberg, J., Escobar, N. M., Wanner, G., Giavalisco, P., and Witte, C. P. (2014). Uric acid accumulation in an *Arabidopsis* urate oxidase mutant impairs seedling establishment by blocking peroxisome maintenance. *Plant Cell* 26, 3090–3100. doi: 10.1105/tpc.114.124008

Hinojosa, L., Sanad, M. N. M. E., Jarvis, D. E., Steel, P., Murphy, K., and Smertenko, A. (2019). Impact of heat and drought stress on peroxisome proliferation in quinoa. *Plant J.* 99, 1144–1158. doi: 10.1111/tpj.14411

Huang, A. H. C., Moore, T. S., and Trelease, R. N. (1983). *Plant Peroxisomes*. New York, NY: Academic Press.

Huang, J., Willems, P., Wei, B., Tian, C., Ferreira, R. B., Bodra, N., et al. (2019). Mining for protein S-sulfenylation in *Arabidopsis* uncovers redox-sensitive sites. *Proc. Natl. Acad. Sci. U.S.A.* 116, 21256–21261. doi: 10.1073/pnas.1906768116

Ishikawa, T., Yoshimura, K., Sakai, K., Tamoi, M., Takeda, T., and Shigeoka, S. (1998). Molecular characterization and physiological role of a glyoxysome-bound ascorbate peroxidase from spinach. *Plant Cell Physiol.* 39, 23–34. doi: 10.1093/oxfordjournals.pcp.a029285

Jiménez, A., Hernández, J. A., Pastori, G., del Río, L. A., Sevilla, F. (1998). Role of the ascorbate-glutathione cycle of mitochondria and peroxisomes in the senescence of pea leaves. *Plant Physiol.* 118, 1327–35. doi: 10.1104/pp.118.4.1327

Kao, Y. T., Gonzalez, K. L., and Bartel, B. (2018). Peroxisome function, biogenesis, and dynamics in plants. *Plant Physiol.* 176, 162–177. doi: 10.1104/pp.17.01050

Kissner, R., Nauser, T., Bugnon, P., Lye, P. G., and Koppenol, W. H. (1997). Formation and properties of peroxynitrite as studied by laser flash photolysis, high-pressure stopped-flow technique, and pulse radiolysis. *Chem. Res. Toxicol.* 10, 1285–1292. doi: 10.1021/tx970160x

Kohli, S. K., Khanna, K., Bhardwaj, R., Abd Allah, E. F., Ahmad, P., and Corpas, F. J. (2019). Assessment of subcellular ROS and NO metabolism in higher plants: multifunctional signaling molecules. *Antioxidants* 8:641. doi: 10.3390/antiox8120641

Kolbert, Z., Barroso, J. B., Brouquisse, R., Corpas, F. J., Gupta, K. J., Lindermayr, C., et al. (2019). A forty year journey: the generation and roles of NO in plants. *Nitric. Oxide* 93, 53–70.

Kusano, T., Kim, D. W., Liu, T., and Berberich, T. (2015). "Polyamine catabolism in plants," in *Polyamines*, eds T. Kusano, and H. Suzuki, (Tokyo: Springer), 77–88. doi: 10.1007/978-4-431-55212-3_6

León, J., Castillo, M. C., Coego, A., Lozano-Juste, J., and Mir, R. (2014). Diverse functional interactions between nitric oxide and abscisic acid in plant development and responses to stress. *J. Exp. Bot.* 65, 907–921. doi: 10.1093/jxb/ert454

Leterrier, M., Barroso, J. B., Valderrama, R., Begara-Morales, J. C., Sánchez-Calvo, B., Chaki, M., et al. (2016). Peroxisomal NADP-isocitrate dehydrogenase is required for *Arabidopsis* stomatal movement. *Protoplasma* 253, 403–415. doi: 10.1007/s00709-015-0819-0

Leterrier, M., Chaki, M., Airaki, M., Valderrama, R., Palma, J. M., Barroso, J. B., et al. (2011). Function of S-nitrosoglutathione reductase (GSNOR) in plant development and under biotic/abiotic stress. *Plant Signal. Behav.* 6, 789–793. doi: 10.4161/psb.6.6.15161

Leterrier, M., Corpas, F. J., Barroso, J. B., Sandalio, L. M., and del Río, L. A. (2005). Peroxisomal monodehydroascorbate reductase. Genomic clone characterization and functional analysis under environmental stress conditions. *Plant Physiol.* 138, 2111–2123. doi: 10.1104/pp.105.066225

Li, G., Li, J., Hao, R., and Guo, Y. (2017). Activation of catalase activity by a peroxisome-localized small heat shock protein Hsp17.6CII. *J. Genet. Genomics* 44, 395–404. doi: 10.1016/j.jgg.2017.03.009

Lingard, M. J., and Bartel, B. (2009). *Arabidopsis* LON2 is necessary for peroxisomal function and sustained matrix protein import. *Plant Physiol.* 151, 1354–1365. doi: 10.1104/pp.109.142505

Lisenbee, C. S., Lingard, M. J., and Trelease, R. N. (2005). *Arabidopsis* peroxisomes possess functionally redundant membrane and matrix isoforms of monodehydroascorbate reductase. *Plant J.* 43, 900–914. doi: 10.1111/j.1365-313x.2005.02503.x

López-Huertas, E., Charlton, W. L., Johnson, B., Graham, I. A., and Baker, A. (2000). Stress induces peroxisome biogenesis genes. *EMBO J.* 19, 6770–6777. doi: 10.1093/emboj/19.24.6770

López-Huertas, E., and del Río, L. A. (2014). Characterization of antioxidant enzymes and peroxisomes of olive (*Olea europaea* L.) fruits. *J. Plant Physiol.* 171, 1463–1471. doi: 10.1016/j.jplph.2014.06.014

Lounifi, I., Arc, E., Molassiotis, A., Job, D., Rajjou, L., and Tanou, G. (2013). Interplay between protein carbonylation and nitrosylation in plants. *Proteomics* 13, 568–578. doi: 10.1002/pmic.201200304

Mano, J., Nagata, M., Okamura, S., Shiraya, T., and Mitsui, T. (2014). Identification of oxidatively modified proteins in salt-stressed *Arabidopsis*: a carbonyl-targeted proteomics approach. *Plant Cell Physiol.* 55, 1233–1244. doi: 10.1093/pcp/pcu072

Mata-Pérez, C., Begara-Morales, J. C., Chaki, M., Sánchez-Calvo, B., Valderrama, R., Padilla, M. N., et al. (2016). Protein tyrosine nitration during development and abiotic stress response in plants. *Front. Plant Sci.* 7:1699.

Mhamdi, A., Noctor, G., and Baker, A. (2012). Plant catalases: peroxisomal redox guardians. *Arch. Biochem. Biophys.* 525, 181–194. doi: 10.1016/j.abb.2012.04.015

Mhamdi, A., Queval, G., Chaouch, S., Vanderauwera, S., and Van Breusegem, F. (2010). Catalase function in plants: a focus on *Arabidopsis* mutants as stress-mimic models. *J. Exp. Bot.* 61, 4198–4220.

Mishanina, T. V., Libiad, M., and Banerjee, R. (2015). Biogenesis of reactive sulfur species for signaling by hydrogen sulfide oxidation pathways. *Nat. Chem. Biol.* 11, 457–464. doi: 10.1038/nchembio.1834

Mohn, M. A., Thaqi, B., and Fischer-Schrader, K. (2019). Isoform-specific NO synthesis by *Arabidopsis thaliana* nitrate reductase. *Plants* 8:67. doi: 10.3390/plants8030067

Mor, A., Koh, E., Weiner, L., Rosenwasser, S., Sibony-Benyamini, H., and Fluhr, R. (2014). Singlet oxygen signatures are detected independent of light or chloroplasts in response to multiple stresses. *Plant Physiol.* 165, 249–261. doi: 10.1104/pp.114.236380

Moschou, P. N., Sanmartin, M., Andriopoulou, A. H., Rojo, E., Sanchez-Serrano, J. J., and Roubelakis-Angelakis, K. A. (2008). Bridging the gap between plant and mammalian polyamine catabolism: a novel peroxisomal polyamine oxidase responsible for a full back-conversion pathway in *Arabidopsis*. *Plant Physiol.* 147, 1845–1857. doi: 10.1104/pp.108.123802

Müller, M., Zechmann, B., and Zellnig, G. (2004). Ultrastructural localization of glutathione in cucurbita pepo plants. *Protoplasma* 223, 213–219.

Neill, S., Barros, R., Bright, J., Desikan, R., Hancock, J., Harrison, J., et al. (2008). Nitric oxide, stomatal closure, and abiotic stress. *J. Exp. Bot.* 59, 165–176.

Nguyen, A. T., and Donaldson, R. P. (2005). Metal-catalyzed oxidation induces carbonylation of peroxisomal proteins and loss of enzymatic activities. *Arch. Biochem. Biophys.* 2005, 25–31. doi: 10.1016/j.abb.2005.04.018

Niu, L., Yu, J., Liao, W., Xie, J., Yu, J., Lv, J., et al. (2019). Proteomic investigation of S-nitrosylated proteins during NO-induced adventitious rooting of cucumber. *Int. J. Mol. Sci.* 20:5363. doi: 10.3390/ijms20215363

Noctor, G., Veljovic-Jovanovic, S., Driscoll, S., Novitskaya, L., Foyer, C H. (2002). Drought and oxidative load in the leaves of C_3 plants: a predominant role for photorespiration? *Ann. Bot.* 89, 841–50. doi: 10.1093/aob/mcf096

Nowak, K., Luniak, N., Witt, C., Wüstefeld, Y., Wachter, A., Mendel, R. R., et al. (2004). Peroxisomal localization of sulfite oxidase separates it from chloroplast-based sulfur assimilation. *Plant Cell Physiol.* 45, 1889–1894. doi: 10.1093/pcp/pch212

Oikawa, K., Hayashi, M., Hayashi, Y., and Nishimura, M. (2019). Re-evaluation of physical interaction between plant peroxisomes and other organelles using live-cell imaging techniques. *J. Integr. Plant Biol.* 61, 836–852.

Oikawa, K., Matsunaga, S., Mano, S., Kondo, M., Yamada, K., Hayashi, M., et al. (2015). Physical interaction between peroxisomes and chloroplasts elucidated by in situ laser analysis. *Nat. Plants.* 1:15035.

Olson, K. R. (2019). Hydrogen sulfide, reactive sulfur species and coping with reactive oxygen species. *Free Radic. Biol. Med.* 140, 74–83. doi: 10.1016/j.freeradbiomed.2019.01.020

Olson, K. R., Gao, Y., Arif, F., Arora, K., Patel, S., DeLeon, E. R. et al. (2018). Metabolism of hydrogen sulfide (H_2S) and production of reactive sulfur species (RSS) by superoxide dismutase. *Redox Biol.* 15, 74–85. doi: 10.1016/j.redox.2017.11.009

Olson, K. R., Gao, Y., DeLeon, E. R., Arif, M., Arif, F., Arora, N., et al. (2017). Catalase as a sulfide-sulfur oxido-reductase: an ancient (and modern?) regulator of reactive sulfur species (RSS). *Redox Biol.* 12, 325–339. doi: 10.1016/j.redox.2017.02.021

Ono, K., Akaike, T., Sawa, T., Kumagai, Y., Wink, D. A., Tantillo, D. J., et al. (2014). Redox chemistry and chemical biology of H2S, hydropersulfides, and derived species: implications of their possible biological activity and utility. *Free Radic. Biol. Med.* 77, 82–94. doi: 10.1016/j.freeradbiomed.2014.09.007

Palma, J. M., de Morales, P. Á, del Río, L. A., and Corpas, F. J. (2018). The proteome of fruit peroxisomes: sweet pepper (*Capsicum annuum* L.) as a model. *Subcell Biochem.* 89, 323–341. doi: 10.1007/978-981-13-2233-4_14

Palma, J. M., Jiménez, A., Sandalio, L. M., Corpas, F. J., Lundqvist, M., Gómez, M., et al. (2006). Antioxidative enzymes from chloroplasts, mitochondria, and peroxisomes during leaf senescence of nodulated pea plants. *J. Exp. Bot.* 57, 1747–1758. doi: 10.1093/jxb/erj191

Palma, J. M., Mateos, R. M., López-Jaramillo, J., Rodríguez-Ruiz, M., González-Gordo, S., Lechuga-Sancho, A. M., et al. (2020). Plant catalases as NO and H2S targets. *Redox Biol.* 24, 131–137. doi: 10.1016/j.redox.2020.101525

Pan, R., Liu, J., Wang, S., and Hu, J. (2020). Peroxisomes: versatile organelles with diverse roles in plants. *New Phytol.* 225, 1410–1427. doi: 10.1111/nph.16134

Pan, R., Reumann, S., Lisik, P., Tietz, S., Olsen, L. J., and Hu, J. (2018). Proteome analysis of peroxisomes from dark-treated senescent *Arabidopsis* leaves. *J. Integr. Plant Biol.* 60, 1028–1050. doi: 10.1111/jipb.12670

Park, C. M., Weerasinghe, L., Day, J. J., Fukuto, J. M., and Xian, M. (2015). Persulfides: current knowledge and challenges in chemistry and chemical biology. *Mol. Biosyst.* 11, 1775–1785. doi: 10.1039/c5mb00216h

Piacentini, D., Corpas, F. J., D'Angeli, S., Altamura, M. M., and Falasca, G. (2020). Cadmium and arsenic-induced-stress differentially modulates *Arabidopsis* root architecture, peroxisome distribution, enzymatic activities and their nitric oxide content. *Plant Physiol. Biochem.* 148, 312–323. doi: 10.1016/j.plaphy.2020.01.026

Pracharoenwattana, I., and Smith, S. M. (2008). When is a peroxisome not a peroxisome? *Trends Plant Sci.* 13, 522–525. doi: 10.1016/j.tplants.2008.07.003

Prado, A. M., Porterfield, D. M., and Feijó, J. A. (2004). Nitric oxide is involved in growth regulation and re-orientation of pollen tubes. *Development* 131, 2707–2714. doi: 10.1242/dev.01153

Ray, M., Mishra, P., Das, P., and Sabat, S. C. (2012). Expression and purification of soluble bio-active rice plant catalase-A from recombinant *Escherichia coli*. *J. Biotechnol.* 157, 12–19. doi: 10.1016/j.jbiotec.2011.09.022

Reumann, S., and Bartel, B. (2016). Plant peroxisomes: recent discoveries in functional complexity, organelle homeostasis, and morphological dynamics. *Curr. Opt. Plant Biol.* 34, 17–26. doi: 10.1016/j.pbi.2016.07.008

Reumann, S., Quan, S., Aung, K., Yang, P., Manandhar-Shrestha, K., Holbrook, D., et al. (2009). In-depth proteome analysis of *Arabidopsis* leaf peroxisomes combined with in vivo subcellular targeting verification indicates novel metabolic and regulatory functions of peroxisomes. *Plant Physiol.* 150, 125–143. doi: 10.1104/pp.109.137703

Ribeiro, C. W., Korbes, A. P., Garighan, J. A., Jardim-Messeder, D., Carvalho, F. E. L., Sousa, R. H. V., et al. (2017). Rice peroxisomal ascorbate peroxidase knockdown affects ROS signaling and triggers early leaf senescence. *Plant Sci.* 263, 55–65. doi: 10.1016/j.plantsci.2017.07.009

Rodríguez-Ruiz, M., González-Gordo, S., Cañas, A., Campos, M. J., Paradela, A., Corpas, F. J., et al. (2019). Sweet pepper (*Capsicum annuum* L.) fruits contain an atypical peroxisomal catalase that is modulated by reactive oxygen and nitrogen species. *Antioxidants* 8:374. doi: 10.3390/antiox8090374

Rodríguez-Serrano, M., Romero-Puertas, M. C., Pastori, G. M., Corpas, F. J., Sandalio, L. M., del Río, L. A., et al. (2007). Peroxisomal membrane manganese superoxide dismutase: characterization of the isozyme from watermelon (*Citrullus lanatus* Schrad.) cotyledons. *J. Exp. Bot.* 58, 2417–2427. doi: 10.1093/jxb/erm095

Romero-Puertas, M. C., Corpas, F. J., Sandalio, L. M., Leterrier, M., Rodríguez-Serrano, M., del Río, L. A., et al. (2006). Glutathione reductase from pea leaves: response to abiotic stress and characterization of the peroxisomal isozyme. *New Phytol.* 170, 43–52. doi: 10.1111/j.1469-8137.2006.01643.x

Rosenwasser, S., Rot, I., Sollner, E., Meyer, A. J., Smith, Y., Leviatan, N., et al. (2011). Organelles contribute differentially to reactive oxygen species-related events during extended darkness. *Plant Physiol.* 156, 185–201. doi: 10.1104/pp.110.169797

Schlicht, M., Ludwig-Müller, J., Burbach, C., Volkmann, D., and Baluska, F. (2013). Indole-3-butyric acid induces lateral root formation via peroxisome-derived indole-3-acetic acid and nitric oxide. *New Phytol.* 200, 473–482. doi: 10.1111/nph.12377

Schöneich, C. (2016). Thiyl radicals and induction of protein degradation. *Free Radic. Res.* 50, 143–149. doi: 10.3109/10715762.2015.1077385

Shelp, B. J., and Zarei, A. (2017). Subcellular compartmentation of 4-aminobutyrate (GABA) metabolism in *Arabidopsis*: an update. *Plant Signal. Behav.* 12:e1322244. doi: 10.1080/15592324.2017.1322244

Simkin, A. J., Guirimand, G., Papon, N., Courdavault, V., Thabet, I., Ginis, O., et al. (2011). Peroxisomal localisation of the final steps of the mevalonic acid pathway in planta. *Planta* 234, 903–914. doi: 10.1007/s00425-011-1444-6

Sousa, R. H. V., Carvalho, F. E. L., Lima-Melo, Y., Alencar, V. T. C. B., Daloso, D. M., Margis-Pinheiro, M., et al. (2019). Impairment of peroxisomal APX and CAT activities increases protection of photosynthesis under oxidative stress. *J. Exp. Bot.* 70, 627–639. doi: 10.1093/jxb/ery354

Su, T., Li, W., Wang, P., and Ma, C. (2019). Dynamics of peroxisome homeostasis and its role in stress response and signaling in Plants. *Front. Plant Sci.* 10:705.

Su, T., Wang, P., Li, H., Zhao, Y., Lu, Y., Dai, P., et al. (2018). The *Arabidopsis* catalase triple mutant reveals important roles of catalases and peroxisome-derived signaling in plant development. *J. Integr. Plant Biol.* 60, 591–607. doi: 10.1111/jipb.12649

Tolbert, N. E., and Essner, E. (1981). Microbodies: peroxisomes and glyoxysomes. *J. Cell Biol.* 91, 271s–283s. doi: 10.1083/jcb.91.3.271s

Ueda, Y., Uehara, N., Sasaki, H., Kobayashi, K., and Yamakawa, T. (2013). Impacts of acute ozone stress on superoxide dismutase (SOD) expression and reactive oxygen species (ROS) formation in rice leaves. *Plant Physiol. Biochem.* 70, 396–402. doi: 10.1016/j.plaphy.2013.06.009

Veljovic-Jovanovic, S., Oniki, T., and Takahama, U. (1998). Detection of monodehydroascorbic acid radical in sulfite-treated leaves and mechanism of its formation. *Plant Cell Physiol.* 39, 1203–1208. doi: 10.1093/oxfordjournals.pcp.a029321

Wagner, D., Przybyla, D., Op den Camp, R., Kim, C., Landgraf, F., Lee, K. P., et al. (2004). The genetic basis of singlet oxygen-induced stress responses of *Arabidopsis thaliana*. *Science* 306, 1183–1185. doi: 10.1126/science.1103178

Wang, X., Zhu, B., Jiang, Z., and Wang, S. (2019). Calcium-mediation of jasmonate biosynthesis and signaling in plants. *Plant Sci.* 287:110192. doi: 10.1016/j.plantsci.2019.110192

Wang, W., Paschalidis, K., Feng, J. C., Song, J., and Liu, J. H. (2019). Polyamine catabolism in plants: a universal process with diverse functions. *Front. Plant Sci.* 10:561.

Wei, L., Zhang, M., Wei, S., Zhang, J., Wang, C., and Liao, W. (2020). Roles of nitric oxide in heavy metal stress in plants: cross-talk with phytohormones and protein *S*-nitrosylation. *Environ. Pollut.* 259:113943. doi: 10.1016/j.envpol.2020.113943

Wuddineh, W., Minocha, R., and Minocha, S. C. (2018). Polyamines in the context of metabolic networks. *Methods Mol. Biol.* 1694, 1–23. doi: 10.1007/978-1-4939-7398-9_1

Xin, Z., Chen, S., Ge, L., Li, X., and Sun, X. (2019). The involvement of a herbivore-induced acyl-CoA oxidase gene, CsACX1, in the synthesis of jasmonic acid and its expression in flower opening in tea plant (*Camellia sinensis*). *Plant Physiol. Biochem.* 135, 132–140. doi: 10.1016/j.plaphy.2018.11.035

Yamaguchi, K., Mori, H., and Nishimura, M. (1995). A novel isoenzyme of ascorbate peroxidase localized on glyoxysomal and leaf peroxisomal membranes in pumpkin. *Plant Cell Physiol.* 36, 1157–1162. doi: 10.1093/oxfordjournals.pcp.a078862

Yamauchi, S., Mano, S., Oikawa, K., Hikino, K., Teshima, K. M., Kimori, Y., et al. (2019). Autophagy controls reactive oxygen species homeostasis in guard cells that is essential for stomatal opening. *Proc. Natl. Acad. Sci. U.S.A.* 116, 19187–19192. doi: 10.1073/pnas.1910886116

Yang, M., Li, Z., Zhang, K., Zhang, X., Zhang, Y., Wang, X., et al. (2018). Barley stripe mosaic virus γb interacts with glycolate oxidase and inhibits peroxisomal ROS production to facilitate virus infection. *Mol. Plant* 11, 338–341. doi: 10.1016/j.molp.2017.10.007

Yu, L., Fan, J., and Xu, C. (2019). Peroxisomal fatty acid β-oxidation negatively impacts plant survival under salt stress. *Plant Signal. Behav.* 14:1561121. doi: 10.1080/15592324.2018.1561121

Zhang, Z., Xu, Y., Xie, Z., Li, X., He, Z H., Peng, X X. (2016). Association-dissociation of glycolate oxidase with catalase in rice: a potential switch to modulate intracellular H_2O_2 levels. *Mol. Plant*. 9, 737–748. doi: 10.1016/j.molp.2016.02.002

Zarei, A., Trobacher, C. P., Cooke, A. R., Meyers, A. J., Hall, J. C., and Shelp, B. J. (2015). Apple fruit copper amine oxidase isoforms: peroxisomal MdAO1 prefers diamines as substrates, whereas extracellular MdAO2 exclusively utilizes monoamines. *Plant Cell Physiol.* 56, 137–147. doi: 10.1093/pcp/pcu155

Zarepour, M., Kaspari, K., Stagge, S., Rethmeier, R., Mendel, R. R., and Bittner, F. (2010). Xanthine dehydrogenase AtXDH1 from *Arabidopsis thaliana* is a potent producer of superoxide anions via its NADH oxidase activity. *Plant Mol. Biol.* 72, 301–310. doi: 10.1007/s11103-009-9570-2

Conflict of Interest: The authors declare that the research was conducted in the absence of any commercial or financial relationships that could be construed as a potential conflict of interest.

frontiers in Plant Science

REVIEW
published: 16 September 2020
doi: 10.3389/fpls.2020.571399

You Want it Sweeter: How Glycosylation Affects Plant Response to Oxidative Stress

Marc Behr[1], *Godfrey Neutelings*[2], *Mondher El Jaziri*[1] *and Marie Baucher*[1]*

[1] Laboratoire de Biotechnologie Végétale, Université libre de Bruxelles, Gosselies, Belgium, [2] UGSF—Unité de Glycobiologie Structurale et Fonctionnelle, UMR 8576, Université de Lille, CNRS, Lille, France

Oxidative stress is a cellular threat which puts at risk the productivity of most of crops valorized by humankind in terms of food, feed, biomaterial, or bioenergy. It is therefore of crucial importance to understand the mechanisms by which plants mitigate the deleterious effects of oxidizing agents. Glycosylation of antioxidant molecules and phytohormones modifies their chemical properties as well as their cellular and histological repartition. This review emphasizes the mechanisms and the outcomes of this conjugation reaction on plant ability to face growing conditions favoring oxidative stress, in mirror with the activity of deglycosylating enzymes. Pioneer evidence bridging flavonoid, glycosylation, and redox homeostasis paved the way for numerous functional analyses of UDP-glycosyltransferases (UGTs), such as the identification of their substrates and their role to circumvent oxidative stress resulting from various environmental challenges. (De)glycosylation appears as a simple chemical reaction regulating the biosynthesis and/or the activity of a myriad of specialized metabolites partaking in response to pathogen and abiotic stresses. This outcome underlies the possibility to valorize UGTs potential to upgrade plant adaptation and fitness in a rising context of sub-optimal growing conditions subsequent to climate change.

Keywords: abiotic stress, biotic stress, flavonoid, glucosidase, phytohormone, redox homeostasis, ROS—reactive oxygen species, UDP-glycosyltransferase (UGT)

OPEN ACCESS

Edited by:
José Manuel Palma, Consejo Superior de Investigaciones Científicas (CSIC), Spain

Reviewed by:
Yanjie Li, Shandong University, China
Xuebin Zhang, Henan University, China

***Correspondence:**
Marie Baucher
mbaucher@ulb.ac.be

Specialty section:
This article was submitted to Plant Metabolism and Chemodiversity, a section of the journal Frontiers in Plant Science

Received: *10 June 2020*
Accepted: *01 September 2020*
Published: *16 September 2020*

Citation:
Behr M, Neutelings G, El Jaziri M and Baucher M (2020) You Want it Sweeter: How Glycosylation Affects Plant Response to Oxidative Stress. Front. Plant Sci. 11:571399. doi: 10.3389/fpls.2020.571399

INTRODUCTION

Oxidative metabolism is a cornerstone of general cell biology. Plants are characterized by the ability to perform photosynthesis, a biological process supported by high rates of electron transfer in the thylakoids (Waszczak et al., 2018). The metabolism of energy factories, i.e., chloroplasts and mitochondria, generates reactive oxygen species (ROS, Vaahtera et al., 2014; Noctor et al., 2018). Cellular redox status is the balance between ROS abundance and the efficiency of the ROS scavenging system. Under optimal conditions, the deleterious effects of ROS are buffered by multiple ROS-scavenging mechanisms, resulting in a tightly adjusted redox homeostasis ensuring optimal cell metabolism. When ROS production overcomes the capacity of the scavenging systems, cells are facing a situation of oxidative stress. Plant cells have designed intricate signaling pathways to sense and react to this redox imbalance at multiple levels, a mechanism known as redox signaling, to restore redox homeostasis.

In addition to their intrinsic ROS production, plants cells are challenged by a large range of adverse conditions perturbing their redox homeostasis, such as heavy metals, pathogens, drought, salinity, high light, and extreme temperature (Schützendübel and Polle, 2002; Waszczak et al., 2018; Farooq et al., 2019). Oxidative stress is a cellular consequence of these conditions, as reviewed in (Bose et al., 2014; Pospíšil and Prasad, 2014; Anjum et al., 2015; Pospíšil and Yamamoto, 2017; Fryzova et al., 2018), which result in various developmental damages, such as growth arrest, leaf wilting, chlorosis, and impaired reproduction (Gray and Brady, 2016; Lv et al., 2019; Dubois and Inzé, 2020). At the physiological level, oxidative stress leads to lipid peroxidation, oxidative modifications of proteins and DNA damage (Pospíšil and Yamamoto, 2017; Huybrechts et al., 2019). Global warming is likely to increase the frequency and the severity of these events (Diffenbaugh et al., 2017), prompting to decipher and boost ROS scavenging as well as the dissipative mechanisms in species of economical and food interest (Gómez et al., 2019). To overcome their deleterious effects, ROS are scavenged through the actions of enzymes in charge of decreasing their oxidant capacity, such as superoxide dismutase (SOD) or catalase (CAT; Farooq et al., 2019) or by direct reaction with antioxidant molecules, such as redox-regenerable glutathione and ascorbate (Noctor et al., 2018), as well as classes of specialized metabolites such as flavonoids (Montoro et al., 2005; Agati et al., 2007; Nakabayashi et al., 2014). These canonical mechanisms are essentially conserved within the plant kingdom (He et al., 2018; Pan et al., 2020). ROS-removing systems also include molecular actors which indirectly affect redox homeostasis. For instance, some UGTs, which glycosylate a large range of metabolites, also partake in redox homeostasis. Together with glucosidases, UGTs rapidly shape the glycosylation status of a wide range of specialized metabolites to support plant response in various challenging environments. The precise regulation of the balance between glycosylation and deglycosylation applied to antioxidant molecules and to phytohormones allows plant to respond to environmental cues (Verma et al., 2016).

Glycosylation has emerged as a wide conjugation reaction of various molecules, as evidenced by the occurrence in plant extracts of multiple glycosylated forms of different classes of specialized metabolites. The variation in specialized metabolite profiles and the occurrence of UGTs among different species suggest that plant response to equivalent challenging conditions, e.g., redox imbalance, is species-dependent. This specificity highlights the plasticity of UGTs to specifically fit plant requirement, in terms of substrate affinity and environmental conditions (Gachon et al., 2005). This explains the great number of UGTs found in highly evolved plant species. The algae *Chlamydomonas reinhardtii* has only 1 protein with a UGT domain, *versus* 21 for the moss *Physcomitrella patens*, 115 for *Arabidopsis thaliana*, 168 for *Zea mays*, and 236 for *Populus trichocarpa* (Yonekura-Sakakibara and Hanada, 2011). Typically, these enzymes are able to use *in vitro* several substrates (Sun et al., 2019) leading therefore to the glycosylation of a myriad of metabolites with various biological functions *in planta*.

Consistent with the diversity of their substrates, UGTs are part of multiple biosynthetic and signaling networks partaking in redox homeostasis (Tiwari et al., 2016). First, UGTs are able to glycosylate specialized metabolites directly involved in ROS homeostasis, such as some flavonoids and terpenoids. Sugar substitution directly modifies the antioxidant potential when occurring in such substrates (Zheng et al., 2017), but also their cellular and tissular repartition (Taguchi et al., 2000) and retroactively regulates their corresponding biosynthetic pathway (Zhang and Liu, 2015). Second, a large range of phytohormones, which are widely reported to be important during plant developmental processes as well as during response to environmental stresses (Verma et al., 2016), undergoes glycosylation that modulate their activity.

Based on results reporting differential sensitivity of plants with altered *UGT* expression toward these stresses, we will explain and discuss how the glycosylation of selected substrates contribute to the equilibrium of the redox status during challenging conditions. In order to provide a reader's guide, the main information dealing with the UGTs which have been thoroughly investigated so far are presented in **Table 1**. All these results are depicted by the UGT potential substrate(s) and will be further explained in the upcoming sections.

We will first sum up the first elements highlighting the involvement of some UGTs toward chemically-induced oxidative stress. The second part will be devoted to the study of UGTs related to redox homeostasis during pathogen infection. The third part will explain how the glycosylation of antioxidant molecules can mitigate oxidative stress arising from abiotic stresses. Finally, the last part will address the participation of the glycosylation of selected phytohormones during plant response to abiotic constrains. The conclusion will open perspectives to the potential interactions between glycosylation and redox retrograde signaling.

FIRST EVIDENCES CONNECTING GLYCOSYLATION TO PLANT RESPONSE TO OXIDATIVE STRESS

The first molecular characterization of an UGT, demonstrated to guide flavonoid glycosylation, was reported in maize (Dooner and Nelson, 1977). The sequencing and the annotation of several plant genomes, especially of model species such as *A. thaliana*, highlighted the diversity of the UGT families. Since then, an unceasing effort has been undertaken to decipher the cellular functions of UGTs and to provide evidences for their roles *in planta*. Meanwhile, the importance of flavonoids regarding protection to oxidative damages was highlighted (Landry et al., 1995), underlying the relevance of studying flavonoid glycosylation in the context of oxidative stress. One of these first studies focused on the role of Arabidopsis *UGT73B1*, *UGT73B2*, and *UGT73B3* concerning methyl viologen (MV) tolerance (Chae et al., 2006). In the acceptor side of photosystem I, MV catalyzes reduction of oxygen into superoxide ion $O_2^{\bullet -}$, a potent oxidant agent (Noctor et al., 2016). MV is widely used experimentally to specifically induce ROS production. While

TABLE 1 | Main UGTs described in this review.

UGT	Substrate	Role *in planta*	Inducing factor
		Flavonoids	
UGT71C1 (Arabidopsis)	Flavonoids, lignans	Flavonoid aglycones are potentially more antioxidant than their glycosylated forms, explaining the better tolerance of knockout mutants to methyl viologen.	Unknown
UGT73B1, UGT73B2, UGT73B3 (Arabidopsis)	Flavonoids		Pathogen infection, SA, methyl jasmonate, oxidative stress
UGT78A14 (*Camellia sinensis*)	Kaempferol, quercetin	Kaempferol and quercetin glycosylation products have higher ROS scavenging activity (FRAP, DPPH and ABTS) than their corresponding aglycones and contribute to cold stress tolerance.	Cold stress
UGT79B2/UGT79B3 (Arabidopsis)	Cyanidin/cyanidin-3-*O*-glucoside	Glycosylation of anthocyanins results in their storage in the vacuole, derepressing the product feedback inhibition on PAL and increasing total anthocyanin content. Plants are therefore more tolerant to cold, salt, and drought stresses.	Cold, salt, and drought stresses
UFGT2 (*Zea mays*)	Quercetin, kaempferol	Flavonoids can protect the plant from oxidative stress resulting from exposure to salt, H_2O_2 and high osmotic condition. Glycosylation supports the biosynthesis of these flavonoids.	Salt, drought and oxidative stresses
		Phytohormones	
SDG8i (*Sporobolus stapfianus*)	Strigolactones	Overexpression of this gene in Arabidopsis results in higher tolerance to salt, freezing and drought stresses. Strigolactones favour the biosynthesis of anthocyanins and strigolactones glycosylation may ease their translocation between different organs.	Water stress
UGT71B6, UGT71B7, UGT71B8 (Arabidopsis)	ABA	These UGTs maintain an optimal ABA content under non-limiting growing conditions and may mitigate ABA response during salt and osmotic stress.	ABA, salt and osmotic stresses
UGT74E2 (Arabidopsis)	Indole-3-butyric acid	The enzymatic activity of UGT74E2 may modify auxin gradient and distribution to support plant acclimation under drought and salt stress conditions, in interaction with flavonoids.	Osmotic, oxidative, ultraviolet B and salt stresses
UGT90A1 (*Oryza sativa*)	Possibly auxins and cytokinins	Overexpression in rice and Arabidopsis leads to higher tolerance to cold and salt stress, with lower accumulation of ROS and higher catalase and soluble PRX activities.	Low temperature, salt stress
		Miscellaneous	
TOGT (*Nicotiana tabacum*)	Scopoletin	Scopoletin is an antiviral and a potent antioxidant in plant defense response. Scopoletin regulates ROI accumulation in cells surrounding necrosis (as substrate of PRX or direct ROI scavenger).	SA- and pathogen-inducible
UGT73B3, UGT73B5 (Arabidopsis)	Phytoprostanes, camalexin degradation products	These UGTs contribute to the regulation of redox status and general detoxification of ROS-reactive specialized metabolites, limitation of cell death establishment during HR.	Early-SA induced gene, paraquat, ozone, bacteria
UGT85A5 (Arabidopsis)	Unknown	Ectopic expression increases tolerance to salt stress, as indicated by lower loss of chlorophyll and lower malondialdehyde equivalents content.	Salt stress
UGT91Q2 (*Camellia sinensis*)	Nerolidol	Nerolidol glucoside has a higher ROS scavenging activity than its aglycone, possibly protects PSII during cold stress and prevents lipid peroxidation.	Cold stress

ABA, abscisic acid; ABTS, 2,2'-azino-bis(3-ethylbenzothiazoline-6-sulfonic acid); DPPH, 2,2-diphenyl-1-picrylhydrazyl; FRAP, ferric reducing ability of plasma; HR, hypersensitive response; PAL, phenylalanine ammonia lyase; PRX, peroxidase; PSII, photosystem II; ROI, reactive oxygen intermediates; ROS, reactive oxygen species; SA, salicylic acid. Additional details and corresponding references are provided in the main text.

Arabidopsis T-DNA insertional mutants of each of these genes did not display any obvious phenotype under normal growth conditions, they turned to be more tolerant to MV in terms of biomass and chlorophyll content as compared to the wild-type (25- to 55-fold higher chlorophyll a content at 1.5 μM MV and higher total chlorophyll content). Compared to the WT, this increased tolerance to MV may have two origins. The first one is a lower $O_2^{\bullet -}$ production, as suggested by the decreased nitroblue tetrazolium (NBT) staining of the *ugt73b2* mutant following MV exposure (Kim et al., 2010). The second one is an increased redox buffer potential able to maintain a ROS concentration compatible with survival, which lays in more abundant/efficient ROS scavenging through enzymatic, such as SOD and CAT, and/or non-enzymatic (antioxidant molecules) systems. The tolerance to MV in *ugt73b1*, *ugt73b2*, and *ugt73b3* mutants might be a consequence of the accumulation of flavonoid aglycones (Lim et al., 2008; Kim et al., 2010), as proteins of these UGT families glycosylate flavonoids (Jones et al., 2003; Chae et al., 2006; Lim et al., 2008; Sun et al., 2019). For instance, UGT73B1 and UGT73B2 show *in vitro* glucose-conjugating activity toward the flavanones eriodictyol and naringenin, the flavones apigenin and luteolin, and the flavonols kaempferol and quercetin (Kim et al., 2006b; Kim et al., 2006a). As kaempferol and quercetin glycosides naturally occur in Arabidopsis leaves and flowers (Jones et al., 2003), it is likely that they are natural substrates of these UGT73. Since quercetin and kaempferol are major flavonoids (Deng and Lu, 2017), we may hypothesize that the depletion of their glycosylated forms entails increased pool of their aglycones, explaining the tolerance to MV-induced oxidative stress in the *ugt73b* mutants. In addition, exogenous naringenin was shown to protect chloroplasts from oxidative damages through activation of H_2O_2 scavenging mechanisms (Yildiztugay et al., 2020), which may also account for increased MV tolerance of *ugt73b1* and *ugt73b2* mutants.

Results similar to those reported for *ugt73b2* mutant have been obtained with an *ugt71c1* mutant. While no obvious phenotype was observed in control conditions, this line retains higher total chlorophyll and carotenoid content following MV treatment (0.5 and 1 μM) as compared to the wild-type

(Lim et al., 2008). When facing a MV concentration of 1.5 μM, the radical scavenging activity of seedlings, as assessed with 2,2-diphenyl-1-picrylhydrazyl (DPPH) assay, was significantly higher in the *ugt71c1* mutant than in the wild-type. The expression of eight genes involved in ROS response (such as *ALTERNATIVE OXIDASE*, *CAT*s, *SOD*s, and *PEROXIREDOXIN*) was lower in the *ugt71c1* mutant under various MV concentrations, as compared to the wild-type (Lim et al., 2008). In absence of MV, the expression of these genes was similar in the two genotypes. This strongly suggests that MV tolerance of this line does not rely on ROS scavenging by enzymatic detoxication process. As further explained below, a possible involvement of flavonoids is suspected.

In point of fact, the *ugt71c1* mutant showed decreased amounts of quercetin 3,7-*O*-glucoside and kaempferol 3,7-*O*-glucoside (25% and 70% of wild-type level, respectively; Lim et al., 2008) as well as reduced lariciresinol- and pinoresinol-glucosides content (Okazawa et al., 2014). In addition to quercetin and luteolin (Lim et al., 2003), recombinant UGT71C1 is able to glycosylate the lignans lariciresinol and pinoresinol (Okazawa et al., 2014). Lariciresinol efficiently inhibits lipid peroxidation *in vitro* (Zhang et al., 2004). Isolariciresinol is an isomer of lariciresinol and its 4'-β-D-glucoside form is less antioxidant than its aglycon (Baderschneider and Winterhalter, 2001). These data are consistent with increased MV tolerance of the *ugt71c1* mutant. Lignans are biosynthesized in response to various adverse conditions, comprising oxidative stress (Paniagua et al., 2017). Interestingly, reduced neolignans such as isodihydrodehydrodiconiferyl alcohol contribute to cytosolic H_2O_2 scavenging in poplar during xylem differentiation (Niculaes et al., 2014). This further suggests that lignan glycosylation may impact on redox homeostasis.

Flavonoid aglycones are considered as more effective antioxidants than their glycosides (Rice-Evans et al., 1996; Hopia and Heinonen, 1999; Baderschneider and Winterhalter, 2001; Montoro et al., 2005). Zheng and colleagues showed that hydroxyl groups in B-ring and C-ring (**Figure 1**) contribute mainly to the antioxidative activities of quercetin and its glucosides, as compared with A-ring (Zheng et al., 2017). Rice-Evans et al. (1996) also demonstrated in quercetin that i) blocking the 3-hydroxyl group in the C-ring with a glycoside and ii) removing the 3-hydroxyl group in the C-ring, reduces its antioxidant activity. Some examples of quercetin derivatives detected in Arabidopsis are depicted in **Figure 1**. Dihydroxy B-ring substituted flavonoids such as quercetin and luteolin occur in the vacuole as well as in the chloroplastic and nuclear compartments, where they scavenge ROS with different mechanisms (Agati et al., 2012; Chapman et al., 2019). In the vacuole, they reduce H_2O_2 to H_2O in a peroxidase-dependent reaction (mechanism extensively explained in Pourcel et al., 2007), leading to the formation of flavonoid radicals (**Figure 2**). Ascorbate recycles these radicals to their reduced form, allowing the reduction of additional H_2O_2 molecules (Yamasaki et al., 1997; Pérez et al., 2002; Ferreres et al., 2011). The main vacuolar peroxidase from *Catharanthus roseus* showed higher affinity for quercetin than for quercetin-3-*O*-arabinoside (Km of 0.045 mM for quercetin vs. 1.589 mM for the glycoside), providing a biological explanation to the antioxidant value of flavonoid aglycones and their high H_2O_2 scavenging capacity (Ferreres et al., 2011). When localized in chloroplasts, these flavonoids efficiently scavenge singlet oxygen, while in the nucleus, they protect DNA from oxidative damages (**Figure 2**) (Naoumkina and Dixon, 2008; Brunetti et al., 2019). The main structural feature explaining the free radical scavenging capacity of flavonoids consists in the high reactivity of their hydroxyl substituents, as explained by (Heim et al., 2002):

$$Flavonoid - OH + R^{\cdot} \rightarrow Flavonoid - O^{\cdot} + RH$$

The results obtained in Arabidopsis lines with altered *UGT71* and *UGT73* expression demonstrate that glycosylation directly modifies plant cellular redox scavenging potential and demonstrate the role of UGTs in redox homeostasis.

GLYCOSYLATION REGULATES REDOX STATUS DURING RESPONSE TO PATHOGENS

UGT73B3 and UGT73B5 were also investigated in the context of plant response to bacterial infection. An untargeted metabolite analysis show that three kaempferol glucosides are slightly more accumulated in the wild-type than in the *ugt73b3* and *ugt73b5* mutants (Simon et al., 2014), providing additional evidence that

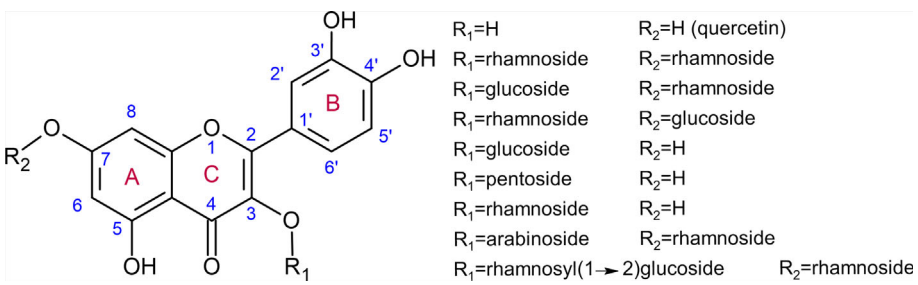

FIGURE 1 | Quercetin and examples of quercetin glycosides detected in various organs of *Arabidopsis thaliana* using ultraperformance liquid chromatography–photodiode array–electrospray ionization/quadrupole time-of-flight/mass spectrometry (Yonekura-Sakakibara et al., 2008).

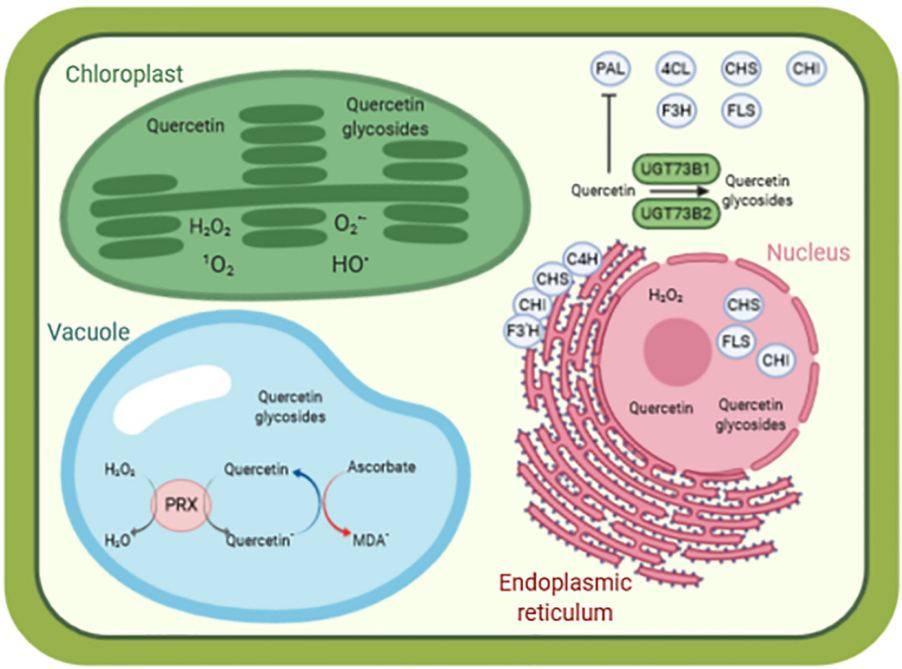

FIGURE 2 | A simplified model of quercetin as antioxidant molecule in a cellular context. The biosynthesis of quercetin is performed by enzymes located in the cytosol (PAL, C4H, CHS, F3H, FLS), anchored to the endoplasmic reticulum (C4H, CHS, CHI, F3'H) and present in the nucleus (CHS, CHI, FLS). Quercetin is glycosylated by various UGTs, such as UGT73B1 and UGT73B2 in *Arabidopsis thaliana*. Quercetin and quercetin glycosides are found in various compartments (such as cytosol, nucleus, chloroplasts, and vacuole), contributing to redox homeostasis and preventing oxidative damages caused by reactive species, for instance, in the chloroplasts. In the vacuole, quercetin reduces H_2O_2 to H_2O in a peroxidase-dependent reaction, leading to the formation of quercetin radical. This radical is then recycled back to quercetin by oxidation of ascorbate to monodehydroascorbate radical. Data from (Burbulis and Winkel-Shirley, 1999; Saslowsky et al., 2005; Fujino et al., 2018; Khorobrykh et al., 2020). $^1O_2$ singlet state of molecular oxygen, HO$^\bullet$ hydroxyl radical, H_2O_2 hydrogen peroxide, and O2$^{\bullet-}$ superoxide anion radical. 4CL, 4-coumaroyl:CoA-ligase; C4H, cinnamate 4-hydroxylase; CHI, chalcone isomerase; CHS, chalcone synthase; F3H, flavanone 3-hydroxylase; F3'H, flavonoid 3'-hydroxylase; FLS, flavonol synthase; MDA$^\bullet$, monodehydroascorbate radical; PAL, phenylalanine ammonia lyase; PRX, peroxidase. Picture designed with Biorender.

kaempferol is a substrate of UGT73B3 and UGT73B5 (Kim et al., 2006b; Kim et al., 2006a). The *ugt73b3 ugt73b5* double mutant was also characterized by a lower ascorbate pool (Simon et al., 2014), which is part of the H_2O_2 scavenging system in combination with ascorbate peroxidase (Asada, 1992; Smirnoff and Arnaud, 2019). During hypersensitive response (HR) to *Pst-AvrRpm1*, an avirulent strain of the biotrophic bacteria *Pseudomonas syringae* pv. *tomato*, *ugt73b3 ugt73b5* double mutant exhibited, as compared to wild-type, slightly enhanced cell death (ca. 10%) as measured by electrolyte leakage in the leaves (Simon et al., 2014). While no genotypic difference in H_2O_2 content was observed in absence of infection, the interaction between *Pst-AvrRpm1* and the single or double mutants resulted, as compared to wild type, in a higher accumulation of H_2O_2 (18%, 36%, and 42% in *ugt73b3*, *ugt73b5*, and *ugt73b3 ugt73b5*, respectively), which usually activate defense mechanisms (Smirnoff and Arnaud, 2019). Since this H_2O_2 accumulation did not correlate with decreased bacterial growth in leaves (Simon et al., 2014), it seems that the higher sensitivity of the double mutant is directly related to the absence of UGT73B3 and UGT73B5 and not to subsequent downstream consequences. This also suggests the important role of the ROS scavenging system, including UGT73B3 and UGT73B5, in response to *Pst-AvrRpm1* (Simon et al., 2014). It is also surprising that, while kaempferol prevents $O_2^{\bullet-}$ accumulation caused by MV in the *ugt73b1-2-3* backgrounds (Chae et al., 2006), it does not seem efficient to prevent H_2O_2 accumulation generated by *Pst-AvrRpm1* infection during HR in *ugt73b3* and *ugt73b5* mutants. In other words, the production of ROS during HR overcomes the redox scavenging capacity of the cell. However, this ROS burst, whose role is to enable a more efficient defense system, is not able to lower bacterial growth in infected leaves. This may be hypothetically related to the different metabolic profile of *ugt73b3* and *ugt73b5* after *Pst-AvrRpm1* infection, explaining the large spreading of the pathogen in the mutants. For instance, both glutathione content and oxidation status were altered in the mutants as compared to wild-type. *UGT73B3* and *UGT73B5* are co-expressed with genes associated to cellular redox status and detoxification (such as several *glutathione S-transferases* and ROS-induced genes). In the wild-type, oxidative stress, here caused by a pathogen attack, induces the expression of this subset of genes, which in turn contributes to limit cell death establishment during HR through regulation of redox homeostasis. It is important to notice that the Arabidopsis *tt4* mutant, depleted in flavonoids and kaempferol glycosides, displays essentially the same sensitivity to *P. syringae*

than its corresponding wild-type (Hagemeier et al., 2001), indicating that these molecules do not significantly account for the higher sensitivity of the *ugt73b3* and *ugt73b5* mutants. Instead, several elements suggest that during HR, UGT73B3 and UGT73B5 may accept as substrates, i) phytoprostanes, which are reactive lipids accumulating under oxidative conditions, to change their redox activity, and ii) phytoalexin by-products, such as hydroxycamalexin, whose accumulation is induced by H_2O_2 and several microorganisms (Simon et al., 2014). Such hypotheses remain however to be further validated.

Two tobacco salicylic acid- and pathogen-inducible UGTs (TOGTs) belonging to the UGT73B subfamily preferentially catalyze the glycosylation of the hydroxycoumarin scopoletin into scopolin (Fraissinet-Tachet et al., 1998; Chong et al., 2002). Simultaneous down-regulation of the two corresponding genes with an antisense construction coupled to tobacco mosaic virus (TMV) infection decreased scopoletin and scopolin content (three- to four-fold), enhanced lesion size (23 to 28%) while increasing reactive oxygen intermediates (ROI, i.e., $O_2^{\bullet-}$and H_2O_2) content (1.5- to 2.2-fold) in comparison with empty-vector transformed plants. The diminution of the scopoletin-scopolin pool therefore leads to increased accumulation of ROI. Besides, treatment of tobacco protoplasts with scopoletin significantly reduces TMV multiplication in a dose-dependent manner (Chong et al., 2002). Overall, scopoletin may act at two distinct levels: as an antiviral molecule in the tissues infected by TMV and as an antioxidant in cells surrounding the infected area to mitigate the effects of HR-induced ROI accumulation. The scopoletin antioxidant capacity is probably related to its ability to directly scavenge ROI and/or to its use as a substrate for peroxidase-mediated H_2O_2 detoxification (Yamasaki et al., 1997; Chong et al., 2002; Agati et al., 2012).

Overexpression of *TOGT* in tobacco results in both scopoletin and scopolin over-accumulation as compared to wild-type (Gachon et al., 2004), demonstrating that up-regulation of glycosylating activity toward a specific substrate does not necessarily result in lower accumulation of the corresponding aglycone form. This may be explained by their differential accumulation within cellular compartments (Taguchi et al., 2000). In tobacco T-13 cells, scopolin indeed preferentially accumulates in the vacuole (93% of the total pool), while the proportion of scopoletin is higher in the protoplast excluding the vacuole (70% of the total pool) (Taguchi et al., 2000). Glycosylation therefore decreases scopoletin cytoplasmic content by increasing vacuolar scopolin content, and this conversion mainly occurs in the cytosol (Taguchi et al., 2000). The transcription and activity of phenylalanine ammonia lyase (PAL), the first enzyme of the phenylpropanoid biosynthesis pathway from which is derived scopoletin, is well known to be negatively regulated by downstream metabolic products, such as *trans*-cinnamate and flavonols (**Figure 2**) (Zhang and Liu, 2015). Therefore, glycosylation and subsequent accumulation of its glycosylated form in the vacuole favors scopoletin biosynthesis and associated antioxidant activity by avoiding PAL feedback inhibition.

Thus, UGT activity may have, for various substrates, an important role in the homeostasis of their respective metabolic pathway. Such a regulation is of crucial importance for maintenance of redox stability when the aglycone/glycosylated form of a given molecule is involved in this subtle equilibrium. Collectively, these results show that UGT may participate in redox homeostasis through a panel of biochemical mechanisms in order to support global plant response to oxidative stress related to pathogen infection. Scopoletin accumulation supported by TOGT activity both inhibits viral multiplication and buffers the redox status of infected cells, while UGT73B3 and UGT73B5 may detoxify molecules produced by infected cells.

GLYCOSYLATION OF SPECIALIZED METABOLITES SHAPES OXIDATIVE STATUS DURING ABIOTIC STRESSES

Abiotic stresses result in accumulation of ROS and disturbance of the redox homeostasis (Keunen et al., 2013; Xie et al., 2019). Plants exposed to these stresses usually accumulate more antioxidant molecules, such as phenolics, carotenoids, and tocopherols (Wang and Frei, 2011) to re-equilibrate their oxidative balance. Consistent with the accumulation of phenolics, PAL is strongly induced at both transcriptional and enzymatic activity levels (Wang and Frei, 2011; Xing et al., 2013), similarly to other genes involved in flavonoids biosynthesis (Cheynier et al., 2013). Flavonoids accumulation significantly increases tolerance to oxidative stress resulting from high irradiance or drought in various plant species (Agati et al., 2007; Gómez et al., 2019).

Strikingly, there is also a pure energy rationale behind specialized metabolites biosynthesis (Selmar and Kleinwächter, 2013). Various abiotic stresses, such as drought and high temperature, result in partial stomatal closure, implying decreased requirement of ATP and reduction equivalents ($NADPH+H^+$) for CO_2 fixation in the Calvin cycle. Consequently, the pool of $NADP^+$ accepting electrons becomes depleted. Instead, these electrons would be transferred to oxygen, resulting in the production of superoxide radicals. The biosynthesis of highly reduced specialized metabolites (such as monoterpenes, alkaloids, aromatic amino acids, and phenolics) aims at regenerating the pool of $NADP^+$ through consumption of the reduction equivalents which cannot be directed to the Calvin cycle (Selmar and Kleinwächter, 2013).

The expression of several *UGT*s is induced during particular abiotic conditions (Rehman et al., 2018). Moreover, *UGT*s may also be co-expressed with genes from a specific biosynthesis pathway such as flavonols and anthocyanins (Tiwari et al., 2016). These observations suggest that UGTs partake in plant global response to abiotic stresses. For instance, the down-regulation of two *UGT*s from tea, *UGT78A14* and *UGT91Q2*, was shown to result in lower tolerance to cold stress (Zhao et al., 2019; Zhao et al., 2020), which also triggers oxidative stress. Interestingly, expression of these two genes is cold-inducible, suggesting that their function *in planta* is closely related to tolerance to this abiotic stress. UGT78A14 accepts kaempferol and quercetin as substrate, with a higher affinity for the first. *UGT78A14*

downregulated tea plants show i) decreased accumulation of total flavonoids, kaempferol-3-*O*-glucoside, kaempferol-7-*O*-glucoside, and kaempferol diglucoside (possibly *via* feedback gene inhibition), ii) reduced ROS scavenging capacity as measured by ferric reducing ability of plasma (FRAP) and DPPH assays, and iii) impaired tolerance to cold stress (lower optimal quantum yield Fv/Fm, an indicator of photoinhibition, after exposure to cold stress). Their leaves are characterized by an increased accumulation of superoxide radicals and H_2O_2, which may result in lipid peroxidation and decreased photosynthetic efficiency. The UGT78A14 glycosylation products of kaempferol and quercetin have higher ROS scavenging activity than their corresponding aglycones as assessed by FRAP, DPPH and 2,2'-azino-bis(3-ethylbenzothiazoline-6-sulfonic acid) (ABTS) assays (Zhao et al., 2019). This result is contradictory to previous observations, which stated that flavonoid aglycones show higher antioxidant capacity than their glycosylated forms, as demonstrated for quercetin and luteolin using another method, the Trolox equivalent antioxidant activity (TEAC) test (Rice-Evans et al., 1996; Hopia and Heinonen, 1999; Montoro et al., 2005). Furthermore, increased kaempferol and quercetin content obtained by transient overexpression in tobacco of the *Crocus sativus CsBGLU12*, coding for a β-glucosidase active on flavonol glycosides, resulted in leaves more tolerant to ultraviolet B, dehydration and salt exposure, as shown by higher chlorophyll content and lower lipid peroxidation after stress application (Baba et al., 2017). We may suggest that the phenotypes related to oxidative stress tolerance observed in tea with down-regulation of *UGT78A14* (Zhao et al., 2019) and tobacco with over-expression of *CsBGLU12* (Baba et al., 2017) are partially explained by different pools of antioxidant molecules, which are not restricted to the few flavonoids developed in this review. Other specialized metabolites, whose molecular structures and contents are highly variable between distinct species, may explain this difference. Moreover, Zhao and colleagues (2019) investigated tolerance to cold stress, while Baba and colleagues (2017) focused on ultraviolet B, dehydration and salt exposure. While all these conditions result in oxidative stress, they most likely do not invoke the same cellular and molecular consequences and responses. For instance, flavonoids involved in protection against ultraviolet B may be preferentially accumulated in the cell wall to protect the cell. In order to cross the plasma membrane, these molecules should be slightly apolar and therefore not glycosylated. Consequently, the glycosylation pattern of a given molecule may not uniformly protect the plant against a range of various stresses. This discrepancy may also lie in the different substitution patterns of investigated flavonoids. Indeed, the glucose substitution pattern of a given aglycone is important to explain its antioxidant potential, as demonstrated for quercetin (Zheng et al., 2017) and previously explained. Two UGT78A14 alleles are reported to yield kaempferol-3-*O*-glucoside, kaempferol-7-*O*-glucoside, and kaempferol diglucoside in different proportions (Zhao et al., 2019), while UGT73B2 preferentially glucosylates kaempferol in the 3-hydroxyl position (Kim et al., 2006a). These different substitution patterns were reported to result in differential antioxidant properties for quercetin and related glycosylation or methoxylation derivatives (Rice-Evans et al., 1996; Montoro et al., 2005). In Arabidopsis, 32 flavonol glycosides showing variable antioxidant capacities have been identified (**Figure 1**) (Yonekura-Sakakibara et al., 2008; Chapman et al., 2019). Reporting of differential ROS scavenging activity between related molecules should therefore be carefully described, for instance, in terms of hydroxyl group substitution, and interpreted with caution.

The maize *UDP glucose:flavonoid glucosyltransferase 2* (*UFGT2*) supports plant response to various abiotic stresses and rescues the flavonols deficiency in the Arabidopsis *ugt78d2* mutant (Li et al., 2018). Arabidopsis *UFGT2* overexpressing lines displayed lower accumulation of H_2O_2 when facing oxidative stress following salt, osmotic, or H_2O_2 conditions while two knock-out maize mutants showed the opposite trend (Li et al., 2018). Quantification of flavonols in these different lines coupled to *in vitro* enzymatic activity consistently demonstrate that UFGT2 glycosylates quercetin and kaempferol. Similarly to *TOGT* (Gachon et al., 2004), overexpression of *UFGT2* in Arabidopsis not only increases the glycosylated forms of these two flavonols, but also the accumulation of their aglycones, through higher expression of core flavonol biosynthesis genes. Consistent with the previously described scopoletin and scopolin translocation mechanism (Taguchi et al., 2000), this equilibrium depends on the differential cellular compartmentalization of these molecules (**Figure 2**). The transport from the site of flavonoids biosynthesis, i.e., the endoplasmic reticulum (ER), to the tonoplast is highly favored by conjugation with either a sugar moiety (resulting in a glycosylated molecule) or a glutathione *S*-transferase group (**Figure 2**). These conjugations therefore maintain flavonoid homeostasis in the cytosol and support their corresponding biosynthetic pathways (Agati et al., 2012).

Anthocyanins are potent antioxidant molecules (Gould, 2004) and they are biosynthesized in response to several stresses. For instance, MV-induced accumulation of chloroplastic H_2O_2 enhances the expression of genes of the anthocyanin biosynthesis pathway as well as anthocyanin content in various Arabidopsis genetic backgrounds (Maruta et al., 2014). The silencing of a major chloroplastic ROS scavenging gene, coding for an ascorbate peroxidase, also resulted in enhanced anthocyanin content (Maruta et al., 2014). Flavonoids present in the chloroplasts are known to scavenge the highly reactive singlet oxygen ($^1O_2$) in order to protect the function of this organelle vs. oxidative stress (Agati et al., 2007). This result has been confirmed using Arabidopsis genotypes overaccumulating flavonoids, including overexpressors of *MYB12* and *PAP1* regulating flavonols and anthocyanins biosynthesis, resulting in better tolerance to MV and drought stress (Nakabayashi et al., 2014). Similarly to flavonols, anthocyanins undergo glycosylation and this conjugation has deep consequences under cold, salt, and drought stresses. For instance, overexpression of *UGT79B2* and *UGT79B3*, which glycosylate cyanidin and cyanidin 3-*O*-glucoside using UDP-rhamnose as sugar donor, resulted in increased tolerance when facing these three stresses, while RNAi line and CRISPR mutant showed enhanced sensitivity (Li et al., 2017). These phenotypes are most likely explained by the PAL feedback repression of anthocyanin intermediates, as previously noted for scopoletin

and kaempferol. Indeed, anthocyanins preferentially locate in the vacuole, while their biosynthesis takes place in the smooth ER (Landi et al., 2015). In addition, two anthocyanins were detected in hydro-alcoholic extracts of vacuoles isolated from protoplasts of *C. roseus* (Ferreres et al., 2011). Once again, these two genes were strongly induced in response to cold, salt, and drought treatments. These genes are part of the cold-regulated genes subset, whose expression may be regulated by the transcription factor CBF1 to scavenge ROS under cold conditions. DAB and NBT staining, together with antioxidant FRAP assay, highlighted the correlation between expression of *UGT79B2* and *UGT79B3* and ROS scavenging capacity, demonstrating the importance of anthocyanin glycosylation in redox homeostasis under several adverse conditions (Li et al., 2017).

The cold-inducible *OsUGT90A1* was isolated from *Oryza sativa* based on its identification as most probable candidate gene explaining the *LOW TEMPERATURE SEEDLING SURVIVABILITY* QTL (Shi et al., 2020). As shown by these authors, *OsUGT90A1* overexpressing rice and Arabidopsis lines display lower electrolyte leakage following exposition at 10°C, 4°C, and −2°C. Membrane integrity was more preserved in these lines because of lower accumulation of ROS, as detected by NBT staining, in addition to higher CAT and soluble peroxidase activities after cold exposure. Opposite results were obtained in two lines with strongly decreased *OsUGT90A1* expression. This gene also increases salt tolerance. While the corresponding enzyme is annotated to glycosylate anthocyanins, no striking differences between these lines were observed in the flavonoid and anthocyanin content. The authors rather suggest, based on modified plant phenotype (longer shoots and shorter roots in line overexpressing *OsUGT90A1*), that OsUGT90A1 may accept auxins and cytokinins as substrates, but no enzymatic activity assays have been performed to further confirm this hypothesis.

Down-regulation of tea *UGT91Q2* reduces nerolidol (a volatile sesquiterpene alcohol) and nerolidol glucoside content, ROS scavenging activity (DPPH assay) and cold stress tolerance (Zhao et al., 2020). Its expression is strongly induced by chilling stress and the corresponding enzyme, while accepting a large range of substrates, has a strong affinity for nerolidol. Nerolidol glucoside has a higher ROS scavenging activity (DPPH assay) than its aglycone and possibly prevents lipid peroxidation to protect PSII during cold stress (Zhao et al., 2020). Glycosylation of volatile terpenoids allows their accumulation in non-volatile forms as a result of their higher water solubility, easing their storage in vacuoles (Yazaki et al., 2017). It is therefore possible that nerolidol glycosylation supports the biosynthesis of its aglycone form and finally contributes to plant cold tolerance.

While its substrate is so far unknown, UGT85A5 protects Arabidopsis plantlets from salt stress. Lines with ectopic expression of this gene indeed show lower loss of chlorophyll as compared to the wild-type (*ca.* 10% at 100 mM NaCl), concomitant with lower concentration of malondialdehyde (*ca.* + 40% in the wild-type at 300 mM NaCl), suggesting that the cells are more successful in keeping ROS at an acceptable level (Sun et al., 2013). *UGT85A5* is induced by salt, further suggesting that this gene is part of the plant response during salt exposure, as well as by abscisic acid (Rehman et al., 2018).

Results gathered from experiments investigating response and tolerance to abiotic stresses demonstrate the importance of several UGTs in this context. Those genes are generally induced under these conditions to mitigate the effects of oxidative stress. While this mechanism is now well described for flavonoids, such as quercetin and anthocyanins, it appears that other families, such as terpenoids (as illustrated here with nerolidol), may also partake in plant redox homeostasis. These findings prompt to study whether glycosylation of other families of molecules may be involved in plant response to unfavorable growth conditions. UGTs, by modulating the cellular repartition of targeted molecules, regulate their corresponding biosynthetic pathways, opening avenues for applications in managing abiotic stress tolerance.

PHYTOHORMONES GLYCOSYLATION AND REDOX STATUS DURING OXIDATIVE STRESSES

Phytohormones undergo various conjugation reactions, with glycosylation being reported for substrates deriving from abscisic acid (ABA), gibberellins, strigolactones, cytokinins, auxins, brassinosteroids, salicylic acid, and jasmonic acid (Piotrowska and Bajguz, 2011; Islam et al., 2013; Maruri-López et al., 2019). These signaling molecules are key regulators with respect to plant acclimation to challenging environmental conditions. This section depicts the importance of phytohormone glycosylation in this context by using ABA, auxins and strigolactones as case studies.

Abscisic Acid

ABA is one of the most thoroughly investigated molecules in the context of abiotic stresses, especially in response to drought (Takahashi et al., 2018; Gómez et al., 2019). Oxidative stress is a notable dimension explaining the cellular damages provoked by drought, especially through production of $^1O_2$ by the photosynthetic electron transport chain in the PSII, resulting in oxidative damages in the chloroplasts (Noctor et al., 2014). The next paragraphs will therefore quickly emphasize the role of ABA in maintaining redox homeostasis during abiotic stresses, before to review the role of ABA glycosylation in terms of acclimation and oxidative damages.

Global transcriptome analyses of Arabidopsis after ABA application demonstrate the crucial role of this phytohormone during response to stress. Indeed, ontology analysis performed with Panther 15.0 (Mi et al., 2019) on Col-0 seedlings subjected to 10 μM ABA (**Supplementary Table S1A**) revealed the up-regulation of genes related to responses to water deprivation, osmotic stress, salt stress, cold, oxidative stress and stress (Goda et al., 2008). These results largely overlap those obtained by Hoth and colleagues (2002) on ecotype Landsberg plantlets cultivated in medium supplemented with 50 μM ABA (**Supplementary Table S1B**), where the biological processes responses to water

deprivation, osmotic stress, salt stress, cold and stress were retrieved. ABA induces the expression of gene coding for transcription factors associated to tolerance to abiotic stress, such as for instance, *ZmHDZ10*, coding for a maize homeodomain–leucine zipper I (Zhao et al., 2014).

ABA-glucose ester (ABA-GE)/ABA equilibrium is considered as an important gatekeeper of plant response to abiotic stresses (Lee et al., 2006; Xu et al., 2012; Chen et al., 2020; Han et al., 2020). ABA-GE is an inactive form of ABA, together with hydroxylated conjugates, but this glycosylation is reversible (Nambara and Marion-Poll, 2005). ABA-GE accumulates in the vacuole and is therefore not able to activate the ABA signaling pathway. This glycosylation is caused by several abiotic stresses. For instance, the expression of an *UGT* from adzuki bean glycosylating ABA is significantly induced by dehydration in hypocotyls (Nambara and Marion-Poll, 2005). Furthermore, UGT71B6, UGT71B7, and UGT71B8 yield ABA-GE and their coding genes are induced by ABA, salt and osmotic stress (Lim et al., 2005; Dong et al., 2014). Their simultaneous silencing through RNAi results in plantlets more tolerant to osmotic stress and to lower water loss in excised plants, but also in smaller rosette leaves, shorter roots and pale green leaves in absence of stress (Dong et al., 2014). Hence, while silencing these *UGT*s responsible for ABA glycosylation results in higher tolerance to dehydration stress, it also penalizes plant growth under optimal conditions. We may therefore suggest that the biological functions of these UGT71s is to maintain an optimal ABA content under non-limiting growing conditions. Since they are ABA-, salt-, and osmotic-inducible, they may also mitigate ABA response under these conditions. A functional analysis of a gene closely related to *UGT71B6/7/8*, *UGT71C5*, reveals similar mechanisms of drought tolerance (Liu et al., 2015). Plants overexpressing *UGT71C5* are less drought-tolerant, with the *ugt71c5* mutant and downregulated lines showing the opposite phenotype. This lower expression of *UGT71C5* results in increased expression of ABA-responsive genes. In addition, *ugt71c5* mutant displays higher drought resistance than *ugt71b6* mutant (Liu et al., 2015). Finally, UGT75B1 is also able to yield ABA-GE, and overexpression of its coding gene results in impaired response to salt and drought stress, downregulation of several ABA-regulated genes involved in stress response and lower ABA content in detached rosette leaves (Chen et al., 2020). ABA-GE may play a key role in desiccation tolerance, since the β-D-glucosidase activity yielding ABA from ABA-GE is enhanced by salinity in several species (Nambara and Marion-Poll, 2005).

By contrast with *de novo* ABA biosynthesis, production of ABA from ABA-GE requires a single enzymatic reaction, which is catalyzed by several β-glucosidases in Arabidopsis. This simple hydrolysis step allows fast plant response when facing adverse challenging environmental conditions. For instance, mutants impaired in *BGLU33*, coding for a β-glucosidase active on ABA-GE, are more sensitive to drought and salt stresses than wild-type, while overexpressing lines are more tolerant (Xu et al., 2012). Similarly, mutant deficient in *BGLU18* is dwarf and highly sensitive to drought stress (Lee et al., 2006). Drought stress enhances BGLU18 activity through homomeric interaction, resulting in a 10-mer complex. This conformation drastically increases ABA content under drought stress as a result of ABA-GE hydrolysis (Lee et al., 2006). Recently, it was shown that the BGLU18 subcellular distribution is modified upon stress conditions (Han et al., 2020). In normal conditions, BGLU18 is mainly found in ER bodies. Following dehydration, osmotic or salt stress, the number of ER bodies significantly increases. These structures consist in temporary storage compartment that release BGLU upon stress, resulting in increased BGLU18-mediated ABA-GE hydrolysis. In addition, there is a relative increase in the BGLU18-microsomal fraction under stress, which also triggers ABA-GE hydrolysis activity. Upon stress, the following mechanisms explain altogether the increased ABA content resulting from BGLU18 activity: i) BGLU18 is organized in an active 10-mer complex, ii) BGLU18 is released from ER bodies, and iii) ABA-GE stored in the vacuole or in apoplastic space is transported to close vicinity of BGLU18.

Altogether, these results highlight the importance of ABA homeostasis and glycosylation status in tolerance to water deprivation or salt stress and subsequent mitigation of oxidative injuries.

Auxins

Besides their developmental roles, auxins translate environmental and stress inputs into adequate plant response (Ludwig-Müller, 2011; Casanova-Sáez and Voß, 2019). The following paragraphs aim at explaining how auxin glycosylation may shape plant response to oxidative stress rising from abiotic constrains.

UGT74E2 enhances, among other biological processes, tolerance to drought and salt stress through glycosylation of the auxin indole-3-butyric acid (IBA), as demonstrated with recombinant enzymatic activity (Tognetti et al., 2010). The importance of UGT74E2 regarding oxidative stress is highlighted in one of the most relevant genetic backgrounds in relation to redox homeostasis, the Arabidopsis mutant deficient in CATALASE 2 (*cat2*), which is a crucial protein for H_2O_2 catabolism in peroxisomes (Pan et al., 2020). When grown in conditions favoring photorespiration and concomitant H_2O_2 accumulation, such as high light, 185 genes which were hardly expressed in conditions repressing photorespiration undergo a massive up-regulation (fold change > 21) in *cat2* (He et al., 2018). Supporting an important role for UGTs in response to H_2O_2 accumulation, five of them were part of these strongly induced genes, including *UGT73B4*, *UGT73B5*, *UGT73C4*, *UGT74E1*, and *UGT74E2*. *UGT74E2* is upregulated by osmotic, oxidative, ultraviolet B and salt stress (Tognetti et al., 2010). Its overexpression increases not only IBA-Glc content, but also free IBA, and modified the levels of IAA-Glc, IAA-Glu, and oxIAA, resulting in a shoot branching phenotype because of loss of apical dominance, often related to altered auxin homeostasis, as well as improved survival under drought and salt stresses (Tognetti et al., 2010). Collectively, these results suggest that UGT74E2 modifies auxin gradient and distribution to support plant acclimation under drought and salt stress conditions (Tognetti et al., 2010). This mechanism may rely on mutual interactions

between flavonoids (especially flavonols) and auxin (Brunetti et al., 2018). More specifically, auxin induces flavonols biosynthesis, which in turn regulate auxin movement and signaling at the cellular and tissue levels by inhibiting the activity of several auxin transport proteins (such as PIN1, PIN2, and PIN5) and modifying the activity of auxin inactivation proteins (e.g., DIOXYGENASE FOR AUXIN OXIDATION). This circuit then invokes a panel of reactions in organelles facing oxidative stress, including chloroplasts, peroxisomes and nucleus (Brunetti et al., 2018). Auxin involvement in redox homeostasis remains however a highly complex picture with several parallel mechanisms whose relative importance remains to be investigated and hierarchized.

UGT85U1 has been isolated from *Crocus sativus* and is involved in response to abiotic stress (Ahrazem et al., 2015). The expression of this gene is inducible by salt, drought and cold stresses. Heterologous overexpression of *UGT85U1* in Arabidopsis resulted in plants with higher total chlorophyll content and increased resistance to oxidative stress caused by H_2O_2 exposure and salt stress as measured by growth parameters. LC-ESI/MS^n analysis revealed an increased content of free and conjugated forms of indole acetic acid (such as IAA-Glc and oxIAA) in the roots, suggesting that auxin may be an *in vivo* substrate of UGT85U1 (Ahrazem et al., 2015), although the authors did not demonstrate this finding with recombinant UGT85U1 assay.

By contrast with ABA, ontology analysis including genes significantly upregulated by auxin (**Supplementary Tables S1C, D**) highlights the absence of biological processes related to response to (a)biotic stresses, in an experiment directly treating Arabidopsis Col-0 seedlings with 1 μM IAA (Goda et al., 2008), and in roots from Arabidopsis Col-0 plantlets transferred to 1 μM IAA medium (Lewis et al., 2013). These transcriptomic analyses underline that auxin does not induce *per se* the expression of genes involved in redox homeostasis and response to stress. Instead, the relative proportion of conjugates and catabolites regulates auxin transport, signaling and plant response to various abiotic stresses.

Strigolactones

Resurrection plants illustrate the ability of various species to adaptation to extreme environmental condition, particularly concerning drought stress. The functional characterization of an UGT isolated from the resurrection grass *Sporobolus stapfianus* illustrates how vital may be a glycosylation (Islam et al., 2013). This UGT is referred to as SDG8i and belongs to the UGT88 family. A protein extract from tobacco leaves infiltrated with an actin promoter-driven *SDG8i* expression is able to glycosylate the strigolactone analogue GR24, while very weak activity was retrieved in leaves infiltrated with the empty vector. No significant activities were detected for other phytohormones. *SDG8i* expression is drastically increased under severe water deficit. The heterologous overexpression of this gene in Arabidopsis results in higher tolerance to salt and drought stresses, as well as increased survival rate following a freezing period (at −8°C and −12°C) (Islam et al., 2013). It is hypothesized that strigolactones positively regulate plant response to drought and salt stress (Ha et al., 2014) and several elements suggest a strigolactones cross-talk with ABA sensitivity and biosynthesis (Cardinale et al., 2018). While the outreach of strigolactone glycosylation remains poorly understood, it was established that strigolactone strongly induces the expression of several key genes of the anthocyanin pathway, such as MYB transcription factors and downstream biosynthesis genes, raising anthocyanin content in Arabidopsis seedlings (Wang et al., 2020). Glycosylation may ease strigolactone translocation between distant organs and induce subsequent anthocyanin biosynthesis upon various abiotic stresses to protect specific tissues, such as leaves, from oxidative damages. SDG8i may therefore be involved in the regulation of strigolactone biosynthesis, which may be of crucial importance during extreme water deficit.

CONCLUSION AND PERSPECTIVES

Oxidative stress results from a wide range of environmental and physiological situations. It is therefore not surprising that plants have designed a large panel of response at many levels to address this deleterious cellular status. As underlined by the large molecule spectrum that may undergo glycosylation, especially phenolics and phytohormones, UGTs and glucosidases are able to support rapid and efficient plant response to numerous environmental conditions. The functional study of genes devoted to ROS detoxication such as CATs, SODs, and soluble peroxidases has demonstrated their importance to maintain redox homeostasis. Antioxidant molecules (such as flavonoids) are also widely acknowledged as efficient players in this respect, notably during abiotic stress events. Redox status is therefore a central hub connecting enzymatic ROS scavenging to biosynthesis and repartition of antioxidant/signaling molecules (partially regulated by glycosylation) in response to various endogenous and exogenous stimuli. The consequences of glycosylation regarding plant response to oxidative stress are multiple. This reaction may i) directly modify the antioxidant property of a molecule, such as flavonoids, ii) favor the biosynthesis of its corresponding aglycone by changing its subcellular location, such as scopolin and scopoletin, and iii) impact on phytohormones translocation, their signaling capacity and downstream gene expression regulation. It is also remarkable that the expression of many *UGTs* is stress-inducible and contributes to the plasticity of plants facing (a)biotic stresses, highlighting their potential valorization for designing plants more tolerant to sub-optimal growing conditions. Humankind benefits from antioxidant molecules, as their biochemical properties are not restricted to plants and strongly contribute to the nutritional values of various fruits and vegetables (Wang and Frei, 2011).

These findings have to be put in perspective with the considerable efforts which have been produced to decipher the molecular basis of redox signaling, now reported to play an important role during plant response to adverse environmental and/or developmental conditions and more specifically to oxidative stress (Waszczak et al., 2018; Farooq et al., 2019).

The chloroplastic compartment, which is the main source of ROS formation under light conditions (Vaahtera et al., 2014), is a sensitive probe of cellular redox status. Under higher accumulation of oxidant markers, such as H_2O_2, chloroplast is able to trigger a signaling cascade leading to expression of nuclear genes to counterbalance the negative effects of oxidant conditions and rescue the functions of not only chloroplasts, but also mitochondria (Leister, 2019).

This ROS-dependent signaling modifies the nuclear transcriptome, but also initiates post-transcriptional, translational, and post-translational regulatory mechanisms (He et al., 2018). ROS may activate these pathways through changes of targeted proteins in either, their conformational state (monomerization, polymerization), interaction with a partner, cleavage from an organelle to allow translocation to the nucleus, enhancement of their DNA binding activity, phosphorylation through the mitogen-activated protein kinase cascade, but also through regulation of general transcription factor activity, such as Mediator (He et al., 2018).

Therefore, any modification related to redox homeostasis, such as concentration of oxidant and antioxidant molecules or proteins, may potentially result in repression or activation of retrograde signaling pathways. Ultimately, it is also possible that impairing the redox homeostasis mechanism causes better resistance to oxidative stress through activation of a retrograde signaling pathway. Since several UGTs are known to regulate the content of specific flavonoids (Chong et al., 2002; Zhao et al., 2019), for instance, in the chloroplasts (Agati et al., 2012), we may hypothesize that this modification of the non-enzymatic ROS scavenging capacity interacts with the chloroplast retrograde signaling wave. Such associations deserve further investigation, especially regarding adaptation required to face the increasingly challenging environmental conditions of the Anthropocene era (Basso et al., 2018).

AUTHOR CONTRIBUTIONS

MBe designed the review, conducted literature review, and wrote the manuscript. GN, MJ, and MBa reviewed and critically revised the manuscript. All authors contributed to the article and approved the submitted version.

FUNDING

MBe is supported by Belgian Fonds de la Recherche Scientifique (FRS-FNRS) research project T.0068.18. MBa is a Senior Research Associate of the FRS-FNRS.

SUPPLEMENTARY MATERIAL

The Supplementary Material for this article can be found online at: https://www.frontiersin.org/articles/10.3389/fpls.2020.571399/full#supplementary-material

REFERENCES

Agati, G., Matteini, P., Goti, A., and Tattini, M. (2007). Chloroplast-located flavonoids can scavenge singlet oxygen. *New Phytol.* 174, 77–89. doi: 10.1111/j.1469-8137.2007.01986.x

Agati, G., Azzarello, E., Pollastri, S., and Tattini, M. (2012). Flavonoids as antioxidants in plants: Location and functional significance. *Plant Sci.* 196, 67–76. doi: 10.1016/j.plantsci.2012.07.014

Ahrazem, O., Rubio-Moraga, A., Trapero-Mozos, A., Climent, M. F. L., Gómez-Cadenas, A., and Gómez-Gómez, L. (2015). Ectopic expression of a stress-inducible glycosyltransferase from saffron enhances salt and oxidative stress tolerance in *Arabidopsis* while alters anchor root formation. *Plant Sci.* 234, 60–73. doi: 10.1016/j.plantsci.2015.02.004

Anjum, N. A., Sofo, A., Scopa, A., Roychoudhury, A., Gill, S. S., Iqbal, M., et al. (2015). Lipids and proteins—major targets of oxidative modifications in abiotic stressed plants. *Environ. Sci. Pollut. Res.* 22, 4099–4121. doi: 10.1007/s11356-014-3917-1

Asada, K. (1992). Ascorbate peroxidase – a hydrogen peroxide-scavenging enzyme in plants. *Physiol. Plant* 85, 235–241. doi: 10.1111/j.1399-3054.1992.tb04728.x

Baba, S. A., Vishwakarma, R. A., and Ashraf, N. (2017). Functional characterization of CsBGlu12, a β-glucosidase from *Crocus sativus*, provides insights into its role in abiotic stress through accumulation of antioxidant flavonols. *J. Biol. Chem.* 292, 4700–4713. doi: 10.1074/jbc.M116.762161

Baderschneider, B., and Winterhalter, P. (2001). Isolation and characterization of novel benzoates, cinnamates, flavonoids, and lignans from Riesling wine and screening for antioxidant activity. *J. Agric. Food Chem.* 49, 2788–2798. doi: 10.1021/jf010396d

Basso, V., De Freitas Pereira, M., Maillard, F., Mallerman, J., Mangeot-Peter, L., Zhang, F., et al. (2018). Facing global change: the millennium challenge for plant scientists. *New Phytol.* 220, 25–29. doi: 10.1111/nph.15376

Bose, J., Rodrigo-Moreno, A., and Shabala, S. (2014). ROS homeostasis in halophytes in the context of salinity stress tolerance. *J. Exp. Bot.* 65, 1241–1257. doi: 10.1093/jxb/ert430

Brunetti, C., Fini, A., Sebastiani, F., Gori, A., and Tattini, M. (2018). Modulation of phytohormone signaling: A primary function of flavonoids in plant–environment interactions. *Front. Plant Sci.* 9:1042:1042. doi: 10.3389/fpls.2018.01042

Brunetti, C., Sebastiani, F., and Tattini, M. (2019). Review: ABA, flavonols, and the evolvability of land plants. *Plant Sci.* 280, 448–454. doi: 10.1016/j.plantsci.2018.12.010

Burbulis, I. E., and Winkel-Shirley, B. (1999). Interactions among enzymes of the *Arabidopsis* flavonoid biosynthetic pathway. *Proc. Natl. Acad. Sci. U. S. A.* 96, 12929–12934. doi: 10.1073/pnas.96.22.12929

Cardinale, F., Krukowski, P. K., Schubert, A., and Visentin, I. (2018). Strigolactones: Mediators of osmotic stress responses with a potential for agrochemical manipulation of crop resilience. *J. Exp. Bot.* 69, 2291–2303. doi: 10.1093/jxb/erx494

Casanova-Sáez, R., and Voß, U. (2019). Auxin Metabolism Controls Developmental Decisions in Land Plants. *Trends Plant Sci.* 24, 741–754. doi: 10.1016/j.tplants.2019.05.006

Chae, E. L., Ahn, J. H., and Lim, J. (2006). Molecular genetic analysis of tandemly located glycosyltransferase genes, *UGT73B1*, *UGT73B2*, and *UGT73B3*, in *Arabidopsis thaliana*. *J. Plant Biol.* 49, 309–314. doi: 10.1007/BF03031161

Chapman, J. M., Muhlemann, J. K., Gayomba, S. R., and Muday, G. K. (2019). RBOH-Dependent ROS Synthesis and ROS Scavenging by Plant Specialized Metabolites to Modulate Plant Development and Stress Responses. *Chem. Res. Toxicol.* 32, 370–396. doi: 10.1021/acs.chemrestox.9b00028

Chen, T. T., Liu, F. F., Xiao, D. W., Jiang, X. Y., Li, P., Zhao, S. M., et al. (2020). The Arabidopsis UDP-glycosyltransferase75B1, conjugates abscisic acid and affects plant response to abiotic stresses. *Plant Mol. Biol.* 102, 389–401. doi: 10.1007/s11103-019-00953-4

Cheynier, V., Comte, G., Davies, K. M., Lattanzio, V., and Martens, S. (2013). Plant phenolics: Recent advances on their biosynthesis, genetics, and ecophysiology. *Plant Physiol. Biochem.* 72, 1–20. doi: 10.1016/j.plaphy.2013.05.009

Chong, J., Baltz, R., Schmitt, C., Beffa, R., Fritig, B., and Saindrenan, P. (2002). Downregulation of a pathogen-responsive tobacco UDP-Glc:phenylpropanoid glucosyltransferase reduces scopoletin glucoside accumulation, enhances

oxidative stress, and weakens virus resistance. *Plant Cell* 14, 1093–1107. doi: 10.1105/tpc.010436

Deng, Y., and Lu, S. (2017). Biosynthesis and Regulation of Phenylpropanoids in Plants. *CRC. Crit. Rev. Plant Sci.* 36, 257–290. doi: 10.1080/07352689.2017.1402852

Diffenbaugh, N. S., Singh, D., Mankin, J. S., Horton, D. E., Swain, D. L., Touma, D., et al. (2017). Quantifying the influence of global warming on unprecedented extreme climate events. *Proc. Natl. Acad. Sci. U. S. A.* 114, 4881–4886. doi: 10.1073/pnas.1618082114

Dong, T., Xu, Z. Y., Park, Y., Kim, D. H., Lee, Y., and Hwang, I. (2014). Abscisic acid uridine diphosphate glucosyltransferases play a crucial role in abscisic acid homeostasis in Arabidopsis. *Plant Physiol.* 165, 277–289. doi: 10.1104/pp.114.239210

Dooner, H. K., and Nelson, O. E. (1977). Controlling element-induced alterations in UDPglucose:flavonoid glucosyltransferase, the enzyme specified by the *bronze* locus in maize. *Proc. Natl. Acad. Sci.* 74, 5623–5627. doi: 10.1073/pnas.74.12.5623

Dubois, M., and Inzé, D. (2020). Plant growth under suboptimal water conditions: Early responses and methods to study them. *J. Exp. Bot.* 71, 1706–1722. doi: 10.1093/jxb/eraa037

Farooq, M. A., Niazi, A. K., Akhtar, J., Saifullah,, Farooq, M., Souri, Z., et al. (2019). Acquiring control: The evolution of ROS-Induced oxidative stress and redox signaling pathways in plant stress responses. *Plant Physiol. Biochem.* 141, 353–369. doi: 10.1016/j.plaphy.2019.04.039

Ferreres, F., Figueiredo, R., Bettencourt, S., Carqueijeiro, I., Oliveira, J., Gil-Izquierdo, A., et al. (2011). Identification of phenolic compounds in isolated vacuoles of the medicinal plant *Catharanthus roseus* and their interaction with vacuolar class III peroxidase: An H2O2 affair? *J. Exp. Bot.* 62, 2841–2854. doi: 10.1093/jxb/erq458

Fraissinet-Tachet, L., Baltz, R., Chong, J., Kauffmann, S., Fritig, B., and Saindrenan, P. (1998). Two tobacco genes induced by infection, elicitor and salicylic acid encode glucosyltransferases acting on phenylpropanoids and benzoic acid derivatives, including salicylic acid. *FEBS Lett.* 437, 319–323. doi: 10.1016/S0014-5793(98)01257-5

Fryzova, R., Pohanka, M., Martinkova, P., Cihlarova, H., Brtnicky, M., Hladky, J., et al. (2018). "Oxidative stress and heavy metals in plants," in *Reviews of Environmental Contamination and Toxicology* (New York: Springer LLC), 129–156. doi: 10.1007/398_2017_7

Fujino, N., Tenma, N., Waki, T., Ito, K., Komatsuzaki, Y., Sugiyama, K., et al. (2018). Physical interactions among flavonoid enzymes in snapdragon and torenia reveal the diversity in the flavonoid metabolon organization of different plant species. *Plant J.* 94, 372–392. doi: 10.1111/tpj.13864

Gachon, C., Baltz, R., and Saindrenan, P. (2004). Over-expression of a scopoletin glucosyltransferase in *Nicotiana tabacum* leads to precocious lesion formation during the hypersensitive response to tobacco mosaic virus but does not affect virus resistance. *Plant Mol. Biol.* 54, 137–146. doi: 10.1023/B:PLAN.0000028775.58537.fe

Gachon, C. M. M., Langlois-Meurinne, M., and Saindrenan, P. (2005). Plant secondary metabolism glycosyltransferases: The emerging functional analysis. *Trends Plant Sci.* 10, 542–549. doi: 10.1016/j.tplants.2005.09.007

Goda, H., Sasaki, E., Akiyama, K., Maruyama-Nakashita, A., Nakabayashi, K., Li, W., et al. (2008). The AtGenExpress hormone and chemical treatment data set: experimental design, data evaluation, model data analysis and data access. *Plant J.* 55, 526–542. doi: 10.1111/j.1365-313X.2008.03510.x

Gómez, R., Vicino, P., Carrillo, N., and Lodeyro, A. F. (2019). Manipulation of oxidative stress responses as a strategy to generate stress-tolerant crops. From damage to signaling to tolerance. *Crit. Rev. Biotechnol.* 39, 693–708. doi: 10.1080/07388551.2019.1597829

Gould, K. S. (2004). Nature's Swiss army knife: The diverse protective roles of anthocyanins in leaves. *J. Biomed. Biotechnol.* 2004, 314–320. doi: 10.1155/S1110724304406147

Gray, S. B., and Brady, S. M. (2016). Plant developmental responses to climate change. *Dev. Biol.* 419, 64–77. doi: 10.1016/j.ydbio.2016.07.023

Ha, C., Van, Leyva-Gonzalez, M. A., Osakabe, Y., Tran, U. T., Nishiyama, R., Watanabe, Y., et al. (2014). Positive regulatory role of strigolactone in plant responses to drought and salt stress. *Proc. Natl. Acad. Sci. U. S. A.* 111, 851–856. doi: 10.1073/pnas.1322135111

Hagemeier, J., Schneider, B., Oldham, N. J., and Hahlbrock, K. (2001). Accumulation of soluble and wall-bound indolic metabolites in *Arabidopsis thaliana* leaves infected with virulent or avirulent *Pseudomonas syringae* pathovar tomato strains. *Proc. Natl. Acad. Sci. U. S. A.* 98, 753–758. doi: 10.1073/pnas.98.2.753

Han, Y., Watanabe, S., Shimada, H., and Sakamoto, A. (2020). Dynamics of the leaf endoplasmic reticulum modulate β-glucosidase-mediated stress-activated ABA production from its glucosyl ester. *J. Exp. Bot.* 71, 2058–2071. doi: 10.1093/jxb/erz528

He, H., Van Breusegem, F., and Mhamdi, A. (2018). Redox-dependent control of nuclear transcription in plants. *J. Exp. Bot.* 69, 3359–3372. doi: 10.1093/jxb/ery130

Heim, K. E., Tagliaferro, A. R., and Bobilya, D. J. (2002). Flavonoid antioxidants: Chemistry, metabolism and structure-activity relationships. *J. Nutr. Biochem.* 13, 572–584. doi: 10.1016/S0955-2863(02)00208-5

Hopia, A., and Heinonen, M. (1999). Antioxidant activity of flavonol aglycones and their glycosides in methyl linoleate. *JAOCS J. Am. Oil Chem. Soc.* 76, 139–144. doi: 10.1007/s11746-999-0060-0

Hoth, S., Morgante, M., Sanchez, J. P., Hanafey, M. K., Tingey, S. V., and Chua, N. H. (2002). Genome-wide gene expression profiling in *Arabidopsis thaliana* reveals new targets of abscisic acid and largely impaired gene regulation in the *abi1-1* mutant. *J. Cell Sci.* 115, 4891–4900. doi: 10.1242/jcs.00175

Huybrechts, M., Cuypers, A., Deckers, J., Iven, V., Vandionant, S., Jozefczak, M., et al. (2019). Cadmium and plant development: An agony from seed to seed. *Int. J. Mol. Sci.* 20:3971. doi: 10.3390/ijms20163971

Islam, S., Griffiths, C. A., Blomstedt, C. K., Le, T.-N., Gaff, D. F., Hamill, J. D., et al. (2013). Increased biomass, seed yield and stress tolerance is conferred in Arabidopsis by a novel enzyme from the resurrection grass *Sporobolus stapfianus* that glycosylates the strigolactone analogue GR24. *PloS One* 8, e80035. doi: 10.1371/journal.pone.0080035

Jones, P., Messner, B., Nakajima, J.II, Schäffner, A. R., and Saito, K. (2003). UGT73C6 and UGT78D1, Glycosyltransferases Involved in Flavonol Glycoside Biosynthesis in *Arabidopsis thaliana*. *J. Biol. Chem.* 278, 43910–43918. doi: 10.1074/jbc.M303523200

Keunen, E., Peshev, D., Vangronsveld, J., Van Den Ende, W., and Cuypers, A. (2013). Plant sugars are crucial players in the oxidative challenge during abiotic stress: Extending the traditional concept. *Plant Cell Environ.* 36, 1242–1255. doi: 10.1111/pce.12061

Khorobrykh, S., Havurinne, V., Mattila, H., and Tyystjärvi, E. (2020). Oxygen and ROS in photosynthesis. *Plants* 9:91. doi: 10.3390/plants9010091

Kim, J. H., Kim, B. G., Ko, J. H., Lee, Y., Hur, H. G., Lim, Y., et al. (2006a). Molecular cloning, expression, and characterization of a flavonoid glycosyltransferase from *Arabidopsis thaliana*. *Plant Sci.* 170, 897–903. doi: 10.1016/j.plantsci.2005.12.013

Kim, J. H., Kim, B. G., Park, Y., Ko, J. H., Lim, C. E., Lim, J., et al. (2006b). Characterization of flavonoid 7-O-glucosyltransferase from *Arabidopsis thaliana*. *Biosci. Biotechnol. Biochem.* 70, 1471–1477. doi: 10.1271/bbb.60006

Kim, I. A., Heo, J. O., Chang, K. S., Lee, S. A., Lee, M. H., Lim, C. E., et al. (2010). Overexpression and inactivation of *UGT73B2* modulate tolerance to oxidative stress in *Arabidopsis*. *J. Plant Biol.* 53, 233–239. doi: 10.1007/s12374-010-9110-2

Landi, M., Tattini, M., and Gould, K. S. (2015). Multiple functional roles of anthocyanins in plant-environment interactions. *Environ. Exp. Bot.* 119, 4–17. doi: 10.1016/j.envexpbot.2015.05.012

Landry, L. G., Chapple, C. C. S., and Last, R. L. (1995). Arabidopsis mutants lacking phenolic sunscreens exhibit enhanced ultraviolet-B injury and oxidative damage. *Plant Physiol.* 109, 1159–1166. doi: 10.1104/pp.109.4.1159

Lee, K. H., Piao, H. L., Kim, H. Y., Choi, S. M., Jiang, F., Hartung, W., et al. (2006). Activation of Glucosidase via Stress-Induced Polymerization Rapidly Increases Active Pools of Abscisic Acid. *Cell* 126, 1109–1120. doi: 10.1016/j.cell.2006.07.034

Leister, D. (2019). Piecing the Puzzle Together: The Central Role of Reactive Oxygen Species and Redox Hubs in Chloroplast Retrograde Signaling. *Antioxid. Redox Signal.* 30, 1206–1219. doi: 10.1089/ars.2017.7392

Lewis, D. R., Olex, A. L., Lundy, S. R., Turkett, W. H., Fetrow, J. S., and Muday, G. K. (2013). A kinetic analysis of the auxin transcriptome reveals cell wall remodeling proteins that modulate lateral root development in Arabidopsis. *Plant Cell* 25, 3329–3346. doi: 10.1105/tpc.113.114868

Li, P., Li, Y.-J., Zhang, F.-J., Zhang, G.-Z., Jiang, X.-Y., Yu, H.-M., et al. (2017). The Arabidopsis UDP-glycosyltransferases UGT79B2 and UGT79B3, contribute to cold, salt and drought stress tolerance via modulating anthocyanin accumulation. *Plant J.* 89, 85–103. doi: 10.1111/tpj.13324

Li, Y. J., Li, P., Wang, T., Zhang, F. J., Huang, X. X., and Hou, B. K. (2018). The maize secondary metabolism glycosyltransferase UFGT2 modifies flavonols and contributes to plant acclimation to abiotic stresses. *Ann. Bot.* 122, 1203–1217. doi: 10.1093/aob/mcy123

Lim, E. K., Higgins, G. S., Li, Y., and Bowles, D. J. (2003). Regioselectivity of glucosylation of caffeic acid by a UDP-glucose:glucosyltransferase is maintained *in planta*. *Biochem. J.* 373, 987–992. doi: 10.1042/BJ20021453

Lim, E. K., Doucet, C. J., Hou, B., Jackson, R. G., Abrams, S. R., and Bowles, D. J. (2005). Resolution of (+)-abscisic acid using an *Arabidopsis* glycosyltransferase. *Tetrahedron Asymmetry* 16, 143–147. doi: 10.1016/j.tetasy.2004.11.062

Lim, C. E., Choi, J. N., Kim, I. A., Lee, S. A., Hwang, Y. S., Lee, C. H., et al. (2008). Improved resistance to oxidative stress by a loss-of-function mutation in the Arabidopsis *UGT71C1* gene. *Mol. Cells* 25, 368–375.

Liu, Z., Yan, J. P., Li, D. K., Luo, Q., Yan, Q., Liu, Z., et al. (2015). UDP-glucosyltransferase71C5, a major glucosyltransferase, mediates abscisic acid homeostasis in Arabidopsis. *Plant Physiol.* 167, 1659–1670. doi: 10.1104/pp.15.00053

Ludwig-Müller, J. (2011). Auxin conjugates: their role for plant development and in the evolution of land plants. *J. Exp. Bot.* 62, 1757–1773. doi: 10.1093/jxb/erq412

Lv, M. J., Wan, W., Yu, F., and Meng, L. S. (2019). New Insights into the Molecular Mechanism Underlying Seed Size Control under Drought Stress. *J. Agric. Food Chem.* 67, 9697–9704. doi: 10.1021/acs.jafc.9b02497

Maruri-López, I., Aviles-Baltazar, N. Y., Buchala, A., and Serrano, M. (2019). Intra and extracellular journey of the phytohormone salicylic acid. *Front. Plant Sci.* 10:423:423. doi: 10.3389/fpls.2019.00423

Maruta, T., Noshi, M., Nakamura, M., Matsuda, S., Tamoi, M., Ishikawa, T., et al. (2014). Ferulic acid 5-hydroxylase 1 is essential for expression of anthocyanin biosynthesis-associated genes and anthocyanin accumulation under photooxidative stress in *Arabidopsis*. *Plant Sci.* 219–220, 61–68. doi: 10.1016/j.plantsci.2014.01.003

Mi, H., Muruganujan, A., Ebert, D., Huang, X., and Thomas, P. D. (2019). PANTHER version 14: More genomes, a new PANTHER GO-slim and improvements in enrichment analysis tools. *Nucleic Acids Res.* 47, D419–D426. doi: 10.1093/nar/gky1038

Montoro, P., Braca, A., Pizza, C., and De Tommasi, N. (2005). Structure-antioxidant activity relationships of flavonoids isolated from different plant species. *Food Chem.* 92, 349–355. doi: 10.1016/j.foodchem.2004.07.028

Nakabayashi, R., Yonekura-Sakakibara, K., Urano, K., Suzuki, M., Yamada, Y., Nishizawa, T., et al. (2014). Enhancement of oxidative and drought tolerance in Arabidopsis by overaccumulation of antioxidant flavonoids. *Plant J.* 77, 367–379. doi: 10.1111/tpj.12388

Nambara, E., and Marion-Poll, A. (2005). Abscisic acid biosynthesis and catabolism. *Annu. Rev. Plant Biol.* 56, 165–185. doi: 10.1146/annurev.arplant.56.032604.144046

Naoumkina, M., and Dixon, R. A. (2008). Subcellular localization of flavonoid natural products: A signaling function? *Plant Signal. Behav.* 3, 573–575. doi: 10.4161/psb.3.8.5731

Niculaes, C., Morreel, K., Kim, H., Lu, F., McKee, L. S., Ivens, B., et al. (2014). Phenylcoumaran Benzylic Ether Reductase Prevents Accumulation of Compounds Formed under Oxidative Conditions in Poplar Xylem. *Plant Cell* 26, 3775–3791. doi: 10.1105/tpc.114.125260

Noctor, G., Mhamdi, A., and Foyer, C. H. (2014). The roles of reactive oxygen metabolism in drought: Not so cut and dried. *Plant Physiol.* 164, 1636–1648. doi: 10.1104/pp.113.233478

Noctor, G., Mhamdi, A., and Foyer, C. H. (2016). Oxidative stress and antioxidative systems: recipes for successful data collection and interpretation. *Plant Cell Environ.* 39, 1140–1160. doi: 10.1111/pce.12726

Noctor, G., Reichheld, J. P., and Foyer, C. H. (2018). ROS-related redox regulation and signaling in plants. *Semin. Cell Dev. Biol.* 80, 3–12. doi: 10.1016/j.semcdb.2017.07.013

Okazawa, A., Kusunose, T., Ono, E., Kim, H. J., Satake, H., Shimizu, B.II, et al. (2014). Glucosyltransferase activity of *Arabidopsis* UGT71C1 towards pinoresinol and lariciresinol. *Plant Biotechnol.* 31, 561–566. doi: 10.5511/plantbiotechnology.14.0910a

Pan, R., Liu, J., Wang, S., and Hu, J. (2020). Peroxisomes: versatile organelles with diverse roles in plants. *New Phytol.* 225, 1410–1427. doi: 10.1111/nph.16134

Paniagua, C., Bilkova, A., Jackson, P., Dabravolski, S., Riber, W., Didi, V., et al. (2017). Dirigent proteins in plants: modulating cell wall metabolism during abiotic and biotic stress exposure. *J. Exp. Bot.* 68, 3287–3301. doi: 10.1093/jxb/erx141

Pérez, F. J., Villegas, D., and Mejia, N. (2002). Ascorbic acid and flavonoid-peroxidase reaction as a detoxifying system of H2O2 in grapevine leaves. *Phytochemistry* 60, 573–580. doi: 10.1016/S0031-9422(02)00146-2

Piotrowska, A., and Bajguz, A. (2011). Conjugates of abscisic acid, brassinosteroids, ethylene, gibberellins, and jasmonates. *Phytochemistry* 72, 2097–2112. doi: 10.1016/J.PHYTOCHEM.2011.08.012

Pospíšil, P., and Prasad, A. (2014). Formation of singlet oxygen and protection against its oxidative damage in Photosystem II under abiotic stress. *J. Photochem. Photobiol. B Biol.* 137, 39–48. doi: 10.1016/j.jphotobiol.2014.04.025

Pospíšil, P., and Yamamoto, Y. (2017). Damage to photosystem II by lipid peroxidation products. *Biochim. Biophys. Acta - Gen. Subj.* 1861, 457–466. doi: 10.1016/j.bbagen.2016.10.005

Pourcel, L., Routaboul, J. M., Cheynier, V., Lepiniec, L., and Debeaujon, I. (2007). Flavonoid oxidation in plants: from biochemical properties to physiological functions. *Trends Plant Sci.* 12, 29–36. doi: 10.1016/j.tplants.2006.11.006

Rehman, H. M., Nawaz, M. A., Shah, Z. H., Ludwig-Müller, J., Chung, G., Ahmad, M. Q., et al. (2018). Comparative genomic and transcriptomic analyses of Family-1 UDP glycosyltransferase in three Brassica species and Arabidopsis indicates stress-responsive regulation. *Sci. Rep.* 8, 1875. doi: 10.1038/s41598-018-19535-3

Rice-Evans, C. A., Miller, N. J., and Paganga, G. (1996). Structure-antioxidant activity relationships of flavonoids and phenolic acids. *Free Radic. Biol. Med.* 20, 933–956. doi: 10.1016/0891-5849(95)02227-9

Saslowsky, D. E., Warek, U., and Winkel, B. S. J. (2005). Nuclear localization of flavonoid enzymes in *Arabidopsis*. *J. Biol. Chem.* 280, 23735–23740. doi: 10.1074/jbc.M413506200

Schützendübel, A., and Polle, A. (2002). Plant responses to abiotic stresses: Heavy metal-induced oxidative stress and protection by mycorrhization. *J. Exp. Bot.* 53, 1351–1365. doi: 10.1093/jxb/53.372.1351

Selmar, D., and Kleinwächter, M. (2013). Stress enhances the synthesis of secondary plant products: The impact of stress-related over-reduction on the accumulation of natural products. *Plant Cell Physiol.* 54, 817–826. doi: 10.1093/pcp/pct054

Shi, Y., Phan, H., Liu, Y., Cao, S., Zhang, Z., Chu, C., et al. (2020). Glycosyltransferase OsUGT90A1 helps protect the plasma membrane during chilling stress in rice. *J. Exp. Bot.* 71, 2723–2739. doi: 10.1093/jxb/eraa025

Simon, C., Langlois-Meurinne, M., Didierlaurent, L., Chaouch, S., Bellvert, F., Massoud, K., et al. (2014). The secondary metabolism glycosyltransferases UGT73B3 and UGT73B5 are components of redox status in resistance of Arabidopsis to *Pseudomonas syringae* pv. *tomato*. *Plant Cell Environ.* 37, 1114–1129. doi: 10.1111/pce.12221

Smirnoff, N., and Arnaud, D. (2019). Hydrogen peroxide metabolism and functions in plants. *New Phytol.* 221, 1197–1214. doi: 10.1111/nph.15488

Sun, Y.-G., Wang, B., Jin, S.-H., Qu, X.-X., Li, Y.-J., and Hou, B.-K. (2013). Ectopic Expression of Arabidopsis Glycosyltransferase *UGT85A5* Enhances Salt Stress Tolerance in Tobacco. *PloS One* 8, e59924. doi: 10.1371/journal.pone.0059924

Sun, G., Strebl, M., Merz, M., Blamberg, R., Huang, F., McGraphery, K., et al. (2019). Glucosylation of the phytoalexin *N* -feruloyl tyramine modulates the levels of pathogen-responsive metabolites in *Nicotiana benthamiana*. *Plant J.* 100, 20–37. doi: 10.1111/tpj.14420

Taguchi, G., Fujikawa, S., Yazawa, T., Kodaira, R., Hayashida, N., Shimosaka, M., et al. (2000). Scopoletin uptake from culture medium and accumulation in the vacuoles after conversion to scopolin in 2,4-D-treated tobacco cells. *Plant Sci.* 151, 153–161. doi: 10.1016/S0168-9452(99)00212-5

Takahashi, F., Suzuki, T., Osakabe, Y., Betsuyaku, S., Kondo, Y., Dohmae, N., et al. (2018). A small peptide modulates stomatal control via abscisic acid in long-distance signaling. *Nature* 556, 235–238. doi: 10.1038/s41586-018-0009-2

Tiwari, P., Sangwan, R. S., and Sangwan, N. S. (2016). Plant secondary metabolism linked glycosyltransferases: An update on expanding knowledge and scopes. *Biotechnol. Adv.* 34, 714–739. doi: 10.1016/j.biotechadv.2016.03.006

Tognetti, V. B., van Aken, O., Morreel, K., Vandenbroucke, K., van de Cotte, B., de Clercq, I., et al. (2010). Perturbation of indole-3-butyric acid homeostasis by the UDP-glucosyltransferase UGT74E2 modulates Arabidopsis architecture and water stress tolerance. *Plant Cell* 22, 2660–2679. doi: 10.1105/tpc.109.071316

Vaahtera, L., Brosché, M., Wrzaczek, M., and Kangasjärvi, J. (2014). Specificity in ROS signaling and transcript signatures. *Antioxid. Redox Signal.* 21, 1422–1441. doi: 10.1089/ars.2013.5662

Verma, V., Ravindran, P., and Kumar, P. P. (2016). Plant hormone-mediated regulation of stress responses. *BMC Plant Biol.* 16:86. doi: 10.1186/s12870-016-0771-y

Wang, Y., and Frei, M. (2011). Stressed food – The impact of abiotic environmental stresses on crop quality. *Agric. Ecosyst. Environ.* 141, 271–286. doi: 10.1016/J.AGEE.2011.03.017

Wang, L., Wang, B., Yu, H., Guo, H., Lin, T., Kou, L., et al. (2020). Transcriptional regulation of strigolactone signalling in *Arabidopsis*. *Nature* 583, 277–281. doi: 10.1038/s41586-020-2382-x

Waszczak, C., Carmody, M., and Kangasjärvi, J. (2018). Reactive Oxygen Species in Plant Signaling. *Annu. Rev. Plant Biol.* 69, 209–236. doi: 10.1146/annurev-arplant-042817-040322

Xie, X., He, Z., Chen, N., Tang, Z., Wang, Q., and Cai, Y. (2019). The Roles of Environmental Factors in Regulation of Oxidative Stress in Plant. *BioMed. Res. Int.* 2019:9732325. doi: 10.1155/2019/9732325

Xing, F., Li, Z., Sun, A., and Xing, D. (2013). Reactive oxygen species promote chloroplast dysfunction and salicylic acid accumulation in fumonisin B1-induced cell death. *FEBS Lett.* 587, 2164–2172. doi: 10.1016/j.febslet.2013.05.034

Xu, Z. Y., Lee, K. H., Dong, T., Jeong, J. C., Jin, J. B., Kanno, Y., et al. (2012). A vacuolar β-Glucosidase homolog that possesses glucose-conjugated abscisic acid hydrolyzing activity plays an important role in osmotic stress responses in *Arabidopsis*. *Plant Cell* 24, 2184–2199. doi: 10.1105/tpc.112.095935

Yamasaki, H., Sakihama, Y., and Ikehara, N. (1997). Flavonoid-peroxidase reaction as a detoxification mechanism of plant cells against H2O2. *Plant Physiol.* 115, 1405–1412. doi: 10.1104/pp.115.4.1405

Yazaki, K., Arimura, G., and Ohnishi, T. (2017). 'Hidden' terpenoids in plants: their biosynthesis, localization and ecological roles. *Plant Cell Physiol.* 50, 1615–1621. doi: 10.1093/pcp/pcx123

Yildiztugay, E., Ozfidan-Konakci, C., Kucukoduk, M., and Turkan, I. (2020). Flavonoid Naringenin Alleviates Short-Term Osmotic and Salinity Stresses Through Regulating Photosynthetic Machinery and Chloroplastic Antioxidant Metabolism in *Phaseolus vulgaris*. *Front. Plant Sci.* 11:682:682. doi: 10.3389/fpls.2020.00682

Yonekura-Sakakibara, K., and Hanada, K. (2011). An evolutionary view of functional diversity in family 1 glycosyltransferases. *Plant J.* 66, 182–193. doi: 10.1111/j.1365-313X.2011.04493.x

Yonekura-Sakakibara, K., Tohge, T., Matsuda, F., Nakabayashi, R., Takayama, H., Niida, R., et al. (2008). Comprehensive flavonol profiling and transcriptome coexpression analysis leading to decoding gene-metabolite correlations in *Arabidopsis*. *Plant Cell* 20, 2160–2176. doi: 10.1105/tpc.108.058040

Zhang, X., and Liu, C.-J. (2015). Multifaceted Regulations of Gateway Enzyme Phenylalanine Ammonia-Lyase in the Biosynthesis of Phenylpropanoids. *Mol. Plant* 8, 17–27. doi: 10.1016/J.MOLP.2014.11.001

Zhang, Y., Cichewicz, R. H., and Nair, M. G. (2004). Lipid peroxidation inhibitory compounds from daylily (*Hemerocallis fulva*) leaves. *Life Sci.* 75, 753–763. doi: 10.1016/j.lfs.2004.03.002

Zhao, Y., Ma, Q., Jin, X., Peng, X., Liu, J., Deng, L., et al. (2014). A Novel Maize Homeodomain–Leucine Zipper (HD-Zip) I Gene, *Zmhdz10*, Positively Regulates Drought and Salt Tolerance in Both Rice and Arabidopsis. *Plant Cell Physiol.* 55, 1142–1156. doi: 10.1093/pcp/pcu054

Zhao, M., Jin, J., Gao, T., Zhang, N., Jing, T., Wang, J., et al. (2019). Glucosyltransferase CsUGT78A14 Regulates Flavonols Accumulation and Reactive Oxygen Species Scavenging in Response to Cold Stress in Camellia sinensis. *Front. Plant Sci.* 10:1675:1675. doi: 10.3389/fpls.2019.01675

Zhao, M., Zhang, N., Gao, T., Jin, J., Jing, T., Wang, J., et al. (2020). Sesquiterpene glucosylation mediated by glucosyltransferase UGT91Q2 is involved in the modulation of cold stress tolerance in tea plants. *New Phytol.* 226, 362–372. doi: 10.1111/nph.16364

Zheng, Y. Z., Deng, G., Liang, Q., Chen, D. F., Guo, R., and Lai, R. C. (2017). Antioxidant activity of quercetin and its glucosides from propolis: A theoretical study. *Sci. Rep.* 7, 7543. doi: 10.1038/s41598-017-08024-8

Conflict of Interest: The authors declare that the research was conducted in the absence of any commercial or financial relationships that could be construed as a potential conflict of interest.

frontiers in Plant Science

REVIEW
published: 23 September 2020
doi: 10.3389/fpls.2020.571288

Thioredoxin Network in Plant Mitochondria: Cysteine S-Posttranslational Modifications and Stress Conditions

María Carmen Martí, Ana Jiménez and Francisca Sevilla *

Abiotic Stress, Production and Quality Laboratory, Department of Stress Biology and Plant Pathology, Centre of Edaphology and Applied Biology of Segura, Spanish National Research Council, Murcia, Spain

Plants are sessile organisms presenting different adaptation mechanisms that allow their survival under adverse situations. Among them, reactive oxygen and nitrogen species (ROS, RNS) and H_2S are emerging as components not only of cell development and differentiation but of signaling pathways involved in the response to both biotic and abiotic attacks. The study of the posttranslational modifications (PTMs) of proteins produced by those signaling molecules is revealing a modulation on specific targets that are involved in many metabolic pathways in the different cell compartments. These modifications are able to translate the imbalance of the redox state caused by exposure to the stress situation in a cascade of responses that finally allow the plant to cope with the adverse condition. In this review we give a generalized vision of the production of ROS, RNS, and H_2S in plant mitochondria. We focus on how the principal mitochondrial processes mainly the electron transport chain, the tricarboxylic acid cycle and photorespiration are affected by PTMs on cysteine residues that are produced by the previously mentioned signaling molecules in the respiratory organelle. These PTMs include S-oxidation, S-glutathionylation, S-nitrosation, and persulfidation under normal and stress conditions. We pay special attention to the mitochondrial Thioredoxin/Peroxiredoxin system in terms of its oxidation-reduction posttranslational targets and its response to environmental stress.

Keywords: abiotic stress, mitochondria, persulfidation, redox regulation, S-glutathionylation, S-nitrosation, S-oxidation, thioredoxin

OPEN ACCESS

Edited by:
José Manuel Palma, Consejo Superior de Investigaciones Científicas (CSIC), Spain

Reviewed by:
Cecilia Gotor, Institute of Plant Biochemistry and Photosynthesis (IBVF), Spain
Irene García, Institute of Plant Biochemistry and Photosynthesis (IBVF), Spain

***Correspondence:**
Francisca Sevilla
fsevilla@cebas.csic.es

Specialty section:
This article was submitted to Plant Metabolism and Chemodiversity, a section of the journal Frontiers in Plant Science

Received: *10 June 2020*
Accepted: *08 September 2020*
Published: *23 September 2020*

Citation:
Martí MC, Jiménez A and Sevilla F (2020) Thioredoxin Network in Plant Mitochondria: Cysteine S-Posttranslational Modifications and Stress Conditions. Front. Plant Sci. 11:571288. doi: 10.3389/fpls.2020.571288

INTRODUCTION

Reactive oxygen species (ROS) are considered unavoidable byproducts of aerobic metabolism. Mitochondria play a pivotal role in plant cells providing the energy in the form of adenosine triphosphate (ATP) during oxidative phosphorylation, but also providing intermediates of the tricarboxylic acid cycle (TCA) for major biosynthetic pathways. Mitochondria are also one of the main cellular ROS source but also a source and a target of nitric oxide (NO) and derived reactive nitrogen species (RNS) (Foyer and Noctor, 2013; Lázaro et al., 2013; Albert et al., 2017; Jayawardhane et al., 2020). Balanced ROS and RNS production and scavenging is an essential characteristic of mitochondrial function for ensuring cellular growth and plant maintenance. Local

changes of ROS and RNS homeostasis mediate downstream signaling events *via* interactions with individual proteins and signaling. Similar to ROS and RNS, a new player in mitochondrial signaling is H_2S (Filipovic and Jovanović, 2017). Proteins sense redox changes and transmit information by posttranslational modifications (PTMs) of cysteine sensitive thiols, which are oxidized to proteins disulfide, trisulfides, sulfenic, sulfinic or sulfonic acid derivates, as well as S-glutathionylated and S-nitrosated forms. Additionally, H_2S does not spontaneously react with reduced thiol groups but it can react with oxidized ones leading to protein persulfidation (Sevilla et al., 2015a; Wang et al., 2018; Huang et al., 2019).

In the process of ROS elimination and redox signal integration, mitochondria contain antioxidants enzymes such as Mn-superoxide dismutase (Mn-SOD) and ascorbate dependent peroxidase (APX) (Jiménez et al., 1997; Chew et al., 2003) as well as redox sensitive proteins, which are classified into two classes: redox sensors, including peroxiredoxin (PRX) and glutathione peroxidase-like (GPXL) and redox transmitters, containing thioredoxin (TRX) and glutaredoxin (GRX). However, in contrast to that occurring in plastids, cytosol, and nucleus, the TRX/PRX and glutathione/GRX systems are not very well studied in mitochondria. The scarce information about TRX/PRX system in mitochondria is striking, taking into account that posttranscriptional/translational regulation is a likely determinant of the mitochondrial stress response as well as the role of this redox system as sensor and initiator of signaling cascades in a variety of processes and stress conditions (Sevilla et al., 2015a; Zannini et al., 2018).

This review is focused on summarizing the information about ROS, RNS and H_2S dependent mitochondrial PTMs, as regulatory mechanisms of plant mitochondria function under normal and stress conditions. We focus on the main enzymes from the major biological processes occurring in the mitochondria such us the ETC, the TCA and photorespiration and on how PTMs affecting cysteine residues (S-oxidation, S-glutathionylation, S-nitrosation, and persulfidation) exert their regulatory mechanisms on plant mitochondrial enzymes. We pay special attention to the mitochondrial TRX/PRX system in terms of its posttranslational control and its response to environmental stress.

MITOCHONDRIAL ROS, RNS, AND H_2S GENERATION

ROS Generation in Mitochondria

Oxygen is essential for the aerobic life and due to its chemical feature as a molecule containing two unpaired electrons it can suffer monovalent reduction generating ROS with a bimodal action. Their beneficial aspects are related to the effect on the cellular redox state and the role in signaling cascades while their detrimental aspect is related to an overproduction or insufficient endogenous antioxidant defenses which can damage all kind of cellular structures leading, in the worst case scenario, to cell death (Mhamdi and Van Breusegem, 2018). As signaling molecules, ROS have a special importance during developmental and physiological processes in plants. A redox compartmentalization exists for a proper function of ROS-dependent signaling pathways and ROS production, which depend on the reaction with other reactive species and interaction with antioxidants and scavengers (Waszczak et al., 2018; Foyer et al., 2020). Mitochondria generate energy in form of ATP by oxidative phosphorylation during glucose metabolism, a process coupled with mitochondrial respiration through a generated transmembrane potential *via* mitochondrial complexes I to IV of the electron transport chain (ETC), with the final result of the four-electron reduction of O_2 to H_2O. ROS are generated as byproducts after electron leaking at complex I and III (Hernández et al., 1993; Noctor et al., 2007) and under specific conditions at complex II during the reverse electron transport (Turrens, 2003). Thus, ROS such as superoxide anion ($O_2^{\cdot-}$), hydrogen peroxide (H_2O_2) and hydroxyl radical ($HO^{\cdot}$) are generated after one, two and three-electron reduction, respectively. A role for complex II in H_2O_2 production has been reported to be even more important that complex I with a special influence under stress conditions, and also ubiquinone pool might serve as ROS site in plant mitochondria (Umbach et al., 2005; Gleason et al., 2011). A high proportion of NADH/NAD^+ and/or ADP/ATP can increase the electron transport contributing to a high membrane potential, which is correlated to a higher reduction of the ETC components, increasing the probability of electron leakage to O_2 and thus increasing ROS production. In the presence of transition metal ions, the more reactive $HO^{\cdot}$ is formed. The $O_2^{\cdot-}$ generated in the mitochondrial matrix is rapidly dismutated to H_2O_2 by Mn-SOD contributing to the ROS production in the organelle. This H_2O_2 is scavenged by APX (Jiménez et al., 1997; Jiménez et al., 1998) and PRXIIF (Barranco-Medina et al., 2007). The plant ETC contains other enzymes which do not contribute to the proton gradient and act as security oxidation valves limiting ROS production: type II NAD(P)H-dehydrogenases can avoid the electron transport from complex I and II to ubiquinone while alternative oxidase (AOX) couples the ubiquinol oxidation to the O_2 reduction to water and dissipation of energy in form of heat (Rasmusson and Wallström, 2010; Del-Saz et al., 2017). The increased and/or decreased expression of AOX along with the inhibition of its activity, have been considered as important factors in the establishment of the mitochondrial generation of ROS in signal transduction pathways (Vishwakarma et al., 2015) with the induction of AOX described as a mitochondrial retrograde signaling model (Maxwell et al., 1999; Lázaro et al., 2013). Evidences obtained with respiratory inhibitors and/or mutants have shown that fully functional mitochondria are also determinant for optimal photosynthesis. That dependency was linked to both cytochrome c oxidase (COX) and AOX pathway as well as to uncoupled protein (UCP) activity, which may modify the oxidation rate of ETC substrates by an increase of ubiquinol oxidation when the electrochemical proton gradient decreases across the inner membrane (Millar et al., 2011). Together with AOX, the terminal enzyme of ascorbate (ASC) biosynthesis, L-galactone-1,4-lactone dehydrogenase (GLDH), has been described to be a dual-function enzyme as structural assembly

factor of complex I and as associated to the cytochrome respiratory pathway (Schimmeyer et al., 2016; Rodríguez-Ruiz et al., 2017) allowing the synthesis of ASC when coupled as an alternative electron donor for the respiratory chain. In this way, this protein may have an specific role under conditions of possible inhibition of components of the TCA as occurring under oxidative stress (Dumont and Rivoal, 2019). Interestingly, the last step of ASC biosynthesis does not produce H_2O_2 as it happens in animals where the activity is carried out by an oxidase instead of a dehydrogenase, altering the cellular redox state (reviewed by Fenech et al., 2019).

RNS Generation in Mitochondria

Nitric oxide (NO) refers to its nitrosyl radical ($^{\cdot}NO$). In many species, including plants, NO is a key signalling molecule that plays a role in a large number of biological processes (Kolbert et al., 2019) due to its chemistry. Reactive nitrogen species (RNS) are a family of molecules derived from NO, such as S-nitrosothiols (SNOs), S-nitrosoglutathione (GSNO), peroxynitrite (ONOO-), nitrogen dioxide (NO_2), and nitro-fatty acids (NO_2-FA), among others (Romero-Puertas et al., 2008; Martínez-Ruiz et al., 2013; Mata-Pérez et al., 2017).

In mitochondria both, an oxidative and a reductive pathway have been described for the NO generation. Regarding the oxidative route involving an L-Arg-dependent NOS-like activity, a mitochondrial Arabidopsis NO synthase 1 (AtNOS1) implicated in mitochondrial biogenesis was identified (Guo and Crawford, 2005). However, this enzyme was later on characterized as a small GTPase and not a NO synthase, being renamed as AtNOA1 (nitric oxide associated 1). In contrast to animals, a NOS-like enzyme has not been identified in plants (Astier et al., 2018; Kolbert et al., 2019). The reductive route of NO generation is dependent on nitrite and occurs in the inner membrane probably *via* cytochrome c oxidase (CCO) and/or reductase, generating ATP under hypoxia (Jayawardhane et al., 2020). Using different inhibitors, the involvement of the respiratory chain mainly complex III, CCO, and AOX was later reported although with clear results for CCO again under hypoxia (Gupta and Igamberdiev, 2016). The NO generated, can accept or loose an electron to generate nitrosyl anion (NO^-) or the nitrosonium cation (NO^+) or other RNS including higher oxides such as NO_2 and N_2O_3, or it can react immediately with superoxide originated from ETC, to form peroxynitrite (ONOO–) (Leitner et al., 2009). NO can also react with GSH to form GSNO, considered as an *in vivo* reservoir of NO.

H_2S Generation in Mitochondria

Sulfur is an essential macronutrient, taken up as sulfate and assimilated into cysteine. Volatile H_2S is an inflammable gas considered as a pollutant but also as a new signaling molecule in both plants and animals (Filipovic and Jovanović, 2017). In plants it has been involved in multiple processes including response to abiotic stresses, regulation of photosynthesis, stomatal closure or autophagy (Aroca et al., 2018; Zhou et al., 2020). Opposite to ROS and RNS, H_2S does not spontaneously react with reduced thiol groups, but it can react with oxidized ones leading to protein S-sulfhydration (now named persulfidation) (Paul and Snyder, 2012; Dumont and Rivoal, 2019). The increasing interest on H_2S resides, among others, in that when administered exogenously, it has a positive effect in regulating plants adaptation (Zhang et al., 2009; Jin et al., 2017; Aroca et al., 2018), although the mechanism is not fully understood.

In plant systems, H_2S is generated mainly in chloroplasts *via* the photosynthetic sulfate-assimilation pathway (García et al., 2015) although in mitochondria, the enzyme cyanoalanine synthase c1 (CAS-C1) also generates sulfide (Álvarez et al., 2012). Other enzymes described in mitochondria are certain desulfydrases which decomposes D/L-cysteine into pyruvate, H_2S, and NH_3 (Riemenschneider et al., 2005).

POST-TRASLATIONAL MODIFICATIONS AFFECTING CYSTEINE RESIDUES: S-OXIDATION, S-GLUTATHIONYLATION, S-NITROSATION, AND PERSULFIDATION

S-Oxidation

The –SH group of cysteine has a pKa of about 8.3 in free amino acids. However, in oxidoreductases proteins, such as TRXs and glutaredoxins (GRXs) this pKa is lower, because it is affected by the surrounding micro-environment (Mailloux et al., 2014). Therefore, the –SH group of this type of cysteine residues will appear predominantly as more reactive thiolate and will react with close -SH groups to form a disulfide bridge (Meyer et al., 2012; Sevilla et al., 2015a). Additionally, –SH cysteine residues will suffer different oxidation states in response to redox signals mediates by ROS (**Figure 1**).

The key player ROS that provokes oxidative reactions is H_2O_2, due to three main characteristics: reactivity with cysteine, prolonged half-life relative to other ROS, and capacity to diffuse through membranes. The significance of the oxidation produced by H_2O_2 on cysteine residues depends on the levels of H_2O_2. At high levels of H_2O_2, proteins can be oxidized irreversibly and lost their ability to function. Thus, H_2O_2 levels are tightly controlled by antioxidant systems to avoid overoxidation of functional proteins. In this sense, enzymes as catalase, multiple Cys-based peroxidases including PRXs, GPX, and those enzymes of ASC-GSH cycle, exert a fine control of H_2O_2 cellular levels (Dietz, 2011; Foyer and Noctor, 2011; Lázaro et al., 2013).

As the levels of H_2O_2 rise, it oxidizes the thiolate anion of protein cysteine residues to the sulfenic form (Cys–SOH). The sulfenic form can form an intra-or intermolecular disulfide bond by reaction with a neighboring thiolate or can be reduced and reverted to the thiolate form. A typical example of this kind of protein is the PRX, which by the action of TRXs and/or GRXs can be converted back to the reduced thiol group (Dietz, 2011; Sevilla et al., 2015a). Cysteine residues involved in dithiol-disulfide redox exchange frequently are located at catalytic sites of enzymes or are cysteines involved in metal binding and usually show a high degree of conservation. This dithiol-disulfide

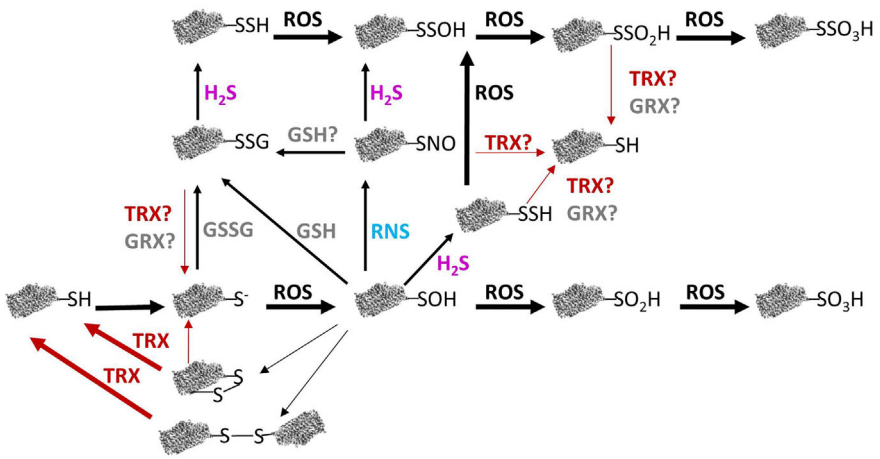

FIGURE 1 | Relation between redox modifications of protein cysteine thiols and their reversibility in plant mitochondria. Reactive oxygen species (ROS)-mediated oxidation of protein thiols leads to different redox modifications. Reactive nitrogen species (RNS) can produce S-nitrosation of cysteine residues and GSH and GSSG provoke S-glutathionylation whereas H_2S can lead to persulfidation. Some of these modifications may be reversed by TRX or GRX (see text for details). GRX, glutaredoxin; GSH, reduced glutathione; GSSG, oxidized glutathione; H_2S, hydrogen sulfide; RNS, reactive nitrogen species; ROS, reactive oxygen species; R-S–, thiolate anion; R-SH, reduced thiol; R-SNO, S-nitrosation; R-SOH, sulfenic acid; RO_2H, sulfinic acid; RO_3H, sulfonic acid; R-SSG, S-glutathionylation; R-SSH, persulfidation; R-SSOH, persulfenic acid; R-SSO_2H, persulfonic acid; R-SSO_3H, persulfinic acid; R-SS-R, disulfide bond; TRX, thioredoxin.

modification is transient and can act as a molecular switch altering protein activity, conformation, subcellular localization, and/or binding properties (Van Ruyskensvelde et al., 2018). In fact, protein cysteine sulfenylation is considered to play a key role in sensing and redox signalling (Huang et al., 2019). Alternatively, Cys–SOH can react with low-molecular weight thiols, such as GSH, to form S-glutathionylated disulfides. If the levels of H_2O_2 increases, the sulfenic form can suffer two more oxidation steps and become sulfinic (SO_2H) or sulfonic (SO_3H) species. The sulfinic form can be reduced by sulfiredoxin (SRX) through an ATP-dependent reaction (Iglesias-Baena et al., 2011), however the hyperoxidized sulfonic form, to date, has been shown to be irreversible (**Figure 1**).

S-Glutathionylation

The presence of GSH in plant mitochondria (Jiménez et al., 1997; Fernández-García et al., 2009; Foyer and Noctor, 2011) allows the posttranslational modification (PTM) of proteins *via* reversible S-glutathionylation of protein cysteine residues. S-glutathionylation can occur by spontaneous disulfide bond formation between the cysteine sulfenic form and GSH or a thiolate form derived from a reduced cysteine with GSSG, being the extend of the reactions dependent on the GSH/GSSG ratio in mitochondria, which is usually high in normal conditions (Dumont and Rivoal, 2019) (**Figure 1**). S-glutathionylation can be considered as a defense mechanism against the overoxidation of cysteine residues during oxidative stress that decreases the GSH/GSSG ratio (Zechmann, 2014; Sevilla et al., 2015b). After glutathionylation, disulfide bonds may be formed with another protein thiol and both forms can be reversed by GSH, GRX, or TRX as it has been described in animal systems (Beer et al., 2004) (**Figure 1**). In plants, several TRXs *h* present a de-glutathionylation activity although with a lower efficiency than GRXs as demonstrated for Arabidopsis cytosolic glyceraldehyde-3-phosphate dehydrogenase (Bedhomme et al., 2012), explaining the absence of GRX in plant mitochondria with de-glutathionylation activity (Zannini et al., 2018). In fact, mitochondrial TRX *h* undergoes glutationylation and the thiolation alters its redox potential as identified by MS (Gelhaye et al., 2004).

S-Nitrosation

The presence of RNS in mitochondria and the PTMs that they produce, allow mitochondria to be involved in many biological processes. RNS exert their role mainly by protein tyrosine nitration, metal nitrosylation and S-nitrosation (Romero-Puertas et al., 2008; Camejo et al., 2013; Corpas et al., 2013; Camejo et al., 2015; Lamotte et al., 2015). Tyrosine nitration is mediated by ONOO- and NO_2 which are generated respectively, by reaction of $O_2^{\cdot-}$ and O_2 with NO. During this process, a 3-nitrotyrosine group is produced by addition of a nitro group at the ortho position of the phenolic group of tyrosine (Ischiropoulos et al., 1992). During metal nitrosylation, NO binds to transition metals in metalloproteins (Keilin and Hartree, 1937). Finally, the most important pathway by which RNS execute their action is by protein S-nitrosylation. S-nitrosylation can occur by different mechanisms depending of the NO source, all of them resulting in the addition of a NO group to a cysteine residue in the target protein (**Figure 1**). During S-nitrosation, the S-nitrosothiol can be formed through NO reaction with thiyl radicals formed from one electron oxidation of thiolates *via* NO_2 or NO_2 and NO can react to form N_2O_3, which reacts with the cysteine thiolate (Hess et al., 2005). Additionally, S-nitrosation can occur *via*

trans-nitrosylation, by which an S-nitrosylated group transfers its NO to another thiolate group or to GSH to form the NO reservoir GSNO, which in turn can also transfer its NO to S-nitrosylate proteins or its GSH to S-glutationylate proteins. In fact, GSNO is a mobile NO pool which effectively transduces NO signalling. To do that, GNSO levels are tightly controlled by its production and degradation. Previously we mentioned that GSNO is formed by the transfer of NO to GSH. GSNO degradation can be *via* non-enzymatic and *via* GSNO reductase (GSNOR) enzymatic activity (Lindermayr, 2018). S-nitrosylation and therefore, GSNOR, can regulate a large amount of cellular functions and signaling events due to the capacity of alter the activity, stability, conformation, interactions with other molecules or subcellular localization of the S-nitrosated proteins, playing an essential role to protect cells under nitrosative stress (Sevilla et al., 2015a; Romero-Puertas and Sandalio, 2016; Corpas et al., 2019a).

Persulfidation

H_2S can exert its function through persulfidation, a PTM affecting the thiol group of cysteine (-SH) in proteins to be modified into a persulfide group (-SSH) (Gotor et al., 2019; Sandalio et al., 2019). H_2S reacts with either disulfides or sulfenic acids to yield persulfides which are highly reactive to ROS, being oxidized to perthiosulfenic acids (–SSOH), perthiosulfinic ($–SSO_2H$), and perthiosulfonic ($–SSO_3H$) acids (**Figure 1**). Oxidized persulfides, can be then reduced back to their thiol forms by TRXs or GRXs (Wedmann et al., 2016; Zhou et al., 2020), so the presence in plant mitochondria of TRX*o*1 (Martí et al., 2009) may be a key component of the action of this PTM in the organelle, allowing the recycling and reusing of H_2S by the cell.

MITOCHONDRIAL TARGETS OF S-OXIDATION, S-GLUTATHIONYLATION, S-NITROSYLATION, AND PERSUFIDATION

In this review, we focus on the cysteine S-oxidation described for mitochondrial TRX targets and other cysteine PTMs that affect those proteins and/or proteins that are key players in the TCA, the ETC and photorespiration (**Figures 2**, **3**).

Targets of S-Oxidation

TRXs are small ubiquitous proteins with a conserved CPGC motif in the active center enabling the reduction of disulfides bonds of specific target proteins through a dithiol-disulfide exchange mechanism. In Arabidopsis, at least 20 *TRX* genes have been reported, classified into eight subgroups (*f, h, m, o, s, x, y*, and z-type) (Alkhalfioui et al., 2008; Meyer et al., 2012). The mitochondrial TRX isoforms belong to the TRX*h* and TRX*o* groups. The presence of TRX and NADPH-TRX reductase (NTR) activities was initially detected in plant mitochondria (Marcus et al., 1991; Konrad et al., 1996), but the native proteins were not identified and characterized. Laloi et al. (2001) identified *AtTRX-o1* and *AtTRX-o2* genes encoding two TRX*o* isoforms in Arabidopsis, being TRX*o*1 unequivocally present in mitochondria whereas the TRX*o*2 cellular location is still not clear (Zannini et al., 2018). Later on, Gelhaye et al. (2004) found that poplar mitochondria also contain a TRX isoform belonging to the TRX*h* type (PtTRX*h*2), earlier identified in the cytosol. More recently, a new *TRXo1* gene was identified in *Pisum sativum* L. and located in both mitochondria and nucleus under physiological non –stress conditions (Martí et al., 2009). TRXs regeneration relies on the NTRA and/or NTRB being both

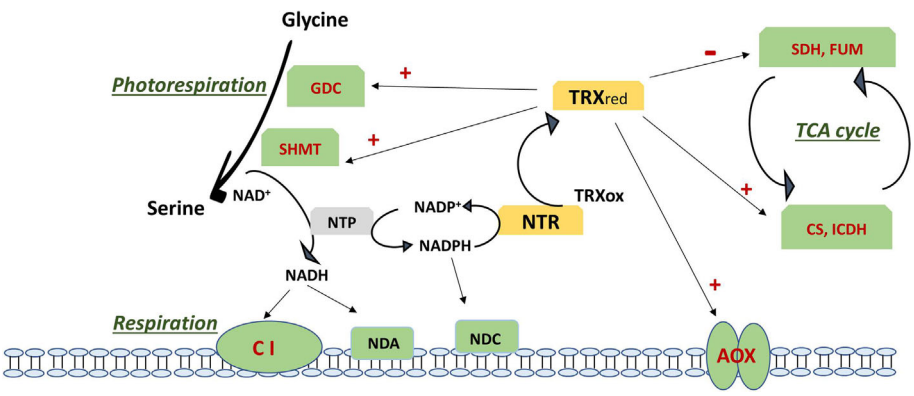

FIGURE 2 | Regulation of photorespiration, respiration and TCA cycle *via* the action of thioredoxin on specific targets (in red). Negative regulation is shown as – and positive regulation as +. TCA cycle is regulated by inhibition of SDH and FUM and the activation of CS and ICDH. Respiration is regulated *via* activation of AOX and by the NADH generated by an active photorespiration with the Gly to Ser conversion regulated by the TRX-mediated activation of GDC an SHMT, which generates an increase in NADH. NADH excess can be oxidised *via* complex I and internal dehydrogenase NDA or can be transhydrogenated by NTP with formation of NADPH. NADPH is used by NTR to reduce back TRX from its oxidised form or can be oxidized *via* the internal dehydrogenase NDC. Updated scheme based on the previously reported one (Bykova and Igamberdiev, 2016). AOX, alternative oxidase; CI, complex I; CS, citrate synthase; FUM, fumarase; GDC, glycine decarboxylase complex; ICDH, isocitrate dehydrogenase; NDA, internal NADH dehydrogenase; NDC, internal NADPH dehydrogenase; NTP, NAD(P)transhydrogenase; NTR, NADPH thioredoxin reductase; Ox, oxidized; Red, reduced; SDH, succinate dehydrogenase; SHMT, serine hydroxymethyl transferase; TCA, tricarboxylic acid; TRX, thioredoxin.

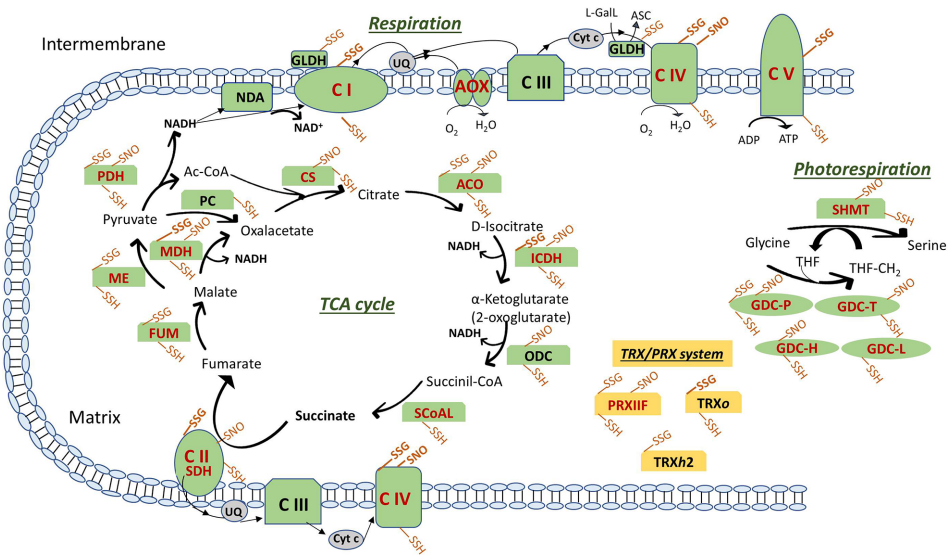

FIGURE 3 | Posttranslational modifications of cysteine residues of ETC components, TCA cycle, photorespiration enzymes and TRX/PRX system in plant mitochondria. Modifications are shown as SSG (S-glutathionylation), SNO (S-nitrosylation) and SSH (Persulfidation). In bold the modifications described only in mitochondria from animal systems. Enzymes are in red when reported as thioredoxin targets (see text for details and references). ASC, ascorbate; ETC, electron transport chain: NDA, internal NADH dehydrogenase; Complex (C) I: NADH Dehydrogenase; CII: SDH, succinate dehydrogenase; CIII: Cytochrome (Cyt) b-c reductase; CIV: Cyt c oxidase; CV: ATP synthase; AOX: alternative oxidase; GLDH, L-galactono-1,4-lactone dehydrogenase; L-GalL, L-galactono-1,4-lactone; UQ, ubiquinone. TCA, tricarboxylic acid cycle: ACO, aconitase; CS, citrate synthase; FUM, fumarase; ICDH, isocitrate dehydrogenase; MDH, malate dehydrogenase; ME, malic enzyme; ODC, 2-oxoglutarate decarboxylase; PC, pyruvate carboxylase; PDH, pyruvate dehydrogenase; SCoAL, Succinyl-CoA synthetase. Photorespiration: GDC, glycine decarboxylase (P, T, H and L proteins); SHMT, serine hydroxymethyltransferase; THF, tetrahydrofolate; THF-CH2, N-5, N-10-methylenetetrahydrofolate. TRX/PRX system: PRX, peroxiredoxin; TRX, thioredoxin.

genes expressed in mitochondria and cytosol, although *NTRA* has been also found in the nucleus (Reichheld et al., 2005).

In Arabidopsis, a recent structure-function analysis of both TRX*o* isoforms, has demonstrated that both recombinant proteins expressed in *E. coli* bind a Fe-S cluster. In TRX*o*2, the Fe-S cluster ligation depends on the cysteine residues found in the active conserved motif, but the physiological relevance of this observation remains unclear. Furthermore, it was observed a possible connection between TRXs *o* with the mitochondrial Fe-S cluster as both TRXs *o* shown the same capacity to reduce oxidized nitrogen-fixation-subunit-U 4 (NFU4) or NFU5. These NFU proteins were previously isolated as putative TRX partners and known to participate in the maturation of certain mitochondrial Fe-S proteins (Braymer and Lill, 2017; Ciofi-Baffoni et al., 2018).

An important advance in the research on the physiological role of TRX in plants has been carried out in the last two decades, but the specific role in mitochondria remains to be fully elucidated and only Arabidopsis and pea TRX*o*1 have been deeper studied. Several redox-proteomics studies using TRX affinity chromatography approaches have identified potentially redox regulated proteins in plant mitochondria. Thus, the TRX*o*1 function has been related with mitochondrial processes including, the respiratory AOX pathway, the detoxification of ROS *via* mitochondrial PRXIIF, the TCA cycle enzymes, the energy (ATP) synthesis and protein translation (Balmer et al., 2004; Barranco-Medina et al., 2008; Martí et al., 2009; Yoshida et al., 2013). In parallel, transcriptional regulation and redox regulation *via* TRXs is believed to play a crucial role in adapting photorespiration to changing environmental conditions (Reinholdt et al., 2019a).

Over-reducing conditions of mitochondrial ETC activate AOX by promoting the conversion of its dimeric oxidase form into the active reduced dimers as a consequence of the reduction of a functional disulfide bond (Day et al., 1994). Although AOX protein has not been identified as a putative mitochondrial TRX target using affinity chromatography, it has been shown to be activated by TRX-dependent reversible thiol-disulfide switch, being the mitochondrial TRX the candidate to this redox regulation (Lázaro et al., 2013; Selinski et al., 2018). AOX reduction and activation by mitochondrial PtTRX*h*2 and its effector pyruvate was initially described (Gelhaye et al., 2004; Umbach et al., 2005). Further, the addition of recombinant NADPH/NTR/PsTRX*o*1 to isolated pea and soybean mitochondria preparations induced both the reduction of AOX homodimers through the thiol redox switch of the protein and the activation of the AOX capacity (Martí et al., 2009). A similar induced AOX thiol redox switch has been linked to recombinant TRX*o*1 system in Arabidopsis and recently in thermogenic skunk cabbage (Yoshida et al., 2013; Umekawa and Ito, 2019). However, aside from these studies in isolated mitochondria, there is still no conclusive evidence showing that AOX is indeed regulated by the TRX system *in vivo* (Sevilla et al., 2015a; Geigenberger et al., 2017) (**Figure 2**).

PRXIIF is considered as partner of TRX*o* and was captured by PsTRX*o*1 affinity chromatography using mitochondrial preparations (Martí et al., 2009). PRXs are dimeric thiol-based peroxidases involved in H_2O_2 and alkyl hydroperoxide reduction to water and the corresponding alcohol, respectively. PRXs play an important role as redox sensors, antioxidant defense and in signaling. The mitochondrial location of Arabidopsis and pea PRXIIF was reported by Finkemeier et al. (2005) and Barranco-Medina et al. (2007), respectively. A biochemical characterization analysis, the use of recombinant proteins and microcalorimetric (ITC) titrations techniques reported the binding of PsTRX*o*1 and PsPrxIIF, sustaining a role of TRX*o*1 as a physiological electron donor to PrxIIF (Barranco-Medina et al., 2007; Barranco-Medina et al., 2008). A common characteristic for PRXs from plants and mammalians is the presence of at least one conserved cysteine at the active site called peroxidatic cysteine Cp (Barranco-Medina et al., 2007; Dietz, 2011; Toledo et al., 2011). Under the normal catalytic mechanism, reaction of Cp with H_2O_2 is very fast generating the sulfenic acid (Cys-SOH), which then form an inter-or intramolecular disulfide bond with a resolving cysteine (Cr) (Toledo et al., 2011). The disulfide or sulfenic from of PRXs is subsequently reduced by TRX/GRX (Barranco-Medina et al., 2009; Meyer et al., 2012). The cysteine sulfenic form may be overoxidized to the sulfinic form (Cys-SO_2H), which can be reduced by SRX in the presence of ATP. Finally, a thiosulfinate intermediate between both PRX and SRX is formed (Iglesias-Baena et al., 2010). The regeneration step is catalyzed by a thiol reductant like NTR/TRX and/or GSH (Iglesias-Baena et al., 2011; Liebthal et al., 2018). In pea and Arabidopsis plants, the small thiol reductase protein, SRX has also been described to be localized in mitochondria and in chloroplasts (Iglesias-Baena et al., 2010; Iglesias-Baena et al., 2011). In mitochondria, SRX presents a broader specificity than in chloroplasts, catalyzing the retro-reduction of hyperoxidized (sulfinic) atypical mitochondrial PRXIIF and atypical human PRXV (Rey et al., 2007; Iglesias-Baena et al., 2010; Iglesias-Baena et al., 2011).

Some TCA enzymes were described to be highly susceptible to oxidative stress as citrate synthase (CS) and isocitrate dehydrogenase (ICDH) (Geigenberger et al., 2017). CS activity in Arabidopsis was demonstrated to be inhibited by oxidation (Stevens et al., 1997). Later on, the mitochondrial CS isoform was also shown to be regulated by TRX*o* (Schmidtmann et al., 2014). In contrast to other TCA cycle enzymes, CS is exclusively localized in mitochondria in green tissues, so the TCA cycle cannot be bypassed *via* cytosolic isoforms in those tissues. By site-directed mutagenesis of its six cysteine residues the authors reported that oxidation inhibited enzyme activity by the formation of diverse disulfide bridges, as the partially oxidized enzyme forms large redox-dependent aggregates. TRX can cleave those intra- and intermolecular disulfide bridges, reversing the enzyme to the active state and strongly enhancing the activity (**Figure 2**). Daloso et al. (2015) described an activation by TRX*o*1 *in vitro* although an increase in the leaf enzyme activities in *trxo1* and *ntra ntrb* mutants suggested that this activation may not occur *in vivo*. Mitochondrial NAD^+-dependent isocitrate dehydrogenase (mICDH) was also captured using TRX affinity chromatography. This enzyme forms only intramolecular disulfide bridges under oxidizing conditions (Yoshida and Hisabori, 2014). Recombinant Arabidopsis mICDH has a heterodimeric structure composed of two subunits: ICDH-c and ICDH-r and unlike yeast ICDH, it did not show adenylated-dependent enzyme activity. Upon oxidation of the subunit ICDH-r, ICDH activity was largely diminished *via* intermolecular disulfide–mediated oligomer formation of ICDH-r. A recent study has confirmed that AtTRX*o* was effective in the reduction of oxidized ICDH-r likely leading to a recovery of ICDH activity (Yoshida and Hisabori, 2014) (**Figure 2**). In the first studies using the double T-DNA mutant of Arabidopsis with downregulated *NTRA* and *B* expression (*ntra ntrb*) and the mitochondrial located thioredoxin *o*1 (*trxo1*) mutant, Daloso et al. (2015) demonstrated that the mitochondrial TRX system regulates *in vivo* the activity of different enzymes of the TCA cycle. In particular, the mitochondrial TRX*o*1 deactivates fumarase (FUM) and succinate dehydrogenase (SDH) both previously reported as potential TRX target proteins (Yoshida et al., 2013). These enzymes bear a considerable proportion of the flux control of TCA pathway, with SDH linking the TCA cycle and ETC. Curiously, TRX*o* activates the cytosolic citrate lyase. On the basis on these findings, the authors point out a role of mitochondrial TRX*o* as crucial mediator of mitochondria-cytosol cross-talk controlling carbon fluxes in the cell (Daloso et al., 2015). The enzyme ATP-citrate lyase is involved in fatty acid biosynthesis, a noncyclic mode of TCA function, using citrate exported from the mitochondria. It has been suggested that this TRX*o*1/citrate lyase regulation might be favored under reducing conditions characterized by a high NAD(P)H/NAD $(P)^+$ ratio, which allows a deceleration from the TCA cycle (Møller, 2015) (**Figure 2**). Other TCA cycle enzyme that was trapped on TRX affinity columns is malate dehydrogenase (MDH). In plants, two mitochondrial NAD-dependent MDHs have been described with a role in central metabolism and redox homeostasis (Selinski et al., 2014; Huang et al., 2017). Initially, it was reported that mitMDH could be regulated *via* mitochondrial TRX*o*. However, Daloso et al. (2015) described an unaltered effect by TRX*o*1 finding similar activity in WT and *trxo1* and *ntra ntrb* mutant plants (**Figure 2**). Additionally, mitMDH activity has been shown to be regulated by adenin nucleotides (Yoshida and Hisabori, 2016).

Photorespiration or "respiration in light" links photosynthetic carbon assimilation with nitrogen and sulfur assimilation and carbon metabolism, contributing to balancing the redox state between mitochondria, chloroplasts, peroxisomes and cytoplasm. In mitochondria, a key step in photorespiration is the conversion of glycine from peroxisomes into serine which will be back to peroxisomes for its deamination (Engel et al., 2007). This step is carried out by the action of a multienzyme system composed of the complex glycine decarboxylase (GDC, with 4 subunits: P, T, L and H) and serine hydroxymethyl transferase (SHMT; Bauwe and Kolukisaoglu, 2003). The NADH generated by GDC is oxidized by the respiratory ETC leading to higher NADH/NAD^+ ratio in the organelle and

increased cytosolic ATP/ADP under photorespiratory conditions (Eisenhut et al., 2019) (**Figure 2**). GDC proteins have been identified as potential targets of mitochondrial TRX*o*1 in different plants as well as in *Synechocystis* PCC 6803. In pea, mitochondrial P and T components were identified as PsTRX*o*1 targets together with SHMT (Martí et al., 2009). More recent research has shown that, the lack of *TRXo1* caused a slow-down of GDC activity with an impaired glycine to serine turnover. Results evidenced that *TRXo1* contributes to redox-regulation of GDC due to TRX*o*-mediated redox regulation of lipoamide dehydrogenase (GDC-L or LPD), since its activity decreases in plant and cyanobacteria when reduced *via* NTRA/TRX*o*1 system. Redox regulation of LPD has also been suggested in *Chlamydomonas reinhardtii* (Pérez-Pérez et al., 2017). It was concluded that TRX*o*1 contributes to adjust photorespiration in response to environmental fluctuations *via* the regulation of GDC and possibly other mitochondrial multienzyme systems in which LPD is involved (Reinholdt et al., 2019a). Not only TRX*o*1, but also AtTRX*h*2, contributes to the redox regulation of mitochondrial photorespiratory metabolism (Da Fonseca-Pereira et al., 2019a) (**Figure 2**). AtTRX*h*2 regulates the redox state of GDC-L protein, which is altered in *trxh2* mutants *in vivo*. The recombinant TRX*h*2 can also deactivate GDC-L *in vitro*. Decreased abundance of SHMT and GDC H and L subunits as well as reduced NADH/NAD^+ ratio, were also found.

All the described evidences allow us to conclude that a consistent overall picture is emerging indicating that central carbon metabolism is controlled by protein thiol switches that affect enzymatic activity. To determine the physiological and molecular function of mitochondrial TRX on the *in vivo* regulation of the identified targets and metabolism, plant mutants have been recently probe to be useful, therefore plants mutants needs to be analyzed further.

Targets of Glutathionylation

Glutathionylation in cells represents the major form of S-thiolation mainly occurring under oxidative stress conditions although it may also be important under normal conditions and the exact mechanism *in vivo* is not clearly elucidated (Gao et al., 2009). Several methods have been developed to glutathionylate proteins *in vitro* and also to induce glutathionylation by oxidative stress in proteomic studies. Among them, GSSG-biotin is considered a component of oxidation because of the shift in the glutathione redox towards the oxidized state (Brennan et al., 2006). Other glutathionylating agents as GSH-biotin or biotin-amide that do not induce oxidative stress are usually used together with oxidants as diamide, ter-buthyl hydroperoxide (TBHP) or H_2O_2. Also, anti-GSH antibody is used to identify thiolation in protein extracts or in specific purified proteins after immunoprecipitation and western blot assay, although a major concern is related to its specificity and sensitivity (Gao et al., 2009).

Some TCA cycle enzymes have been identified as thiolated such as FUM, malic enzyme and pyruvate decarboxylase in Arabidopsis cell cultures treated with GSSG-biotin and TBHP and identification by MS (Dixon et al., 2005). Glutathionylation may be also important to modulate ACO activity under oxidative and nitrosative stress, due to the fact that apart from the cysteine thiol oxidation to sulfonic acid, using anti-GSH, the purified enzyme was shown to be glutathionylated, and both modifications decreased its activity (Han et al., 2005). Other TCA enzymes identified as glutathionylated but in different animal systems are succinate dehydrogenase (SDH) and MDH (Kil and Park, 2005; Niture et al., 2005; Chen et al., 2007) (**Figure 3**).

Among respiratory enzymes, in plants only GLDH is sensitive to oxidative stress induced by H_2O_2 (Leferink et al., 2009) due to the modification of Cys-340 presumably *via* reversible S-glutathionylation. In this way, glutathione (GSH) may protect the enzyme from overoxidation allowing production of ASC. However, in animal systems, the glutathionylation of mitochondrial respiratory proteins such as complex I, II, ATP synthase, and COX have been described as a modulator of mitochondrial redox status (Fratelli et al., 2003; Chen et al., 2007; Hurd et al., 2008; García et al., 2010) (**Figure 3**).

Related to glutathionylation of photorespiratory enzymes in mitochondria, the inhibition of GDC-P subunit activity by glutathionylation has been described by Palmieri et al. (2010) using partially purified P subunit from Arabidopsis leaf mitochondria. The fact that NO is also able to modulate GDC activity suggests the possibility of certain competitive effect of S-glutathionylation and S-nitrosation which may depend of the susceptibility of each protein to undergo these modifications (**Figure 3**).

Some possible targets of TRXs has been identified as glutathionylated in mammals, so the overlap between regulation by TRX and glutathionylation may be important to better understand the complex network of redox-regulated processes in plant cells (Gao et al., 2009). Human thioredoxin was identified as glutathionylated and the modification likely decreased its activity (Casagrande et al., 2002). In plants, Arabidopsis chloroplastic TRX*f* was identified as glutathionylated (Michelet et al., 2005) and interestingly, thiolation of poplar mitochondrial TRX*h*2 in an additional cysteine not belonging to the active site was shown to increase the redox potential of the enzyme (Gelhaye et al., 2004) (**Figure 3**). Also, PRXs undergo glutathionylation as in pea chloroplastic 2-Cys PRX in which the glutathionylation of the decameric form induced a change to its dimeric glutathionylated form (Calderón et al., 2017b) or in the poplar 1-Cys PRXIIB with a conformational dissociation of homodimers into monomers (Noguera-Mazon et al., 2006). This suggested the existence of a redox-dependent oligomerization switch in the PRX family by thiolation although it does not occur for all PRXs: this is the case of mitochondrial PRXIIF in which glutathionylation did not provoke a change in its oligomeric state, being GSSG able to glutathionylate both peroxidatic (Cys59) and resolving (Cys84) cysteine, provoking a decrease in the peroxidatic activity of the protein (Calderón et al., 2017b) (**Figure 3**). Interestingly, pea 2-Cys PRX and PRXIIF were differentially sensitive to small changes in GSH/GSSG ratio pointing to a fine regulation by the intensity of the oxidative stress. This could be a key step during cellular metabolism but mainly during stress conditions

modulating the peroxidase activity and thus affecting H_2O_2 signaling. Both pea chloroplastic 2-Cys PRX and mitochondrial PRXIIF are regenerated from their overoxidized forms by pea SRX, which is then reduced by TRX (Iglesias-Baena et al., 2010; Iglesias-Baena et al., 2011). Interestingly, SRX deglutathionylated pea 2-Cys PRX but not PRXIIF, so the glutathionylation/deglutathionylation processes may have an important role during plant development and response to stress in which redox changes influence the posttranslational regulation of key proteins as the ones involved in the TRX/PRX/SRX system.

Targets of S-Nitrosation

A large number of mass spectrometry (MS)-based analytical methods has been developed to face the challenge of analyzing S-nitrosylated proteins. However, the most often-used method is the biotin-switch assay (BST) (Jaffrey and Snyder, 2001). This methodology includes firstly the blocking of all the free thiols groups of cysteine residues, then selective reduction of modified cysteine and switch with a stable functional group usually with a biotin molecule that also serves as a handle for enrichment and detection. Despite this method is time consuming, tedious, and unsuitable for monitoring dynamic changes of this PTM *in vivo* (Feng et al., 2019), it has allowed to gain insight into the processes affected by S-nitrosation and into the study of the mechanism and effect that this PTM has on protein functions. Recently, newer strategies have been reported to overcome these issues. A S-nitrosoproteomic analysis using iodo-TMT (iodo-tandem mass tag) labelling, affinity enrichment, and high-resolution LC-MS/MS has been used to identify S-nitrosated proteins in tea plants (Qiu et al., 2019). Also, in animals, a new chemical proteomics strategy for quantitative analysis of reversibly modified cysteine using bioorthogonal cleavable-linker and switch technique (Cys-BOOST) has been reported. This method shows a higher sensitivity and considerably higher specificity and precision than other methods. It allows the proteome wide identification of SNO even from low abundance proteins and under basal conditions (Mnatsakanyan et al., 2019).

Similar to glutathionylation, several TCA enzymes including ACO, MDH, ICDH, α-ketoglutarate dehydrogenase, FUM, CS, and pyruvate dehydrogenase have been found to be S-nitrosylated in several plant species using different methodological approaches (Fares et al., 2011; Puyaubert et al., 2014; Hu et al., 2015; Lindermayr et al., 2015; Qiu et al., 2019) (**Figure 3**). However, the mechanisms by which this PTM happens, how S-nitrosation affects the enzymes activity or how S-nitrosation is affected by stress conditions are not well known. Previously it has been reported that ACO is reversibly inhibited by NO by a mechanism which promotes the loss of the iron-sulfur cluster, which can subsequently be reassembled under the proper conditions (Drapier, 1997). Recently it has been also shown that this inhibition under hypoxia results in accumulation of citrate, the latter in turn induces AOX and causes a shift of metabolism towards amino acid biosynthesis (Gupta et al., 2012). Regarding MDH, it has also been found to be S-nitrosated in peroxisomes which activity has been shown to be inhibited by NO donors (Ortega-Galisteo et al., 2012). Additionally, ICDH has been reported to be slightly over-nitrosylated in Arabidopsis cell suspension submitted to salt stress (Fares et al., 2011). In plants, the effect of S-nitrosation on ICDH has not been described unlike in animals, where this PTM leads to an inactivation of the enzyme and to a pro-oxidant condition in the cell (Yang et al., 2002; Lee et al., 2003).

SDH in plants is susceptible to S-nitrosation *in vivo* (Fares et al., 2011; Hu et al., 2015; Qiu et al., 2019) (**Figure 3**) under normal but not under saline stress conditions (Camejo et al., 2013). To our knowledge, in plants the effect of the S-nitrosylation in SDH activity is not known, although an inhibitory effect has been described in animals (Rizza et al., 2016).

Among the enzymes involved in the photorespiratory process, GDH has been reported to be S-nitrosated *in vivo* in Arabidopsis (Palmieri et al., 2010; Puyaubert et al., 2014; Hu et al., 2015) (**Figure 3**). As previously mentioned, *in vitro* studies have shown the effect of S-nitrosation on GDC-P subunit activity (Palmieri et al., 2010). Additionally, our laboratory has also found that in pea, both subunits P and T of GDC showed the same S-nitrosation pattern in control plants and salt-treated plants, with no changes in protein levels during plant development and salt stress, although loosing S-nitrosation in older plants (Camejo et al., 2013). S-nitrosation of SHMT has been reported by Camejo et al. (2013); Hu et al. (2015) and Tanou et al. (2009) in Arabidopsis, pea, and citrus plants, respectively (**Figure 3**). Despite of previous report where photorespiration has been shown to increase under salinity (Hoshida et al., 2000), our lab has reported that SHMT did not change its protein levels during salt stress although it was found S-nitrosated in control pea mitochondria but not in those from stressed plants. We hypothesized that its denitrosation after long period of salt stress may allow photorespiration to be functional under these conditions.

Among the RNS targets in plant mitochondria are some ETC components, with NO inhibiting cytochrome c pathway whereas AOX is only partially inhibited (Martí et al., 2012). The different inhibitory effect may be involved in the regulation of ROS generation and energy metabolism in the organelle collaborating in the stress response. In fact, the reported effect of NO on different enzymes components of the antioxidant system as the lack of inhibition on Mn-SOD or on the majority of the ASC-GSH cycle except APX in pea plants could be part of a NO redox signalling through the H_2O_2 and NO cross-talk (Martí et al., 2012). However, similar to AOX, COX has not been found to be S-nitrosated in plants according to the references checked for this review, although it has been reported to be S-nitrosated in animals (**Figure 3**) (Zhang et al., 2005).

Under both, normal and stress conditions, PRXs from animals and plants have been shown to be targets of S-nitrosylation (**Figure 3**). In Arabidopsis and citrus plants under normal and salinity conditions, respectively, PRX is one of the proteins reported to be S-nitrosated (Tanou et al., 2009; Lindermayr et al., 2015). Deeper studies have also shown that S-nitrosation of plants PRXs leads to a change in their protein

activity. In this sense, in chloroplasts, both the hydroperoxide-reducing peroxidase activity during the plant hypersensitive disease resistance response and the ONOO− detoxification activity of PRXIIE are inhibited by S-nitrosation (Romero-Puertas et al., 2007; Romero-Puertas et al., 2008). Recently, mitochondrial PRXIIF has been found by our lab to be S-nitrosated *in vivo* under long saline stress conditions, a situation in which NO levels were also increased (Camejo et al., 2013). The effect of NO and S-nitrosation on the protein function has been further investigated in our lab (Camejo et al., 2015). Under *in vitro* conditions, we found that both catalytic cysteines of PsPRXIIF (C59 and/or C84) are susceptible of S-nitrosation depending of its oligomerization state. We also found that the S-nitrosation leads to a conformational change that inhibits the PsPRXII peroxidase activity in favour of the transnitrosylase activity. These data together with the previous finding of PRXIIF being nitrosated only under long saline conditions and the reversibility of S-nitrosation and, consequently, of its peroxidase activity, suggest that the S-nitrosation of PRXIIF might act as a mechanism that is activated under oxidative and nitrosative stress, a situation that is presented in long saline conditions and that is reversed by reducing conditions, in which the TRX system may function in the mitochondria.

The level of S-nitrosated proteins depends on NO levels in the cells, which are regulated by several mechanisms. They depend on GSNO which is regulated by GSNOR activity (Liu et al., 2001; Holzmeister et al., 2011) and on Tyr nitration of proteins which consumes NO. Another important mechanism affecting S-nitrosation state of proteins may be through TRX activity, which similarly to GSNOR, can degrade S-nitrosothiols to increase their turnover ratio (Benhar et al., 2008). Several S-nitrosated enzymes that are summarized in this review have been also shown to be targets of mitochondrial TRX (see review in Møller et al., 2020). From plant S-nitrosation studies under abiotic stresses (Fares et al., 2011; Camejo et al., 2013; Puyaubert et al., 2014), it could be suggested that under those conditions, the effect of the stress does not produce large changes on the S-nitrosation status of the cells, probably due to other mechanisms that could be competing with the S-nitrosation process. Therefore, in the future, it might be more important to answer which cysteine residues in a specific protein are differentially S-nitrosated under normal and stress conditions and in which proportion, and also, which are the biochemical mechanisms involved.

Targets of Persulfidation

The chemical reactivity of H_2S provokes the modification of cysteine residues to form persulfides, a PTM that may cause functional changes in protein structures and activities.This modification has been reported to increase under oxidative stress and it has been postulated as a defense mechanism against protein oxidative damage, avoiding the formation of dangerous -SO_2H or irreversible -SO_3H. Trying to identify the target proteins of persulfidation, a few works have been carried out in plant extracts. In a first approach, using a modified BST with S-methyl-methanothiosulfonate (MMTS) to block free thiols and the thiol-specific biotinylating agent biotin-HPDP, 106 proteins were identified as persulfidated in Arabidopsis mainly involved in photosynthesis, protein synthesis, and cell organization (Aroca et al., 2015). More recently, using methylsulfonylbenzothiazole (MSBT) to block both thiols and persulfide groups and cyanoacetate-based reagent CN-biotin as labelling agent, more than 3,000 proteins were identified as possible targets in cytosol-enriched leaf extracts of Arabidopsis plants grown under physiological conditions (Aroca et al., 2017). The bioinformatic analysis revealed that persulfidated cysteines are involved regulating important processes such as plant growth, plant response to abiotic and biotic stresses, carbon metabolism, and RNA translation. Several mitochondrial proteins were described as possible targets of persulfidation, including among others, proteins involved in ATP synthesis, respiration, chaperone function, protein synthesis, and all the TCA and photorespiratory enzymes (**Figure 3**). Interestingly, TRX*o*1 and almost all the described PsTRX*o*1 targets (Martí et al., 2009) were also found as persulfidated (ATP synthase subunit alpha, thiosulfate/3-mercaptopyruvate sulfurtransferase, elongation factor Tu and PRXIIF), implying that the role of this mitochondrial TRX*o*1 is related to persulfidation as it has been described for other TRXs (Filipovic and Jovanović, 2017) (**Figure 3**). Some of them were also demonstrated as S-nitrosylated and/or glutathionylated as described above, that reinforces the role of these PTMs in the processes in which the proteins are involved in mitochondria.

Another mechanism of action of H_2S independent of its persulfidation effect is its coordination with the metal center of metalloproteins, attaching covalently to heme porphyrins. In this way, H_2S acts as a potent inhibitor of plant and animal COX. Additionally, both COX and NADH dehydrogenase have been found among the persulfidated proteins in Arabidopsis (Aroca et al., 2017) (**Figure 3**).

A beneficial effect of exogenous application of H_2S on plants subjected to different abiotic stresses has been described (see review by Corpas and Palma, 2020), including heavy metals, arsenic, low and high temperature, salinity, or drought. In fact, a reduction of oxidative stress on lipids and proteins as well as an increase in antioxidant components have been observed in the treated plants, contributing to a better response under the stress situation. However, to our knowledge, the effect on specific mitochondrial targets of persulfidation is scarcely reported.

Cross Talk Among H_2S and Reactive Oxygen and Nitrogen Species

The crosstalk between H_2S and RNS/ROS is important for the biological functions of all these molecules (Scuffi et al., 2014; Corpas et al., 2019b). H_2S can act as a reductant reacting with biological oxidants, such as $NO^{\cdot}$, H_2O_2, $O_2^{\cdot-}$, peroxynitrite, hypochlorite, and S-nitrosothiols although the direct reactions have not been quantified in plants (Gotor et al., 2019). Several examples point to the existence of the mentioned crosstalk. It has been described that H_2S enhanced antioxidant capacity and salt tolerance of cucumber hypocotyls and radicles (Yu et al., 2013). The overlap between persulfidation and sulfenylation has been

described by proteomic studies [reviewed by Zhou (2020)], with 437 proteins being modified by both. However, the effect of each modification can be opposite. As examples, activities of glyceraldehyde- 3-phosphate dehydrogenase (GAPC) and cytosolic APX are inhibited by sulfenylation and increased by persulfidation (Kitajima et al., 2008; Zaffagnini et al., 2013; Aroca et al., 2015), pointing to a fine regulation of the proteins by different PTMs. Related to RNS, an increase in NO occurs after H_2S treatments of nitrate-treated tomato (Guo et al., 2018). Also, among 927 S-nitrosated proteins in Arabidopsis, 639 may be persulfidated (Hu et al., 2015; Aroca et al., 2018) with different functions on specific targets: both PTMs increased cAPX activity while S-nitrosation inhibited GAPC and persulfidation increased it (Begara-Morales et al., 2014; Lindermayr et al., 2015; Yang et al., 2015). As another example, exogenous treatments of H_2S and NO alleviated some abiotic stresses and maintained the quality of post-harvested fruits (Ziogas et al., 2015; Corpas and Palma, 2018). Although the cascade of action is not fully elucidated, some experiments have reported that H_2S could act upstream of NO signaling during stomatal closure while downstream in response to abiotic stress (Scuffi et al., 2014).

All these examples evidence that the interaction among H_2S, RNS, and ROS may occur to regulate physiological processes not only under control conditions during plant development but also under stressed environments, allowing signal transduction pathways through the posttranslational regulation of key proteins involved in the response. The identification of the target proteins of each modification driven by H_2S, RNS, and ROS and their effects on enzyme structure and activity are essential to understand the complexity of interactions and will help to reveal the modulating effect of redox components.

THE TRX-PRX SYSTEM UNDER STRESS CONDITIONS

Stress conditions provoke changes in cellular redox homeostasis mainly by dangerous increase in ROS/RNS generation (Noctor et al., 2015; Calderón et al., 2018a). APX, a component of the ASC-GSH cycle together with monodehydroascorbate reductase (MDHAR), dehydroascorbate (DHA) reductase (DHAR) and glutathione reductase (GR), is the responsible of H_2O_2 scavenging in mitochondria (Jiménez et al., 1997; Locato et al., 2018). Also, GPX, GRX, and TRX/PRX system play an important role in cellular ROS homeostasis. In this context, either mitochondria as chloroplasts are essential in maintaining the cellular redox balance under stress conditions (Cejudo et al., 2014; Sevilla et al., 2015b; Ojeda et al., 2017).

Changes in redox state and its significance in cellular signaling process can be evaluated in plant tissues using different approaches. Mutants are useful tools for investigating the involvement of specific proteins *in vivo* on redox metabolism in plant cells. Also, a parallel approach is to analyze stress conditions affecting the intracellular redox balance. In this sense, loss of function *trxo*1-*1* and *trxo*1-*2* mutants have been used not only to corroborate a role for the TRX system in regulating different metabolic processes in mitochondria but also to define the importance of mitochondrial TRXs under stress conditions (Daloso et al., 2015; Calderón et al., 2018a). However, in these studies, no extreme phenotype has been described, either in standard or stress conditions, possibly due to the redundancy or overlapping functions with mitochondrial or cytosolic proteins as other TRXs and GRXs (Daloso et al., 2015; Geigenberger et al., 2017; Ortiz-Espín et al., 2017; Calderón et al., 2018a; Calderón et al., 2018b; Sánchez-Guerrero et al., 2019). The information related to the physiological mitochondrial TRX*o*1/TRX*h*2 function in plant stress acclimation is scarce. *In silico* studies on *AtTRXo1* gene expression have revealed that it does not vary as a response to different environment conditions including salinity. Contrary, in pea plants, an adaptative response to a short-term high salinity levels (150 mM NaCl), including increased *PsTRXo1* gene expression was demonstrated, while longer salinity treatment downregulated it, with a parallel increase in PsTRX*o*1 protein and activity. Interestingly, these TRX*o*1 related changes were correlated with an increase in the AOX capacity in purified mitochondria preparations as well as a higher demand to regenerate the oxidized form of PRXIIF involved in ROS detoxification. Also, a maintained *MnSOD* gene expression, protein and activity levels were observed. Overall, the results demonstrated the participation of PsTRX*o*1 as a component in the mitochondrial antioxidant response allowing plant salinity adaptation (Martí et al., 2011). In order to gain further insight into the physiological and metabolic function of the mitochondrial TRX*o*1 in the plant acclimation to saline stress, we have recently used two independent mitochondrial *Attrxo1* mutants (*Attrxo1-1, Attrxo1-2*) (Calderón et al., 2018b). Their responses to salinity fit well with those reported by Martí et al. (2011) in pea plants, all pointing that TRX*o*1 is required for the proper functioning of the antioxidant metabolism including compensatory mechanisms, as higher levels of H_2O_2 and NO, an upregulation of all SOD isoforms, catalase and GR, alterations in the glutathione redox state, due to maintained GSH content in *Attrxo1* plants and changes in stomatal density, stomatal closure with lower water loss, which may be also a key factor for the adaptative response to salinity (Calderón et al., 2018b) (**Figure 4**). At mitochondrial level, a more recent study has revealed the impact of the lack of TRX*o*1 in the acclimation to salinity, with an important *in vivo* reorganization of the respiratory and antioxidant enzymes as well as metabolic responses (Sánchez-Guerrero et al., 2019). Compelling evidences from several plants indicated that *AOX* transcript and protein increase during salinity (Smith et al., 2009; Martí et al., 2011; Lázaro et al., 2013; Del-Saz et al., 2016). Using *Attrxo1-1* and *Attrxo1-2* mutants under a long-term saline stress, we described that AOX protein displayed a reduction of its *in vivo* activity in all genotypes and that exits a higher electron partitioning to the AOX pathway under salinity which denotes a relatively higher response of the AOX that can act preventing the generation of $O_2^{\cdot-}$ at the UQ level (Purvis, 1997; Cvetkovska and Vanlerberghe, 2012). In parallel, the high constitutive mitochondrial GR and

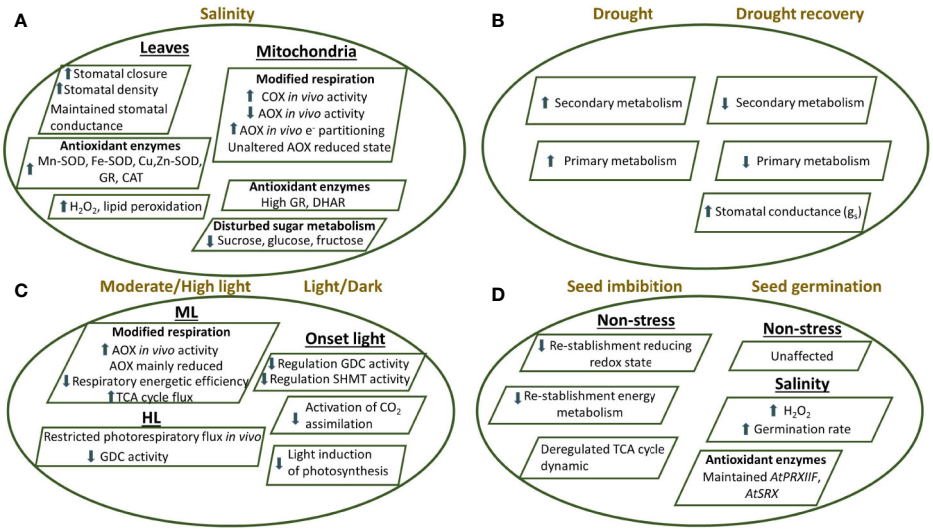

FIGURE 4 | Proposed model showing the response of *Arabidopsis thaliana* plants knockout of the mitochondrial TRX*o*1 under different stress conditions as **(A)** salinity in leaves and mitochondria, **(B)** drought and drought recovery, **(C)** moderate light/high light and **(D)** during seed imbibition and germination, as detailed in the main text (Daloso et al., 2015; Ortiz-Espín et al., 2017; Calderón et al., 2018b; Florez-Sarasa et al., 2019; Sánchez-Guerrero et al., 2019; Da Fonseca-Pereira et al., 2019b; Da Fonseca-Pereira et al., 2019c). Effect on stomatal behaviour, antioxidant and oxidative metabolism, respiration and photorespiration, photosynthesis, TCA cycle as well as primary and secondary metabolism are shown in the KO plants compared to non-transformed plants. AOX, alternative oxidase; CAT, catalase; COX, cytochrome oxidase; Cu/Zn-SOD, copper-zinc superoxide dismutase; DHAR, dehydroascorbate reductase; GDC, glycine decarboxylase; Fe-SOD, iron superoxide dismutase; GR, glutathione reductase; Mn-SOD, manganese superoxide dismutase; PRXIIF, peroxiredoxin IIF; SHMT, serine hydroxymethyl transferase; SRX, sulfiredoxin; TCA, tricarboxylic acid.

DHAR activities in A*ttrxo1* mutants, could act helping to decrease H_2O_2 content and to increase GSH recycling. Importantly, we observed a change in AOX isoforms pattern but AOX protein was not decreased and was also maintained in its reduced state under control and saline conditions in both *Attrxo1* mutants. These observations suggested that *in vivo*, the mitochondrial TRX*o*1 system could perform a maintenance of reductive function rather than an AOX regulation, as it has been proposed. This possibility was also suggested recently by Nietzel et al. (2017) (**Figure 4**). Furthermore, a pronounced decrease on glucose and fructose levels occurred in both *Attrxo1 mutants* under control and salinity, coinciding with an increased *in vivo* respiration through the cytochrome c (COX) pathway (Sánchez-Guerrero et al., 2019). These results indicated a reorganization in central carbon metabolism and reflect a higher use of these sugars in the glycolytic pathway, causing an increased respiration, probably driven by an increased carbon flow through the TCA cycle as previously suggested (Daloso et al., 2015). The increase in ATP-coupled respiration is an indicator of a higher demand on the leaf energy of the mutants under control conditions (**Figure 3**).

A similar metabolic adjustment could be also taking place during seed germination, a process in which a function for AtTRX*o*1 has also been described (Ortiz-Espín et al., 2017). Arabidopsis *AtTrxo1* transcript levels were particularly high in dry seeds and cotyledons, where it reached a maximum coinciding with 50% germination. However, expression was lower in seeds germinating under salinity. We reported that seeds of both *Attrxo1-1* and *Attrxo1-2* mutant lines failed to show any important difference in the germination rate compared to WT, but the physiological and metabolic analysis of these mutants showed diverse and complex responses, showing higher H_2O_2 levels in dry seeds. Moreover, A*ttrxo1* mutant seeds germinated faster and accumulated higher H_2O_2 content under salinity (**Figure 4**). This peak of H_2O_2 at the beginning of germination might be a factor in the observed early germination rate and fits well with that proposed for the accumulated mitochondrial H_2O_2 at early stages of germination (Zhang et al., 2014). Thus, a role for AtTRX*o*1 in redox homeostasis during seed germination, acting as a possible sensor of saline stress and/or an inducer of H_2O_2 accumulation was proposed. This specific role of TRX*o*1 under stress may in turn be related to its targets following seed germination, an aspect that deserves further investigations (Ortiz-Espín et al., 2017).

Recently, the earliest events in energy and redox metabolism of Arabidopsis seeds at imbibition, as a physiological step of metabolic reactivation, have been investigated (Nietzel et al., 2020). RoGFP-based *in vivo* sensing experiments, have suggested that the reestablishment to a more reducing thiol redox status of the mitochondrial matrix and the cytosol within minutes in intact seeds, is intimately linked to the reestablishment of energy metabolism. Redox proteomic analysis has shown that active site cysteine peptides of GR 2, NTR a/b, and TRX*o*1 present the

strongest change in redox state. Seeds germination of the three mutants *gr2, ntra/b*, and *trx-o1* was associated with increased respiratory rates and deregulated TCA cycle dynamics, suggesting decreased resource efficiency of energy metabolism. NAD-malic enzyme (NAD-ME) and aconitase (ACO) also showed a quantitative redox-dependent response, but this was not the case for enzymes as 2-oxoglutarate dehydrogenase (OGDH), NAD-isocitrate dehydrogenase (ICDH), and ICDH which only showed a marginal response at imbibition. These differences indicated that the functional impact of cysteine redox switch operation is enzyme-specific. An important contribution of redox regulation to efficient metabolism during early seed germination was proposed.

The importance of the mitochondrial NTR/TRX system under drought episodes was recently investigated using both *Attrxo1* mutant and At*ntra ntrb* double mutant plants (Da Fonseca-Pereira et al., 2019b). Under these conditions, all the genotypes lacking functional NTR/TRX system, showed enhanced drought tolerance. Interestingly, *TRXo1* transcript was more highly expressed under drought, an effect even stronger mainly during repetitive drought/recovery events. Results on the changes in secondary metabolites with a large number of metabolites increasing in at least one of the *Attrxo1* mutants following two cycles of drought, reinforces the idea that secondary metabolism is redox regulated by TRX system (**Figure 4**). Finally, the analysis of the increased stomatal conductance following drought recovery suggested a TRX*o*1 redox regulation of stoma function (**Figure 4**) which fits well with the previously reported involvement of TRX*o*1 mediated redox regulation of stomatal dynamic and function under salinity (Calderón et al., 2018b).

Regarding the effects of different light conditions, it has been observed that an altered *in vivo* AOX activity and carbon metabolism occur in both Arabidopsis *trxo1* mutants under medium light (ML) and high light (HL) conditions (Florez-Sarasa et al., 2019). Contrary to the effects under salinity (Sánchez-Guerrero et al., 2019), the results showed that the *in vivo* AOX activity was higher in the *Attrxo1* mutants at ML while the AOX redox state was apparently unaltered as we have commented above. Moreover, the authors claim that the negative regulation of the TCA cycle by the TRX system is coordinated with the increased input of electrons into the AOX pathway. Under HL conditions, AOX and photosynthesis displayed similar patterns in the mutants. Furthermore, changes on photorespiration were observed under HL conditions, being restricted at the level of glycine decarboxylation, most likely as a consequence of the redox imbalance. These results denote the relevance of TRX*o*1 on the interaction between mitochondrial redox and carbon metabolism under light stress conditions (**Figure 4**). In a parallel study, the alteration of photorespiratory activity in the absence of TRX*o*1 was described. In this sense, it has been shown that a functional TRX*o*1 allowing the rapid induction of mitochondrial steps of the photorespiration process *via* GDC system in conjunction with SHMT is necessary to facilitate light-induction of photosynthesis (Reinholdt et al., 2019b).

Some other TRX*o*1 functional studies were focused on determining the effect of high *PsTRXo1* expression on processes linked to oxidative treatment and on the functional PsTRX*o*1 role in the nucleus. Under a situation of high H_2O_2 level treatment, the analysis of different hallmarks of programmed cell death (PCD) demonstrated that the over-expression of PsTrx*o*1 in tobacco (*Nicotiana tabacum*) BY-2 cells, was able to increase the cell viability in that oxidative situation, contrasting with a severe decrease in viability and marked oxidative stress, with a rapid cell death, observed in non-overexpressing lines. The decreased content in endogenous H_2O_2, an increased catalase activity, with the practically maintained *PRXII* expression, would be involved in the delayed cell death found in over-expressing cells, in which changes in oxidative parameters and GSH/ASC redox state were less extended after the H_2O_2 treatment, than in non-overexpressing lines. These data pointed to PsTRX*o*1 as an important factor responsible for the delay in the PCD provoked by the oxidative treatment (Ortiz-Espín et al., 2015) (**Figure 5**). In pea leaves TRX*o*1 is constitutively found in mitochondria and nucleus (Martí et al., 2009). Nuclear localization has been reported for several cytosolic TRX*h* isoforms but only during oxidative stress (Pulido et al., 2009). While subsequent reports describing a functional TRX system in the plant nucleus have appeared, little evidence on the nuclear TRXs targets *in vivo* has been reported and only a few candidate protein targets have been experimentally validated (Delorme-Hinoux et al., 2016). Among them, proliferating cellular nuclear antigen (PCNA) has been demonstrated to interact with PsTRX*o*1 in the nucleus (Calderón et al., 2017a). In *Medicago* and barley seed embryos, PCNA was also reported as a candidate targets of TRX*h*, but the interaction was not conclusively demonstrated (Alkhalfioui et al., 2007; Hägglund et al., 2008). In TBY-2 cells it was reported that the over-expressed PsTRX*o*1 was localized in mitochondria and nucleus and the over-expression correlated with changes in the growth of the culture, increase in the rate of cell proliferation and a decrease in the total cellular GSH content, but maintained nuclear GSH accumulation (Calderón et al., 2017a). Changes in GSH content were accompanied by a higher mitotic index, unlike non-expressing TBY-2 cells. All these findings suggest that TRX*o*1 is involved in the cell cycle progression of TBY-2 cultures, possibly through its link with both GSH and PCNA (**Figure 5**).

The information on the involvement of the mitochondrial PRXIIF in stress is scarce, being the chloroplastic and cytosolic isoforms more studied. Among ROS sensors during stress, reactive thiols may play a key role in the signal transduction, and as example, the action of SRX on the oxidized PRX has been reported (Lázaro et al., 2013). A link between redox changes and gene regulation has been described during the stress response (Astier et al., 2011) being *AtPRXIIF* one of the responsive genes in oxidative-induced stress situations such as treatments of Arabidopsis cell cultures with H_2O_2, menadione

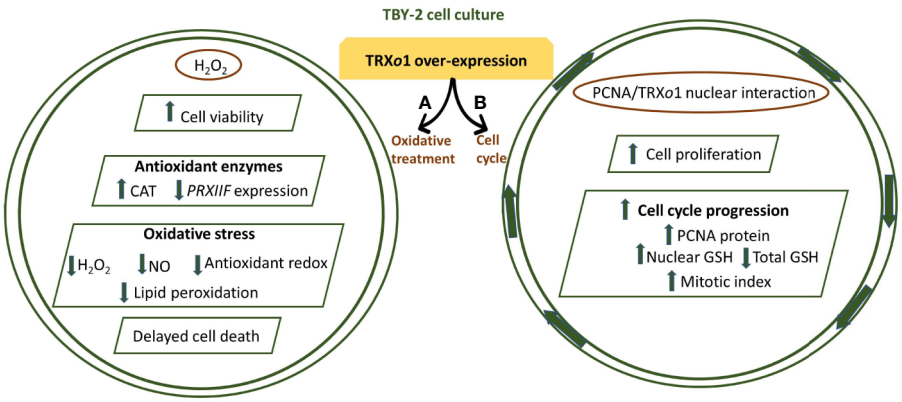

FIGURE 5 | **(A)** PsTRX*o*1 function in cell response to high H_2O_2 treatment. TBY-2 cell lines over-expressing PsTRX*o*1 showed higher and maintained viability than control lines. The high catalase (CAT) activity, decrease in ASC and GSH redox state are parallel and might contribute to decreased H_2O_2, NO, and lipid peroxidation, protecting together with TRX*o*1, against increased oxidative stress, thus allowing delayed programmed cell death (PCD) (Ortiz-Espín et al., 2015). **(B)** Proliferating cell nuclear antigen (PCNA) interacts with PsTRX*o*1 in the nucleus and showed an efficient *in vitro* disulfide reductase activity reducing oxidized PCNA. Flow cytometry showed that TRX*o*1 increased the rate of cell proliferation and cell cycle progression. Higher amount of PCNA protein in over-expressing TRX*o*1 cells occurred in the growth phases when high mitotic index and percentage of cells in S-G2/M phases were more evident and different to that in control lines. These changes were parallel to maintained GSH level in the nucleus but decreased in total cellular GSH in over-expressing lines, when the percentage of cells in G2/M phase was higher. Overall, these changes suggest that TRX*o*1 is involved in cell cycle progression providing a reductive environment and interacting with PCNA (Calderón et al., 2017a).

or antimycin A (Sweetlove et al., 2002) or in pea and poplar leaves under cold stress (Barranco-Medina et al., 2007; Gama et al., 2007). Also under salinity and Cd stress in pea leaves but not in roots, both transcripts and protein levels were upregulated (Barranco-Medina et al., 2007), while in more resistant species as Arabidopsis, the leaf mRNA level did not change significantly under salt, ozone, H_2O_2, or light stress (Horling et al., 2002; Horling et al., 2003). In another study, PRXIIF presented a biphasic response in pea plants under salinity, being the gene upregulated after 5 days of 150 mM NaCl treatment while downregulated after 14 days (Martí et al., 2011). However, the protein content remained constant although a regulation by S-nitrosylation was described affecting structure and function as commented above (Camejo et al., 2013; Camejo et al., 2015). Also, under these conditions salinity provoked a change in the oligomerization pattern of PRXIIF, increasing the oligomeric forms of the protein, similar to that occurring when recombinant protein was treated with H_2O_2 (Camejo et al., 2015). Also, the analysis of mutants lacking AtPRXIIF has allowed the knowledge of the physiological role of the protein not only under control (where a compensatory mechanism by mitochondrial antioxidant system seems to occur) but also under stress situations (Lázaro et al., 2013). The mutants' behaviour has revealed a role for PRXIIF in root growth under Cd stress in Arabidopsis seedlings (Finkemeier et al., 2005), water stress in *Vitis vinifera* and in Arabidopsis mature leaves (Gama et al., 2007; Vidigal et al., 2013). All these examples imply the important involvement of PRXIIF in the antioxidant defence and redox signalling in plant cells.

CONCLUSION AND PERSPECTIVES

In the last years, the advance in the analysis and characterization of TRX*o*1 mutants has allowed to obtain wide information on the function of this protein, unveiling the key processes by which TRX system regulates mitochondrial respiration, TCA cycle, photorespiration, plant acclimation to stress through a proper functioning of the antioxidant metabolism, as well as its link with the germination process and cell cycle progression. In general, in the scarce studies describing processes as germination and plants acclimation under different conditions, the lack of TRX*o*1 generates a decrease in the energetic efficiency, but the connection between TRX*o*1 and *in vivo* respiratory AOX, needs to be explored in more detail. Also, the compelling evidences that both, TRX*h*2 and *o*1 systems play a role in the redox regulation of the mitochondrial photorespiratory metabolism needs to be further investigated. Another interesting point is the possible existence of compensatory and redundant mechanisms as the existence of other TRX isoforms. The use of multiple mutants in different redox systems present in the cellular compartments will aid to unravel their functionality in which, the PTMs may play a key role. Understanding which is the signature of the signal that triggers the specific PTM associated to a specific stress and also how plants distinguish these signals, will help to get insight on how plants responds to the different environmental cues. Hopefully, the development of new mass-spectrometry proteomic techniques will allow in the near future to expand the knowledge on the dynamic and interaction among the different PTMs. This is important not only for fundamental research but also for crop improvement in the actual climate-changing environment.

AUTHOR CONTRIBUTIONS

MM, AJ, and FS conceived the idea and wrote the manuscript.

FUNDING

The review was funded by a Saavedra Fajardo 20402/SF/17 (Fundación Séneca, Murcia, Spain) and a Ramón y Cajal (Ministry of Science and Innovation, Spain) Fellowship both awarded to MM and Spanish grants MINECO/FEDER (BFU2017-86585-P) and Seneca Excellence Project (19876/GERM/15).

ACKNOWLEDGMENTS

The authors apologize to the scientists that are not cited because of space limitation.

REFERENCES

Albert, N. A., Sivanesan, H., and Vanlerberghe, G. C. (2017). The occurrence and control of nitric oxide generation by the plant mitochondrial electron transport chain. *Plant Cell Environ.* 40, 1074–1085. doi: 10.1111/pce.12884

Alkhalfioui, F., Renard, M., Frendo, P., Keichinger, C., Meyer, Y., Gelhaye, E., et al. (2008). A Novel Type of Thioredoxin Dedicated to Symbiosis in Legumes. *Plant Physiol.* 148, 424–435. doi: 10.1104/pp.108.123778

Alkhalfioui, F., Renard, M., Vensel, W. H., Wong, J., Tanaka, C. K., Hurkman, W. J., et al. (2007). Thioredoxin-linked proteins are reduced during germination of *Medicago truncatula* seeds. *Plant Physiol.* 144, 1559–1579. doi: 10.1104/pp.107.098103

Álvarez, C., García, I., Romero, L. C., and Gotor, C. (2012). Mitochondrial sulfide detoxification requires a functional isoform O-acetylserine (thiol) lyase C in *Arabidopsis thaliana*. *Mol. Plant* 5, 1217–1226. doi: 10.1093/mp/sss043

Aroca, A., Serna, A., Gotor, C., and Romero, L. C. (2015). S-sulfhydration: a cysteine posttranslational modification in plant systems. *Plant Physiol.* 168, 334–342. doi: 10.1104/pp.15.00009

Aroca, A., Benito, J. M., Gotor, C., and Romero, L. C. (2017). Persulfidation proteome reveals the regulation of protein function by hydrogen sulfide in diverse biological processes in Arabidopsis. *J. Exp. Bot.* 68, 4915–4927. doi: 10.1093/jxb/erx294

Aroca, A., Gotor, C., and Romero, L. C. (2018). Hydrogen Sulfide Signaling in Plants: Emerging Roles of Protein Persulfidation. *Front. Plant Sci.* 9, 1369. doi: 10.3389/fpls.2018.01369

Astier, J., Rasul, S., Koen, E., Manzoor, H., Besson-Bard, A., Lamotte, O., et al. (2011). S-nitrosylation: an emerging post-translational protein modification in plants. *Plant Sci.* 181, 527–533. doi: 10.1016/j.plantsci.2011.02.011

Astier, J., Gross, I., and Durner, J. (2018). Nitric oxide production in plants: an update. *J. Exp. Bot.* 69, 3401–3411. doi: 10.1093/jxb/erx420

Balmer, Y., Vensel, W. H., Tanaka, C. K., Hurkman, W. J., Gelhaye, E., Rouhier, N., et al. (2004). Thioredoxin links redox to the regulation of fundamental processes of plant mitochondria. *Proc. Natl. Acad. Sci. U.S.A.* 101, 2642–2647. doi: 10.1073/pnas.0308583101

Barranco-Medina, S., Krell, T., Finkemeier, I., Sevilla, F., Lázaro, J. J., and Dietz, K. J. (2007). Biochemical and molecular characterization of the mitochondrial peroxiredoxin PsPrxII F from *Pisum sativum*. *Plant Physiol. Biochem.* 45, 729–739. doi: 10.1016/j.plaphy.2007.07.017

Barranco-Medina, S., Bernier-Villamor, L., Krell, T., Sevilla, F., Lázaro, J. J., and Dietz, K. J. (2008). Hexameric oligomerization of mitochondrial peroxiredoxin PrxII F and formation of an ultrahigh affinity complex with its electron donor thioredoxin Trx-*o*. *J. Exp. Bot.* 59, 3259–3269. doi: 10.1093/jxb/ern177

Barranco-Medina, S., Lázaro, J. J., and Dietz, K. J. (2009). The oligomeric conformation of peroxiredoxins links redox state to function. *FEBS Lett.* 583, 1809–1816. doi: 10.1016/j.febslet.2009.05.029

Bauwe, H., and Kolukisaoglu, U. (2003). Genetic manipulation of glycine decarboxylation. *J. Exp. Bot.* 54, 1523–1535. doi: 10.1093/jxb/erg171

Bedhomme, M., Adamo, M., Marchand, C. H., Couturier, J., Rouhier, N., Lemaire, S. D., et al. (2012). Glutathionylation of cytosolic glyceraldehyde-3-phosphate dehydrogenase from the model plant *Arabidopsis thaliana* is reversed by both glutaredoxins and thioredoxins in vitro. *Biochem. J.* 445, 337–347. doi: 10.1042/BJ20120505

Beer, S. M., Taylor, E. R., Brown, S. E., Dahm, C. C., Costa, N. J., Runswick, M. J., et al. (2004). Glutaredoxin 2 catalyzes the reversible oxidation and glutathionylation of mitochondrial membrane thiol proteins: implications for mitochondrial redox regulation and antioxidant defense. *J. Biol. Chem.* 279, 47939–47951. doi: 10.1074/jbc.M408011200

Begara-Morales, J. C., Sánchez-Calvo, B., Chaki, M., Valderrama, R., Mata-Pérez, C., López-Jaramillo, J., et al. (2014). Dual regulation of cytosolic ascorbate peroxidase (APX) by tyrosine nitration and S-nitrosylation. J. *Exp. Bot.* 65, 527–538. doi: 10.1093/jxb/ert396

Benhar, M., Forrester, M. T., Hess, D. T., and Stamler, J. S. (2008). Regulated protein denitrosylation by cytosolic and mitochondrial thioredoxins. *Science* 320, 1050–1054. doi: 10.1126/science.1158265

Braymer, J. J., and Lill, R. (2017). Iron–sulfur cluster biogenesis and trafficking in mitochondria. *J. Biol. Chem.* 292, 12754–12763. doi: 10.1074/jbc.R117.787101

Brennan, J. P., Miller, J. I., Fuller, W., Wait, R., Begum, S., Dunn, M. J., et al. (2006). The utility of N,N-biotinyl glutathione disulfide in the study of protein S-glutathiolation. *Mol. Cell Proteom.* 5, 215–225. doi: 10.1074/mcp.M500212-MCP200

Bykova, N. V., and Igamberdiev, A. U. (2016). "Redox state in plant mitochondria and its role in stress tolerance", in *Redox State as a Central Regulator of Plant-Cell Stress Responses*. Ed. D. K. Gupta, J. M. Palma and F. J. Corpas (Switzerland: Springer International Publishing), 93–115.

Calderón, A., Ortiz-Espín, A., Iglesias-Fernández, R., Carbonero, P., Pallardó, F. V., Sevilla, F., et al. (2017a). Thioredoxin (Trx*o*1) interacts with proliferating cell nuclear antigen (PCNA) and its overexpression affects the growth of tobacco cell culture. *Redox Biol.* 11, 688–700. doi: 10.1016/j.redox.2017.01.018

Calderón, A., Lázaro-Payo, A., Iglesias-Baena, I., Camejo, D., Lázaro, J. J., Sevilla, F., et al. (2017b). Glutathionylation of pea chloroplast 2-Cys Prx and mitochondrial PrxIIF affects their structure and peroxidase activity and sulfiredoxin deglutathionylates only the 2-Cys Prx. *Front. Plant Sci.* 8, 118. doi: 10.3389/fpls.2017.00118

Calderón, A., Sevilla, F., and Jiménez, A. (2018a). "Redox protein thioredoxins: function under salinity, drought and extreme temperature condition," in *Antioxidants and Antioxidant Enzymes in Higher Plants*. Ed. D. K. Gupta, J. M. Palma and F. J. Corpas (Switzerland: Springer International Publishing), 132–162.

Calderón, A., Sánchez-Guerrero, A., Ortiz, A., Martínez-Alcalá, I., Camejo, D., Jiménez, A., et al. (2018b). Lack of mitochondrial thioredoxin o1 is compensated by antioxidant components under salinity in *Arabidopsis thaliana* plants. *Physiol. Plant* 164, 251–267. doi: 10.1111/ppl.12708

Camejo, D., Romero-Puertas, M. C., Rodríguez-Serrano, M., Sandalio, L. M., Lázaro, J. J., Jiménez, A., et al. (2013). Salinity-induced changes in S-nitrosylation of pea mitochondrial proteins. *J. Proteom.* 79, 87–99. doi: 10.1016/j.jprot.2012.12.003

Camejo, D., Ortiz-Espín, A., Lázaro, J. J., Romero-Puertas, M. C., Lázaro-Payo, A., Sevilla, F., et al. (2015). Functional and structural changes in plant mitochondrial PrxIIF caused by NO. *J. Proteom.* 119, 112–125. doi: 10.1016/j.jprot.2015.01.022

Casagrande, S., Bonetto, V., Fratelli, M., Gianazza, E., Eberini, I., Massignan, T., et al. (2002). Glutathionylation of human thioredoxin: a possible crosstalk between the glutathione and thioredoxin systems. *Proc. Natl. Acad. Sci. U. S. A.* 99, 9745–9749. doi: 10.1073/pnas.152168599

Cejudo, F. J., Meyer, A. J., Reichheld, J.-P., Rouhier, N., Traverso, J. A., and Huber, S. C. (2014). Thiol-based redox homeostasis and signaling. *Front. Plant Sci.* 5, 266. doi: 10.3389/fpls.2014.00266

Chen, Y.-R., Chen, C. H.-L., Pfeiffer, D. R., and Zweier, J. L. (2007). Mitochondrial complex II in the post-ischemic heart. Oxidative injury and the role of

proteins-glutathionylation. *J. Biol. Chem.* 282, 32640–32654. doi: 10.1074/jbc.M702294200

Chew, O., Whelan, J., and Millar, A. H. (2003). Molecular definition of the ascorbate-glutathione cycle in Arabidopsis mitochondria reveals dual targeting of antioxidant defenses in plants. *J. Biol. Chem.* 278, 46869–46877. doi: 10.1074/jbc.M307525200

Ciofi-Baffoni, S., Nasta, V., and Banci, L. (2018). Protein networks in the maturation of human iron–sulfur proteins. *Metallomics* 10, 4972. doi: 10.1039/C7MT00269F

Corpas, F. J., and Palma, J. M. (2018). Nitric oxide on/off in fruit ripening. *Plant Biol.* 20, 805–807. doi: 10.1111/plb.12852

Corpas, F. J., and Palma, J. M. (2020). H_2S signaling in plants and applications in agriculture. *J. Adv. Res.* 24, 131–137. doi: 10.1016/j.jare.2020.03.011

Corpas, F. J., Alché, J. D., and Barroso, J. B. (2013). Current overview of S-nitrosoglutathione (GSNO) in higher plants. *Front. Plant Sci.* 4, 126. doi: 10.3389/fpls.2013.00126

Corpas, F. J., Río, L. A. D., and Palma, J. M. (2019a). Impact of Nitric Oxide (NO) on the ROS Metabolism of Peroxisomes. *Plants (Basel)* 8, e37. doi: 10.3390/plants8020037

Corpas, F. J., González-Gordo, S., Cañas, A., and Palma, J. M. (2019b). Nitric oxide and hydrogen sulfide in plants: which comes first? *J. Exp. Bot.* 70, 4391–4404. doi: 10.1093/jxb/erz031

Cvetkovska, M., and Vanlerberghe, G. C. (2012). Alternative oxidase impacts the plant response to biotic stress by influencing the mitochondrial generation of reactive oxygen species. *Plant Cell Environ.* 36, 721–732. doi: 10.1111/pce.12009

Da Fonseca-Pereira, P., Souza, P. V. L., Hou, L. Y., Schwab, S., Geigenberger, P., Nunes-Nesi, A., et al. (2019a). Thioredoxin h2 contributes to the redox regulation of mitocondrial photorespiratory metabolism. *Plant Cell Environ.* 43, 188–208. doi: 10.1111/pce.13640

Da Fonseca-Pereira, P., Daloso, D. M., Gago, J., Magnum, F., Silva, O., Condori-Apfata, J. A., et al. (2019b). The Mitochondrial Thioredoxin System Contributes to the Metabolic Responses Under Drought Episodes in Arabidopsis. *Plant Cell Physiol.* 60, 213–229. doi: 10.1093/pcp/pcy194

Da Fonseca-Pereira, P., Daloso, D. M., Gago, J., Nunes-Nesi, A., and Araújo, W. L. (2019c). On the role of the plant mitochondrial thioredoxin system during abiotic stress. *Plant Signal. Behav.* 14, 1592536. doi: 10.1080/15592324.2019.1592536

Daloso, D. M., Müller, K., Obata, T., Florian, A., Tohge, T., Bottcher, A., et al. (2015). Thioredoxin, a master regulator of the tricarboxylic acid cycle in plant mitochondria. *Proc. Natl. Acad. Sci. U.S.A.* 112, 1392–1400. doi: 10.1073/pnas.1424840112

Day, D. A., Millar, A. H., Wiskich, J. T., and Whelan, J. (1994). Regulation of Alternative Oxidase Activity by Pyruvate in Soybean Mitochondria. *Plant Physiol.* 106, 1421–1427. doi: 10.1104/pp.106.4.1421

Delorme-Hinoux, V., Bangash, S. A., Meyer, A. J., and Reichheld, J. P. (2016). Nuclear thiol redox systems in plants. *Plant Sci.* 243, 84–95. doi: 10.1016/j.plantsci.2015.12.002

Del-Saz, N. F., Florez-Sarasa, I., Clemente-Moreno, M. J., Mhadhbi, H., Flexas, J., Fernie, A. R., et al. (2016). Salinity tolerance is related to cyanide-resistant alternative respiration in *Medicago truncatula* under sudden severe stress. *Plant Cell Environ.* 39, 2361–2369. doi: 10.1111/pce.12776

Del-Saz, N. F., Ribas-Carbo, M., McDonald, A. E., Lambers, H., Fernie, A. R., and Florez-Sarasa, I. (2017). An *In Vivo* Perspective of the Role(s) of the Alternative Oxidase Pathway. *Trends Plant Sci.* 23, 206–219. doi: 10.1016/j.tplants.2017.11.006

Dietz, K.-J. (2011). Peroxiredoxins in plants and cyanobacteria. *Antioxid. Redox Signal.* 15, 1129–1159. doi: 10.1089/ars.2010.3657

Dixon, D. P., Skipsey, M., Grundy, N. M., and Edwards, R. (2005). Stress-induced protein Sglutathionylation in Arabidopsis. *Plant Physiol.* 138, 2233–2244. doi: 10.1104/pp.104.058917

Drapier, J. C. (1997). Interplay between NO and [Fe-S] clusters: relevance to biological systems. *Methods* 11, 319–329. doi: 10.1006/meth.1996.0426

Dumont, S., and Rivoal, J. (2019). Consequences of Oxidative Stress on Plant Glycolytic and Respiratory Metabolism. *Front. Plant Sci.* 10, 166. doi: 10.3389/fpls.2019.00166

Eisenhut, M., Roelland, M. S., and Weber, A. P. M. (2019). Mechanistic understanding of photorespiration paves the way to a new green revolution. *New Phytol.* 223, 1762–1769. doi: 10.1111/nph.15872

Engel, N., van den Daele, K., Kolukisaoglu, U., Morgenthal, K., Weckwerth, W., Pärnik, T., et al. (2007). Deletion of glycine decar-boxylase in Arabidopsis is lethal under non photorespiratory conditions. *Plant Physiol.* 144, 1328–1335. doi: 10.1104/pp.107.099317

Fares, A., Rossignol, M., and Peltier, J. B. (2011). Proteomics investigation of endogenous S-nitrosylation in Arabidopsis. *Biochem. Biophys. Res. Commun.* 416, 331–336. doi: 10.1016/j.bbrc.2011.11.036

Fenech, M., Amaya, I., Valpuesta, V., and Botella, M. A. (2019). Vitamin C Content in Fruits: Biosynthesis and Regulation. *Front. Plant Sci.* 9:2006:2006. doi: 10.3389/fpls.2018.02006

Feng, J., Chen, L., and Zuo, L. (2019). Protein S-Nitrosylation in plants: Current progresses and challenges. *J. Integr. Plant Biol.* 61, 1206–1223. doi: 10.1111/jipb.12780

Fernández-García, N., Martí, M. C., Jiménez, A., Sevilla, F., and Olmos, E. (2009). Sub-cellular distribution of glutathione in an Arabidopsis mutant (vtc1) deficient in ascorbate. *J. Plant Physiol.* 166, 2004–2012. doi: 10.1016/j.jplph.2009.06.006

Filipovic, M. R., and Jovanović, V. M. (2017). More than just an intermediate: hydrogen sulfide signalling in plants. *J. Exp. Bot.* 68, 4733–4736. doi: 10.1093/jxb/erx352

Finkemeier, I., Goodman, M., Lankemeyer, P., Kandlbinder, A., Sweetlove, L. J., and Dietz, K. J. (2005). The mitochondrial type II peroxiredoxin F is essential for redox homeostasis and root growth of *Arabidopsis thaliana* under stress. *J. Biol. Chem.* 280, 12168–12180. doi: 10.1074/jbc.M413189200

Florez-Sarasa, I., Obata, T., Del-Saz, N. S. F. N., Reichheld, J. P., Meyer, E. H., Rodriguez-Concepcion, M., et al. (2019). The lack of mitochondrial thioredoxin TRX*o*1 affects *in vivo* alternative oxidase activity and carbon metabolism under different light conditions. *Plant Cell Physiol.* 60, 2369–2381. doi: 10.1093/pcp/pcz123

Foyer, C. H., and Noctor, G. (2011). Ascorbate and Glutathione: The Heart of the Redox Hub. *Plant Physiol.* 155, 2–18. doi: 10.1104/pp.110.167569

Foyer, C. H., and Noctor, G. (2013). Redox signaling in plants. *Antioxid. Redox Signal.* 18, 2087–2090. doi: 10.1089/ars.2013.5278

Foyer, C. H., Baker, A., Wright, M., Sparkes, I. A., Mhamdi, A., Schippers, J. H. M., et al. (2020). On the move: redox-dependent protein relocation in plants. *J. Exp. Bot.* 71, 620–631. doi: 10.1093/jxb/erz330

Fratelli, M., Demol, H., Puype, M., Casagrande, S., Villa, P., Eberini, I., et al. (2003). Identification of proteins undergoing glutathionylation in oxidatively stressed hepatocytes and hepatoma cells. *Proteomics* 3, 1154–1161. doi: 10.1002/pmic.200300436

Gama, O., Keech, F., Eymery, F., Finkemeier, I., Gelhaye, E., Gardeström, P., et al. (2007). The mitochondrial type II peroxiredoxin from poplar. *Physiol. Plant* 129, 196–206. doi: 10.1111/j.1399-3054.2006.00785.x

Gao, X. H., Bedhomme, M., Veyel, D., Zaffagnini, M., and Lemaire, S. D. (2009). Methods for Analysis of Protein Glutathionylation and their Application to Photosynthetic Organisms. *Mol. Plant* 2, 218–235. doi: 10.1093/mp/ssn072

García, J., Han, D., Sancheti, H., Yap, L. P., Kaplowitz, N., and Cadenas, E. (2010). Regulation of mitochondrial glutathione redox status and protein glutathionylation by respiratory substrates. *J. Biol. Chem.* 285, 39646–39654. doi: 10.1074/jbc.M110.164160

García, I., Gotor, C., and Romero, L. C. (2015). "Cysteine homeostasis," in *Amino Acids in Higher Plants*. Ed. J. P. F. D'Mello (Wallingford, UK: CABI Publishing), 219–233.

Geigenberger, P., Thormählen, I., Daloso, D. M., and Fernie, A. R. (2017). The unprecedented versatility of the plant thioredoxin system. *Trends Plant Sci.* 22, 249–262. doi: 10.1016/j.tplants.2016.12.008

Gelhaye, E., Rouhier, N., Gérard, J., Jolivet, Y., Gualberto, J., Navrot, N., et al. (2004). A specific form of thioredoxin h occurs in plant mitochondria and regulates the alternative oxidase. *Proc. Natl. Acad. Sci. U.S.A.* 101, 14545–14550. doi: 10.1073/pnas.0405282101

Gleason, C., Huang, S., Thatcher, L. F., Foley, R. C., Anderson, C. R., Carroll, A. J., et al. (2011). Mitochondrial complex II has a key role in mitochondrial-derived reactive oxygen species influence on plant stress gene regulation and defense. *Proc. Natl. Acad. Sci. U.S.A.* 108, 10768–10773. doi: 10.1073/pnas.1016060108

Gotor, C., García, I., Aroca, Á., Laureano-Marín, A. M., Arenas-Alfonseca, L., Jurado-Flores, A., et al. (2019). Signaling by hydrogen sulfide and cyanide through post-translational modification. *J. Exp. Bot.* 70, 4251–4265. doi: 10.1093/jxb/erz225

Guo, F. Q., and Crawford, N. M. (2005). Arabidopsis nitric oxide synthase 1 is targeted to mitochondria and protects against oxidative damage and dark-induced senescence. *Plant Cell* 17, 3436–3450. doi: 10.1105/tpc.105.037770

Guo, Z., Liang, Y., Yan, J., Yang, E., Li, K., and Xu, H. (2018). Physiological response and transcription profiling analysis reveals the role of H_2S in alleviating excess nitrate stress tolerance in tomato roots. *Plant Physiol. Biochem.* 124, 59–69. doi: 10.1016/j.plaphy.2018.01.006

Gupta, K. J., and Igamberdiev, A. U. (2016). Reactive nitrogen species in mitochondria and their implications in plant energy status and hypoxic stress tolerance. *Front. Plant Sci.* 7, 369. doi: 10.3389/fpls.2016.00369

Gupta, K. J., Shah, J. K., Brotman, Y., Jahnke, K., Willmitzer, L., Kaiser, W. M., et al. (2012). Inhibition of aconitase by nitric oxide leads to induction of the alternative oxidase and to a shift of metabolism towards biosynthesis of amino acids. *J. Exp. Bot.* 63, 1773–1784. doi: 10.1093/jxb/ers053

Hägglund, P., Bunkenborg, J., Maeda, K., and Svensson, B. (2008). Identification of thioredoxin disulfide targets using a quantitative proteomics approach based on isotope-coded affinity tags. *J. Prot. Res.* 7, 5270–5276. doi: 10.1021/pr800633y

Han, D., Canali, R., García, J., Aguilera, R., Gallaher, T. K., and Cadenas, E. (2005). Sites and mechanisms of aconitase inactivation by peroxynitrite: modulation by citrate and glutathione. *Biochemistry* 44, 11986–11996. doi: 10.1021/bi0509393

Hernández, J. A., Corpas, F. J., Gómez, M., del Río, L. A., and Sevilla, F. (1993). Salt-induced oxidative stress mediated by activated oxygen species in pea leaf mitochondria. *Physiol. Planta* 89, 103–110. doi: 10.1111/j.1399-3054.1993.tb01792.x

Hess, D. T., Matsumoto, A., Kim, S. O., Marshall, H. E., and Stamler, J. S. (2005). Protein S-nitrosylation: Purview and parameters. *Nat. Rev. Mol. Cell Biol.* 6, 150–166. doi: 10.1038/nrm1569

Holzmeister, C., Fröhlich, A., Sarioglu, H., Bauer, N., Durner, J., and Lindermayr, C. (2011). Proteomic analysis of defense response of wildtype *Arabidopsis thaliana* and plants with impaired NO-homeostasis. *Proteomics* 11, 1664–1683. doi: 10.1002/pmic.201000652

Horling, F., König, J., and Dietz, K. J. (2002). Type II peroxiredoxin C, a member of the peroxiredoxin family of *Arabidopsis thaliana*: its expression and activity in comparison with other peroxiredoxins. *Plant Physiol. Biochem.* 40, 491–499. doi: 10.1016/S0981-9428(02)01396-7

Horling, F., Lamkemeyer, P., Konig, J., Finkemeier, I., Kandlbinder, A., Baier, M., et al. (2003). Divergent light, ascorbate, and oxidative stress-dependent regulation of expression of the peroxiredoxin gene family in Arabidopsis. *Plant Physiol.* 131, 317–325. doi: 10.1104/pp.010017

Hoshida, H., Tanaka, K., Hibino, T., Hayashi, Y., Tanaka, A., Takabe, T., et al. (2000). Enhanced tolerance to salt stress in transgenic rice that overexpresses chloroplast glutamine synthetase. *Plant Mol. Biol.* 43, 103–111. doi: 10.1023/A:1006408712416

Hu, J., Huang, X., Chen, L., Sun, X., Lu, C., Zhang, L., et al. (2015). Site-specific nitrosoproteomic identification of endogenously S-nitrosylated proteins in Arabidopsis. *Plant Physiol.* 167, 1731–1746. doi: 10.1104/pp.15.00026

Huang, J., Niazi, A. K., Young, D., Rosado, L. A., Vertommen, D., and Bodra, N. (2017). Self-protection of cytosolic malate dehydrogenase against oxidative stress in Arabidopsis. *J. Exp. Bot.* 69, 3491–3505. doi: 10.1093/jxb/erx396

Huang, J., Willems, P., Wei, B., Tian, C., Ferreira, R. B., Bodra, N., et al. (2019). Mining for protein S-sulfenylation in Arabidopsis uncovers redox-sensitive sites. *PNAS* 116, 21256–21261. doi: 10.1073/pnas.1906768116

Hurd, T. R., Raquejo, R., Filipovska, A., Brown, S., Prime, T. A., Robinson, A. J., et al. (2008). Complex I within oxidatively-stressed bovine heart mitochondria is glutathionylated on Cys-531 and Cys-704 of the 75-kDa subunit: potential role of Cys residues in decreasing oxidative damage. *J. Biol. Chem.* 283, 24801–24815. doi: 10.1074/jbc.M803432200

Iglesias-Baena, I., Barranco-Medina, S., Lázaro-Payo, A., López-Jaramillo, F. J., Sevilla, F., and Lázaro, J. J. (2010). Characterization of plant sulfiredoxin and role of sulphinic form of 2-Cys peroxiredoxin. *J. Exp. Bot.* 6, 1509–1521. doi: 10.1093/jxb/erq016

Iglesias-Baena, I., Barranco-Medina, S., Sevilla, F., and Lázaro, J. J. (2011). The dual targeted plant sulfiredoxin retroreduces the sulfinic form of atypical mitochondrial peroxiredoxin. *Plant Physiol.* 155, 944–955. doi: 10.1104/pp.110.166504

Ischiropoulos, H., Zhu, L., Chen, J., Tsai, M., Martin, J. C., and Smith, C. D. (1992). Peroxynitrite-mediated tyrosine nitration catalyzed by superoxide dismutase. *Arch. Biochem. Biophys.* 298, 431–437. doi: 10.1016/0003-9861(92)90431-u

Jaffrey, S. R., and Snyder, S. H. (2001). The biotin switch method for the detection of S-nitrosylated proteins. *Sci. Signal.* 2001, pl1. doi: 10.1126/stke.2001.86.pl1

Jayawardhane, J., Cochrane, D. W., Vyas, P. V., Bykova, N. V., Vanlerberghe, G. C., and Igamberdiev, A. U. (2020). Roles for Plant Mitochondrial Alternative Oxidase Under Normoxia, Hypoxia, and Reoxygenation Conditions. *Front. Plant Sci.* 11, 566. doi: 10.3389/fpls.2020.00566

Jiménez, A., Hernández, J. A., del Rio, L. A., and Sevilla, F. (1997). Evidence for the Presence of the Ascorbate-Glutathione Cycle in Mitochondria and Peroxisomes of Pea Leaves. *Plant Physiol.* 114, 275–284. doi: 10.1104/pp.114.1.275

Jiménez, A., Hernández, J. A., Barcelo, A. R., Sandalio, L. M., del Rio, L. A., and Sevilla, F. (1998). Mitochondrial and peroxisomal ascorbate peroxidase of pea leaves. *Physiol. Planta* 104, 687–692. doi: 10.1034/j.1399-3054.1998.1040424.x

Jin, Z., Wang, Z., Ma, Q., Sun, L., Zhang, L., Liu, Z., et al. (2017). Hydrogen sulfide mediates ion fluxes inducing stomatal closure in response to drought stress in *Arabidopsis thaliana*. *Plant Soil* 419, 141–152. doi: 10.1007/s11104-017-3335-5

Keilin, D., and Hartree, E. F. (1937). Reaction of nitric oxide with haemoglobin and methaemoglobin. *Nature* 139, 548. doi: 10.1038/139548a0

Kil, I. S., and Park, J.-W. (2005). Regulation of Mitochondrial NADP+-dependent Isocitrate Dehydrogenase Activity by Glutathionylation. *J. Biol. Chem.* 280, 10846–10854. doi: 10.1074/jbc.M411306200

Kitajima, S., Kurioka, M., Yoshimoto, T., Shindo, M., Kanaori, K., Tajima, K., et al. (2008). A cysteine residue near the propionate side chain of heme is the radical site in ascorbate peroxidase. *FEBS J.* 275, 470–480. doi: 10.1111/j.1742-4658.2007.06214.x

Kolbert, Zs., Barroso, J. B., Brouquisse, R., Corpas, F. J., Gupta, K. J., Lindermayr, C., et al. (2019). A forty year journey: The generation and roles of NO in plants. *Nitric. Oxide* 93, 53–70. doi: 10.1016/j.niox.2019.09.006

Konrad, A., Banze, M., and Follman, H. (1996). Mitochondria of plant leaves contain two thioredoxins. Completion of the thioredoxin profile of higher plants. *J. Plant Physiol.* 149, 317–321. doi: 10.1016/S0176-1617(96)80128-3

Laloi, C., Rayapuram, N., Chartier, Y., Grienenberger, J. M., Bonnard, G., and Meyer, Y. (2001). Identification and characterization of a mitochondrial thioredoxin system in plants. *Proc. Natl. Acad. Sci. U.S.A.* 98, 14144–14149. doi: 10.1073/pnas.241340898

Lamotte, O., Bertoldo, J. B., Besson-Bard, A., Rosnoblet, C., Aimé, S., Hichami, S., et al. (2015). Protein S-nitrosylation: specificity and identification strategies in plants. *Front. Chem.* 2:114:114. doi: 10.3389/fchem.2014.00114

Lázaro, J. J., Jiménez, A., Camejo, D., Iglesias-Baena, I., Martí, M., Lázaro-Payo, A., et al. (2013). Dissecting the integrative antioxidant and redox systems in plant mitochondria. Effect of stress and S-nitrosylation. *Front. Plant Sci.* 4, 460. doi: 10.3389/fpls.2013.00460

Lee, J. H., Yang, E. S., and Park, J. W. (2003). Inactivation of NADP+-dependent Isocitrate Dehydrogenase by Peroxynitrite: implications for cytotoxicity and alcohol-induced liver injury. *J. Biol. Chem.* 27, 51360–51371. doi: 10.1074/jbc.M302332200

Leferink, N. G. H., van Duijn, E., Barendregt, A., Heck, A. J. R., and van Berkel, W. J. H. (2009). Galactonolactone Dehydrogenase Requires a Redox-Sensitive Thiol for Optimal Production of Vitamin C. *Plant Physiol.* 150, 596–605. doi: 10.1104/pp.109.136929

Leitner, M., Vandelle, E., Gaupels, F., Bellin, D., and Delledonne, M. (2009). NO signals in the haze. Nitric oxide signalling in plant defence. *Curr. Opin. Plant Biol.* 12, 451–458. doi: 10.1016/j.pbi.2009.05.012

Liebthal, M., Maynard, D., and Dietz, K.-J. (2018). Peroxiredoxins and Redox Signaling in Plants. *Antioxid. Redox Signal.* 28, 609–624. doi: 10.1089/ars.2017.7164

Lindermayr, C., Saalbach, G., and Durner, J. (2015). Proteomic identification of S-Nitrosylated proteins in Arabidopsis. *Plant Physiol.* 137, 921–930. doi: 10.1104/pp.104.058719

Lindermayr, C. (2018). Crosstalk between reactive oxygen species and nitric oxide in plants: Key role of S-nitrosoglutathione reductase. *Free Radic. Biol. Med.* 122, 110–115. doi: 10.1016/j.freeradbiomed.2017.11.027

Liu, L., Hausladen, A., Zeng, M., Que, L., Heitman, J., and Stamler, J. S. (2001). A metabolic enzyme for S-nitrosothiol conserved from bacteria to humans. *Nature* 410, 490–494. doi: 10.1038/35068596

Locato, V., Cimini, S., and De Gara, L. (2018). ROS and redox balance as multifaceted players of cross-tolerance: epigenetic and retrograde control of gene expression. *J. Exp. Bot.* 69, 3373–3391. doi: 10.1093/jxb/ery168

Mailloux, R. J., Jin, X., and Willmore, W. G. (2014). Redox regulation of mitochondrial function with emphasis on cysteine oxidation reactions. *Redox Biol.* 2, 123–139. doi: 10.1016/j.redox.2013.12.011

Marcus, F., Chamberlain, S. H., Che, C., Masiarz, F. R., Shin, S., Yee, B. C., et al. (1991). Plant thioredoxin h: an animal-like thioredoxin occurring in multiple cell compartments. *Arch. Biochem. Biophys.* 287, 195–198. doi: 10.1016/0003-9861(91)90406-9

Martí, M. C., Olmos, E., Calvete, J. J., Díaz, I., Barranco-Medina, S., Whelan, J., et al. (2009). Mitochondrial and nuclear localization of a novel pea thioredoxin: identification of its mitochondrial target proteins. *Plant Physiol.* 150, 646–657. doi: 10.1104/pp.109.138073

Martí, M. C., Florez-Sarasa, I., Camejo, D., Ribas-Carbó, M., Lázaro, J. J., Sevilla, F., et al. (2011). Response of the mitochondrial antioxidant redox system and respiration to salinity in pea plants. *J. Exp. Bot.* 62, 3863–3874. doi: 10.1093/jxb/err076

Martí, M. C., Florez-Sarasa, I., Camejo, D., Pallol, B., Ortiz, A., Ribas-Carbó, M., et al. (2012). Response of mitocondrial antioxidant system and respiratory pathways to reactive nitrogen species in pea leaves. *Physiol. Plant.* 147, 194–206. doi: 10.1111/j.1399-3054.2012.01654.x

Martínez-Ruiz, A., Araújo, I. M., Izquierdo-Álvarez, A., Hernansanz-Agustín, P., Lamas, S., and Serrador, J. (2013). Specificity in S-nitrosylation: A short-range mechanism for NO signaling? *Antioxid. Redox Signal.* 19, 1220–1235. doi: 10.1089/ars.2012.5066

Mata-Pérez, C., Sánchez-Calvo, B., Padilla, M. N., Begara-Morales, J. C., Valderrama, R., Corpas, F. J., et al. (2017). Nitro-fatty acids in plant signaling: New key mediators of nitric oxide metabolism. *Redox Biol.* 11, 554–561. doi: 10.1016/j.redox.2017.01.002

Maxwell, D. P., Wang, Y., and McIntosh, L. (1999). The alternative oxidase lowers mitochondrial reactive oxygen production in plant cells. *Proc. Natl. Acad. Sci. U.S.A.* 96, 8271–8276. doi: 10.1016/0003-9861(91)90406-9

Meyer, Y., Belin, C., Delorme-Hinoux, V., Reichheld, J. P., and Riondet, C. (2012). Thioredoxin and glutaredoxin systems in plants: molecular mechanisms, crosstalks, and functional significance. *Antioxid. Redox Signal.* 17, 1124–1160. doi: 10.1089/ars.2011.4327

Mhamdi, A., and Van Breusegem, F. (2018). Reactive oxygen species in plant development. *Development* 145, dev164376. doi: 10.1242/dev.164376

Michelet, L., Zaffagnini, M., Marchand, C., Collin, V., Decottignies, P., Tsan, P., et al. (2005). Glutathionylation of chloroplast thioredoxin f is a redox signaling mechanism in plants. *Proc. Natl. Acad. Sci. U. S. A.* 102, 16478–16483. doi: 10.1073/pnas.0507498102

Millar, A. H., Whelan, J., Soole, K. L., and Day, D. A. (2011). Organization and regulation of mitochondrial respiration in plants. *Annu. Rev. Plant Biol.* 62, 79–104. doi: 10.1146/annurev-arplant-042110-103857

Mnatsakanyan, R., Markoutsa, S., Walbrunn, K., Roos, A., Verhelst, S. H. L., and Zahedi, R. P. (2019). Proteome-wide detection of S-nitrosylation targets and motifs using bioorthogonal cleavable-linker-based enrichment and switch technique. *Nat. Commun.* 10, 2195. doi: 10.1038/s41467-019-10182-4

Møller, I. M., Igamberdiev, A. U., Bykova, N. V., Finkemeier, I., Rasmusson, L. G., and Schwarzländer, M. (2020). Matrix Redox Physiology Governs the Regulation of Plant Mitochondrial Metabolism through Posttranslational Protein Modifications. *Plant Cell* 32, 573–594. doi: 10.1105/tpc.19.00535

Møller, I. M. (2015). Mitochondrial metabolism is regulated by thioredoxin. *Proc. Natl. Acad. Sci. U.S.A.* 112, 3180–3181. doi: 10.1073/pnas.1502425112

Nietzel, T., Mostertz, J., Hochgräfe, F., and Schwarzländer, M. (2017). Redox regulation of mitochondrial proteins and proteomes by cysteine thiol switches. *Mitochondrion* 33, 72–83. doi: 10.1016/j.mito.2016.07.010

Nietzel, T., Mostertz, J., Ruberti, C., Née, G., Fuchs, P., Wagner, S., et al. (2020). Redox-mediated kickstart of mitochondrial energy metabolism drives resource-efficient seed germination. *Proc. Natl. Acad. Sci. U.S.A.* 117, 741–751. doi: 10.1073/pnas.1910501117

Niture, S. K., Velu, C. S., Bailey, N. I., and Srivenugopal, K. S. (2005). S-thiolation mimicry: quantitative and kinetic analysis of redox status of protein cysteines by glutathione-affinity chromatography. *Arch. Biochem. Biophys.* 444, 174–184. doi: 10.1016/j.abb.2005.10.013

Noctor, G., De Paepe, R., and Foyer, C. H. (2007). Mitochondrial redox biology and homeostasis in plants. *Trends Plant Sci.* 12, 125–134. doi: 10.1016/j.tplants.2007.01.005

Noctor, G., Lelarge-Trouverie, C., and Mhamdi, A. (2015). The metabolomics of oxidative stress. *Phytochemistry* 112, 33–53. doi: 10.1016/j.phytochem.2014.09.002

Noguera-Mazon, V., Lemoine, J., Walker, O., Rouhier, N., Salvador, A., Jacquot, J. P., et al. (2006). Glutathionylation induces the dissociation of 1-Cys D-peroxiredoxin non-covalent homodimer. *J. Biol. Chem.* 281, 31736–31742. doi: 10.1074/jbc.M602188200

Ojeda, V., Pérez-Ruiz, J. M., González, M., Nájera, V. A., Sahrawy, M., Serrato, A. J., et al. (2017). NADPH thioredoxin reductase C and thioredoxins act concertedly in seedling development. *Plant Physiol.* 174, 1436–1448. doi: 10.1104/pp.17.00481

Ortega-Galisteo, A. P., Rodríguez-Serrano, M., Pazmiño, D. M., Gupta, D. K., Sandalio, L. M., and Romero-Puertas, M. C. (2012). S-Nitrosylated proteins in pea (*Pisum sativum* L.) leaf peroxisomes: changes under abiotic stress. *J. Exp. Bot.* 63, 2089–2103. doi: 10.1093/jxb/err414

Ortiz-Espín, A., Locato, V., Camejo, D., Schiermeyer, A., De Gara, L., Sevilla, F., et al. (2015). Over-expression of Trx*o*1 increases the viability of tobacco BY-2 cells under H_2O_2 treatment. *Ann. Bot.* 116, 571–582. doi: 10.1093/aob/mcv076

Ortiz-Espín, A., Iglesias-Fernández, R., Calderón, A., Carbonero, P., Sevilla, F., and Jiménez, A. (2017). Mitochondrial AtTrx*o*1 is transcriptionally regulated by AtbZIP9 and AtAZF2 and affects seed germination under saline conditions. *J. Exp. Bot.* 68, 1025–1038. doi: 10.1093/jxb/erx012

Palmieri, M. C., Lindermayr, C., Bauwe, H., Steinhauser, C., and Durner, J. (2010). Regulation of plant glycine decarboxylase by s-nitrosylation and glutathionylation. *Plant Physiol.* 152, 1514–1528. doi: 10.1104/pp.109.152579

Paul, B. D., and Snyder, S. H. (2012). H_2S signaling through protein sulfhydration and beyond. *Nat. Rev. Mol. Cell Biol.* 13, 499–507. doi: 10.1038/nrm3391

Pérez-Pérez, M. E., Mauriès, A., Maes, A., Tourasse, N. J., Hamon, M., Lemaire, S. D., et al. (2017). The deep thioredoxome in *Chlamydomonas reinhardtii*: New insights into redox regulation. *Mol. Plant* 10, 1107–1125. doi: 10.1016/j.molp.2017.07.009

Pulido, P., Cazalis, R., and Cejudo, F. J. (2009). An antioxidant redox system in the nucleus of wheat seed cells suffering oxidative stress. *Plant J.* 57, 132–145. doi: 10.1111/j.1365-313X.2008.03675.x

Purvis, A. C. (1997). Role of the alternative oxidase in limiting superoxide production in plant mitochondria. *Physiol. Plant* 100, 165–170. doi: 10.1111/j.1399-3054.1997.tb03468.x

Puyaubert, J., Fares, A., Reze, N., Peltier, J. B., and Baudouin, E. (2014). Identification of endogenously S-nitrosylated proteins in Arabidopsis plantlets: effect of cold stress on cysteine nitrosylation level. *Plant Sci.* 215-216, 150–156. doi: 10.1016/j.plantsci.2013.10.014

Qiu, C., Sun, J., Wang, Y., Sun, L., Xie, H., Ding, Y., et al. (2019). First nitrosoproteomic profiling deciphers the cysteine S-nitrosylation involved in multiple metabolic pathways of tea leaves. *Sci. Rep.* 9, 17525. doi: 10.1038/s41598-019-54077-2

Rasmusson, A. G., and Wallström, S. V. (2010). Involvement of mitochondria in the control of plant cell NAD(P)H reduction levels. *Biochem. Soc Trans.* 38, 661–666. doi: 10.1042/bst0380661

Reichheld, J. P., Meyer, E., Khafif, M., Bonnard, G., and Meyer, Y. (2005). AtNTRB is the major mitochondrial thioredoxin reductase in *Arabidopsis thaliana*. *FEBS Lett.* 579, 337–342. doi: 10.1016/j.febslet.2004.11.094

Reinholdt, O., Schwab, S., Zhang, Y., Reichheld, J.-P., Fernie, A. R., Hagemann, M., et al. (2019a). Redox-regulation of photorespiration through mitochondrial thioredoxin *o*1. *Plant Physiol.* 181, 442–457. doi: 10.1104/pp.19.00559

Reinholdt, O., Bauwe, H., Hagemann, M., and Timm, S. (2019b). Redox-regulation of mitochondrial metabolism through thioredoxin *o*1 facilitates light induction of photosynthesis. *Plant Signal. Behav.* 14, 1674607. doi: 10.1080/15592324.2019.1674607

Rey, P., Becuwe, N., Barrault, M. B., Rumeau, D., Havaux, M., Biteau, B., et al. (2007). The *Arabidopsis thaliana* sulfiredoxin is a plastidic cysteine-sulfinic

acid reductase involved in the photooxidative stress response. *Plant J.* 49, 505–514. doi: 10.1111/j.1365-313X.2006.02969.x

Riemenschneider, A., Wegele, R., Schmidt, A., and Papenbrock, J. (2005). Isolation and characterization of a D-cysteine desulfhydrase protein from *Arabidopsis thaliana*. *FEBS J.* 272, 1291–1304. doi: 10.1111/j.1742-4658.2005.04567.x

Rizza, S., Montagna, C., Cardaci, S., Maiani, E., Di Giacomo, G., Sanchez-Quiles, V., et al. (2016). S-nitrosylation of the Mitochondrial Chaperone TRAP1 Sensitizes Hepatocellular Carcinoma Cells to Inhibitors of Succinate Dehydrogenase. *Cancer Res.* 76, 4170–4182. doi: 10.1158/0008-5472.CAN-15-2637

Rodríguez-Ruiz, M., Mateos, R. M., Codesido, V., Corpas, F. J., and Palma, J. M. (2017). Characterization of the galactono-1,4-lactone dehydrogenase from pepper fruits and its modulation in the ascorbate biosynthesis. *Role Nitric. Oxide Redox Biol.* 12, 171–181. doi: 10.1016/j.redox.2017.02.009

Romero-Puertas, M. C., and Sandalio, L. M. (2016). Nitric Oxide Level Is Self-Regulating and Also Regulates Its ROS Partners. *Front. Plant Sci.* 7, 316. doi: 10.3389/fpls.2016.00316

Romero-Puertas, M. C., Laxa, M., Matte, A., Zaninotto, F., Finkemeier, I., Jones, A. M., et al. (2007). S-Nitrosylation of peroxiredoxin II E promotes peroxynitrite-mediated tyrosine nitration. *Plant Cell* 19, 4120–4130. doi: 10.1105/tpc.107.055061

Romero-Puertas, M. C., Campostrini, N., Matte, A., Righetti, P. G., Perazzolli, M., Zolla, L., et al. (2008). Proteomic analysis of S-nitrosylated proteins in *Arabidopsis thaliana* undergoing hypersensitive response. *Proteomics* 8, 1459–1469. doi: 10.1002/pmic.200700536

Sánchez-Guerrero, A., Fernández del-Saz, N., Florez-Sarasa, I., Ribas-Carbó, M., Ferni, A. R., Jiménez, A., et al. (2019). Coordinated responses of mitochondrial antioxidative enzymes, respiratory pathways and metabolism in *Arabidopsis thaliana* thioredoxin trxo1 mutants under salinity. *Env. Exp. Bot.* 162, 212–222. doi: 10.1016/j.envexpbot.2019.02.026

Sandalio, L. M., Gotor, C., Romero, L. C., and Romero-Puertas, M. C. (2019). Multilevel regulation of peroxisomal proteome by posttranslational modifications. *Int. J. Mol. Sci.* 20, 4881. doi: 10.3390/ijms20194881

Schimmeyer, J., Bock, R., and Meyer, E. H. (2016). L-Galactono-1,4-lactone dehydrogenase is an assembly factor of the membrane arm of mitochondrial complex I in Arabidopsis. *Plant Mol. Biol.* 90, 117–126. doi: 10.1007/s11103-015-0400-4

Schmidtmann, E., König, A.-C., Orwat, A., Leister, D., Hartl, M., and Finkemeier, I. (2014). Redox regulation of Arabidopsis mitochondrial citrate synthase. *Mol. Plant* 7, 156–169. doi: 10.1093/mp/sst144

Scuffi, D., Álvarez, C., Laspina, N., Gotor, C., Lamattina, L., and García-Mata, C. (2014). Hydrogen sulfide generated by L-cysteine desulfhydrase acts upstream of nitric oxide to modulate abscisic acid-dependent stomatal closure. *Plant Physiol.* 166, 2065–2076. doi: 10.1104/pp.114.245373

Selinski, J., König, N., Wellmeyer, B., Hanke, G. T., Linke, V., Neuhaus, H. E., et al. (2014). The plastid-localized NAD-dependent malate dehydrogenase is crucial for energy homeostasis in developing *Arabidopsis thaliana* seeds. *Mol. Plant* 7, 170–186. doi: 10.1093/mp/sst151

Selinski, J., Scheibe, R., Day, D. A., and Whelan, J. (2018). Alternative Oxidase Is Positive for Plant Performance. *Trends Plant Sci.* 23, 588–597. doi: 10.1016/j.tplants.2018.03.012

Sevilla, F., Camejo, D., Ortiz-Espín, A., Calderón, A., Lázaro, J. J., and Jiménez, A. (2015a). The thioredoxin/peroxiredoxin/sulfiredoxin system: current overview on its redox function in plants and regulation by reactive oxygen and nitrogen species. *J. Exp. Bot.* 66, 2945–2955. doi: 10.1093/jxb/erv146

Sevilla, F., Jiménez, A., and Lázaro, J. J. (2015b). "What do the plant mitochondrial antioxidant and redox systems have to say in salinity, drought and extreme temperature abiotic stress situations?," in *Reactive oxygen species and oxidative damage in plants under stress*. Eds. D. K. Gupta, J. M. Palma and F. J. Corpas (Switzerland: Springer Cham), 23–55.

Smith, C. A., Melino, V. J., Sweetman, C., and Soole, K. L. (2009). Manipulation of alternative oxidase can influence salt tolerance in *Arabidopsis thaliana*. *Physiol. Plant* 137, 459–472. doi: 10.1111/j.1399-3054.2009.01305.x

Stevens, F. J., Li, A. D., Lateef, S. S., and Anderson, L. E. (1997). Identification of potential inter-domain disulfides in three higher plant mitochondrial citrate synthases: paradoxical differences in redox-sensitivity as compared with the animal enzyme. *Photosynth. Res.* 54, 185–197. doi: 10.1023/A:1005991423503

Sweetlove, L. J., Heazlewood, J. L., Herald, V., Holtzapffel, R., Day, D. A., Leaver, C. J., et al. (2002). The impact of oxidative stress on Arabidopsis mitochondria. *Plant J.* 32, 891–904. doi: 10.1046/j.1365-313X.2002.01474.x

Tanou, G., Job, C., Rajjou, L., Arc, E., Belghazi, M., Diamantidis, G., et al. (2009). Proteomics reveals the overlapping roles of hydrogen peroxide and nitric oxide in the acclimation of citrus plants to salinity. *Plant J.* 60, 795–804. doi: 10.1111/j.1365-313X.2009.04000.x

Toledo, J. C., Audi, R., Ogusucu, R., Monteiro, G., Netto, L. E. S., and Augusto, O. (2011). Horseradish peroxidase compound I as a tool to investigate reactive protein-cysteine residues: from quantification to kinetics. *Free Radic. Biol. Med.* 50, 1032–1038. doi: 10.1016/j.freeradbiomed.2011.02.020

Turrens, J. F. (2003). Mitochondrial formation of reactive oxygen species. *J. Physiol.* 552, 335–344. doi: 10.1111/j.1469-7793.2003.00335.x

Umbach, A. L., Fiorani, F., and Siedow, J. N. (2005). Characterization of transformed Arabidopsis with altered alternative oxidase levels and analysis of effects on reactive oxygen species in tissue. *Plant Physiol.* 139, 1806–1820. doi: 10.1104/pp.105.070763

Umekawa, Y., and Ito, K. (2019). Thioredoxin o- mediated reduction of mitocondrial alternative oxidase. *J. Biol. Chem.* 165, 57–65. doi: 10.1093/jb/mvy082

Van Ruyskensvelde, V., Van Breusegem, F., and Van Der Kelen, K. (2018). Post-transcriptional regulation of the oxidative stress response in plants. *Free Rad. Biol. Med.* 122, 181–192. doi: 10.1016/j.freeradbiomed.2018.02.032

Vidigal, P., Carvalho, R., Amancio, S., and Carvalho, L. (2013). Peroxiredoxins are involved in two independent signalling pathways in the abiotic stress protection in *Vitis vinifera*. *Biol. Planta* 57, 675–683. doi: 10.1007/s10535-013-0346-9

Vishwakarma, A., Tetali, S. D., Selinski, J., Scheibe, R., and Padmasree, K. (2015). Importance of the alternative oxidase (AOX) pathway in regulating cellular redox and ROS homeostasis to optimize photosynthesis during restriction of the cytochrome oxidase pathway in *Arabidopsis thaliana*. *Annu. Bot.* 116, 555–569. doi: 10.1093/aob/mcv122

Wang, Y., Berkowitz, O., Selinski, J., Xu, Y., Hartmann, A., and Whelan, J. (2018). Stress responsive mitochondrial proteins in *Arabidopsis thaliana*. *Free Rad. Biol. Med.* 122, 28–39. doi: 10.1016/j.freeradbiomed.2018.03.031

Waszczak, C., Carmody, M., and Kangasjärvi, J. (2018). Reactive Oxygen Species in Plant Signaling. *Annu. Rev. Plant Biol.* 69, 209–236. doi: 10.1146/annurev-arplant-042817-040322

Wedmann, R., Onderka, C., Wei, S., Szijártó, I. A., Miljkovic, J. L., Mitrovic, A., et al. (2016). Improved tag-switch method reveals that thioredoxin acts as depersulfidase and controls the intracellular levels of protein persulfidation. *Chem. Sci.* 7, 3414–3426. doi: 10.1039/c5sc04818d

Yang, E. S., Richter, C. H., Chun, J. S., Huh, T. L., Kang, S. S., and Park, J. W. (2002). Inactivation of NADP-dependent isocitrate dehydrogenase by nitric oxide. *Free Radic. Biol. Med.* 33, 927–937. doi: 10.1016/s0891-5849(02)00981-4

Yang, H., Mu, J., Chen, L., Feng, J., Hu, J., Li, L., et al. (2015). S-nitrosylation positively regulates ascorbate peroxidase activity during plant stress responses. *Plant Physiol.* 167, 1604–1615. doi: 10.1104/pp.114.255216

Yoshida, K., and Hisabori, T. (2014). Mitochondrial isocitrate dehydrogenase is inactivated upon oxidation and reactivated by thioredoxin-dependent reduction in Arabidopsis. *Front. Environ. Sci.* 2, 38. doi: 10.3389/fenvs.2014.00038

Yoshida, K., and Hisabori, T. (2016). Adenine nucleotide-dependent and redox-independent control of mitochondrial malate dehydrogenase activity in *Arabidopsis thaliana*. *Biochim. Biophys. Acta* 1857, 810–818. doi: 10.1016/j.bbabio.2016.03.001

Yoshida, K., Noguchi, K., Motohashi, K., and Hisabori, T. (2013). Systematic exploration of thioredoxin target proteins in plant mitochondria. *Plant Cell Physiol.* 54, 875–892. doi: 10.1093/pcp/pct037

Yu, L.-X., Zhang, C.-J., Shang, H.-Q., Wang, X.-F., Wei, M., Yang, F.-J., et al. (2013). Exogenous hydrogen sulfide enhanced antioxidant capacity, amylase activities and salt tolerance of cucumber hypocotyls and radicles. *J. Integr. Agric.* 12, 445–456. doi: 10.1016/S2095-3119(13)60245-2

Zaffagnini, M., Fermani, S., Costa, A., Lemaire, S. D., and Trost, P. (2013). Plant cytoplasmic GAPDH: redox post-translational modifications and moonlighting properties. *Front. Plant Sci.* 4, 450. doi: 10.3389/fpls.2013.00450

Zannini, F., Roret, T., Przybyla-Toscano, J., Dhalleine, T., Rouhier, N., and Couturier, J. (2018). Mitochondrial *Arabidopsis thaliana* TRX*o* Isoforms Bind an Iron–Sulfur Cluster and Reduce NFU Proteins *In Vitro*. *Antioxidants* 7, 142. doi: 10.3390/antiox7100142

Zechmann, B. (2014). Compartment-specific importance of glutathione during abiotic and biotic stress. *Front. Plant Sci.* 5, 566. doi: 10.3389/fpls.2014.00566

Zhang, J., Jin, B., Li, L., Block, E. R., and Patel, J. M. (2005). Nitric oxide-induced persistent inhibition and nitrosylation of active site cysteine residues of mitochondrial cytochrome-c oxidase in lung endothelial cells. *Am. J. Physiol. Cell Physiol.* 288, C840–C849. doi: 10.1152/ajpcell.00325.2004

Zhang, H., Ye, Y. K., Wang, S. H., Luo, J. P., Tang, J., and Ma, D. F. (2009). Hydrogen sulfide counteracts chlorophyll loss in sweetpotato seedling leaves and alleviates oxidative damage against osmotic stress. *Plant Growth Regul.* 58, 243–250. doi: 10.1007/s10725-009-9372-1

Zhang, H., Wu, Z., Wang, C., Li, Y., and Xu, J.-R. (2014). Germination and infectivity of microconidia in the rice blast fungus *Magnaporthe oryzae*. *Nat. Commun.* 5, 4518. doi: 10.1038/ncomms5518

Zhou, H., Zhang, J., Shen, J., Zhou, M., Yuan, X., and Xie, Y. (2020). Redox-based protein persulfidation in guard cell ABA signaling. *Plant Signal. Behav.* 15, 1741987. doi: 10.1080/15592324.2020.1741987

Ziogas, V., Tanou, G., Belghazi, M., Filippou, P., Fotopoulos, V., Grigorios, D., et al. (2015). Roles of sodium hydrosulfide and sodium nitroprusside as priming molecules during drought acclimation in citrus plants. *Plant Mol. Biol.* 89, 433–450. doi: 10.1007/s11103-015-0379-x

Conflict of Interest: The authors declare that this review article was written in the absence of any commercial or financial relationships that could be construed as a potential conflict of interest.

frontiers in Plant Science

MINI REVIEW
published: 12 November 2020
doi: 10.3389/fpls.2020.572686

The Chloroplast Reactive Oxygen Species-Redox System in Plant Immunity and Disease

Elżbieta Kuźniak and Tomasz Kopczewski*

Department of Plant Physiology and Biochemistry, Faculty of Biology and Environmental Protection, University of Lodz, Lodz, Poland

Pathogen infections limit plant growth and productivity, thus contributing to crop losses. As the site of photosynthesis, the chloroplast is vital for plant productivity. This organelle, communicating with other cellular compartments challenged by infection (e.g., apoplast, mitochondria, and peroxisomes), is also a key battlefield in the plant–pathogen interaction. Here, we focus on the relation between reactive oxygen species (ROS)—redox signaling, photosynthesis which is governed by redox control, and biotic stress response. We also discuss the pathogen strategies to weaken the chloroplast-mediated defense responses and to promote pathogenesis. As in the next decades crop yield increase may depend on the improvement of photosynthetic efficiency, a comprehensive understanding of the integration between photosynthesis and plant immunity is required to meet the future food demand.

Keywords: chloroplasts, defense response, pathogens, redox signaling, stress hormones

OPEN ACCESS

Edited by:
José Manuel Palma, Consejo Superior de Investigaciones Científicas (CSIC), Spain

Reviewed by:
Néstor Carrillo, Consejo Nacional de Investigaciones Científicas y Técnicas (CONICET), Argentina
Agepati S. Raghavendra, University of Hyderabad, India

****Correspondence:***
Elżbieta Kuźniak
elzbieta.kuzniak@biol.uni.lodz.pl

Specialty section:
This article was submitted to Plant Metabolism and Chemodiversity, a section of the journal Frontiers in Plant Science

Received: *15 June 2020*
Accepted: *27 October 2020*
Published: *12 November 2020*

Citation:
Kuźniak E and Kopczewski T (2020) The Chloroplast Reactive Oxygen Species-Redox System in Plant Immunity and Disease. Front. Plant Sci. 11:572686. doi: 10.3389/fpls.2020.572686

THE IMPLICATION OF CHLOROPLASTS IN PLANT DEFENSE

Plant diseases significantly reduce the yield of agricultural production worldwide (Nelson, 2020). In plants, there is an antagonistic relationship between immunity and growth, known as the growth—immunity trade-off. Immune responses temporarily suppress plant growth and *vice versa*—intense growth can hinder the defense reactions. A likely mechanism of this trade-off is the diversion of photosynthesis-derived energy and metabolites to the defense-related pathways instead of growth. The recognition of pathogen results in downregulation of growth mediated by phytohormones and upregulation of defense-related genes (Karasov et al., 2017). In *Arabidopsis*, constitutive accumulation of salicylic acid (SA) correlates with increased resistance to *Peronospora parasitica* but negatively affects growth (Mauch et al., 2001). Other studies also indicate that SA, a plant defense hormone, contributes to the homeostasis of plant growth and immunity (Ding and Ding, 2020).

Chloroplasts are not only vital for plant productivity, but they are also active sensors of the environment integrating the cellular response to stress. They significantly participate in the generation of ROS and NO, play a central role in redox homeostasis and retrograde signaling regulating nuclear gene expression (Foyer, 2018; Dietz et al., 2019). Their role in immunity is supported by observations that plant resistance to pathogens differ between light and dark,

and light and functional chloroplasts are needed for defense responses (Roden and Ingle, 2009; Kuźniak et al., 2010).

Chloroplasts are also involved in stress hormone signaling by providing biosynthetic precursors for SA, jasmonic acid (JA), abscisic acid (ABA), and ethylene (ET) (Baier and Dietz, 2005; Lu and Yao, 2018).

As a signaling hub for regulating plant stress responses, chloroplasts are also targets for pathogen effectors and phytotoxins to suppress host defense, which makes them a key battlefield in plant–pathogen interactions (Park et al., 2018).

Here, we discuss the contribution of chloroplasts to plant immunity and their role as a target to pathogen manipulation weakening plant defense. Considering the internal redox environment of the chloroplast and the role of redox regulations in mediating plant responses to stress, we focus on the processes that directly or indirectly depend on chloroplast-associated ROS and redox changes. The role of ROS and redox components in retrograde signaling is not emphasized as it has recently been extensively reviewed (Dietz et al., 2019).

THE PTI/ETI MODEL OF PLANT IMMUNITY

The plant immune system relies on patterns-triggered immunity (PTI) and effector-triggered immunity (ETI) which are defined by the recognition mechanism of invading pathogens. PTI, responsible for the non-host-specific resistance, is activated following recognition of pathogen-associated molecular patterns (PAMP) by receptors at the cell surface. PTI initiates defense responses associated with ROS generation, stomata closure, activation of mitogen-activated protein kinases (MAPK) and induction of defense genes. Recognition of the avirulence (*Avr*) genes-coded pathogen effector proteins by cytoplasmic resistance (R) protein receptors triggers ETI which is more robust than PTI and includes the local hypersensitive response (HR) often followed by systemic acquired resistance in the host (Cook et al., 2015). HR is a specialized form of programmed cell death (PCD) characterized by a rapid cell death at the point of pathogen penetration that usually leads to or is linked to resistance associated with Nucleotide Binding Site and Leucine-Rich Repeat domains (NBS–LRR) R-proteins, but is not restricted to the ETI. HR is competent against biotrophs which grow and reproduce in living hosts but it may be beneficial for necrotrophs feeding on dead tissues (Balint-Kurti, 2019).

Oxidative burst associated with a biphasic accumulation of ROS, mainly O_2^- and H_2O_2, is a hallmark of plant interactions with incompatible pathogens. The first, non-specific phase of ROS generation is linked to the activity of NADPH oxidase respiratory burst homolog (RBOH) and class III cell wall peroxidases in the apoplast whereas the second one is specifically associated with ETI and occurs in chloroplasts (Shapiguzov et al., 2012). Apoplastic ROS accumulation is sensed in all cellular compartments via different redox-based mechanisms, and ROS produced in the apoplast and in chloroplasts, mitochondria, and peroxisomes are involved in interorganellar communication to trigger the immune response (Mignolet-Spruyt et al., 2016). The oxidative burst originating in different compartments trigger redox-modulated SA signaling with NPR1 (non-expressor of pathogenesis-related gene 1) being the master redox sensor for SA-mediated gene expression in the defense response (Seyfferth and Tsuda, 2014; Herrera-Vásquez et al., 2015).

STRUCTURAL PATHWAYS UNDERLYING CHLOROPLAST SIGNALING

The decrease in the number and size of chloroplasts, the occurrence of plastoglobules and degradation of thylakoids were found markers of biotic stress (Gabara et al., 2012; Zechmann, 2019). In *Botrytis cinerea*-infected plants these changes have been attributed to the accumulation of ROS, especially H_2O_2 in chloroplasts (Rossi et al., 2017). Chloroplasts communicate with other organelles via signaling networks and by establishing physical contact with them (Park et al., 2018). Activation of PTI, ETI, and PCD-promoting signals such as H_2O_2 and SA, trigger chloroplast re-localization, clustering around the nucleus, and extending stromules, the stroma-filled tubules (Caplan et al., 2015; Ding et al., 2019). A decline in photosynthesis, often accompanying plant immunity, and increase in ROS generation within chloroplasts are likely pre-requisites for stromule formation (Brunkard et al., 2015; de Torres Zabala et al., 2015). During HR, chloroplasts are the major source of H_2O_2 which is a defense signaling molecule and induces nuclear gene expression (Yao and Greenberg, 2006). Stromules could facilitate the direct transfer of chloroplast-sourced H_2O_2 to the nucleus. Stromule formation increases with enhanced ROS generation in chloroplasts and its frequency is regulated in response to the chloroplast redox status (Brunkard et al., 2015; Caplan et al., 2015; Exposito-Rodriguez et al., 2017). Specific sub-sets of chloroplasts harboring the MSH1 (MUTS HOMOLOG1) protein function as sensory plastids and participate in epigenetic stress memory in plants (Foyer, 2018). *MSH1* silencing results in differential expression of biotic stress-related genes and the function of MSH1 is associated with redox state of these chloroplasts (Virdi et al., 2015).

THE CHLOROPLASTIC ELECTRON TRANSPORT CHAIN CARRIERS AND THEIR LINKS TO PLANT DEFENSE

The chloroplast redox state is determined by electron flow through the photosynthetic electron transport chain (PETC) with plastoquinone (PQ) proposed to be the central redox regulator (Potters et al., 2010; Liu and Lu, 2016). PQ is also involved in plant immune response. Light-induced redox changes of the PQ pool regulated HR and defense gene expression (Mühlenbock et al., 2008). PQ content increased in plants treated with pathogen-derived elicitor and acting as an antioxidant, PQ mediated

the ROS balance during oxidative stress induced by elicitation (Maciejewska et al., 2002). In *Mesembryanthemum crystallinum*, the PQ redox state modified the response to *B. cinerea* by affecting the activity of antioxidant enzymes and the HR-like response was promoted when the PQ pool was reduced (Nosek et al., 2015). PQ is involved in ABA biosynthesis through the oxidative cleavage of epoxy-carotenoids (Rock and Zeevaart, 1991) and thus linked with the hormone-regulated defense. As PQ reduces O_2 to $O_2^{\cdot-}$ by semiquinone and $O_2^{\cdot-}$ to H_2O_2 by hydroquinone, PQ also regulates defense signaling mediated by these two ROS (Camejo et al., 2016). In *Arabidopsis*, 50 nuclear genes is regulated by the redox state of PQ and the kinases STN7 and CSK1 are involved in this signaling. PQ may also regulate gene expression indirectly through the generation of H_2O_2 (Adamiec et al., 2008; Pfannschmidt et al., 2009).

Ferredoxin, the most upstream electron acceptor in PETC, determines the redox status of downstream reductants, e.g., NADPH and thioredoxins. NADPH produced in chloroplasts by ferredoxin-$NADP^+$ reductase is used in defense-related anabolic processes and in the regeneration of antioxidants by NADPH-dependent enzymes (Noctor et al., 2006). Ferredoxin and NADPH are involved in redox signaling via ferredoxin- and NADPH-dependent thioredoxin reductases localized in chloroplasts as well as maintenance of redox balance mediated by ascorbate–glutathione cycle. Both processes are implicated in regulating disease resistance (Kuźniak and Skłodowska, 2005; Potters et al., 2010; Hanke and Mulo, 2013). In *Arabidopsis*, NADPH-dependent thioredoxin reductase C (NTRC) working together with H_2O_2-reducing 2-Cys peroxiredoxin play a role in innate immunity to non-host *Pseudomonas syringae* pathogens. This redox detoxification system regulates H_2O_2 generated in chloroplasts and functions as a negative regulator of disease-associated cell death. The increased susceptibility of *Arabidopsis ntrc* mutant to non-host *P. syringae* correlated with enhanced JA-dependent signaling (Ishiga et al., 2016).

The main leaf ferredoxin, Fd2 is required for resistance against pathogens. Fd2 plays a positive role in PTI-mediated ROS accumulation but negatively regulates the ETI response. The Fd2-knockout mutants exhibited increased susceptibility to virulent *P. syringae* pv. *tomato* DC3000 and the powdery mildew *Golovinomyces cichoracearum*. The Fd2-knockout mutant accumulated more JA following *P. syringae* pv. *tomato* DC3000 infection whereas the SA-mediated defense was compromised (Wang et al., 2018).

Imbalance in PETC may initiate and modulate defense responses, e.g., via ROS-mediated chloroplast-to-nucleus signaling (Karpiński et al., 2013). As activation of immune responses requires redox-mediated transcriptome reprogramming, the ferredoxin-dependent availability of NADPH and redox status of chloroplast thioredoxins may modify chloroplast retrograde signaling and affect nuclear gene expression (Rintamäki et al., 2009). In *Arabidopsis*, 286 nuclear genes were identified to be under the photosynthetic redox control and 76 of these genes encoded products with known functions, e.g., stress response (Fey et al., 2005). Moreover, Fd2 localizes in stromules and therefore it could reduce the redox-regulated transcription factors (TFs), including those required for the expression of SA-dependent genes (Fobert and Després, 2005; Wang et al., 2018).

CAROTENOID, UNSATURATED FATTY ACIDS, AND TOCOPHEROL DERIVED SIGNALING

In the chloroplast membranes, unsaturated fatty acids, carotenoids, and tocopherols act as ROS quenchers and their oxidation products can regulate defense responses. Tocopherols transfer the stress signals outside the chloroplast, possibly by influencing redox signaling in other organelles. Recently, tocopherols were shown to access endoplasmic reticulum (ER) via hemifused-membranes at plastid-ER contact sites (Mehrshahi et al., 2014). Under stress, changes in the content and composition of tocopherols modulate nuclear gene expression, the profiles of SA, JA, ABA, and ET as well as the formation of defense-related lipid peroxidation products. A link between redox and hormone signaling mediated, respectively, by γ-tocopherol and Ethylene Response Factors (ERFs) which integrates ABA, JA, and ET response to infection, found in vitamin E-deficient *Arabidopsis* mutant, likely represents a mechanism of chloroplast to nucleus retrograde signaling (Müller and Munné-Bosch, 2015; Allu et al., 2017). Altered tocopherol composition in chloroplasts negatively influenced *Arabidopsis* response to *B. cinerea* through enhanced lipid peroxidation and delayed defense activation (Cela et al., 2018).

Apocarotenoids are the products of oxidative cleavage of carotenoids. Interestingly, SA content increase in response to excess light which inhibits ROS accumulation in chloroplasts is dependent on apocarotenoid, β-cyclocitral which interferes with the SA signaling by regulating the localization of NPR1 in the nucleus (Hou et al., 2016).

Pathogens elicit the accumulation of oxylipins which are the products of peroxidation of polyunsaturated fatty acids (PUFA), and those with α,β-unsaturated carbonyls are reactive electrophilic species (RES). The generation of oxylipins in chloroplasts can activate defense signaling and has an impact on gene expression (Farmer and Mueller, 2013). JA originated form PUFA controls gene expression through CORONATINE-INSENSITIVE 1 (COI1), JASMONATE-ZIM DOMAIN (JAZ) proteins, and MYC TFs (Pieterse et al., 2009). RES signal transduction involves the class II TGA TFs and is enhanced by SA, known to inhibit JA signaling. Thus, JA and RES play distinct roles in mediating plant-defense responses (Findling et al., 2018). Moreover, oxylipins identified as signaling molecules, contribute to defense as antimicrobial agents inhibiting pathogen spore germination and growth (Prost et al., 2005).

The production of $^1O_2$, the predominant ROS in chloroplasts, can increase during pathogenesis favoring oxidative burst. PUFA in thylakoid membranes may act as structural $^1O_2$ scavengers (Farmer and Mueller, 2013). The protective role of PUFA during pathogenesis was shown in *Arabidopsis* where genetic removal of triunsaturated fatty acids led to increased susceptibility to *B. cinerea* (Mène-Saffrané et al., 2009). Moreover, in *Arabidopsis–P. syringae* interaction, massive lipid oxidation is confined to

plastid lipids and the HR-related PCD is preceded by $^1O_2$-dependent lipid peroxidation (Zoeller et al., 2012).

There is compelling evidence that tetrapyrrole signaling contributes to abiotic stress tolerance (Larkin, 2016) but to the best of our knowledge there are no data directly indicating its role in plant–pathogen interactions.

CHLOROPLAST-GENERATED ROS IN PLANT–PATHOGEN INTERACTIONS

Chloroplasts can perceive and propagate PTI signals generated in the apoplast following pathogen recognition. Application of flg22, a conserved peptide of bacterial flagellin, to *Arabidopsis* leaves induces CAS (Calcium-Sensing Sensor)-mediated calcium signaling in the chloroplast stroma. CAS mediated both the basal defense responses (PTI) and HR (ETI) leading to downregulation of photosynthesis-related genes and upregulation of the defensive genes (Nomura et al., 2012). ROS production in chloroplasts was linked to PAMP-induced downregulation of non-photochemical quenching (NPQ) due to weaker accumulation of PSII protein subunits. These PAMP-induced changes in redox balance prime chloroplasts to respond with massive ROS burst upon recognition of effectors during ETI (Göhre et al., 2012). Increased ETI-related ROS contribute to HR-like cell death mediated by MAPK and light-dependent ROS generation in chloroplasts is preceded by inhibition of photosynthetic CO_2 fixation (Liu et al., 2007; Zurbriggen et al., 2009). Moreover, *Arabidopsis* plants in which H_2O_2 generation at PSI was abolished were more susceptible to *P. syringae* pv *tomato* mutant which lacks the ability to secrete effectors, and so only elicits PTI. In this system the pathogenicity of the mutant was rescued (Göhre et al., 2012).

The level of ferredoxin decreases under stress and functional replacement of ferredoxin by a cyanobacterial flavodoxin confer resistance to biotic stress in tobacco. These plants infected with *B. cinerea* showed sustained photosynthetic electron flow, decreased ROS accumulation and enhanced resistance to this necrotroph which invasion is known to be facilitated by HR and oxidative processes mediated by ROS (Govrin and Levine, 2000; Rossi et al., 2017).

ROS-related signaling and the expression of defense require fine-tuning of the prooxidant-antioxidant balance in chloroplasts (Das and Roychoudhury, 2014). Pathogens could activate abiotic stress tolerance mechanisms related to ROS managements to promote virulence and plants defective in these systems and overproducing ROS show increased resistance to pathogens (Sowden et al., 2018). However, the effects depend on ROS amount, timing, and the plant–pathogen interaction. For example, during a non-host interaction of tobacco-*Xanthomonas campestris* pv *vesicatoria*, ROS generated in chloroplasts were essential for the development of HR but not for the induction of pathogenesis-related (PR) genes, and JA and SA accumulation (Zurbriggen et al., 2009). Moreover, the ROS homeostasis is coordinated by NO and the interplay of H_2O_2 and NO affects the immune response. The interaction of these redox molecules is required for HR, NO inhibits NADPH oxidase and PCD, and NO-mediated modifications of ascorbate peroxidase and other antioxidant enzymes have regulatory functions under biotic stress (Frederickson Matika and Loake, 2014; Saxena et al., 2016). Moreover, nitrosoglutathione (GSNO), a NO-derived molecule, facilitates the oligomerization of NPR1 through thiol S-nitrosylation (Lindermayr et al., 2010; Corpas et al., 2013).

Infected plants experience episodes of reduced CO_2 availability to photosynthesis because both foliar pathogenesis and resistance responses can result in stomata closure (Melotto et al., 2008; Grimmer et al., 2012). Consequently, photorespiration is increased and the metabolic integration of chloroplasts with mitochondria and peroxisomes via this pathway contributes to defense (Sørhagen et al., 2013). Photorespiration provides photoprotection by dissipating excess excitation energy in the absence of sufficient CO_2 as an electron acceptor and reducing ROS generation as well as contributes to redox homeostasis during biotic challenge (Reumann and Corpas, 2010; Eisenhut et al., 2017). Elevated activity of the photorespiratory enzyme, serine:glyoxylate aminotransferase likely confers pathogen resistance in melon by stimulating glycolate oxidase and the intraperoxisomal production of H_2O_2, and thereby activating the immune response (Taler et al., 2004). Moreover, H_2O_2 originated in chloroplasts and peroxisomes can elicit different responses, and H_2O_2 from peroxisomes stimulates stress tolerance whereas that from chloroplasts induces early defense signaling (Sewelam et al., 2014). In *Arabidopsis* overexpressing glycolate oxidase in chloroplasts and the peroxisomal catalase deficient mutant *cat2-2*, producing increased amounts of H_2O_2 from the respective organelles, only signals generated by H_2O_2 in chloroplasts enhanced resistance to *Colletotrichum higginssianum* (Schmidt et al., 2020).

CHLOROPLASTS AS TARGETS FOR PATHOGEN MANIPULATION

Pathogens modify chloroplast functions for their benefit. During interactions with hemibiotrophs, this mechanism often relays on suppressing redox-linked SA pathway by activating the antagonistic JA signaling (Robert-Seilaniantz et al., 2011). *Ralstonia solanacearum* uses type III effector proteins called Rips (*Ralstonia*-injected protein) to induce JA accumulation by releasing linolenic acid with its lipase activity. Simultaneously, Rips promote bacterial pathogen growth by suppressing SA and SA-dependent signaling in infected cells (Nakano and Mukaihara, 2018). Coronatine, *P. syringae* phytotoxin with structural similarity to JA which promotes bacterial entry and growth, targets photosynthesis and modulates ROS balance in chloroplasts (Ishiga et al., 2009). The *P. syringae* toxin syringolin and the *Xanthomonas campestris* effector XopJ interfere with the degradation of NPR1 which redox-dependent turnover is required for SA signaling (Büttner, 2016).

Sclerotinia sclerotiorum induces stomata opening at the early stages of infection. Oxalic acid secreted by this fungus acidifies the infected tissues, stimulates NPQ by enhancing the conversion of violaxanthin to zeaxanthin and attenuates ROS generation, affecting chloroplast redox status. The dysfunction of the xanthophyll cycle limits ABA biosynthesis by decreasing the violaxanthin precursor for ABA synthesis in chloroplasts. This affects defense responses such as ROS induction and callose

TABLE 1 | Chloroplast factors involved in plant immune response.

Factor	Role in plant immunity	References
Photosynthesis-derived reactive oxygen species (ROS)	Contribute to pattern-triggered immunity (PTI) and effector triggered immunity (ETI) and chloroplasts are the main source of ROS during hypersensitive response. Chloroplast ROS-mediated retrograde signaling leads to the induction of defense gene expression. ROS generation and signaling in chloroplasts follows ROS bursts in the apoplast triggered by pathogen recognition. The signaling specificity of ROS depends on the chemical characteristics and the ROS-antioxidants balance in chloroplast	Zurbriggen et al., 2009; Göhre et al., 2012; Nomura et al., 2012; Mignolet-Spruyt et al., 2016
Plastoquinone	Regulates defense signaling and gene expression through O_2^- and H_2O_2 generation. Mediates ROS balance and affects the activities of antioxidant enzymes. Is linked with abscisic acid (ABA)-regulated defense by contributing to ABA biosynthesis	Rock and Zeevaart, 1991; Maciejewska et al., 2002; Adamiec et al., 2008; Pfannschmidt et al., 2009; Nosek et al., 2015; Camejo et al., 2016
Ferredoxin	Determines the redox status of NADPH and ferredoxin-dependent thioredoxins involved in defense signaling. The increased susceptibility to biotrophic and hemibiotrophic pathogens of ferredoxin-knockout mutants relays on suppressing salicylic acid (SA) pathway and activating the antagonistic jasmonic acid (JA) signaling; Ferredoxin localized in stromules could be involved in redox-mediated transcriptome reprogramming required for activation of immune response	Robert-Seilaniantz et al., 2011; Wang et al., 2018
NADPH	Chloroplast-produced NADPH is involved in redox signaling via NTRC and used in the regeneration of ascorbate and glutathione by NADPH-dependent enzymes in the ascorbate-glutathione cycle which is implicated in regulating disease resistance	Kuźniak and Skłodowska, 2005; Potters et al., 2010; Hanke and Mulo, 2013
NADPH-dependent thioredoxin reductase (NTRC)	The importance of the NTRC in plant immunity is shown by elevated JA signaling and enhanced susceptibility of the *ntrc Arabidopsis* mutant to non-host pathogens	Ishiga et al., 2016
Thioredoxin Trx-h	NtTRXh3 protein localized in chloroplasts is involved in tobacco resistance to viruses by contributing to ROS scavenging and cellular reducing conditions. The redox status of thioredoxins affects nuclear gene expression by modifying chloroplasts retrograde signaling	Rintamäki et al., 2009; Sun et al., 2010
Tocopherols	Involved in the antioxidant protection of chloroplast membranes and in the transfer of stress signals outside the chloroplast via plastid- endoplasmic reticulum contact sites Tocopherols content and composition modulate nuclear gene expression, the profiles of defense hormones and PUFA-derived defense products	Mehrshahi et al., 2014; Müller and Munné-Bosch, 2015; Allu et al., 2017; Cela et al., 2018
Apocarotenoids	Chloroplast-generated signaling molecules produced by carotenoid cleavage link chloroplast activity and nuclear gene expression. They interfere with SA signaling by regulating the localization of NPR1, a redox-sensitive transcription co-activator, in the nucleus	Bobik and Burch-Smith, 2015; Brunkard et al., 2015; Hou et al., 2016
Polyunsaturated fatty acids (PUFA)	Biosynthetic precursors of JA which is central to modulating defense against necrotrophs, participates in systemic acquired resistance and usually antagonizes SA-mediated defense Independently of being the precursors of JA, PUFA are sinks for ROS in chloroplasts	Mène-Saffrané et al., 2009; Farmer and Mueller, 2013
Oxylipins	Reactive electrophilic species signaling molecules interfering with TGA transcription factors-mediated SA pathway which also exhibit antimicrobial activity	Prost et al., 2005; Findling et al., 2018
Calcium sensor protein (CAS)	Thylakoid-localized calcium-binding protein which connects chloroplasts to immune responses triggered during PTI and ETI and regulates the biosynthesis of SA via the chloroplast isochorismate pathway. CAS is involved in PAMP-induced defense gene expression, including SA biosynthesis genes, through $^1O_2$-mediated retrograde signaling. SA generally mediates defense against biotrophic/hemibiotrophic pathogens and systemic acquired resistance	Nomura et al., 2012; Bobik and Burch-Smith, 2015

deposition which increases plant susceptibility to *Sclerotinia* (Zhou et al., 2015; Zeng et al., 2020).

P. syringae effector HopN1 targets the oxygen-evolving complex of PSII, suppresses cell death, attenuates ROS production, callose deposition, and the formation of defense signals in *Arabidopsis* chloroplasts (Rodríguez-Herva et al., 2012). HopI1, the *P. syringae* pv *maculicola* effector localizes to chloroplasts, suppresses SA accumulation, and affects thylakoid stacking (Jelenska et al., 2007). It also recruits cytosolic Hsp70 to chloroplasts suppressing the function of cytosolic Hsp70 in basal defense (Jelenska et al., 2010). Chloroplast proteins identified as targets of virus effectors are components of the PETC (e.g., ferredoxin, Rieske Fe–S), the PSII oxygen-evolving complex and Rubisco, which supports the chloroplast role in plant defense (Bobik and Burch-Smith, 2015).

CONCLUSION

The organelle–organelle contacts and inter-compartment communication initiated at the plasma membrane on pathogen recognition are essential for defense. Chloroplasts have emerged as regulatory hubs connecting the primary metabolism and plant defense. They participate in PTI and ETI through ROS/redox systems, retrograde signaling, and phytohormones (**Table 1**). Chloroplasts are the source and the target of redox regulations which are integrated to the interorganellar signaling network and contribute to the outcome of the plant immune response. Therefore, our integrated understanding of the redox-mediated functions of chloroplasts in photosynthesis and plant immunity will be highly relevant in developing new crops with broad-spectrum resistance to pathogens.

AUTHOR CONTRIBUTIONS

EK and TK took responsibility for the integrity of the work as a whole. Both authors contributed to the article and approved the submitted version.

ACKNOWLEDGMENTS

This work was supported by Grant No. 2013/11/N/NZ9/00116 from the National Science Centre (NCN, Poland).

REFERENCES

Adamiec, M., Drath, M., and Jackowski, G. (2008). Redox state of plastoquionone pool regulates expression of *Arabidopsis thaliana* genes in response to elevated irradiance .*Acta Biochim. Pol.* 55, 161–173. doi: 10.18388/abp.2008_3176

Allu, A. D., Simancas, B., Balazadeh, S., and Munné-Bosch, S. (2017). Defense-related transcriptional reprogramming in vitamin E-deficient *Arabidopsis* mutants exposed to contrasting phosphate availability. *Front. Plant Sci.* 8:1396. doi: 10.3389/fpls.2017.01396

Baier, M., and Dietz, K. J. (2005). Chloroplasts as source and target of cellular redox regulation: a discussion on chloroplast redox signals in the context of plant physiology. *J. Exp. Bot.* 56, 1449–1462. doi: 10.1093/jxb/eri161

Balint-Kurti, P. (2019). The plant hypersensitive response: concepts, control and consequences. *Mol. Plant Pathol.* 20, 1163–1178. doi: 10.1111/mpp.12821

Bobik, K., and Burch-Smith, T. M. (2015). Chloroplast signaling within, between and beyond cells. *Front. Plant Sci.* 6:781. doi: 10.3389/fpls.2015.00781

Brunkard, J. O., Runkel, A. M., and Zambryski, P. C. (2015). Chloroplasts extend stromules independently and in response to internal redox signals. *Proc. Natl. Acad. Sci. U.S.A.* 112, 10044–10049. doi: 10.1073/pnas.1511570112

Büttner, D. (2016). Behind the lines-actions of bacterial type III effector proteins in plant cells. *FEMS Microbiol. Rev.* 40, 894–937. doi: 10.1093/femsre/fuw026

Camejo, D., Guzmán-Cedeño, Á, and Moreno, A. (2016). Reactive oxygen species, essential molecules, during plant-pathogen interactions. *Plant Physiol. Biochem.* 103, 10–23. doi: 10.1016/j.plaphy.2016.02.035

Caplan, J. L., Kumar, A. S., Park, E., Padmanabhan, M. S., Hoban, K., Modla, S., et al. (2015). Chloroplast stromules function during innate immunity. *Dev. Cell* 34, 45–57. doi: 10.1016/j.devcel.2015.05.011

Cela, J., Tweed, J. K. S., Sivakumaran, A., Lee, M. R. F., Mur, L. A. J., and Munné-Bosch, S. (2018). An altered tocopherol composition in chloroplasts reduces plant resistance to *Botrytis cinerea*. *Plant Physiol. Biochem.* 127, 200–210. doi: 10.1016/j.plaphy.2018.03.033

Cook, D. E., Mesarich, C. H., and Thomma, B. P. H. J. (2015). Understanding plant immunity as a surveillance system to detect invasion. *Annu. Rev. Phytopathol.* 53, 541–563. doi: 10.1146/annurev-phyto-080614-120114

Corpas, F. J., Alché, J. D., and Barroso, J. B. (2013). Current overview of S-nitrosoglutathione (GSNO) in higher plants. *Front. Plant Sci.* 4:126. doi: 10.3389/fpls.2013.00126

Das, K., and Roychoudhury, A. (2014). Reactive oxygen species (ROS) and response of antioxidants as ROS-scavengers during environmental stress in plants. *Front. Environ. Sci.* 2:53. doi: 10.3389/fenvs.2014.00053

de Torres Zabala, M., Littlejohn, G., Jayaraman, S., Studholme, D., Bailey, T., Lawson, T., et al. (2015). Chloroplasts play a central role in plant defence and are targeted by pathogen effectors. *Nat. Plants* 1:15074. doi: 10.1038/NPLANTS.2015.74

Dietz, K.-J., Wesemann, C., Wegener, M., and Seidel, T. (2019). Toward an integrated understanding of retrograde control of photosynthesis. *Antioxid. Redox Signal.* 30, 1186–1205. doi: 10.1089/ars.2018.7519

Ding, P., and Ding, Y. (2020). Stories of salicylic acid: a plant defense hormone. *Trends Plant Sci.* 1, 1–17. doi: 10.1016/j.tplants.2020.01.004

Ding, X., Jimenez-Gongora, T., Krenz, B., and Lozano-Duran, R. (2019). Chloroplast clustering around the nucleus is a general response to pathogen perception in *Nicotiana benthamiana*. *Mol. Plant Pathol.* 20, 1298–1306. doi: 10.1111/mpp.12840

Eisenhut, M., Bräutigam, A., Timm, S., Florian, A., Tohge, T., Fernie, A. R., et al. (2017). Photorespirationis crucial for dynamic response of photosynthetic metabolism and stomatal movement to altered CO2 availability. *Mol. Plant* 10, 47–61. doi: 10.1016/j.molp.2016.09.011

Exposito-Rodriguez, M., Laissue, P. P., Yvon-Durocher, G., Smirnoff, N., and Mullineaux, P. M. (2017). Photosynthesis-dependent H2O2 transfer from chloroplasts to nuclei provides a high-light signalling mechanism. *Nat. Commun.* 8:49. doi: 10.1038/s41467-017-00074-w

Farmer, E. E., and Mueller, M. J. (2013). ROS-mediated lipid peroxidation and RES-activated signaling. *Annu. Rev. Plant Biol.* 64, 429–450. doi: 10.1146/annurev-arplant-050312-120132

Fey, V., Wagner, R., Bräutigam, K., Wirtz, M., Hell, R., Dietzmann, A., et al. (2005). Retrograde plastid redox signals in the expression of nuclear genes for chloroplast proteins of *Arabidopsis thaliana*. *J. Biol. Chem.* 280, 5318–5328. doi: 10.1074/jbc.M406358200

Findling, S., Stotz, H. U., Zoeller, M., Krischke, M., Zander, M., Gatz, C., et al. (2018). TGA2 signaling in response to reactive electrophile species is not dependent on cysteine modification of TGA2. *PLoS One* 13:e0195398. doi: 10.1371/journal.pone.0195398

Fobert, P. R., and Després, C. (2005). Redox control of systemic acquired resistance. *Curr. Opin. Plant Biol.* 8, 378–382. doi: 10.1016/j.pbi.2005.05.003

Foyer, C. H. (2018). Reactive oxygen species, oxidative signaling and the regulation of photosynthesis. *Environ. Exp. Bot.* 154, 134–142. doi: 10.1016/j.envexpbot.2018.05.003

Frederickson Matika, D. E., and Loake, G. J. (2014). Redox regulation in plant immune function. *Antioxid. Redox Signal.* 21, 1373–1388. doi: 10.1089/ars.2013.5679

Gabara, B., Kuźniak, E., Skłodowska, M., Surówka, E., and Miszalski, Z. (2012). Ultrastructural and metabolic modifications at the plant-pathogen interface in *Mesembryanthemum crystallinum* leaves infected by *Botrytis cinerea*. *Environ. Exp. Bot.* 77, 33–43. doi: 10.1016/j.envexpbot.2011.10.010

Göhre, V., Jones, A. M. E., Sklenář, J., Robatzek, S., and Weber, A. P. M. (2012). Molecular crosstalk between PAMP-triggered immunity and photosynthesis. *Mol. Plant Microbe Interact.* 25, 1083–1092. doi: 10.1094/MPMI-11-11-0301

Govrin, E. M., and Levine, A. (2000). The hypersensitive response facilitates plant infection by the necrotrophic pathogen *Botrytis cinerea*. *Curr. Biol.* 10, 751–757. doi: 10.1016/S0960-9822(00)00560-1

Grimmer, M. K., John Foulkes, M., and Paveley, N. D. (2012). Foliar pathogenesis and plant water relations: a review. *J. Exp. Bot.* 63, 4321–4331. doi: 10.1093/jxb/ers143

Hanke, G., and Mulo, P. (2013). Plant type ferredoxins and ferredoxin-dependent metabolism. *Plant Cell Environ.* 36, 1071–1084. doi: 10.1111/pce.12046

Herrera-Vásquez, A., Salinas, P., and Holuigue, L. (2015). Salicylic acid and reactive oxygen species interplay in the transcriptional control of defense genes expression. *Front. Plant Sci.* 6:171. doi: 10.3389/fpls.2015.00171

Hou, X., Rivers, J., León, P., McQuinn, R. P., and Pogson, B. J. (2016). Synthesis and function of apocarotenoid signals in plants. *Trends Plant Sci.* 21, 792–803. doi: 10.1016/j.tplants.2016.06.001

Ishiga, Y., Ishiga, T., Ikeda, Y., Matsuura, T., and Mysore, K. S. (2016). NADPH-dependent thioredoxin reductase C plays a role in nonhost disease resistance against *Pseudomonas syringae* pathogens by regulating chloroplast-generated reactive oxygen species. *PeerJ* 4:e1938. doi: 10.7717/peerj.1938

Ishiga, Y., Uppalapati, S. R., Ishiga, T., Elavarthi, S., Martin, B., and Bender, C. L. (2009). The phytotoxin coronatine induces light-dependent reactive oxygen species in tomato seedlings. *New Phytol.* 181, 147–160. doi: 10.1111/j.1469-8137.2008.02639.x

Jelenska, J., Van Hal, J. A., and Greenberg, J. T. (2010). *Pseudomonas* syringae hijacks plant stress chaperone machinery for virulence. *Proc. Natl. Acad. Sci. U.S.A.* 107, 13177–13182. doi: 10.1073/pnas.0910943107

Jelenska, J., Yao, N., Vinatzer, B. A., Wright, C. M., Brodsky, J. L., and Greenberg, J. T. (2007). A J domain virulence effector of *Pseudomonas syringae* remodels host chloroplasts and suppresses defenses. *Curr. Biol.* 17, 499–508. doi: 10.1016/j.cub.2007.02.028

Karasov, T. L., Chae, E., Herman, J. J., and Bergelson, J. (2017). Mechanisms to mitigate the trade-off between growth and defense. *Plant Cell* 29, 666–680. doi: 10.1105/tpc.16.00931

Karpiński, S., Szechyńska-Hebda, M., Wituszyńska, W., and Burdiak, P. (2013). Light acclimation, retrograde signalling, cell death and immune defences in plants. *Plant Cell Environ.* 36, 736–744. doi: 10.1111/pce.12018

Kuźniak, E., Kornas, A., Gabara, B., Ullrich, C., Skłodowska, M., and Miszalski, Z. (2010). Interaction of *Botrytis cinerea* with the intermediate C3-CAM plant *Mesembryanthemum crystallinum*. *Environ. Exp. Bot.* 69, 137–147. doi: 10.1016/j.envexpbot.2010.03.010

Kuźniak, E., and Skłodowska, M. (2005). Compartment-specific role of the ascorbate-glutathione cycle in the response of tomato leaf cells to *Botrytis cinerea* infection. *J. Exp. Bot.* 56, 921–933. doi: 10.1093/jxb/eri086

Larkin, R. M. (2016). Tetrapyrrole signaling in plants. *Front. Plant Sci.* 7:1586. doi: 10.3389/fpls.2016.01586

Lindermayr, C., Sell, S., Müller, B., Leister, D., and Durner, J. (2010). Redox regulation of the NPR1-TGA1 system of *Arabidopsis thaliana* by nitric oxide. *Plant Cell* 22, 2894–2907. doi: 10.1105/tpc.109.066464

Liu, M., and Lu, S. (2016). Plastoquinone and ubiquinone in plants: biosynthesis, physiological function and metabolic engineering. *Front. Plant Sci.* 7:1898. doi: 10.3389/fpls.2016.01898

Liu, Y., Ren, D., Pike, S., Pallardy, S., Gassmann, W., and Zhang, S. (2007). Chloroplast-generated reactive oxygen species are involved in hypersensitive response-like cell death mediated by a mitogen-activated protein kinase cascade. *Plant J.* 51, 941–954. doi: 10.1111/j.1365-313X.2007.03191.x

Lu, Y., and Yao, J. (2018). Chloroplasts at the crossroad of photosynthesis, pathogen infection and plant defense. *Int. J. Mol. Sci.* 19, 1–37. doi: 10.3390/ijms19123900

Maciejewska, U., Polkowska-Kowalczyk, L., Swiezewska, E., and Szkopinska, A. (2002). Plastoquinone: possible involvement in plant disease resistance. *Acta Biochim. Pol.* 49, 775–780. doi: 10.18388/abp.2002_3785

Mauch, F., Mauch-Mani, B., Gaille, C., Kull, B., Haas, D., and Reimmann, C. (2001). Manipulation of salicylate content in *Arabidopsis thaliana* by the expression of an engineered bacterial salicylate. *Plant J.* 25, 67–77. doi: 10.1046/j.1365-313X.2001.00940.x

Mehrshahi, P., Johnny, C., and DellaPenna, D. (2014). Redefining the metabolic continuity of chloroplasts and ER. *Trends Plant Sci.* 19, 501–507. doi: 10.1016/j.tplants.2014.02.013

Melotto, M., Underwood, W., and He, S. Y. (2008). Role of stomata in plant innate immunity and foliar bacterial diseases. *Annu. Rev. Phytopathol.* 46, 101–122. doi: 10.1146/annurev.phyto.121107.104959

Mène-Saffrané, L., Dubugnon, L., Chételat, A., Stolz, S., Gouhier-Darimont, C., and Farmer, E. E. (2009). Nonenzymatic oxidation of trienoic fatty acids contributes to reactive oxygen species management in *Arabidopsis*. *J. Biol. Chem.* 284, 1702–1708. doi: 10.1074/jbc.M807114200

Mignolet-Spruyt, L., Xu, E., Idänheimo, N., Hoeberichts, F. A., Mühlenbock, P., Brosche, M., et al. (2016). Spreading the news: subcellular and organellar reactive oxygen species production and signalling. *J. Exp. Bot.* 67, 3831–3844. doi: 10.1093/jxb/erw080

Mühlenbock, P., Szechyńska-Hebda, M., Płaszczyca, M., Baudo, M., Mateo, A., Mullineaux, P. M., et al. (2008). Chloroplast signaling and lesion simulating disease1 regulate crosstalk between light acclimation and immunity in *Arabidopsis*. *Plant Cell* 20, 2339–2356. doi: 10.1105/tpc.108.059618

Müller, M., and Munné-Bosch, S. (2015). Ethylene response factors: a key regulatory hub in hormone and stress signaling. *Plant Physiol.* 169, 32–41. doi: 10.1104/pp.15.00677

Nakano, M., and Mukaihara, T. (2018). Ralstonia solanacearum type III effector RipAL targets chloroplasts and induces jasmonic acid production to suppress salicylic acid-mediated defense responses in plants. *Plant Cell Physiol.* 59, 2576–2589. doi: 10.1093/pcp/pcy177

Nelson, R. (2020). International plant pathology: past and future contributions to global food security. *Phytopathology* 110, 245–253. doi: 10.1094/PHYTO-08-19-0300-IA

Noctor, G., Queval, G., and Gakière, B. (2006). NAD(P) synthesis and pyridine nucleotide cycling in plants and their potential importance in stress conditions. *J. Exp. Bot.* 57, 1603–1620. doi: 10.1093/jxb/erj202

Nomura, H., Komori, T., Uemura, S., Kanda, Y., Shimotani, K., Nakai, K., et al. (2012). Chloroplast-mediated activation of plant immune signalling in *Arabidopsis*. *Nat. Commun.* 3:926. doi: 10.1038/ncomms1926

Nosek, M., Kornaś, A., Kuźniak, E., and Miszalski, Z. (2015). Plastoquinone redox state modifies plant response to pathogen. *Plant Physiol. Biochem.* 96, 163–170. doi: 10.1016/j.plaphy.2015.07.028

Park, E., Nedo, A., Caplan, J. L., and Dinesh-Kumar, S. P. (2018). Plant–microbe interactions: organelles and the cytoskeleton in action. *New Phytol.* 217, 1012–1028. doi: 10.1111/nph.14959

Pfannschmidt, T., Bräutigam, K., Wagner, R., Dietzel, L., Schröter, Y., Steiner, S., et al. (2009). Potential regulation of gene expression in photosynthetic cells by redox and energy state: approaches towards better understanding. *Ann. Bot.* 103, 599–607. doi: 10.1093/aob/mcn081

Pieterse, C. M. J., Leon-Reyes, A., Van Der Ent, S., and Van Wees, S. C. M. (2009). Networking by small-molecule hormones in plant immunity. *Nat. Chem. Biol.* 5, 308–316. doi: 10.1038/nchembio.164

Potters, G., Horemans, N., and Jansen, M. A. K. (2010). The cellular redox state in plant stress biology – a charging concept. *Plant Physiol. Biochem.* 48, 292–300. doi: 10.1016/j.plaphy.2009.12.007

Prost, I., Dhondt, S., Rothe, G., Vicente, J., Rodriguez, M. J., Kift, N., et al. (2005). Evaluation of the antimicrobial activities of plant oxylipins supports their involvement in defense against pathogens. *Plant Physiol.* 139, 1902–1913. doi: 10.1104/pp.105.066274

Reumann, S., and Corpas, F. J. (2010). "The peroxisomal ascorbate– glutathione pathway: molecular identification and insights into its essential role under environmental stress conditions," in *Ascorbate-Glutathione Pathway and Stress Tolerance in Plants*, eds N. A. Anjum, M.-T. Chan, and S. Umar (Dordrecht: Springer), 387–404. doi: 10.1007/978-90-481-9404-9_14

Rintamäki, E., Lepistö, A., and Kangasjärvi, S. (2009). Implication of chlorophyll biosynthesis on chloroplast-to-nucleus retrograde signaling. *Plant Signal. Behav.* 4, 545–547. doi: 10.4161/psb.4.6.8711

Robert-Seilaniantz, A., Grant, M., and Jones, J. D. G. (2011). Hormone crosstalk in plant disease and defense: more than just jasmonate-salicylate antagonism. *Annu. Rev. Phytopathol.* 49, 317–343. doi: 10.1146/annurev-phyto-073009-114447

Rock, C. D., and Zeevaart, J. A. D. (1991). The aba mutant of *Arabidopsis thaliana* is impaired in epoxy-carotenoid biosynthesis. *Proc. Natl. Acad. Sci. U.S.A.* 88, 7496–7499. doi: 10.1073/pnas.88.17.7496

Roden, L. C., and Ingle, R. A. (2009). Lights, rhythms, infection: the role of light and the circadian clock in determining the outcome of plant-pathogen interactions. *Plant Cell* 21, 2546–2552. doi: 10.1105/tpc.109.069922

Rodríguez-Herva, J. J., González-Melendi, P., Cuartas-Lanza, R., Antúnez-Lamas, M., Río-Alvarez, I., Li, Z., et al. (2012). A bacterial cysteine protease effector protein interferes with photosynthesis to suppress plant innate immune responses. *Cell. Microbiol.* 14, 669–681. doi: 10.1111/j.1462-5822.2012.01749.x

Rossi, F. R., Krapp, A. R., Bisaro, F., Maiale, S. J., Pieckenstain, F. L., and Carrillo, N. (2017). Reactive oxygen species generated in chloroplasts contribute to tobacco leaf infection by the necrotrophic fungus *Botrytis cinerea*. *Plant J.* 92, 761–773. doi: 10.1111/tpj.13718

Saxena, I., Srikanth, S., and Chen, Z. (2016). Cross talk between H2O2 and interacting signal molecules under plant stress response. *Front. Plant Sci.* 7:570. doi: 10.3389/fpls.2016.00570

Schmidt, A., Mächtel, R., Ammon, A., Engelsdorf, T., Schmitz, J., Maurino, V. G., et al. (2020). Reactive oxygen species dosage in *Arabidopsis* chloroplasts can improve resistance towards *Colletotrichum higginsianum* by the induction of WRKY33. *New Phytol.* 226, 189–204. doi: 10.1111/nph.16332

Sewelam, N., Jaspert, N., Van Der Kelen, K., Tognetti, V. B., Schmitz, J., Frerigmann, H., et al. (2014). Spatial H2O2 signaling specificity: H2O2 from chloroplasts and peroxisomes modulates the plant transcriptome differentially. *Mol. Plant* 7, 1191–1210. doi: 10.1093/mp/ssu070

Seyfferth, C., and Tsuda, K. (2014). Salicylic acid signal transduction: the initiation of biosynthesis, perception and transcriptional reprogramming. *Front. Plant Sci.* 5:697. doi: 10.3389/fpls.2014.00697

Shapiguzov, A., Vainonen, J. P., Wrzaczek, M., and Kangasjärvi, J. (2012). ROS-talk – how the apoplast, the chloroplast, and the nucleus get the message through. *Front. Plant Sci.* 3:292. doi: 10.3389/fpls.2012.00292

Sørhagen, K., Laxa, M., Peterhänsel, C., and Reumann, S. (2013). The emerging role of photorespiration and non-photorespiratory peroxisomal metabolism in pathogen defence. *Plant Biol.* 15, 723–736. doi: 10.1111/j.1438-8677.2012.00723.x

Sowden, R. G., Watson, S. J., and Jarvis, P. (2018). The role of chloroplasts in plant pathology. *Essays Biochem.* 62, 21–39. doi: 10.1042/EBC20170020

Sun, L., Ren, H., Liu, R., Li, B., Wu, T., Sun, F., et al. (2010). An h-Type thioredoxin functions in tobacco defense responses to two species of viruses and an abiotic oxidative stress. *Mol. Plant-Microbe Interact.* 23, 1470–1485. doi: 10.1094/MPMI-01-10-0029

Taler, D., Galperin, M., Benjamin, I., Cohen, Y., and Kenigsbuch, D. (2004). Plant eR genes that encode photorespiratory enzymes confer resistance against disease. *Plant Cell* 16, 172–184. doi: 10.1105/tpc.016352

Virdi, K. S., Laurie, J. D., Xu, Y. Z., Yu, J., Shao, M. R., Sanchez, R., et al. (2015). *Arabidopsis* MSH1 mutation alters the epigenome and produces heritable changes in plant growth. *Nat. Commun.* 6:6386. doi: 10.1038/ncomms7386

Wang, M., Rui, L., Yan, H., Shi, H., Zhao, W., Lin, J. E., et al. (2018). The major leaf ferredoxin Fd2 regulates plant innate immunity in *Arabidopsis*. *Mol. Plant Pathol.* 19, 1377–1390. doi: 10.1111/mpp.12621

Yao, N., and Greenberg, J. T. (2006). *Arabidopsis* accelerated cell death2 modulates programmed cell death. *Philos. Trans. R. Soc. B* 18, 397–411. doi: 10.1105/tpc.105.036251

Zechmann, B. (2019). Ultrastructure of plastids serves as reliable abiotic and biotic stress marker. *PLoS One* 14:e0214811. doi: 10.1371/journal.pone.0214811

Zeng, L., Yang, X., and Zhou, J. (2020). The xanthophyll cycle as an early pathogenic target to deregulate guard cells during *Sclerotinia sclerotiorum* infection. *Plant Signal. Behav.* 15, 1. doi: 10.1080/15592324.2019.1691704

Zhou, J., Zeng, L., Liu, J., and Xing, D. (2015). Manipulation of the xanthophyll cycle increases plant susceptibility to *Sclerotinia sclerotiorum*. *PLoS Pathog.* 11:e1004878. doi: 10.1371/journal.ppat.1004878

Zoeller, M., Stingl, N., Krischke, M., Fekete, A., Waller, F., Berger, S., et al. (2012). Lipid profiling of the *Arabidopsis* hypersensitive response reveals specific lipid peroxidation and fragmentation processes: biogenesis of pimelic and azelaic acid. *Plant Physiol.* 160, 365–378. doi: 10.1104/pp.112.202846

Zurbriggen, M. D., Carrillo, N., Tognetti, V. B., Melzer, M., Peisker, M., Hause, B., et al. (2009). Chloroplast-generated reactive oxygen species play a major role in localized cell death during the non-host interaction between tobacco and *Xanthomonas campestris* pv. vesicatoria. *Plant J.* 60, 962–973. doi: 10.1111/j.1365-313X.2009.04010.x

Conflict of Interest: The authors declare that the research was conducted in the absence of any commercial or financial relationships that could be construed as a potential conflict of interest.

frontiers in Plant Science

ORIGINAL RESEARCH
published: 04 December 2020
doi: 10.3389/fpls.2020.576718

Synergistic Regulation of Nitrogen and Sulfur on Redox Balance of Maize Leaves and Amino Acids Balance of Grains

*Shuoran Liu[1], Shuai Cui[1], Xue Zhang[1], Yin Wang[1], Guohua Mi[2] and Qiang Gao[1]**

[1] Key Laboratory of Sustainable Utilization of Soil Resources in The Commodity Grain Bases of Jilin Province, College of Resource and Environmental Sciences, Jilin Agricultural University, Changchun, China, [2] College of Resources and Environmental Science, China Agricultural University, Beijing, China

As a primary food crop, maize is widely grown around the world. However, the deficiency of essential amino acids, such as lysine, tryptophan, and methionine, results in poor nutritional quality of maize. In addition, the protein concentration of maize declines with the increase in yield, which further reduces the nutritional quality. Here, the photosynthesis of leaves, grain amino acid composition, and stoichiometry of N and S are explored. The results show that N and S maintained the redox balance by increasing the content of glutathione in maize leaves, thereby enhancing the photosynthetic rate and maize yield. Simultaneously, the synergy of N and S increased the grain protein concentration and promoted amino acid balance by increasing the cysteine concentration in maize grains. The maize yield, grain protein concentration, and concentration of essential amino acids, such as lysine, tryptophan, and methionine, could be simultaneously increased in the N:S ratio range of 11.0 to 12.0. Overall, the synergy of N and S simultaneously improved the maize yield and nutritional quality by regulating the redox balance of maize leaves and the amino acids balance of grains, which provides a new theoretical basis and practical method for sustainable production of maize.

Keywords: cysteine, glutathione, maize, nitrogen, photosynthesis, Rubisco, sulfur

OPEN ACCESS

Edited by:
Francisco J. Corpas, Estación Experimental del Zaidín, Spain

Reviewed by:
Jiwang Zhang, Shandong Agricultural University, China
Shiwei Guo, Nanjing Agricultural University, China

****Correspondence:***
Qiang Gao
gyt9962@126.com

Specialty section:
This article was submitted to Plant Abiotic Stress, a section of the journal Frontiers in Plant Science

Received: *26 June 2020*
Accepted: *23 October 2020*
Published: *04 December 2020*

Citation:
Liu S, Cui S, Zhang X, Wang Y, Mi G and Gao Q (2020) Synergistic Regulation of Nitrogen and Sulfur on Redox Balance of Maize Leaves and Amino Acids Balance of Grains. Front. Plant Sci. 11:576718. doi: 10.3389/fpls.2020.576718

INTRODUCTION

Contemporary grain production faces great challenges, including that more than 1 in 10 people still do not have access to sufficient energy and protein in their diets even with recent productivity gains (Food and Agriculture Organization of the United Nations, 2018). As one of the main food crops, maize (*Zea mays* L.) provides 20% of the calories and 15% of the protein in the global diet, making an important contribution to global food security (Bhatnagar et al., 2004). In terms of production, maize has become the most productive cereal crop (Liu et al., 2020). However, the serious deficiency of essential amino acids (EAA), such as lysine, tryptophan, and methionine, results in an amino acid imbalance in the grain, which often requires expensive dietary supplementation (Ali et al., 2011; Li et al., 2020). Simultaneously, in maize production, a yield increase usually results in a continuous decline in protein concentration, which decreases by an average of 0.3% per decade

(Duvick, 2005; Chen et al., 2015). One study based on 45 maize varieties from the 1920s through 2001 shows that the increase in maize yield was mainly achieved by enhancing the starch concentration in the grains. The concentration of EAA, such as lysine, tryptophan, and methionine, in maize grains decreased as the yield increased (Scott et al., 2006). In addition, climate change also seriously affects food yield and nutritional quality (Li et al., 2009; Soares et al., 2019). Therefore, how to synchronously improve grain yield and nutritional quality is a great challenge in maize production.

Among the many strategies to increase crop yield, increasing the efficiency and productivity of photosynthesis is widely accepted as the pivotal measure (Leister, 2012; Long et al., 2015; Foyer et al., 2017; Wu et al., 2019). However, because it is a key catalytic enzyme for photosynthesis, the low efficiency of ribose-1,5-bisphosphate carboxylase/oxygenase (Rubisco) has always plagued attempts at the improvement of photosynthesis (Igamberdiev, 2015; Sharwood, 2016). Consequently, plants need a significant nitrogen (N) investment to synthesize a large amount of Rubisco for carbohydrate synthesis (Whitney and Sharwood, 2014). In fact, Rubisco is the most abundant protein in plants, accounting for 50% of the soluble protein in the leaves, and 25% of the N in the leaves is used to synthesize Rubisco (Parry et al., 2013). It has been suggested that N deficiency causes concentration of Rubisco to be significantly reduced in leaves, which leads to decreased rates of chloroplast electron transport (Osaki et al., 1993; von Caemmerer et al., 2004). Furthermore, N deficiency severely reduces the maximum carboxylation rate of Rubisco, the photosynthetic rate, and the use of triose-P parameters (Rubio-Wilhelmi et al., 2014). Similarly, as an important component of Rubisco, sulfur (S) also affects its metabolism and activity (Ashida et al., 2005). In plants of S deficiency, the levels of chlorophyll and the Rubisco in leaves are reduced twofold and sixfold, respectively, and PSII efficiency is reduced by 31%, which results in a significant reduction in photosynthesis efficiency (Lunde et al., 2008). In addition, some studies show that the deficiency of N and S can reduce the intensity of photosynthesis by affecting the content of hydrogen peroxide (H_2O_2) and glutathione (GSH) in maize plants (Bashir et al., 2020; Nemat Alla and Hassan, 2020). In conclusion, the deficiency of N and S inhibits the photosynthesis of crops and ultimately leads to yield reduction (Resurreccion et al., 2002; Ding et al., 2005).

In terms of the nutritional quality of maize, it is thought that increasing the protein concentration of grains could improve the nutritional quality of maize. However, an imbalance of amino acids in the diet could cause serious negative effects (Maurin et al., 2014). Therefore, in order to obtain balanced nutrition, it is not enough to consider the accumulation of protein; the proportion of amino acids in dietary protein should also be considered (Kim et al., 2019). Studies show that simply increasing the protein concentration of maize grains may not necessarily improve its nutritional quality and even has a negative impact (Wu and Messing, 2012). MacGregor et al. (1961) found that N application could significantly increase the protein concentration of maize grains, but the concentration of each amino acid in the protein did not increase uniformly. Among all amino acids, the concentration of non-essential amino acids (NAA), such as glutamic acid and proline, continuously increase with the increase of N application rates, and EAA, such as lysine and methionine, continuously decrease with the increase of N application rates. Tsai et al. (1983) reported that, as the N application rates increased, zein accumulated preferentially in maize grains, and the concentration of lysine and tryptophan continuously decreased as the protein concentration increased. Subsequent studies show that, with the N application rates increased, the zeins lacking EAA significantly increased, and the concentration of EAA, such as lysine and threonine, continuously decreased, which exacerbated the imbalance of amino acids in grains (Tsai et al., 1992; Lošák et al., 2010).

Contrary to N, S can increase the concentration of EAA in maize grains, especially the concentration of sulfur-containing amino acids, such as cysteine and methionine (Habtegebrial and Singh, 2009). Many studies show that the nutritional quality of crops can be improved by increasing the concentration of methionine and cysteine in crops (Galili and Amir, 2013; Krishnan and Jez, 2018). It is argued that enhanced S storage can increase the concentration of methionine and cysteine in maize grains, thereby promoting the balance of amino acids in grains (Wu et al., 2012; Planta et al., 2017). In fact, the concentration of methionine and cysteine in S-deficient maize grains decreased by 25% and 30%, respectively, and the concentration of asparagine and aspartic acid increased by 30%, which seriously reduced the nutritional quality of maize (Baudet et al., 1986). It can be seen that the regulation effects of N and S on the amino acids in maize grains are different. It is worth optimizing the amino acid balance of maize grains by coordinating the supply of N and S.

As essential mineral nutrient elements for proteins, enzymes, coenzymes, prosthetic groups, vitamins, amino acids, GSH, and secondary metabolites, N and S have important regulatory effects on crop growth, yield, and nutritional quality (Hawkesford et al., 2012; Gigolashvili and Kopriva, 2014). In actual agricultural production, N and S not only independently exert their functions, but also interact with each other. Some studies show that the application rates of N and S and the stoichiometry of N and S in maize plants have an impact on maize yield and nutrient use efficiency (Li et al., 2019; Carciochi et al., 2020). However, synergistically improving maize yield and nutritional quality by regulation of N and S is seldom reported. Therefore, a pot experiment combining N and S fertilization was established to investigate the regulation mechanism of N and S for synergistically improving maize yield and grain protein quality. The relationship between yield, protein concentration, amino acid composition of grains and stoichiometry of N and S in grains was analyzed in this experiment. Besides that, the response of the GSH content, H_2O_2 content, Rubisco activity, photosynthetic rate, and concentration of N and S in leaves to application rates of N and S was also investigated at important growth stages of maize. In this study, the regulation mechanism of N and S was proposed to synergistically enhance maize yield and nutritional quality by maintaining the redox

balance in maize leaves and promoting amino acid balance in maize grains.

MATERIALS AND METHODS

Experimental Design

The experiment was undertaken in a greenhouse at the experimental base of Jilin Agricultural University in 2017 and 2018. The greenhouse temperature was the same as the outdoor temperature. During this experiment, soil samples used for the test were sandy soils with the following characteristics: pH 5.77 (1:2.5 m/v), soil organic matter (SOM) 16.2 g kg^{-1}, available nitrogen (alkali-hydrolyzable N) 61.71 mg kg^{-1}, available phosphorus (Olsen-P) 24.96 mg kg^{-1}, available potassium (1 mol L^{-1} NH_4OAc extracting) 120.92 mg kg^{-1}, and available sulfur [0.008 mol L^{-1} $Ca(H_2PO_4)_2$ extracting] 11.36 mg kg^{-1}. Maize (cv. Liangyu 99) seeds were planted in plastic pots ($\Phi \times h$ = 30 cm × 35 cm) filled with an equal quantity of soil (25 kg pot^{-1}). In each pot, the same amount of water (70%–75% of the maximum water-holding capacity of the soil) was maintained, and the weight of water was controlled using a weighing method. The experiment was a two-factor interaction design of different N and S fertilization levels. Sixteen treatments of a combination of N and S and four repetitions for each treatment were undertaken. Four rates of N, i.e., no N (N0), low N (N1), moderate N (N2), and high N (N3) were applied. The amount of fertilization (g fertilizer kg $soil^{-1}$) was 0, 0.06, 0.24, and 0.48 g kg^{-1}. Four rates of S, i.e., no S (S0), low S (S1), moderate S (S2), and high S (S3) were applied. The amount of fertilization was 0, 0.04, 0.12, and 0.24 g kg^{-1}. The fertilizers used for the test were all AR grade. The types were as follows: nitrogen (N) [$CO(NH_2)_2$, N = 46.2%], phosphorus (P) (KH_2PO_4, P_2O_5 = 52.1%, K_2O = 34.6%), potassium (K) (KCl, K_2O = 62.5%), and sulfur (S) ($MgSO_4 \cdot 7H_2O$, S = 13.0%). The same amount of P (P_2O_5 = 0.15 g kg^{-1}) and K (K_2O = 0.15 g kg^{-1}) fertilizers were maintained in each pot. In the course of filling the pots with soil, total N of the N1 treatment; 1/3 N of the N2 and N3 treatments; and total P, K, and S were applied in every pot as a basal fertilizer mixed with the soil. The remaining 2/3 N of the N2 and N3 treatments was used a topdressing fertilizer in the corresponding pots at the stage when the maize unfolds the eighth leaf. Initially, five maize seeds per pot were planted to a depth of 2 cm. When the seedlings had grown six leaves, one representative seedling was reserved, and the remaining seedlings were removed from the pots. During the entire plant's growth, conventional management for prevention and control of pests and plant diseases was conducted.

Photosynthetic Rate Measurements

The photosynthetic rate of maize leaves (the first leaf above the ear of the maize plant in each experimental treatment) was measured by a Li-6400XT portable photosynthesis system (Li-6400XT, Li-Cor, Inc., Lincoln, NE, United States) at the silking stage and the grain-filling stage (75 and 100 days after planting, DAP), respectively. The measurements were performed during the morning of a sunny day (9:00–11:00). The leaf chamber light intensity of the head light source was set to 1600 μmol m^{-2} s^{-1} photosynthetic photon flux density (PPFD).

H_2O_2 Content, GSH Content, and Rubisco Activity Measurements

The collection of samples for biochemical measurement was performed simultaneously with the determination of photosynthesis. The 10-cm^2 leaf disks collected from the first leaf above the maize ear were quickly placed in liquid nitrogen and stored in a refrigerator at −80°C until extraction (Perdomo et al., 2017). According to the relevant measurement method (Pan et al., 2017; Hou et al., 2018), the H_2O_2 content, GSH content, and Rubisco activity of maize leaves were determined by an enzyme-linked immunosorbent assay method with commercial kits (Jiangsu Kete Biological Science and Technology Co., Ltd., China).

Maize Yield Measurements

At the maturity stage (140 DAP), the plant was cut along the soil surface, and the grains were threshed. All maize grains from each plant were collected and placed in a constant temperature oven at 70°C to dry to a constant weight and weighed.

Grain Ultrastructure Analysis

The grain samples were placed overnight in 2% (v/v) glutaraldehyde in a 0.1 mol L^{-1} phosphate buffer (Buffer A) with a pH of 7.2. The samples were rinsed three times in buffer A for 5 min each time and dehydrated with a gradient series of ethanol (25–100%). The maize grains were horizontally cut into slices (1 mm) and dried in a lyophilizer. The prepared samples were observed and photographed using a scanning electron microscope (SEM) (SU8000, HITACHI, Japan).

Concentration and Stoichiometry of N and S Measurements

At the silking (75 DAP), grain-filling (100 DAP), and maturity stages (140 DAP), a portion (about 50 g, fresh weight, FW) of the leaf near the maize ear was cut and dried in a constant temperature oven at 70°C and then ground into powder for measuring the N and S concentration. Similarly, the maize grains at maturity were dried and ground to measure the N and S concentration. The samples were digested with acid (H_2SO_4-H_2O_2), cooled to room temperature, and equilibrated with deionized water. Then, the N concentration was measured by a Kjeldahl instrument (KDY-9820, KETUO, China). After the samples were digested with acid (HNO_3-$HClO_4$), the S concentration was measured using an inductively coupled plasma instrument (SHIMADZU, I-7500, Japan). The stoichiometry of N and S was determined by the ratio of N to S concentration in the samples.

Grain Protein Concentration Measurements

The concentration of protein in maize grains (P_c) was converted from the N concentration of grains (N_c) measured by the Kjeldahl method using the following equation:

$$P_c = N_c \times 6.25$$

Amino Acid Analysis

An appropriate amount (0.05 g) of the sample was placed in a 20-ml hydrolysis tube, and 20 ml of 6 mol L^{-1} HCl was added. The tube was sealed with nitrogen and hydrolyzed at 110°C for 24 h. The sample used for the determination of tryptophan was hydrolyzed with 5 mol L^{-1} NaOH for 24 h, and the pH of the solution was adjusted to 6 with 6 mol L^{-1} HCl. The amino acid analysis was carried out using a high-performance liquid chromatography instrument (1260 Infinity II, Agilent, United States).

Statistical Analysis

The statistically experimental data were compared using two-way analysis of variance (ANOVA). The least significant difference (LSD) test was used to compare significant differences based on P values < 0.05. Statistical computations and analysis were conducted using the Statistical Analysis System (SAS 9.2, SAS Institute Inc., United States).

RESULTS

Physiological Response in Photosynthesis

During the silking and grain-filling stages of the maize plant, N and S application had significant effects on the concentration of N and S in leaves (**Table 1**), photosynthetic rate (**Figures 1A,B**), and Rubisco activity (**Figures 1C,D**) although their interactions were not significant. Simultaneously, N and S application markedly affected the GSH (**Figures 1E,F**) and H_2O_2 content (**Figures 1G,H**), and their interaction reached a significant level. During the silking stage, the photosynthetic rate (**Figure 1A**), Rubisco activity (**Figure 1C**), and GSH content (**Figure 1E**) of the leaves increased with N application rates. At the N2 and N3 levels, the photosynthetic rate increased with the S application rate and reached a maximum (33.0 μmol m^{-2} s^{-1}) at the N2S3 treatment, which was significantly higher than the N0S0 treatment (21.4 μmol m^{-2} s^{-1}). For each N level, the Rubisco activity and GSH content increased with the increase of S application rates and reached a maximum (267.2 nmol min^{-1} g^{-1}, 16.9 nmol mg^{-1}) at the N3S3 and N2S3 treatments, which was significantly higher than the N0S0 treatment (113.2 nmol min^{-1} g^{-1}, 6.2 nmol mg^{-1}). During the grain-filling stage, the photosynthetic rate (**Figure 1B**) and Rubisco activity (**Figure 1D**) increased with N application rates. Except for the N0 level, the photosynthetic rate and Rubisco

TABLE 1 | N and S stoichiometry and photosynthetic rate in maize leaves of different growth stages.

Treatment		Silking stage (75 DAP)				Grain-filling stage (100 DAP)			
		N_c	S_c	N:S	Pn	N_c	S_c	N:S	Pn
		(mg g^{-1})	(mg g^{-1})		(μ mol m^{-2} s^{-1})	(mg g^{-1})	(mg g^{-1})		(μ mol m^{-2} s^{-1})
N0	S0	22.2 a D	1.51 b A	14.8 a C	21.4 a A	16.9 a D	1.35 b A	12.8 a C	15.3 a A
	S1	21.9 a D	1.65 ab A	13.4 a C	22.8 a A	17.0 a D	1.47 ab A	11.8 a C	16.3 a B
	S2	21.4 a C	1.74 ab B	12.4 a C	23.5 a B	16.5 a C	1.56 ab A	10.8 a C	17.9 a B
	S3	20.8 a D	1.80 a B	11.7 a C	22.9 a B	15.9 a D	1.61 a A	10.0 a C	17.9 a B
N1	S0	27.9 a C	1.59 b A	17.8 a BC	23.4 a A	22.0 a C	1.39 b A	16.0 a BC	18.2 b A
	S1	29.5 a C	1.71 ab A	17.4 a B	24.9 a A	23.6 a C	1.52 ab A	15.7 a BC	21.4 ab A
	S2	30.6 a B	1.93 a AB	16.0 a BC	29.0 a AB	24.2 a B	1.68 a A	14.6 a BC	25.8 a A
	S3	30.2 a C	1.98 a AB	15.4 a B	28.4 a AB	23.4 a C	1.74 a A	13.6 a BC	25.2 a A
N2	S0	33.5 b B	1.65 b A	20.5 a AB	24.9 b A	26.3 b B	1.43 b A	18.6 a AB	18.9 b A
	S1	35.7 ab B	1.87 b A	19.3 ab AB	27.1 ab A	28.3 ab B	1.63 ab A	17.7 a AB	23.5 b A
	S2	37.7 a A	2.16 a A	17.6 ab AB	31.3 ab A	30.2 a A	1.83 a A	16.7 a AB	29.9 a A
	S3	36.6 a B	2.22 a A	16.6 b B	33.0 a A	29.7 ab B	1.89 a A	15.9 a AB	29.3 a A
N3	S0	37.9 a A	1.64 b A	23.2 a A	23.7 b A	30.3 a A	1.42 b A	21.6 a A	18.2 c A
	S1	39.6 a A	1.85 ab A	21.7 a A	28.4 ab A	31.6 a A	1.59 ab A	20.0 a A	23.1 bc A
	S2	40.7 a A	2.01 a AB	20.6 a A	33.7 a A	32.7 a A	1.72 a A	19.3 a A	28.7 a A
	S3	40.5 a A	2.04 a AB	20.0 a A	32.9 a A	33.2 a A	1.87 a A	18.1 a A	27.4 ab A
ANOVA									
N		**	**	**	**	**	*	**	**
S		*	**	**	**	*	**	*	**
N × S		*ns*	*ns*	*ns*	*ns*	*ns*	*ns*	*ns*	*ns*

*The data are the means of four replicates (N = 4). Different lowercase letters after the data indicate the significant differences between the different S rates at the same N level ($P < 0.05$), and different capital letters after the data indicate the significant differences between the different N rates at the same S level ($P < 0.05$). The variance analysis used two-way ANOVA (**$P < 0.01$, *$P < 0.05$, ns $P > 0.05$). N_c, nitrogen concentration in leaves; S_c, sulfur concentration in leaves; Pn, net photosynthetic rate.*

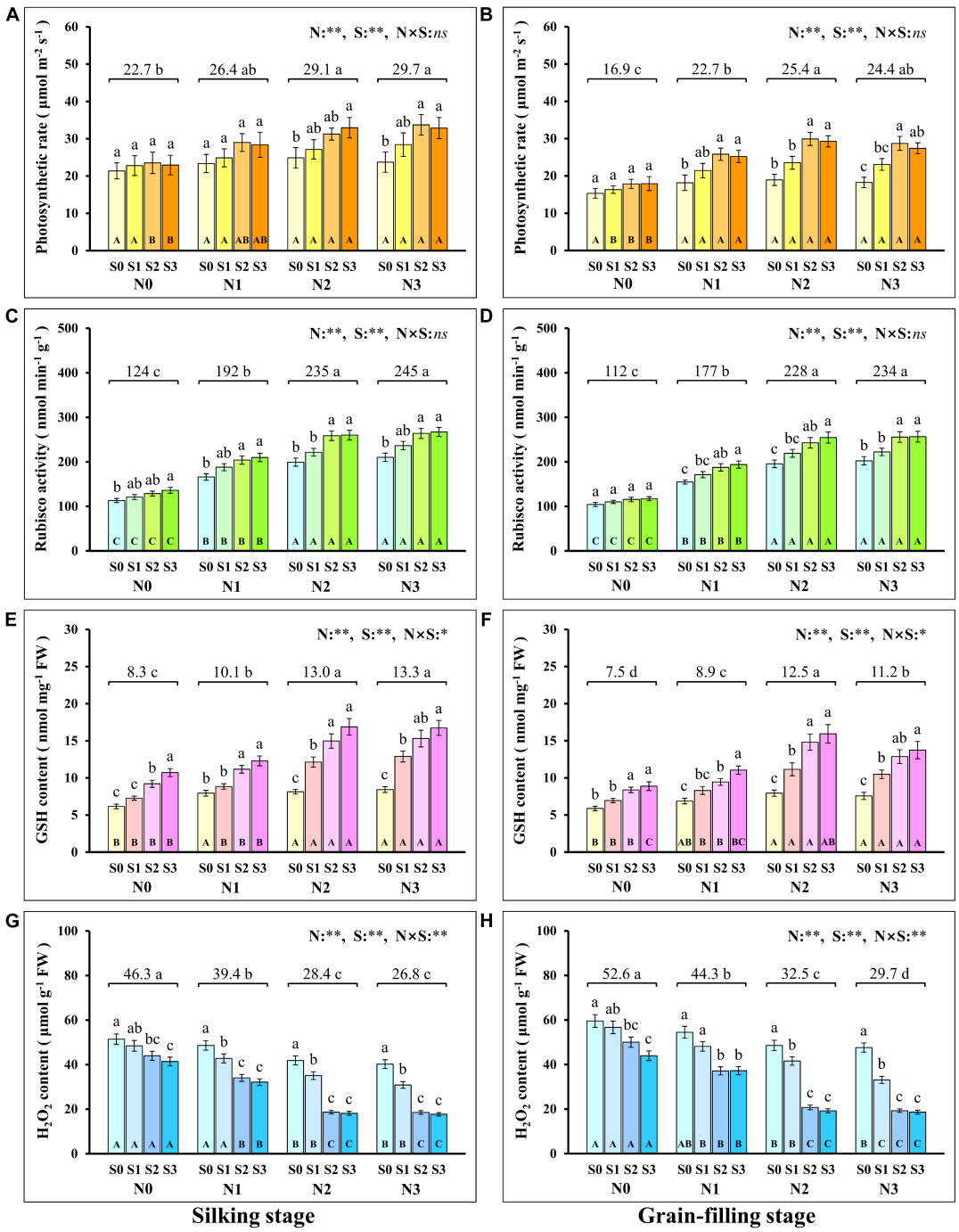

FIGURE 1 | Physiological response during photosynthesis at different N and S rates. The data are the means of four replicates, and the error bars represent the standard deviations. The lowercase letters above the bars indicate the significant differences between the different S rates at the same N level, and the different uppercase letters in the bars indicate the significant differences between the different N rates at the same S level. The number on the horizontal line above each group of bars indicates the average value of the corresponding indicator represented by the ordinate axis at different N levels, and the lowercase letters after the number indicate that the indicator has significant differences at different N levels. The variance analysis used two-way ANOVA (**$P < 0.01$, *$P < 0.05$, *ns* $P > 0.05$). Response of photosynthetic rate **(A,B)**, Rubisco activity **(C,D)**, GSH **(E,F)**, H_2O_2 content **(G,H)** in silking and grain-filling stage to different N and S rates.

activity at other N levels increased with S application rates and reached a maximum (29.9 μmol m^{-2} s^{-1}, 256.6 nmol min^{-1} g^{-1}) at the N2S2 and N3S3 treatments, respectively. During the grain-filling stage, the GSH content (**Figure 1F**) increased with N application rates, reached a maximum at the N2 level, and then decreased at the N3 level. For each N level,

the GSH content increased with the S application and reached a maximum (15.9 nmol mg^{-1}) at the N2S3 treatment. During the silking and the grain-filling, the H_2O_2 content (**Figures 1G,H**) continuously decreased with the increase of S application rates at each N level. For each S level, the H_2O_2 content continuously decreased with the increase of N application rates and reached a maximum (17.7 nmol g^{-1}, 18.6 nmol g^{-1}) at the N3S3 treatment, which has no significant difference compared with

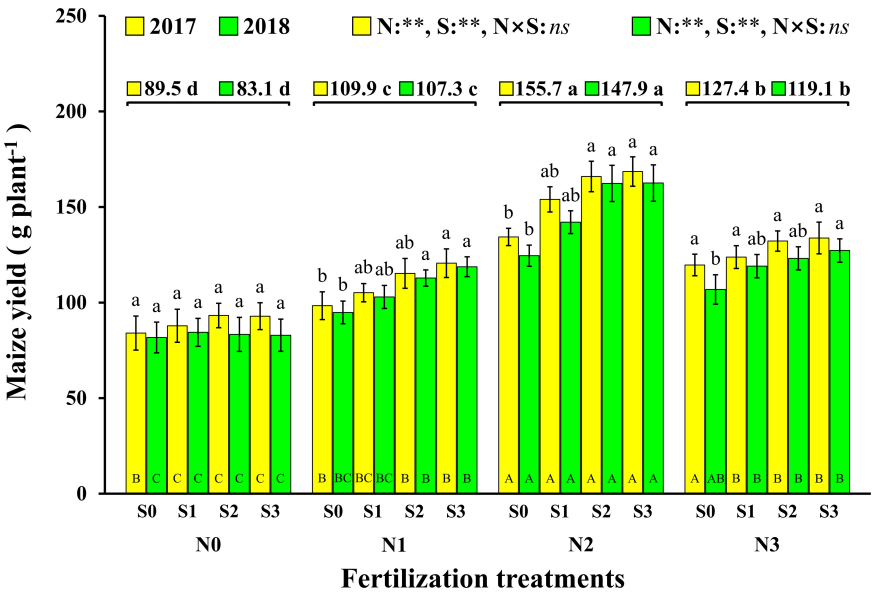

FIGURE 2 | Effect of N and S on maize yield. The data are the means of four replicates, and the error bars represent the standard deviations. The lowercase letters above the bars indicate the significant differences between the different S rates at the same N level in the same year, and the different uppercase letters in the bars indicate the significant differences between the different N rates at the same S level in the same year. The number on the horizontal line above each group of bars indicates the average value of grain yield of maize at different N levels in the same year, and the lowercase letters after the numbers indicate the significant difference in yield at different N levels. The variance analysis used two-way ANOVA (**$P < 0.01$, *ns* $P > 0.05$).

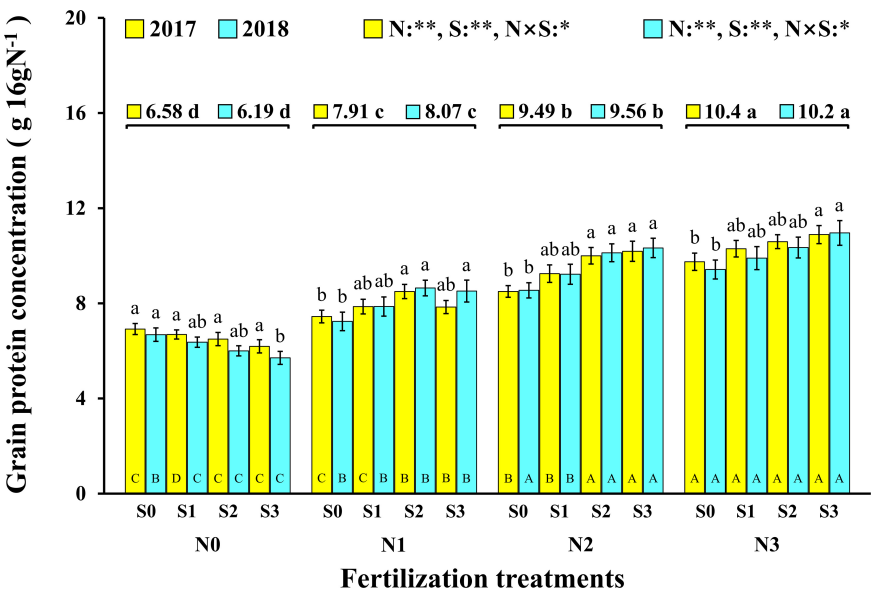

FIGURE 3 | Effect of N and S on grain protein concentration of maize. The data are the means of four replicates, and the error bars represent the standard deviation. The lowercase letters above the bars indicate the significant differences between the different S rates at the same N level in the same year, and the different uppercase letters in the bars indicate the significant differences between the different N rates at the same S level in the same year. The number on the horizontal line above each group of bars indicates the average value of protein concentration of maize at different N levels in the same year, and the lowercase letters after the numbers indicate the significant difference in protein concentration at different N levels. The variance analysis used two-way ANOVA (**$P < 0.01$, *$P < 0.05$).

TABLE 2 | N and S stoichiometry of maize leaves and grains during maturity stage (140 DAP).

Treatment		Leaf			Grain		
		N_c	S_c	N:S	N_c	S_c	N:S
		(mg g^{-1})	(mg g^{-1})		(mg g^{-1})	(mg g^{-1})	
N0	S0	14.6 a D	1.27 b A	11.6 a C	10.7 a B	0.89 b A	12.4 a A
	S1	14.7 a D	1.36 ab A	10.9 a B	10.2 ab C	0.99 ab A	11.1 ab A
	S2	13.9 ab D	1.45 ab A	9.66 ab C	9.60 ab C	1.18 ab A	8.29 b C
	S3	12.8 b D	1.54 a A	8.39 b C	9.13 b C	1.27 a A	7.31 b B
N1	S0	19.1 a C	1.29 b A	15.0 a B	11.6 b B	0.89 c A	13.4 a A
	S1	20.5 a C	1.41 ab A	14.6 a A	12.6 ab B	1.12 b A	11.4 ab A
	S2	20.4 a C	1.52 a A	13.5 ab B	13.8 a B	1.32 ab A	10.6 ab BC
	S3	18.9 a C	1.58 a A	12.0 b B	13.6 a B	1.43 a A	9.60 b BC
N2	S0	22.5 a B	1.31 b A	17.3 a AB	13.7 b A	0.97 b A	14.2 a A
	S1	23.8 a B	1.48 ab A	16.3 ab A	14.8 ab A	1.14 b A	13.3 ab A
	S2	24.2 a B	1.60 a A	15.3 ab AB	16.2 a A	1.38 a A	11.9 ab AB
	S3	23.5 a B	1.68 a A	14.2 b A	16.5 a A	1.50 a A	11.1 b AB
N3	S0	25.7 a A	1.40 b A	18.5 a A	15.1 b A	0.96 c A	15.8 a A
	S1	26.7 a A	1.57 ab A	17.1 ab A	15.8 ab A	1.10 bc A	14.4 ab A
	S2	27.1 a A	1.67 ab A	16.4 ab A	16.6 ab A	1.17 b A	14.2 ab A
	S3	26.7 a A	1.77 a A	15.2 b A	17.5 a A	1.34 a A	13.2 b A
ANOVA							
N		**	**	**	**	*	**
S		*	**	**	*	**	**
N × S		*ns*	*ns*	*ns*	*	*ns*	*ns*

*The data are the means of four replicates (N = 4). Different lowercase letters after the data indicate the significant differences between the different S rates at the same N level ($P < 0.05$), and different capital letters after the data indicate the significant differences between the different N rates at the same S level ($P < 0.05$). The variance analysis used two-way ANOVA, (**$P < 0.01$, *$P < 0.05$, ns $P > 0.05$). N_c, nitrogen concentration of samples; S_c, sulfur concentration of samples.*

the N2S2, N2S3, and N3S2 treatments, but was significantly lower than the N0S0 treatment (51.4 nmol g^{-1}, 59.6 nmol g^{-1}). Overall, the photosynthetic rate was directly proportional to Rubisco activity and GSH content and inversely proportional to H_2O_2 content.

Grain Yield of Maize

The change trend in maize yield in 2017 and 2018 was same, and the results show that both N and S had significant effects on maize yield, but there were no significant interactions between the two elements (**Figure 2**). The effect of N on maize yield was analyzed, and it is demonstrated that the maize yield with N application was significantly higher than that without N application (N0). Compared to N0 (89.5 g $plant^{-1}$ and 83.1 g $plant^{-1}$, 2017 and 2018), the maize yield with the N1, N2, and N3 levels increased by 22.8% and 29.0% (2017 and 2018), 74.0% and 78.0% (2017 and 2018), and 42.3% and 43.3% (2017 and 2018), respectively. The maize yield of S application was also significantly higher than that without S application (S0). Compared to S0 (109.1 g $plant^{-1}$ and 94.5 g $plant^{-1}$, 2017 and 2018), the maize yields with the S1, S2, and S3 levels increased by 7.9% and 9.4% (2017 and 2018), 16.1% and 20.8% (2017 and 2018), and 18.1% and 22.8% (2017 and 2018), respectively. At the N1 and N2 levels, maize yield increased with S application rates. For each S level, maize yield increased with N application rates and reached a maximum at the N2 level and then decreased at the N3 level. The highest yields were observed under the N2S2 and N2S3 treatments with yields of 166.0 g $plant^{-1}$ and 162.3 g $plant^{-1}$ (2017 and 2018), 168.6 g $plant^{-1}$ and 162.6 g $plant^{-1}$ (2017 and 2018), respectively.

Grain Protein Concentration of Maize

In this experiment, the change trend in the grain protein concentration was the same in the two consecutive years (**Figure 3**). In 2017 and 2018, both N and S had significant effects on the grain protein concentration of maize, and their interaction reached a significant level. Correspondingly, the concentration of N and S in leaves and maize grains during the maturity stage (2018) increased significantly with the application of N and S, and there were significant interactions between N and S on grain N concentration (**Table 2**). For each S level, grain protein concentration in maize continuously increased with N application rates. The grain protein concentration in maize decreased as S application rates increased at the N0 level, which may be ascribed to the S application inhibiting the N absorption of maize at a low N supply. Under N application conditions, grain protein concentration was directly proportional to S application rates and reached a maximum (10.9 g $16gN^{-1}$, 11.0 g $16gN^{-1}$, 2017 and 2018) at the N3S3 treatment. It is worth emphasizing that the N2S3 treatment achieved the highest maize yield, but its grain protein concentration still reached a high level (10.2 g $16gN^{-1}$, 10.3 g $16gN^{-1}$, 2017 and 2018) and had no significant difference from the N3S3 treatment although it was significantly higher than the N0S0 treatment (6.9 g $16gN^{-1}$, 6.7 g $16gN^{-1}$, 2017 and 2018).

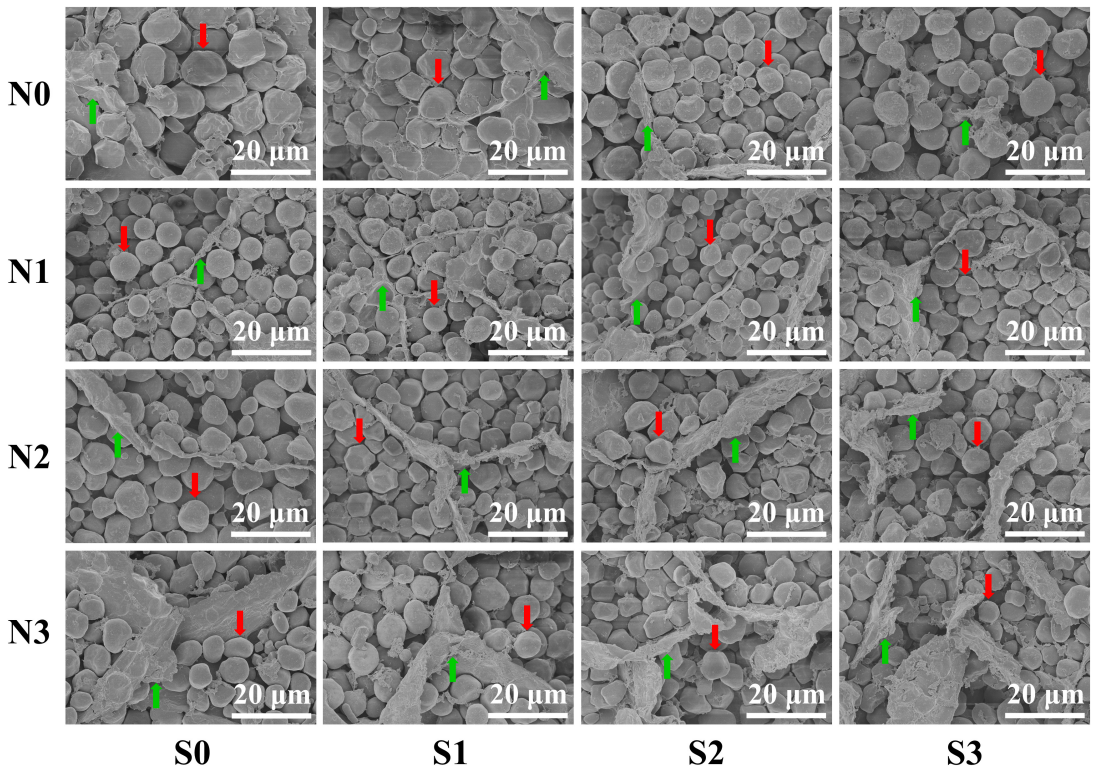

FIGURE 4 | Grain endosperm ultrastructure of maize at different N and S rates. The weight of individual grains was calculated based on the grain weight per hundred kernels of the maize, and the grains equal to the average grain weight were selected by weighing with an electronic balance. The selected samples of maize grains were sliced with a blade (thickness ≈ 1 mm). The prepared samples were observed and photographed using a scanning electron microscope. In this image, the red arrows indicate the starch granules, the green arrows indicate the matrix proteins, and the bars represent 20 μm.

Grain Ultrastructure of Maize

To verify the regularity of the changes in protein concentration in grains, the ultrastructure of maize grains was tested. An SEM image showed that the change trend of the matrix proteins was completely consistent with the measured value of protein concentration in grains (**Figure 4**). At the N0 level, the starch granules in the maize grains were larger and irregularly shaped, and their arrangement was loose with a small number of matrix proteins interspersed in the gaps of the starch granules. At the N1 level, the starch granules in maize grains were small and spheroidal, which were arranged closely and orderly and had a large amount, and the divided matrix proteins were interspersed in the gaps of the starch granules. At the N2 and N3 levels, the starch granules in maize grains were closely arranged, and a large number of matrix proteins was interspersed in the gaps of the starch granules. In terms of S application, the matrix proteins in maize grains at other N levels increased as S application rates increased except for the N0 level.

Grain Amino Acids Analysis of Maize

To evaluate the nutritional quality of maize grains, the concentration of amino acids in maize grains was measured and analyzed in 2018 (**Figure 5**). At the N0 level, various amino acids in maize grains were at their lowest level. At the N1 level, except for tyrosine and threonine, the concentration of other amino acids was at a lower level and slightly higher than that of the N0 treatment. At the N2 level, the concentrations of aspartic acid, histidine, tyrosine, phenylalanine, threonine, valine, leucine, isoleucine, methionine, lysine, and tryptophan were highest, and among these amino acids, other amino acids were EAA except for aspartic acid. At the N3 level, the concentration of glutamate, proline, glycine, arginine, alanine, serine, and cysteine were highest, and among these amino acids, other amino acids were NAA except for cysteine. In addition to the N0 level, the various NAA concentration of S application at other N levels was lower than the S0 level, but at each N level, the various EAA concentration of S application was higher than S0 level. In particular, as a sulfur-containing amino acid, the concentration of cysteine in maize grains increased with N application rates. At the N2 and N3 levels, the concentration of cysteine in maize grains increased with the S application rate (**Figure 6**).

Analysis of the proportion of amino acids in grain protein showed that the total EAA (**Figure 7A**) in grain protein increased first and then decreased with the increase of N application rates and reached the minimum (34.6%) at the N3 level. At each N level, the total EAA in grain protein increased with S application rates and reached the maximum (45.8%) at N1S3 treatment. For each S level, the total EAA in grain protein had no significant

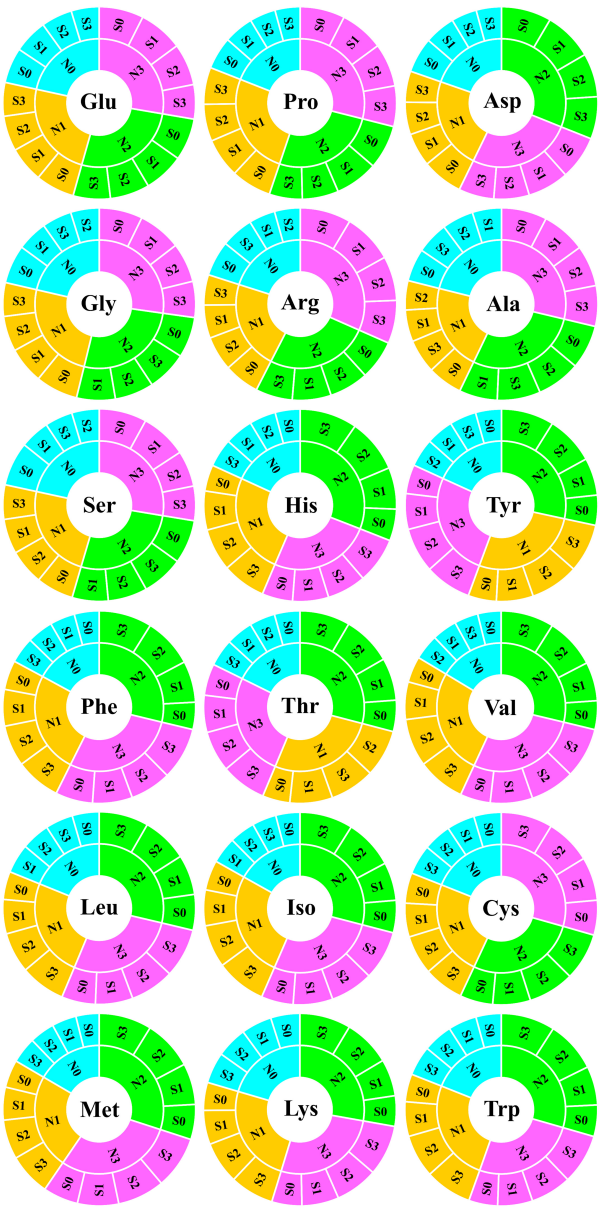

FIGURE 5 | Analysis of amino acids in maize grains. In this image, the abbreviations at the center of the circle represent the amino acid type. The fan-shaped regions of different colors indicate the amino acid concentration of grains at different N rates, and each grid surrounding the outer ring of the same color region indicates the amino acid concentration of different S rates at the same N level. Both the fan-shaped area and the outer ring grid are arranged in descending clockwise order according to the area size. Glu, glutamate; Pro, proline; Asp, aspartic acid; Gly, glycine; Arg, arginine; Ala, alanine; Ser, serine; His, histidine; Tyr, tyrosine; Phe, phenylalanine; Thr, threonine; Val, valine; Leu, leucine; Iso, isoleucine; Cys, cysteine; Met, methionine; Lys, lysine; Trp, tryptophan.

difference at each N application rate. Notably, the highest maize yield was obtained at the N2S3 treatment, but its proportion (42.8%) of EAA in grain protein was not significantly different from the N1S3 treatment.

To further evaluate the balance of amino acids in grain protein, the changes in several amino acids that were usually deficient in maize grains were analyzed emphatically. Methionine (**Figure 7B**) in grain protein increased with N application rates and reached a maximum (2.96%) at the N2 level. At each N level, methionine in protein increased as S application rates increased and reached the maximum (3.26%) at the N2S3 treatment. For each S level, methionine in protein had no significant difference at each N application rate. The lysine (**Figure 7C**) in protein continuously decreased as N application rates increased, and the minimum (2.10%) was observed at the N3 level. At the S0 level, lysine in protein decreased with N application rates and reached a minimum (1.70%) at the N3 level. At each N level, lysine in protein increased with S application rates, and the maximum (2.89%) was observed at the N1S3 treatment. Except for the S0 level, there was no significant difference in lysine with N application rates at other S levels. Compared with the N0 level, a small amount (N1 level) and a proper amount (N2 level) of N application had no significant effect on tryptophan (**Figure 7D**) in grain protein, but excessive N application (N3 level) significantly reduced the concentration of tryptophan in grain protein. Except for the N0 level, tryptophan in protein at other N levels increased as S application rates increased and reached the maximum (1.28%) at the N1S3 treatment. For each S level, tryptophan in grain protein had no significant difference at each N application rate.

DISCUSSION

Regulation of N and S to Increase Maize Yield by Enhancing Photosynthesis

Photosynthesis is the biochemical basis of the synthesis of photosynthates, such as sucrose and starch, which directly determine the crop yield (Lunn and Hatch, 1995; Kruger and Volin, 2006). Enhancing photosynthesis is an important guarantee for high crop yield (Lawson et al., 2012). In this study, coordinated application of N and S significantly enhanced GSH content (**Figures 1E,F**), Rubisco activity (**Figures 1C,D**), and photosynthetic rate (**Figures 1A,B**) of maize leaves, which was consistent with the change in maize yield. The increase in photosynthetic rate may benefit from the removal of excessively accumulated H_2O_2 (**Figures 1G,H**) in leaves by GSH to reduce oxidative damage to the Rubisco, which can be inferred from the result that the Rubisco activity was directly proportional to the GSH content, and it was inversely proportional to H_2O_2 content. Actually, plants inevitably produce reactive oxygen species (ROS), such as H_2O_2 during the photosynthesis processes (Foyer, 2018; Smirnoff and Arnaud, 2019). An ROS, such as H_2O_2, has a dual role in plant biology; it is a key regulator of plant growth, development, and defense pathways, and it is a toxic by-product of aerobic metabolism (Mittler et al., 2004; Saxena et al., 2016; Exposito-Rodriguez et al., 2017). H_2O_2, as one of the most stable ROS in plants, can attack Rubisco and cause severe oxidative damage. In this study, Rubisco activity decreased with increasing H_2O_2 content, and the decrease in Rubisco activity directly led to a decrease in photosynthetic

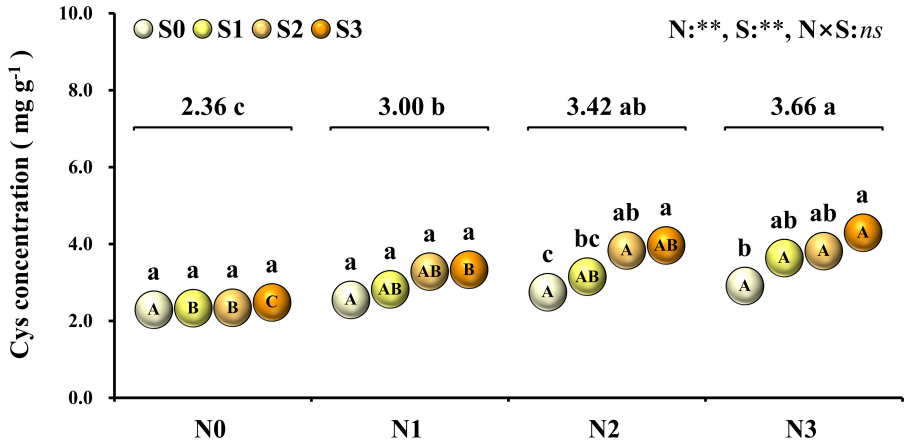

FIGURE 6 | Concentration of cysteine in maize grains at different N and S rates. The data are the means of four replicates. The lowercase letters above the spheres indicate the significant differences between the different S rates at the same N level, and the different uppercase letters in the spheres indicate the significant differences between the different N rates at the same S level. The number on the horizontal line above each group of spheres indicates the average value of concentration of cysteine at different N levels, and the lowercase letters after the numbers indicate the significant difference in concentration of cysteine at different N levels. The variance analysis used two-way ANOVA (**$P < 0.01$, *ns* $P > 0.05$).

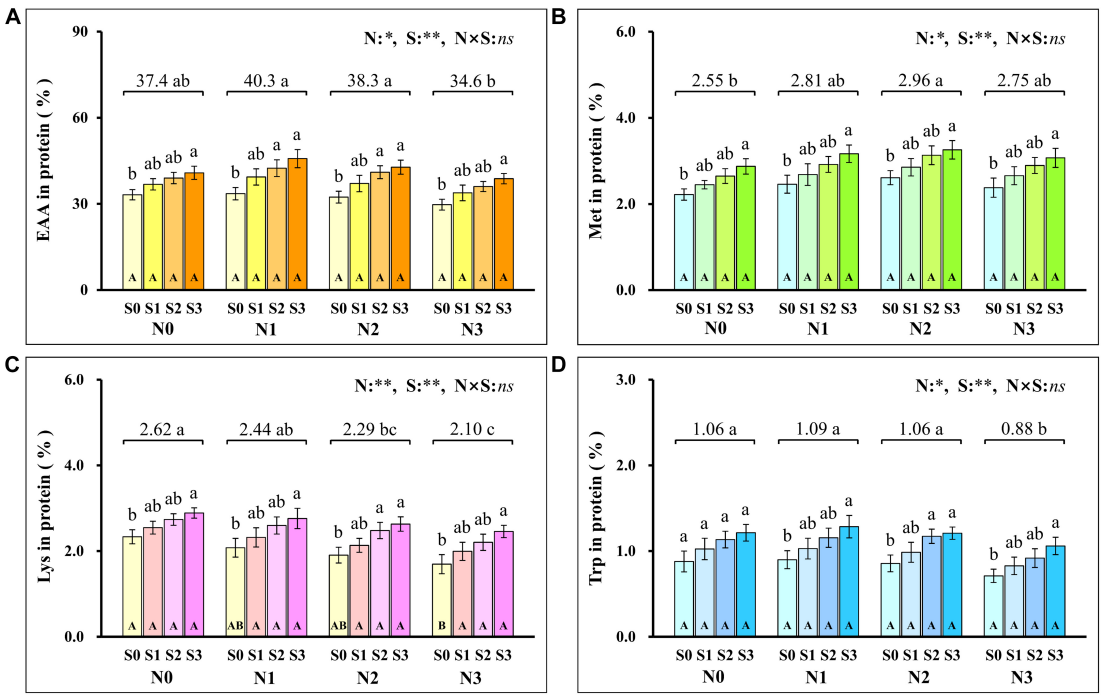

FIGURE 7 | The proportion of total essential amino acids **(A)**, methionine **(B)**, lysine **(C)**, tryptophan **(D)** in protein at different N and S rates. The data are the means of four replicates, and the error bars represent the standard deviation. The lowercase letters above the bars indicate the significant differences between the different S rates at the same N level, and the different uppercase letters in the bars indicate the significant differences between the different N rates at the same S level. The number on the horizontal line above each group of bars indicates the average value of proportion of amino acids in protein at different N levels, and the lowercase letters after the numbers indicate the significant difference in proportion of amino acids in protein at different N levels. The variance analysis used two-way ANOVA (**$P < 0.01$, *$P < 0.05$, *ns* $P > 0.05$). EAA, total essential amino acids; Met, methionine; Lys, lysine; Trp, tryptophan.

rate, which was consistent with previous reports (González-Moro et al., 1997; Li et al., 2004). The redox imbalance in the thiol-disulfide network was ascribed to increased generation of ROS, and GSH can counteract the accumulation of ROS, such as H_2O_2 (König et al., 2018). In this study, the H_2O_2 content decreased with the increase of GSH content, and the photosynthetic rate increased with GSH content, which was consistent with reported results (Fatma et al., 2014). In this study, the GSH content in

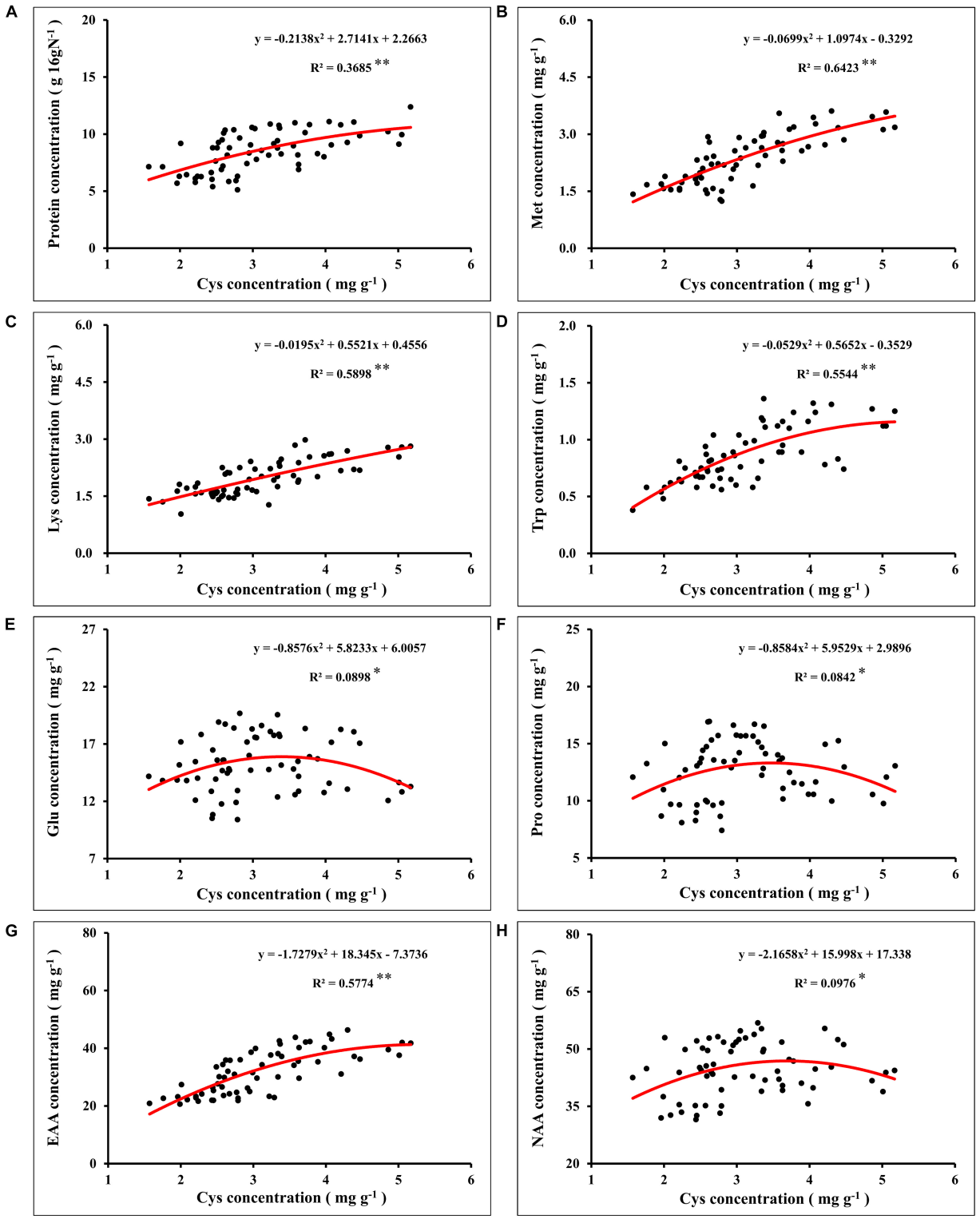

FIGURE 8 | Correlation analysis between the concentration of grain protein **(A)**, methionine **(B)**, lysine **(C)**, tryptophan **(D)**, glutamate **(E)**, proline **(F)**, total essential amino acids **(G)**, total non-essential amino acids **(H)**, and cysteine concentration in maize grains. In this image, the red curve shows the correlation between the concentration of protein, concentration of corresponding amino acids, and cysteine concentration in maize grains (n = 64). Met, methionine; Lys, lysine; Trp, tryptophan; Glu, glutamate; Pro, proline; EAA, total essential amino acids; NAA, total non-essential amino acids.

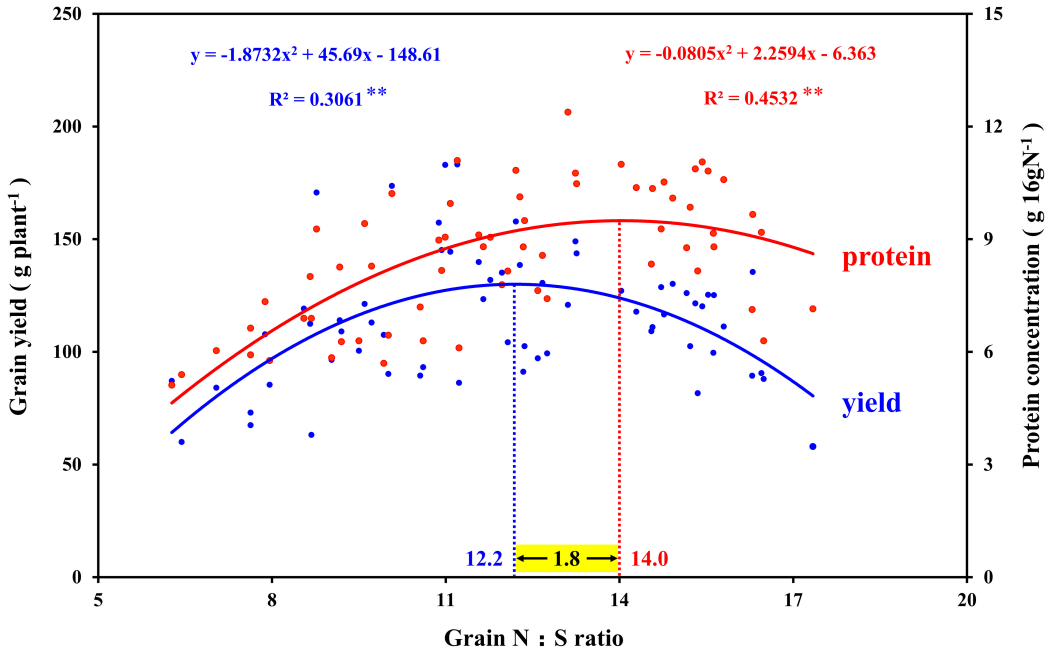

FIGURE 9 | Correlation analysis between the grain yield, grain protein concentration, and N:S ratio in maize grains. In this image, the blue curve shows the correlation between grain yield and N:S ratio in maize grains (n = 64), and the intersection of the blue dotted line and the blue curve indicates the maximum value of the curve. The red curve shows the correlation between grain protein concentration and N:S ratio in maize grains (n = 64), and the intersection of the red dotted line and the red curve indicates the maximum value of the curve.

maize leaves can be achieved by adjusting the application of N and S, which has been confirmed in relevant studies (Gutiérrez-Gamboa et al., 2016; Liang et al., 2016). Therefore, regulating the redox balance of maize leaves by coordinating the supply of N and S nutrients to control the GSH content is an important method for improving photosynthesis. In addition, N and S may also improve photosynthesis by increasing leaf area and chlorophyll concentration of maize, thereby increasing grain yield (Li et al., 2019).

Regulation of N and S to Optimize Grain Protein Concentration and Amino Acid Balance by Increasing Cysteine in Maize Grains

In global maize production, grain protein concentration has shown a downward trend with the increase of grain yield (Duvick and Cassman, 1999; Ciampitti and Vyn, 2012). Nutrient management was an important strategy to simultaneously increase maize yield and grain protein concentration (Zhang et al., 2020). In this study, synergistic application of N and S simultaneously increased maize yield and grain protein concentration, which might have benefited from the mutual promotion of N and S accumulation in grains. The analysis of N and S concentrations in maize leaves during the growth stage (**Table 1**) and maturity stage (**Table 2**) showed that the proper N application (N2 level) promoted the absorption of S. Similarly, suitable S application (S2 level) increased the N accumulation in leaves, which is consistent with the previous report (Li et al., 2019). During the maturity stage, signs of mutual promotion of absorption of N and S were also observed in maize grains (**Table 2**). Grain protein of maize was the main compound that stored N and S, which accumulated in the protein as the form of amino acids (Sriperm et al., 2010). Analysis of the amino acids in maize grains showed that the concentration of various amino acids significantly increased with N application (**Figure 5**). When N supply was sufficient, as a sulfur-containing amino acid, cysteine concentration further increased with the coordinated application of S fertilizer. Cysteine is the basis for the formation of protein disulfide bonds, and the formation of disulfide bonds enhances protein stability (Depuydt et al., 2011). Limited by the conformation of protein, the increase of cysteine concentration provided more possible sites and opportunities for the formation of disulfide bonds, which contributed to the formation and improved stability of protein (Hogg, 2003; Liu et al., 2016). The results showed that protein concentration of grains correlated significantly with cysteine concentration in maize (**Figure 8A**), which indicated that the formation and stability of protein were enhanced with cysteine concentration. Thus, the sufficient formation of disulfide bonds may be the main reason for synergistic application of N and S to increase the protein concentration of maize grains.

Nitrogen supply played a dominant role in determining the quality of storage protein in seeds, and S application could regulate the composition of seed protein under the determined N supply level (Tabe et al., 2002; Li et al., 2016). In this study, the synergistic application of N and S significantly

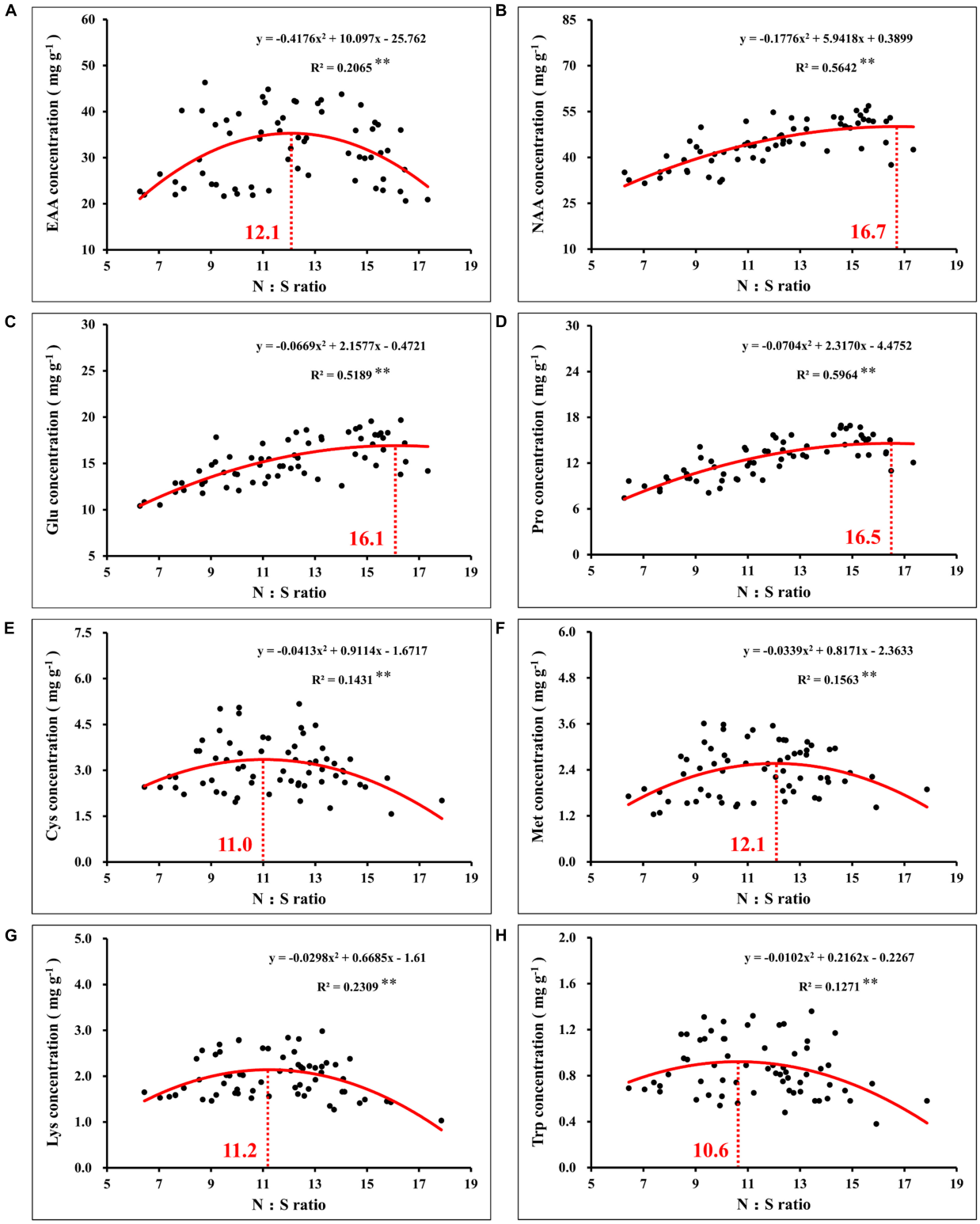

FIGURE 10 | Correlation analysis between the concentration of total essential amino acids **(A)**, total non-essential amino acids **(B)**, glutamate **(C)**, proline **(D)**, cysteine **(E)**, methionine **(F)**, lysine **(G)**, tryptophan **(H)**, and N:S ratio in maize grains. In this image, the red curve shows the correlation between the concentration of amino acids and N:S ratio in maize grains (n = 64), and the intersection of the red dotted line and the red curve indicates the maximum value of the curve. EAA, total essential amino acids; NAA, total non-essential amino acids; Glu, glutamate; Pro, proline; Cys, cysteine; Met, methionine; Lys, lysine; Trp, tryptophan.

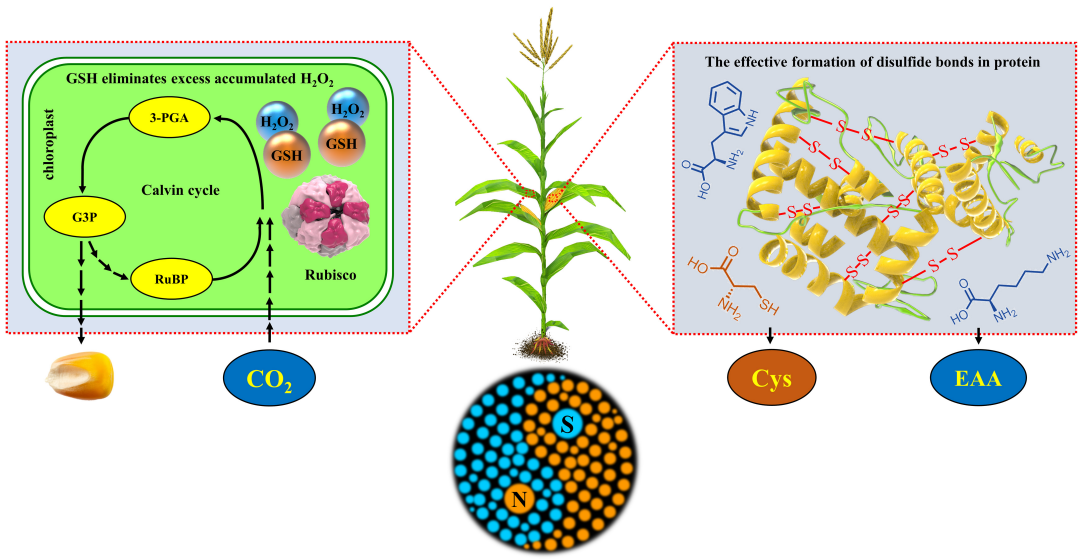

FIGURE 11 | Schematic diagram of the synergistic mechanism of N and S synergistically improving maize yield, grain protein concentration, and quality. The box on the left represents the physiological response during the Calvin cycle in the chloroplast of maize leaves, and the box on the right represents the synthesis and accumulation of protein in maize grains. RuBP, ribulose-1,5-bisphosphate; 3-PGA, 3-phosphoglycerate acid; G3P, glyceraldehyde-3-phosphate; Rubisco, ribulose-1,5-bisphosphate carboxylase/oxygenase; GSH, glutathione; H_2O_2, hydrogen peroxide; Cys, cysteine; EAA, essential amino acids (methionine, lysine, tryptophan, etc.); -S- S-, disulfide bonds in protein.

affected the concentration of various amino acids in the protein (**Figure 5**). According to Salamini and Soavc (1982), grain protein of maize was classified as albumins (3%), globulins (3%), glutelins (34%), and zeins (60%). As the most abundant storage protein in maize endosperm, zeins were high in NAA, such as glutamine, proline, and alanine, and severely lacked EAA, such as lysine, tryptophan, and methionine, which limited the nutritional quality of maize (Coleman and Larkins, 1999). Based on the difference in solubility, zeins were divided into α-, β-, γ-, and δ-zeins (Esen, 1987). Among these types of zeins, γ-zeins are a rich source of cysteine, and δ-zeins contain a high proportion of methionine (Kirihara et al., 1988; Swarup et al., 1995). The β-zeins are high in two sulfur-containing amino acids, cysteine and methionine (Randall et al., 2004). The α-zeins account for more than 70% of the total zeins, but lack lysine and cysteine, and the methionine concentration is poor, which seriously damaged the balance of amino acids in maize grains (Wu et al., 2012). Reducing the α-zein concentration can lead to a compensatory increase of the concentration of β-, γ-, and δ-zein and non-zein protein (Landry, 2002). In this study, under sufficient N supply, the cysteine concentration was increased with S application (**Figure 6**), and the proportion of lysine (**Figure 7C**), tryptophan (**Figure 7D**), and total EAA (**Figure 7A**) in grain protein was also significantly increased. Simultaneously, coordinated application of N and S reduced the NAA concentration, such as glutamic acid and proline, under the premise of ensuring a steady increase of protein concentration, which might benefit from the increase in cysteine regulated by S application, thereby inhibiting the concentration of α-zeins and causing the compensatory increase of EAA-rich non-zein protein. During the development of maize grains, cysteine residues in β- and γ-zeins cross-linked with each other and with other amino acids (Gibbon and Larkins, 2005). However, α-zeins were devoid of cysteine, which reduced the possibility of participation in protein formation, thus providing more opportunities for EAA, such as methionine, lysine, and tryptophan, into proteins. In this study, the concentrations of methionine (**Figure 8B**), lysine (**Figure 8C**), tryptophan (**Figure 8D**), and EAA (**Figure 8G**) continuously increased with cysteine concentration, and the concentrations of glutamic acid (**Figure 8E**), proline (**Figure 8F**), and NAA (**Figure 8H**) increased first and then decreased with cysteine concentration. These relationships indicated that protein formation preferentially accumulated EAA and inhibited NAA at a high enough cysteine concentration, thereby optimizing amino acid composition of protein and achieving amino acid balance.

Stoichiometry of N and S in Synergistically Improving Grain Yield, Grain Protein Concentration, and Quality of Maize

In view of the interaction between crop nutrients, stoichiometry is often used to quantify the interaction between nutrients and determine the nutrients level of crops (Divito et al., 2016; Salvagiotti et al., 2017). The analysis of N and S concentration in maize plants showed good performance in predicting grain yield, which was considered to be an advantageous tool for N and S regulation in crops (Pagani and Echeverría, 2011). In this study, the N:S ratio of leaves that obtained the maximum photosynthetic rate (N2S3 and N2S2 treatments) were 16.6 (silking stage) and 16.7 (grain-filling stage), respectively (**Table 1**).

The N:S ratio of the leaves at the maturity stage decreased in each treatment, which was ascribed to the N export from the leaf being faster than the S export (**Table 2**). At the maturity stage, the N:S ratio of the leaves of the N2S2 and N2S3 treatments that achieved the highest yield were 15.3 and 14.2, respectively. Analogous research showed that the range of the leaves' N:S ratio suitable for maize growth was 14.4–18.7, which is consistent with our results (Li et al., 2019). The correlation analysis between the maize yield, grain protein concentration, and N:S ratio of grains showed that maize yield reached a maximum at 12.2 (N:S ratio), and grain protein concentration reached a maximum at 14.0 (N:S ratio). Obviously, the optimal N:S ratio of yield and grain protein concentration did not coincide (**Figure 9**), which needs to be further analyzed. A lower N:S ratio indicated sufficient or excessive S supply, but it may also be ascribed to N deficiency. Conversely, a higher N:S ratio meant an excessive N supply or an S deficiency (Blake-Kalff et al., 2000). In this study, at the highest S application level (S3 level), the photosynthetic rate of maize leaves, maize yield, and grain protein concentration all achieved the maximum, which indicated that S application was sufficient rather than excessive. Therefore, the lower N:S ratio was ascribed to N deficiency. At the maximum N application level (N3 level), maize yield significantly decreased, which indicated that this N application level has led to an oversupply of N. Thus, the higher N:S ratio was due to the excessive supply of N. In addition, the super-high grain N:S ratio appeared in the experimental treatment of excessive N application without S application (N3S0 treatment). This fertilization method (N3S0 treatment) not only led to low S concentration in maize grains, but also low S concentration in maize leaves, which severely limited the photosynthetic rate of the leaves. The lower photosynthesis rate led to poor grain filling, so the maize yield was lower. When the N:S ratio of grains was at 12.2, it meant that the optimal ratio of N and S concentration in grains was obtained, and thereby, the maximum maize yield was obtained. When the N:S ratio of grains was at 12.2–14.0, it indicated excessive supply of N, and the grain protein concentration increased with N application, which is consistent with previous studies (Hou et al., 2012; Qiu et al., 2015). When the N:S ratio of grain exceeded 14.0, it indicated the deficiency of S, and the grain protein concentration also decreased with S deficiency. However, when maize yield was at the highest level, the grain protein concentration did not decrease significantly, and the total protein accumulation (maize yield × grain protein concentration) reached the maximum value (16.8 g plant^{-1}). Therefore, the most efficient method to obtain the maximum maize yield without sacrificing grain protein concentration was to precisely regulate the N:S ratio of grains.

Notably, correlation analysis between the amino acids and N:S ratio in grains showed that the optimal N:S ratio of EAA (**Figure 10A**), such as cysteine (**Figure 10E**), methionine (**Figure 10F**), lysine (**Figure 10G**), and tryptophan (**Figure 10H**), were all at a lower level (10.6–12.1), and the optimal N:S ratio values of NAA (**Figure 10B**), such as glutamic acid (**Figure 10C**) and proline (**Figure 10D**), were higher (16.1–16.7). Thus, in order to obtain higher nutritional quality of grains, the grain N:S ratio should be controlled at about 11.0–12.0. According to the respective experimental treatments, N2S2 and N2S3 treatments achieved the highest grain yield, and grain protein concentration was also at a high level. The N:S ratio of the N2S2 and N2S3 treatments were 11.9 and 11.1, respectively (**Table 2**), which was highly consistent with the range of grain N:S ratio that achieved the highest nutritional quality. The grain N:S ratio affected maize yield, grain protein concentration, and various amino acid concentration. The maize yield and nutritional quality were simultaneously improved at the suitable range (11.0–12.0) of grain N:S ratio.

Overall, the synergetic regulation of N and S simultaneously improved the yield and nutritional quality of maize by regulating the redox balance of leaves and balance of amino acids in grains (**Figure 11**).

CONCLUSION

Coordinated application of N and S significantly affected maize growth, yield, and nutritional quality. The GSH in the maize leaves increased the photosynthetic rate by maintaining the redox balance, thereby increasing maize yield. The cysteine in grains optimized the concentration of grain protein and balance of amino acids by regulating the ratio of amino acids. The coordinated regulation of N and S synergistically improved the yield and nutritional quality of maize, which met the requirement for sustainable development in maize production and provided a new theoretical basis and method for the high-yield and high-quality production of maize.

DATA AVAILABILITY STATEMENT

The raw data supporting the conclusions of this article will be made available by the authors, without undue reservation.

AUTHOR CONTRIBUTIONS

QG and GM conducted an overall design for this study. SL completed the experiments and wrote the manuscript with guidance from QG and YW. SC, XZ, and GM provided suggestions and edited the manuscript. All authors contributed to the article and approved the submitted version.

FUNDING

This work was supported by the National Key Research and Development Program of China (Grant No. 2016YFD0200101) and Natural Science Foundation of Jilin Province, China (Grant No. 20190201117JC).

REFERENCES

Ali, M., Scott, M. P., and Bakht, J. (2011). Molecular mechanism of methionine differentiation in high and low methionine maize lines. *Afr. J. Biotechnol.* 10, 3747–3752. doi: 10.5897/AJB10.2294

Ashida, H., Danchin, A., and Yokota, A. (2005). Was photosynthetic Rubisco recruited by acquisitive evolution from Rubisco-like proteins involved in sulfur metabolism? *Res. Microbiol.* 156, 611–618. doi: 10.1016/j.resmic.2005.01.014

Bashir, M. A., Naveed, M., Ahmad, Z., Gao, B., Mustafa, A., and Núñez-Delgado, A. (2020). Combined application of biochar and sulfur regulated growth, physiological, antioxidant responses and Cr removal capacity of maize (Zea mays L.) in tannery polluted soils. *J. Environ. Manage.* 259:110051. doi: 10.1016/j.jenvman.2019.110051

Baudet, J., Huet, J. C., Jolivet, E., Lesaint, C., Mossé, J., and Pernollet, J. C. (1986). Chaises in accumulation of seed nitrogen compounds in maize under conditions of sulphur deficiency. *Physiol. Plantarum.* 68, 608–614. doi: 10.1111/j.1399-3054.1986.tb03404.x

Bhatnagar, S., Betrán, F. J., and Rooney, L. W. (2004). Combining abilities of quality protein maize inbreds. *Crop. Sci.* 44, 1997–2005. doi: 10.2135/cropsci2004.1997

Blake-Kalff, M. M. A., Hawkesford, M. J., Zhao, F. J., and McGrath, S. P. (2000). Diagnosing sulfur deficiency in field-grown oilseed rape (*Brassica napus* L.) and wheat (*Triticum aestivum* L.). *Plant Soil* 225, 95–107. doi: 10.1023/A:1026503812267

Carciochi, W. D., Salvagiotti, F., Pagani, A., Reussi Calvo, N. I., Eyherabide, M., Sainz Rozas, H. R., et al. (2020). Nitrogen and sulfur interaction on nutrient use efficiencies and diagnostic tools in maize. *Eur. J. Agron.* 116:126045. doi: 10.1016/j.eja.2020.126045

Chen, Y., Xiao, C., Wu, D., Xia, T., Chen, Q., Chen, F., et al. (2015). Effects of nitrogen application rate on grain yield and grain nitrogen concentration in two maize hybrids with contrasting nitrogen remobilization efficiency. *Eur. J. Agron.* 62, 79–89. doi: 10.1016/j.eja.2014.09.008

Ciampitti, I. A., and Vyn, T. J. (2012). Physiological perspectives of changes over time in maize yield dependency on nitrogen uptake and associated nitrogen efficiencies: a review. *Field Crop. Res.* 133, 48–67. doi: 10.1016/j.fcr.2012.03.008

Coleman, C. E., and Larkins, B. A. (1999). "The prolamins of maize," in *Seed Proteins*, eds P. R. Shewry and R. Casey (Dordrecht: Kluwer Academic Publishers), 109–139. doi: 10.1007/978-94-011-4431-5_6

Depuydt, M., Messens, J., and Collet, J. F. (2011). How proteins form disulfide bonds. *Antioxid. Redox Sign.* 15, 49–66. doi: 10.1089/ars.2010.3575

Ding, L., Wang, K. J., Jiang, G. M., Biswas, D. K., Xu, H., Li, L. F., et al. (2005). Effects of nitrogen deficiency on photosynthetic traits of maize hybrids released in different years. *Ann. Bot.* 96, 925–930. doi: 10.1093/aob/mci244

Divito, G. A., Echeverría, H. E., Andrade, F. H., and Sadras, V. O. (2016). N and S concentration and stoichiometry in soybean during vegetative growth: dynamics of indices for diagnosing the S status. *Field Crop. Res.* 198, 140–147. doi: 10.1016/j.fcr.2016.08.018

Duvick, D. N. (2005). The contribution of breeding to yield advances in maize (*Zea mays* L.). *Adv. Agron.* 86, 83–145. doi: 10.1016/s0065-2113(05)86002-x

Duvick, D. N., and Cassman, K. G. (1999). Post-green revolution trends in yield potential of temperate maize in the North-Central United States. *Crop. Sci.* 39, 1622–1630. doi: 10.2135/cropsci1999.3961622x

Esen, A. (1987). Proposed nomenclature for the alcohol-soluble proteins (zeins) of maize (*Zea mays* L.). *J. Cereal Sci.* 5, 117–128. doi: 10.1016/s0733-5210(87)80015-2

Exposito-Rodriguez, M., Laissue, P. P., Yvon-Durocher, G., Smirnoff, N., and Mullineaux, P. M. (2017). Photosynthesis-dependent H2O2 transfer from chloroplasts to nuclei provides a high-light signalling mechanism. *Nat. Commun.* 8, 49–59. doi: 10.1038/s41467-017-00074-w

Fatma, M., Asgher, M., Masood, A., and Khan, N. A. (2014). Excess sulfur supplementation improves photosynthesis and growth in mustard under salt stress through increased production of glutathione. *Environ. Exp. Bot.* 107, 55–63. doi: 10.1016/j.envexpbot.2014.05.008

Food and Agriculture Organization of the United Nations (2018). *The State of Food Security and Nutrition in the World 2018. Building Climate Resilience for Food Security and Nutrition*. Rome: Food and Agriculture Organization.

Foyer, C. H. (2018). Reactive oxygen species, oxidative signaling and the regulation of photosynthesis. *Environ. Exp. Bot.* 154, 134–142. doi: 10.1016/j.envexpbot.2018.05.003

Foyer, C. H., Ruban, A. V., and Nixon, P. J. (2017). Photosynthesis solutions to enhance productivity. *Philos. T. R. Soc. B.* 372:20160374. doi: 10.1098/rstb.2016.0374

Galili, G., and Amir, R. (2013). Fortifying plants with the essential amino acids lysine and methionine to improve nutritional quality. *Plant Biotechnol. J.* 11, 211–222. doi: 10.1111/pbi.12025

Gibbon, B. C., and Larkins, B. A. (2005). Molecular genetic approaches to developing quality protein maize. *Trends Genet.* 21, 227–233. doi: 10.1016/j.tig.2005.02.009

Gigolashvili, T., and Kopriva, S. (2014). Transporters in plant sulfur metabolism. *Front. Plant Sci.* 5:442. doi: 10.3389/fpls.2014.00442

González-Moro, B., Lacuesta, M., Becerril, J. M., Gonzalez-Murua, C., and Muñoz-Rueda, A. (1997). Glycolate accumulation causes a decrease of photosynthesis by inhibiting Rubisco activity in maize. *J. Plant Physiol.* 150, 388–394. doi: 10.1016/s0176-1617(97)80087-9

Gutiérrez-Gamboa, G., Garde-Cerdán, T., Gonzalo-Diago, A., Moreno-Simunovic, Y., and Martínez-Gil, A. M. (2016). Effect of different foliar nitrogen applications on the must amino acids and glutathione composition in Cabernet Sauvignon vineyard. *LWT Food Sci. Technol.* 75, 147–154. doi: 10.1016/j.lwt.2016.08.039

Habtegebrial, K., and Singh, B. R. (2009). Response of wheat cultivars to nitrogen and sulfur for crop yield, nitrogen use efficiency, and protein quality in the semiarid region. *J. Plant Nutr.* 32, 1768–1787. doi: 10.1080/01904160903152616

Hawkesford, M., Horst, W., Kichey, T., Lambers, H., Schjoerring, J., Møller, I. S., et al. (2012). "Functions of macronutrients," in *Marschner's Mineral Nutrition of Higher Plants*, ed. P. Marschner (Waltham: Academic Press), 135–189.

Hogg, P. J. (2003). Disulfide bonds as switches for protein function. *Trends Biochem. Sci.* 28, 210–214. doi: 10.1016/s0968-0004(03)00057-4

Hou, P., Gao, Q., Xie, R., Li, S., Meng, Q., Kirkby, E. A., et al. (2012). Grain yields in relation to N requirement: optimizing nitrogen management for spring maize grown in China. *Field Crop. Res.* 129, 1–6. doi: 10.1016/j.fcr.2012.01.006

Hou, W., Yan, J., Jakli, B., Lu, J., Ren, T., Cong, R., et al. (2018). Synergistic effects of nitrogen and potassium on quantitative limitations to photosynthesis in rice (*Oryza sativa* L.). *J. Agr. Food Chem.* 66, 5125–5132. doi: 10.1021/acs.jafc.8b01135

Igamberdiev, A. U. (2015). Control of Rubisco function via homeostatic equilibration of CO2 supply. *Front. Plant Sci.* 6:106. doi: 10.3389/fpls.2015.00106

Kim, S. W., Chen, H., and Parnsen, W. (2019). Regulatory role of amino acids in pigs fed on protein-restricted diets. *Curr. Protein Pept. Sci.* 20, 132–138. doi: 10.2174/1389203719666180517100746

Kirihara, J. A., Petri, J. B., and Messing, J. (1988). Isolation and sequence of a gene encoding a methionine-rich 10-kDa zein protein from maize. *Gene* 71, 359–370. doi: 10.1016/0378-1119(88)90053-4

König, K., Vaseghi, M. J., Dreyer, A., and Dietz, K. J. (2018). The significance of glutathione and ascorbate in modulating the retrograde high light response in Arabidopsis thaliana leaves. *Physiol. Plantarum.* 162, 262–273. doi: 10.1111/ppl.12644

Krishnan, H. B., and Jez, J. M. (2018). Review: the promise and limits for enhancing sulfur-containing amino acid content of soybean seed. *Plant Sci.* 272, 14–21. doi: 10.1016/j.plantsci.2018.03.030

Kruger, E. L., and Volin, J. C. (2006). Reexamining the empirical relation between plant growth and leaf photosynthesis. *Funct. Plant Biol.* 33, 421–429. doi: 10.1071/fp05310

Landry, J. (2002). A linear model for quantitating the accumulation of zeins and their fractions (α+δ, β&γ) in developing endosperm of wild-type and mutant maizes. *Plant Sci.* 163, 111–115. doi: 10.1016/s0168-9452(02)00067-5

Lawson, T., Kramer, D. M., and Raines, C. A. (2012). Improving yield by exploiting mechanisms underlying natural variation of photosynthesis. *Curr. Opin. Biotech.* 23, 215–220. doi: 10.1016/j.copbio.2011.12.012

Leister, D. (2012). How can the light reactions of photosynthesis be improved in plants? *Front. Plant Sci.* 3:199. doi: 10.3389/fpls.2012.00199

Li, C. S., Xiang, X. L., Huang, Y. C., Zhou, Y., An, D., Dong, J. Q., et al. (2020). Long-read sequencing reveals genomic structural variations that underlie creation of quality protein maize. *Nat. Commun.* 11:17. doi: 10.1038/s41467-019-14023-2

Li, N., Yang, Y., Wang, L., Zhou, C., Jing, J., Sun, X., et al. (2019). Combined effects of nitrogen and sulfur fertilization on maize growth, physiological traits, N and S uptake, and their diagnosis. *Field Crop. Res.* 242:107593. doi: 10.1016/j.fcr.2019.107593

Li, S., Lu, W., Li, G. F., Gong, Y. D., Zhao, N. M., Zhang, R. X., et al. (2004). Interaction of hydrogen peroxide with ribulose-1,5-bisphosphate carboxylase/oxygenase from rice. *Biochemistry* 69, 1136–1142. doi: 10.1023/b:biry.0000046888.45252.67

Li, X., Zhou, L., Liu, F., Zhou, Q., Cai, J., Wang, X., et al. (2016). Variations in protein concentration and nitrogen sources in different positions of grain in wheat. *Front. Plant Sci.* 7:942. doi: 10.3389/fpls.2016.00942

Li, Y., Ye, W., Wang, M., and Yan, X. (2009). Climate change and drought: a risk assessment of crop-yield impacts. *Clim. Res.* 39, 31–46. doi: 10.3354/cr00797

Liang, T., Ding, H., Wang, G., Kang, J., Pang, H., and Lv, J. (2016). Sulfur decreases cadmium translocation and enhances cadmium tolerance by promoting sulfur assimilation and glutathione metabolism in *Brassica chinensis* L. *Ecotox. Environ. Safe.* 124, 129–137. doi: 10.1016/j.ecoenv.2015.10.011

Liu, J., Fernie, A. R., and Yan, J. B. (2020). The past, present, and future of maize improvement: domestication, genomics, and functional genomic routes toward crop enhancement. *Plant Commun.* 1:100010. doi: 10.1016/j.xplc.2019.100010

Liu, T., Wang, Y., Luo, X., Li, J., Reed, S. A., Xiao, H., et al. (2016). Enhancing protein stability with extended disulfide bonds. *Proc. Natl. Acad. Sci. U.S.A.* 113, 5910–5915. doi: 10.1073/pnas.1605363113

Long, S. P., Marshall-Colon, A., and Zhu, X. G. (2015). Meeting the global food demand of the future by engineering crop photosynthesis and yield potential. *Cell* 161, 56–66. doi: 10.1016/j.cell.2015.03.019

Lošák, T., Hlušek, J., Filipèík, R., Pospíšilová, L., Maòásek, J., Prokeš, K., et al. (2010). Effect of nitrogen fertilization on metabolisms of essential and non-essential amino acids in field-grown grain maize (*Zea mays* L.). *Plant Soil Environ.* 56, 574–579. doi: 10.17221/288/2010-pse

Lunde, C., Zygadlo, A., Simonsen, H. T., Nielsen, P. L., Blennow, A., and Haldrup, A. (2008). Sulfur starvation in rice: the effect on photosynthesis, carbohydrate metabolism, and oxidative stress protective pathways. *Physiol. Plantarum.* 134, 508–521. doi: 10.1111/j.1399-3054.2008.01159.x

Lunn, J. E., and Hatch, M. D. (1995). Primary partitioning and storage of photosynthate in sucrose and starch in leaves of C4 plants. *Planta* 197, 385–391. doi: 10.2307/23384244

MacGregor, J. M., Taskovitch, L. T., and Martin, W. P. (1961). Effect of nitrogen fertilizer and soil type on the amino acid content of corn grain. *Agron. J.* 53, 211–214. doi: 10.2134/agronj1961.00021962005300040001x

Maurin, A.-C., Benani, A., Lorsignol, A., Brenachot, X., Parry, L., Carraro, V., et al. (2014). Hypothalamic eIF2α Signaling Regulates Food Intake. *Cell Rep.* 6, 438–444. doi: 10.1016/j.celrep.2014.01.006

Mittler, R., Vanderauwera, S., Gollery, M., and Van Breusegem, F. (2004). Reactive oxygen gene network of plants. *Trends Plant Sci.* 9, 490–498. doi: 10.1016/j.tplants.2004.08.009

Nemat Alla, M. M., and Hassan, N. M. (2020). Nitrogen alleviates NaCl toxicity in maize seedlings by regulating photosynthetic activity and ROS homeostasis. *Acta Physiol. Plant.* 42, 93–102. doi: 10.1007/s11738-020-03080-6

Osaki, M., Shinano, T., and Tadano, T. (1993). Effect of nitrogen, phosphorus, or potassium deficiency on the accumulation of ribulose-1,5-bisphosphate carboxylase/oxygenase and chlorophyll in several field crops. *Soil Sci. Plant Nutr.* 39, 417–425. doi: 10.1080/00380768.1993.10419782

Pagani, A., and Echeverría, H. E. (2011). Performance of sulfur diagnostic methods for corn. *Agron. J.* 103, 413–421. doi: 10.2134/agronj2010.0265

Pan, D., Li, Q. X., Lin, Z., Chen, Z., Tang, W., Pan, C., et al. (2017). Interactions between salicylic acid and antioxidant enzymes tilting the balance of H2O2 from photorespiration in non-target crops under halosulfuron-methyl stress. *Pestic. Biochem. Phys.* 143, 214–223. doi: 10.1016/j.pestbp.2017.09.007

Parry, M. A. J., Andralojc, P. J., Scales, J. C., Salvucci, M. E., Carmo-Silva, A. E., Alonso, H., et al. (2013). Rubisco activity and regulation as targets for crop improvement. *J. Exp. Bot.* 64, 717–730. doi: 10.1093/jxb/ers336

Perdomo, J. A., Capó-Bauçà, S., Carmo-Silva, E., and Galmés, J. (2017). Rubisco and rubisco activase play an important role in the biochemical limitations of photosynthesis in rice, wheat, and maize under high temperature and water deficit. *Front. Plant Sci.* 8:490. doi: 10.3389/fpls.2017.00490

Planta, J., Xiang, X. L., Leustek, T., and Messing, J. (2017). Engineering sulfur storage in maize seed proteins without apparent yield loss. *Proc. Natl. Acad. Sci. U.S.A.* 114, 11386–11391. doi: 10.1073/pnas.1714805114

Qiu, S. J., He, P., Zhao, S. C., Li, W. J., Xie, J. G., Hou, Y. P., et al. (2015). Impact of nitrogen rate on maize yield and nitrogen use efficiencies in Northeast China. *Agron. J.* 107, 305–313. doi: 10.2134/agronj13.0567

Randall, J., Sutton, D., Ghoshroy, S., Bagga, S., and Kemp, J. D. (2004). Co-ordinate expression of β- and δ-zeins in transgenic tobacco. *Plant Sci.* 167, 367–372. doi: 10.1016/j.plantsci.2004.04.005

Resurreccion, A. P., Makino, A., Bennett, J., and Mae, T. (2002). Effect of light intensity on the growth and photosynthesis of rice under different sulfur concentrations. *Soil Sci. Plant Nutr.* 48, 71–77. doi: 10.1080/00380768.2002.10409173

Rubio-Wilhelmi, M., del, M., Reguera, M., Sanchez-Rodriguez, E., Romero, L., Blumwald, E., et al. (2014). PSARK::IPT expression causes protection of photosynthesis in tobacco plants during N deficiency. *Environ. Exp. Bot.* 98, 40–46. doi: 10.1016/j.envexpbot.2013.10.011

Salamini, S. A., and Soavc, C. (1982). "Zein: genetics and biochemistry," in *Maize for Biological Research*, ed. W. F. Sheridan (Grand Forks: University of North Dakota Press), 155–160.

Salvagiotti, F., Prystupa, P., Ferraris, G., Couretot, L., Magnano, L., Dignani, D., et al. (2017). N:P:S stoichiometry in grains and physiological attributes associated with grain yield in maize as affected by phosphorus and sulfur nutrition. *Field Crop Res.* 203, 128–138. doi: 10.1016/j.fcr.2016.12.019

Saxena, I., Srikanth, S., and Chen, Z. (2016). Cross talk between H2O2 and interacting signal molecules under plant stress response. *Front. Plant Sci.* 7:570. doi: 10.3389/fpls.2016.00570

Scott, M. P., Edwards, J. W., Bell, C. P., Schussler, J. R., and Smith, J. S. (2006). Grain composition and amino acid content in maize cultivars representing 80 years of commercial maize varieties. *Maydica* 51, 417–423.

Sharwood, R. E. (2016). Engineering chloroplasts to improve Rubisco catalysis: prospects for translating improvements into food and fiber crops. *New Phytol.* 213, 494–510. doi: 10.1111/nph.14351

Smirnoff, N., and Arnaud, D. (2019). Hydrogen peroxide metabolism and functions in plants. *New Phytol.* 221, 1197–1214. doi: 10.1111/nph.15488

Soares, J. C., Santos, C. S., Carvalho, S. M. P., Pintado, M. M., and Vasconcelos, M. W. (2019). Preserving the nutritional quality of crop plants under a changing climate: importance and strategies. *Plant Soil* 443, 1–26. doi: 10.1007/s11104-019-04229-0

Sriperm, N., Pesti, G. M., and Tillman, P. B. (2010). The distribution of crude protein and amino acid content in maize grain and soybean meal. *Anim. Feed Sci. Tech.* 159, 131–137. doi: 10.1016/j.anifeedsci.2010.05.009

Swarup, S., Timmermans, M. C., Chaudhuri, S., and Messing, J. (1995). Determinants of the high-methionine trait in wild and exotic germplasm may have escaped selection during early cultivation of maize. *Plant J.* 8, 359–368. doi: 10.1046/j.1365-313x.1995.08030359.x

Tabe, L., Hagan, N., and Higgins, T. J. V. (2002). Plasticity of seed protein composition in response to nitrogen and sulfur availability. *Curr. Opin. Plant Biol.* 5, 212–217. doi: 10.1016/s1369-5266(02)00252-2

Tsai, C. Y., Dweikat, I., Huber, D. M., and Warren, H. L. (1992). Interrelationship of nitrogen nutrition with maize (*Zea mays*) grain yield, nitrogen use efficiency and grain quality. *J. Sci. Food Agr.* 58, 1–8. doi: 10.1002/jsfa.2740580102

Tsai, C. Y., Warren, H. L., Huber, D. M., and Bressan, R. A. (1983). Interactions between the kernel N sink, grain yield and protein nutritional quality of maize. *J. Sci. Food Agr.* 34, 255–263. doi: 10.1002/jsfa.2740340309

von Caemmerer, S., Lawson, T., Oxborough, K., Baker, N. R., Andrews, T. J., and Raines, C. A. (2004). Stomatal conductance does not correlate with photosynthetic capacity in transgenic tobacco with reduced amounts of Rubisco. *J. Exp. Bot.* 55, 1157–1166. doi: 10.1093/jxb/erh128

Whitney, S. M., and Sharwood, R. E. (2014). "Plastid transformation for Rubisco engineering and protocols for assessing expression," in *Methods in Molecular Biology*, ed. P. Maliga (New York, NY: Springer Science+Business Media), 245–262. doi: 10.1007/978-1-62703-995-6_15

Wu, A., Hammer, G. L., Doherty, A., von Caemmerer, S., and Farquhar, G. D. (2019). Quantifying impacts of enhancing photosynthesis on crop yield. *Nat. Plants* 5, 380–388. doi: 10.1038/s41477-019-0398-8

Wu, Y. R., and Messing, J. (2012). RNA interference can rebalance the nitrogen sink of maize seeds without losing hard endosperm. *PLoS One* 7:e32850. doi: 10.1371/journal.pone.0032850

Wu, Y. R., Wang, W. Q., and Messing, J. (2012). Balancing of sulfur storage in maize seed. *BMC Plant Biol.* 12:77. doi: 10.1186/1471-2229-12-77

Zhang, L., Liang, Z. Y., He, X. M., Meng, Q. F., Hu, Y. C., Schmidhalter, U., et al. (2020). Improving grain yield and protein concentration of maize (*Zea mays* L.) simultaneously by appropriate hybrid selection and nitrogen management. *Field Crop. Res.* 249:107754. doi: 10.1016/j.fcr.2020.107754

Conflict of Interest: The authors declare that the research was conducted in the absence of any commercial or financial relationships that could be construed as a potential conflict of interest.

Advantages of publishing in Frontiers

OPEN ACCESS
Articles are free to read for greatest visibility and readership

FAST PUBLICATION
Around 90 days from submission to decision

HIGH QUALITY PEER-REVIEW
Rigorous, collaborative, and constructive peer-review

TRANSPARENT PEER-REVIEW
Editors and reviewers acknowledged by name on published articles

Frontiers
Avenue du Tribunal-Fédéral 34
1005 Lausanne | Switzerland

Visit us: www.frontiersin.org
Contact us: frontiersin.org/about/contact

REPRODUCIBILITY OF RESEARCH
Support open data and methods to enhance research reproducibility

DIGITAL PUBLISHING
Articles designed for optimal readership across devices

FOLLOW US
@frontiersin

IMPACT METRICS
Advanced article metrics track visibility across digital media

EXTENSIVE PROMOTION
Marketing and promotion of impactful research

LOOP RESEARCH NETWORK
Our network increases your article's readership